UNIVERSITY OF SOUTHERN CALIFORNIA

DEPARTMENT OF CIVIL ENGINEERING

MICROZONATION OF A METROPOLITAN AREA

by

V. W. Lee and M. D. Trifunac

Report No. 87-02

May 1987

TABLE OF CONTENTS

ABSTRACT..... 1

INTRODUCTION..... 2

Uniform Risk Spectra..... 6

EXAMPLE: Seismic Microzonation of a Metropolitan Area..... 9

CONCLUSIONS..... 28

REFERENCES..... 29

APPENDIX A: Maps of Uniform Risk Spectra for Scaling with Magnitude..... 32

APPENDIX B: Maps of Uniform Risk Spectra for Scaling with Modified Mercalli Intensity..... 88

ABSTRACT

A method for seismic microzonation of a large metropolitan area (approximately 90 x 90 km) is examined. It utilizes information on the location of active faults and their relative levels of seismicity, the three-dimensional geometry of the source to station and frequency dependent attenuation, the effects of local amplification of wave amplitudes in terms of the depth of sedimentary deposits beneath the site, and two different scaling procedures in terms of earthquake magnitude and the epicentral intensity. It is shown that these two methods of scaling are consistent, and that both can lead to reliable estimates of uniform risk spectra.

The method presented here does not require any new or difficult steps to gather data when compared to other microzonation procedures employed in the United States or abroad. The advantage of the method, however, lies in its ability to properly balance different contributing factors to the seismic risk at a point, in time, space and frequency of strong ground shaking.

INTRODUCTION

The seismic zonation maps, usually presented on a scale which only distinguishes areas as large as states or countries, are intended to show the overall distribution of seismic risk. The quantity plotted in such maps may represent a coefficient for use in seismic resistant design (Roberts and Ulrich, 1951), maximum intensity of shaking (Richter, 1959, Akademia Nauk SSSR, 1980), or some amplitude of the expected future strong ground motion (Goto and Kameda, 1969). Typically, such maps will only include the overall patterns of the geographical distribituion of seismicity and may reflect the presence of only some major fault systems or of large seismically active zones. Most seismic design codes include such maps (IAEE, 1984) and show the zones requiring different lateral force coefficients.

The characteristics of strong earthquake ground shaking at a point, however, also depend on numerous soil and geological features surrounding the site, as well as on the distribution and on the level of activity of the earthquake sources in the area (Gaus and Serif, 1972). These may be too detailed to include in typical seismic zoning maps (IAEE,1984), but can be included in and represent the basis for the detailed microzonation maps. The variety of published microzonation maps results from their many different uses in design (Osaki, 1972; Akademia Nauk, SSSR, 1980), insurance (Steinbrugge, 1978), urban design and in the prediction of earthquake induced soil failures and land slides, for example.

A systematic large scale program to develop zonation maps of the entire country, as well as to develop microzonation maps for large cities started in the U.S.S.R. in the 1930's (Akademia Nauk, 1980). Following the publication of the first U.S.S.R. zoning map in 1937 many researchers there have worked on the development of the microzonation methodology, which today continues to be dominated by the concept of the largest observed intensity and by the local geologic and subsoil conditions at a site (Medvedev, 1962,; Adademia Nauk SSSR, 1980). In Japan the early work on microzonation was influenced by the studies of Sezawa and Kanai on the wave propagation through soil layers and by the effort to measure the transfer function properties of each site experimentally, by studying the local amplitudes of microtremors (Kanai, 1983). In various countries of Europe (Karnik, 1972), Central and South America (Lomnitz, 1974; Kuroiwa et al. 1978) and in China (Liao, 1985), the zonation and microzonation work closely followed and combined the Russian and the Japanese experience. In the United States, with few exceptions (e.g. Richter 1959) the microzonation work has not attracted many researchers. In 1972 and 1978 international conferences were held, first in Seattle, Washington and second in San Francisco, California, to promote international exchange of ideas in microzonation. As can be seen from the proceedings of these two conferences the emphasis in the U.S. seems to be directed towards individual basic or applied studies while an integrated approach to microzonation appears to be lacking.

Following Cornell's pioneering work in 1968, on how to integrate the contributions to the seismic risk at a site, the computational capabilities for evaluating seismic risk have been developed to a point (Der Kiureghian and Ang, 1975; McGuire, 1974; Anderson and Trifunac, 1977, 1978a,b; Lee and Trifunac, 1985) where this approach can be used now for constructing probabilistic microzonation maps. So far this work has been carried out using mainly the peak ground acceleration and the description of seismicity on the scale of the State of California (for example, Tenhaus, 1980; Kiremidjian, 1977). Extending this approach to scaling with frequency dependent spectra directly offers major and new possibilities for the development of microzonation maps in which many contributing factors can be considered simultaneously and in a balanced way. To illustrate this method and its capabilities in this report we present microzonation maps for a hypothetical metropolitan area with geometry corresponding to that of the Los Angeles basin.

One of the most important assumptions underlying almost any microzonation method is that the local geologic and soil conditions possess some intrinsic wave amplification properties which are independent (or almost independent) of the type and of the direction of seismic waves approaching the site. This is the basis of all experimental work of Kanai (1983), who assumes that by measuring the "predominant period" of each site, through the experimental measurement of the site transfer function, it is possible to evaluate the local amplification effects (Allam, 1969). It is also assumed, in this work, that the repeated excitations by different earthquakes will continue to be dominated by the local site effects. For this to be so, it is

essential that the local site transfer functions should play a major role in modifying the input ground motion (Udwadia and Trifunac, 1973). However, this seems to be so only when the local site consists of exceptionally soft soil and alluvium deposits (Herrera and Rosenblueth, 1965), and when the wave excitation arrives from a limited pencil of azimuths. Detailed analysis of the two- and three-dimensional effects of wave propagation shows that the peaks of the transfer function of the local site effects can shift in their "predominant period" and in amplitude, and can disappear altogether with changing the direction of wave incidence (Trifunac, 1971,1973). Though there are many examples of the patterns of building damage following many earthquakes, which are clearly a consequence of the variations of the amplitudes of shaking on a very small (microzonation) scale, there are no adequate data to verify experimentally the extent to which such patterns will be repeated during the future strong earthquake shaking.

Theoretical wave propagation studies and the empirical descriptions of the wave amplitudes do lead to a consistent conclusion that those waves will be amplified which propagate from "hard" to "soft" material (Trifunac, 1971; Wong and Trifunac, 1974). However, this agreement is only in the sense of the mean overall amplitudes and does not involve any detailed description of the spectral amplification or deamplification at given frequencies or at given locations. This observation thus rules out the concept of the predominant period (Kanai, 1983) as it has been associated with the depth of the soft soil deposits (Medvedev, 1962).

The detailed description of the empirical results which describe the dependence of strong earthquake ground motion amplitudes and duration is beyond the scope of this work. The most recent results and detailed references on many earlier studies can be found in the reports by Trifunac and Lee (1985a,b). For the purposes of this work it is sufficient to state that the repeatable site effects are characterized by the amplification of the average wave amplitudes for periods longer than about 0.5 seconds at geologically "soft" sites (Trifunac and Lee, 1985a,b).

Uniform Risk Spectra

The methodology for estimating the uniform risk spectra at a site (Anderson and Trifunac, 1977,1978a; Lee and Trifunac, 1985) involves: (1) Description of the area surrounding the site in terms of all seismic sources, their activity and geometrical extent , (2) Site characteristics in terms of the depth of sedimentary deposits or the site geological classification (Trifunac and Brady, 1975) and (3) Description of attenuation of strong motion amplitudes with distance from the earthquake source (Trifunac and Lee, 1985c). Then the probability $p[S(\omega)]$ that some spectral amplitude will be exceeded at least once in Y years is (Anderson and Trifunac, 1977)

$$p[S(\omega)] = 1 - \exp\{-N_E[S(\omega)]\} \qquad (1)$$

where $N_E[S(\omega)]$ is the expected number of times that $S(\omega)$ will be exceeded at the site. The recurrence time of a given amplitude $S(\omega)$ is

$$T[S(\omega)] = N_E[S(\omega)]^{-1} \quad , \tag{2}$$

where the time unit is Y years (in all examples in this work Y = 50 years). The above equation (2) then gives the recurrence time of $S(\omega)$. Taking the logarithm of equation (1) gives

$$N_E[S(\omega)] = - \ell n\{1-p[S(\omega)]\} \quad . \tag{3}$$

Since, for this example, we are assuming a Poisson sequence of earthquakes in time, equation (3) can be used to alter the probabilities of exceeding $S(\omega)$ during another observation period of Y years. Table I illustrates this. It shows, for example, that amplitude $S(\omega)$ which has the probability of 0.5 of being exceeded in 50 years has the probability of 0.13 of being exceeded during the period of 10 years.

In this report we present the results of microzonation of a metropolitan area assuming that all sources contributing to the risk are represented by a Poissonian sequence in time. However, the computer program we employ (Lee and Trifunac, 1985) is also capable of considering a combination of Poissonian sources in time with events which will occur with certainty. For example, if a reliable prediction is made that an earthquake of certain magnitude will occur at one of the sources in the model, that source can be assigned the Poissonian sequence plus this deterministic sequence (e.g. main shock and its aftershocks) and the resulting Uniform Risk Spectra can be computed. For examples in this report we did not consider such cases. Clearly, when final microzonation maps are developed for a region for a period of Y years, and when at some later time an earthquake prediction is made, it is easy to rerun the probabilistic calculations of the

TABLE I

Examples of using equations (1) and (3), to compute the probability, P, of exceeding spectral amplitudes at least once in Y years, and, N_E, the expected number of times that spectral amplitudes will be exceeded for given P.

Y (years)						
1	P	0.087	0.045	0.014	0.0021	0.000201
	N_E^*	0.09210	0.04605	0.01386	0.00211	0.000201
10	P	0.602	0.369	0.129	0.021	0.0020
	N_E	0.92103	0.46051	0.13863	0.02107	0.00201
30	P	0.937	0.749	0.340	0.061	0.0060
	N_E	2.76310	1.38154	0.41589	0.06322	0.00603
50	P	.990	.900	.500	.100	.010
	N_E	4.60517	2.30258	0.69315	0.105361	0.01005
100	P	0.9999	0.990	0.750	0.190	0.0199
	N_E	9.21034	4.60516	1.38630	0.21072	0.02010

*$N_E = -\ell n\{1-p\}$

microzonation maps to see what is an impact of such a prediction and how and where it may change the previous results based on the Poissonian sequence only, or Poissonian and the predicted sequence but excluding the prediction just made.

EXAMPLE: Seismic Microzonation of a Metropolitan Area

To show how the above methodology could be used to present a microzonation map of a metropolitan area we choose the seismic region and the geometry of the Los Angeles basin in Southern California, but, we select arbitrarily the seismic activity, which, even though it has been chosen to be very similar to the actual one, cannot be taken to represent our interpretation of what we believe it should be. There are too many examples of different zonation maps in literature which have been either misrepresented or overextended relative to the scope of information which they actually contain or which have been erroneously interpreted by the users in an attempt to get quickly an estimate of future seismic risk at a site. Detailed microzonation of a large metropolitan area like Los Angeles will require very detailed studies of the activity and of the distribution of all active zones and will call for much more detailed knowledge of the local soil and geologic conditions than what we have adopted for this illustrative example. While we do believe that many overall features and trends of the "microzonation maps" presented in this report will not change much when such detailed information becomes available, we caution the reader that this report is only an illustration of the methodology

which we wish to present, and is an example of how the results (Pseudo Relative Velocity (PSV) spectral amplitudes with 5% damping) might vary geographically and with local geologic conditions. From the maps presented in this report one may obtain some idea about the difference of the nature of the PSV spectra at two different sites in the Los Angeles Basin, for example, but one cannot take our results to represent reliable estimates of the expected PSV amplitudes for a chosen probability of exceedance.

Figure 1 (modified from Jennings, 1975) suggests the distribution of major quaternary faults in Southern California. Figure 2 shows the same region of Southern California and the faults which we have adopted to represent the geometry of earthquake sources in our example. Table II presents the seismicity parameters which we have assigned to all sources in Figure 2 (identified by arabic numerals) and which have been used in the computer program NEQRISK (Lee and Trifunac, 1985) to calculate the results presented in this report.

There are two sets of inputs for the seismic risk program NEQRISK. The first set of the inputs consists of a description of the seismicity in the region. The second input is the description of the attenuation of seismic waves from the seismic source to the site. Either the magnitude or the M.M.I. models of Trifunac and Lee (1985b) for the attenuation of the amplitudes of the pseudo-relative velocity spectrum (PSV) at period T can be used. In the model with magnitude scaling,

$$\log_{10}\mathrm{PSV}(T) = M_{<} + \mathscr{A}tt(\Delta,M,T) + b_1(T)M_{<>} + b_2(T)h + b_3(T)v + b_5(T) + b_6(T)M_{<>}^{2} \quad , \qquad (4)$$

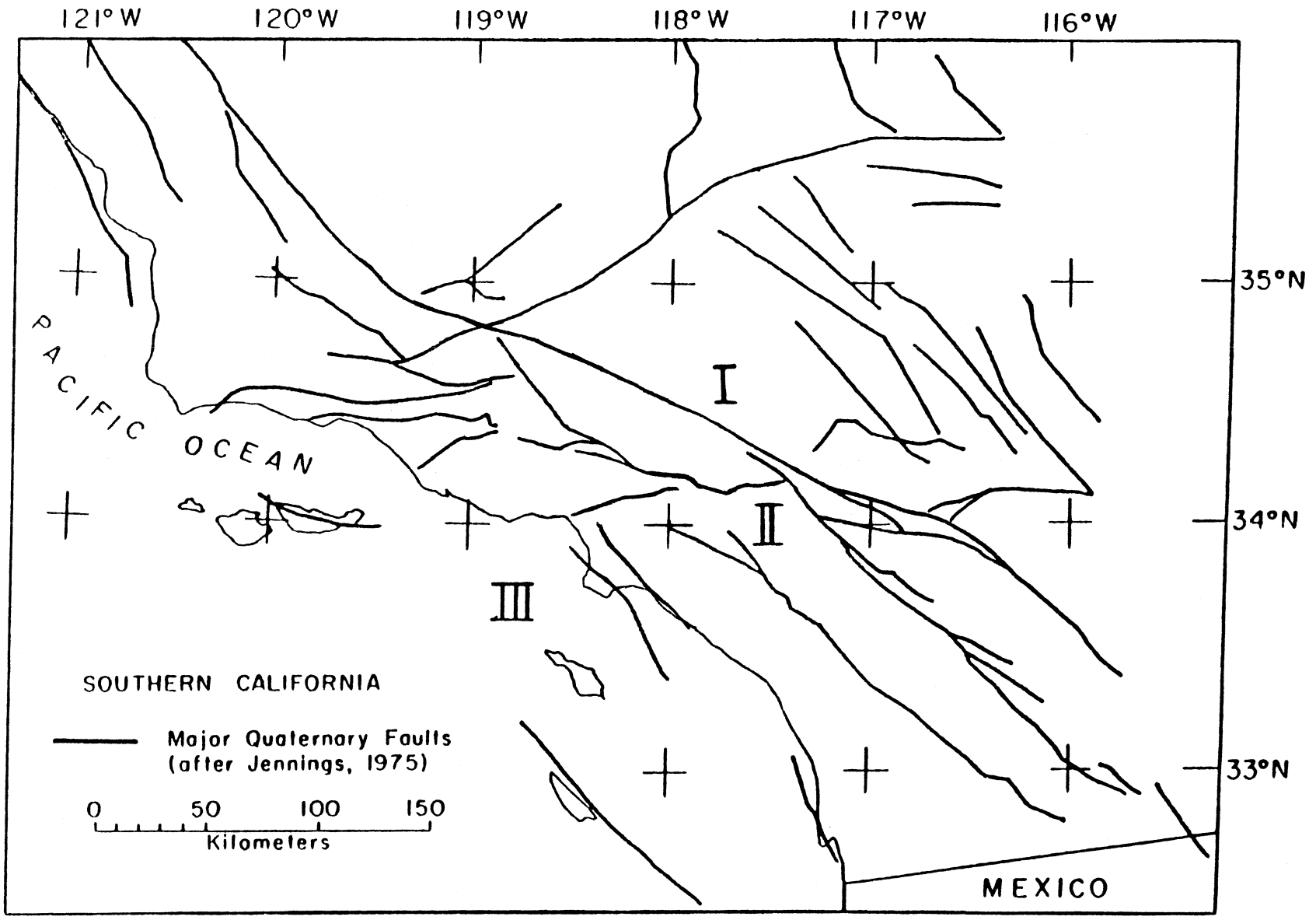
121°W
120°W
119°W
118°W
117°W
116°W
35°N
34°N
33°N
PACIFIC OCEAN
I
II
III
SOUTHERN CALIFORNIA
Major Quaternary Faults
(after Jennings, 1975)
0
50
100
150
Kilometers
MEXICO

Figure 1

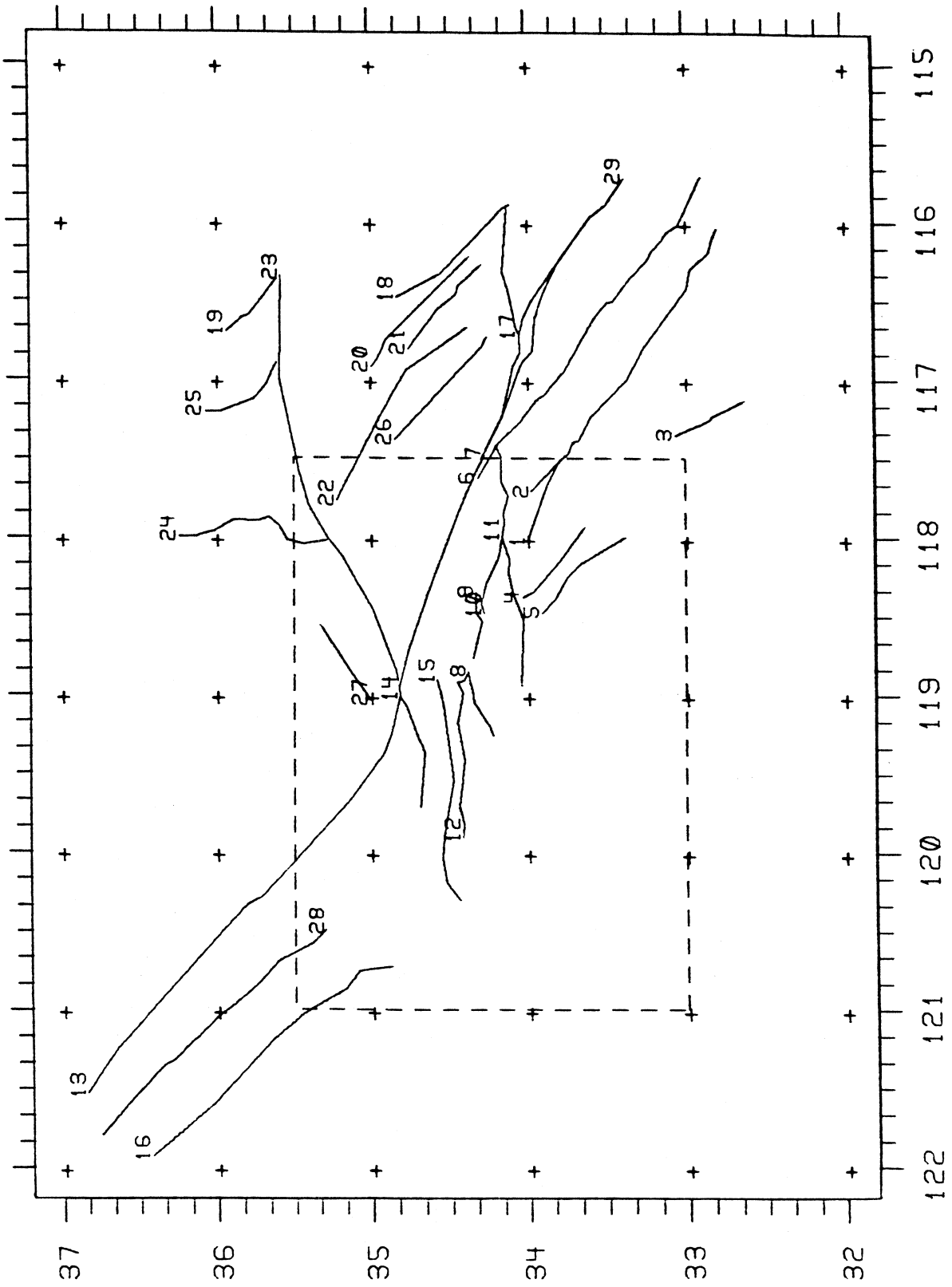
115
116
117
118
119
120
121
122
37
36
35
34
33
32
1
2
3
4
5
6
7
8
10
11
12
13
14
15
16
17
18
19
20
21
22
23
24
25
26
27
28
29

Figure 2

Table II

Coefficients a and a' in equation (15) and the moment rates per year, $\dot{M}_0$ for 29 faults in Figure 2

	FAULT NAME	a (50 YEARS)	a'	MOMENT/YR
1	ELSINORE FAULT - WHITTIER FAULT	3.77	2.69	1.2E+24.
2	CHINO FAULT	1.61	0.55	8.3E+21.
3	ROSE CANYON FAULT	3.28	2.22	3.9E+23.
4	NEWPORT - INGLEWOOD FAULT ZONE	2.92	1.86	1.7E+23.
5	PALOS VERDE FAULT	3.09	2.03	2.5E+23.
6	SAN JACINTO FAULT ZONE	5.05	4.00	2.3E+25.
7	SAN ANDREAS, CAJON TO IMPERIAL VALLEY ON NORTH BRANCH	4.55	3.48	1.5E+25.
8	OAKRIDGE FAULT	2.50	1.44	6.4E+22.
9	SANTA SUSANA FAULT	3.05	2.00	2.3E+23.
10	SIERRA MADRE - CUCAMONGA FAULT ZONE	4.29	3.23	4.0E+24.
11	MALIBU COAST - SANTA MONICA - RAYMOND FAULT SYSTEM	2.50	1.44	6.4E+22.
12	ARROYO PARIDA - SAN CAYETANO FAULT ZONE	2.09	1.03	2.5E+22.
13	SAN ANDREAS FAULT - CAJON PASS TO SAN LUIS OBISPO	5.29	4.23	8.3E+25.
14	BIG PINE FAULT	3.51	2.45	6.6E+23.
15	SANTA YNEZ FAULT - SLIP RATE VERY SPECULATIVE	3.80	2.73	1.3E+24.
16	SAN GREGORIO - HOSGRI FAULT ZONE	4.94	3.88	1.8E+25.
17	PINTO MOUTAIN FAULT	3.25	2.18	3.6E+23.
18	PISGAH - BULLION FAULT	3.67	2.61	9.5E+23.
19	SOUTH DEATH VALLEY FAULT	3.07	2.01	2.4E+23.
20	CALCIO - WEST CALCIO FAULT	3.34	2.29	4.5E+23.
21	CAMP ROCK - EMERSON FAULT ZONE	3.25	2.18	3.6E+23.
22	LOCKHART - LENWOOD FAULT	3.69	2.63	10.0E+23.
23	GARLOCK FAULT	4.68	3.62	9.7E+24.
24	SIERRA NEVADA FAULT	4.03	2.98	2.2E+24.
25	PANAMINT VALLEY FAULT	3.35	2.30	4.6E+23.
26	HELENDALE FAULT	3.32	2.27	4.3E+23.
27	WHITE WOLF FAULT	2.71	1.65	10.4E+22.
28	RINCONADA FAULT	4.14	3.08	2.8E+24.
29	SAN ANDREAS, CAJON TO IMPERIAL VALLEY ON SOUTH BRANCH	4.55	3.48	1.5E+25.
30	DIFFUSE REGION:			

MAG	EXPECTED # IN 50 YRS	MMI	EXPECTED # IN 50 YRS
3.5	480.00	4	400.00
4.0	140.00	5	125.00
4.5	42.00	6	25.00
5.0	12.50	7	2.50
5.5	3.65	8	0.00
6.0	1.10	9	0.00
6.5	0.32	10	0.00

where T is the period, M is the magnitude of the earthquake $\mathcal{A}tt(\Delta,M,T)$ the frequency dependent attenuation function developed by Trifunac and Lee (1985c), $\Delta = \Delta(S,H,R)$ a representative distance from the earthquake source of size S at depth H and at epicentral distance R, h the depth of alluvium, v a component variable set to 0 for horizontal and to 1 for vertical motions and

$$M_{<} = \min(M,M_{max}) \quad ,$$

$$M_{<>} = \max(M_{min},M_{<}) \quad ,$$

where $$M_{min} = -b_1(T)/(2b_6(T)) \quad ,$$

and $$M_{max} = -(1+b_1(T))/(2b_6(T)) \quad . \qquad (5)$$

Using the above two sets of inputs, the seismic risk program calculates the PSV amplitudes for a selected set of probabilities of exceedance and a selected set of periods in the range between 0.04 sec - 7.50 sec at each site (grid point).

In the second model, the distribution of the Modified Mercalli Intensity (M.M.I.) levels for a set of probabilities of exceedance can first be calculated by the seismic risk program at each grid point, and the PSV spectral amplitudes can then be calculated from

$$\log_{10}PSV(T) = C_1(T)\hat{I}_{MM} + C_2(T)h + C_3(T)v + C_4(T) \qquad (6)$$

where $\hat{I}_{MM}$ represents the M.M.I. levels.

The seismicity of each fault in the region may be described by the occurrence rate of earthquakes on the fault. In selecting this occurrence rate we were guided by the work of Anderson and Trifunac (1978b). The seismicity can be estimated from the geological information on the slip of each fault, through the determination of the seismic moment rate, $\dot{M}_o$, which satisfies the following equation,

$$\dot{M}_o = \int_{-\infty}^{\infty} 10^{\gamma} N(\gamma) d\gamma \quad , \tag{7}$$

where $N(\gamma)d\gamma$ is the long term average rate of occurrence of seismic events with moments between $\gamma - d\gamma/2$ and $\gamma + d\gamma/2$, where $\gamma = \log_{10} M_o$. $N(\gamma)$ is usually described by

$$N(\gamma) = 10^{c-d\gamma} \quad . \tag{8}$$

Assuming that $N(\gamma)$ is zero outside some range $\gamma_{min} \leq \gamma \leq \gamma_{max}$, substituting (8) into (7) and integrating gives

$$\dot{M}_o = \frac{10^c}{(1-d)\ell n 10} \left(10^{(1-d)\gamma_{max}} - 10^{(1-d)\gamma_{min}}\right) \quad . \tag{9}$$

For earthquakes in Southern California, Thatcher and Hanks (1973) give, for M representing the local magnitude,

$$\gamma = 16.0 + 3/2\ M \quad . \tag{10}$$

The frequency of the occurrance of earthquakes can be described also directly in terms of magnitude by

$$N(M) = \begin{cases} 10^{a-bM} , & M_{min} \leq M \leq M_{max} \\ 0 & \text{otherwise} \end{cases} , \qquad (11)$$

with $M_{min} \leq M \leq M_{max}$, the range of allowable magnitudes for the fault,

with $$b = 3/2\ d$$

and $$a = c - 16d + \log_{10}(3/2) \quad . \qquad (12)$$

Here $N(M)dM$ gives the number of events with magnitude between M_1 and M_2. In the present analysis we select $b = 0.86$. Then from given $\dot{M}_o$, a can be determined through (9) and (12). In terms of epicentral intensity, I_o, the empirical relation

$$I_o = 1.5(M-1)$$

or $$M = 1 + 2I_o/3 \qquad (13)$$

gives

$$N(I_o) = \begin{cases} 10^{a'-b'I_o} , & I_{min} \leq I_o \leq I_{max} \\ 0 & \text{otherwise} \end{cases} .$$

With $I_{min} \leq I_o \leq I_{max}$ representing the range of allowable epicentral intensities for the fault, and with

$$a' = a-b$$

and $$b' = 2b/3 \quad . \qquad (14)$$

To include the uncertainties in the estimation of seismicity through the use of the parameters a, b and M_{max} in the magnitude model or a', b' and I_{max} in the M.M.I. model (Lee and Trifunac, 1985), a probability distribution is assumed for

$$\log_{10}N(M) = a-bM \quad \text{for} \quad M_{min} \leq M \leq M_{max}$$

and

$$\log_{10}N(I_{MM}) = a'-b'I_{MM} \quad \text{for} \quad I_{min} \leq I \leq I_{max} \quad . \quad (15)$$

In the examples of seismic risk analysis in this report, both $\log_{10}N(M)$ and $\log_{10}N(I_{MM})$ are assumed to follow a triangular distribution (Example b, Section 4.3 of Lee and Trifunac, 1985), which is characterized by additional parameters δa and δb for the magnitude models and by $\delta a'$ and $\delta b'$ for the M.M.I. models. Similarly, we choose M_{max} and I_{max} also to be described by triangular distribution in the range $M_{max} \pm \delta M_{max}$, respectively.

Table II presents all required information for the seismicity of the 29 faults considered in this study. Column 1 lists the fault numbers, from 1 to 29 (see also Figure 2). Column 2 gives the "name" of the fault. Columns 3 and 4 present the coefficients a and a' for calculating N(M) during 50 years. Column 5 gives the adopted moment rate $\dot{M}_o$ per year for each fault. All other coefficients used in the description of seismicity are the same for all the faults, as follows:

For the magnitude scaling model:

$$b = 0.86$$

$$\delta a = 0.42$$

$$\delta b = -.035$$

$$M_{max} = \begin{cases} 7.5 \text{ for faults } \#7,13,29 \\ 7.0 \text{ all other faults} \end{cases}$$

$$\delta M_{max} = 0.5 \quad .$$

For the MMI scaling model:

$$b' = 0.5733$$

$$\delta a' = 0.42$$

$$\delta b' = -0.23$$

$$I_{max} = \begin{cases} 10.5 \text{ for faults } \#7,13,29 \\ 9.0 \quad \text{all other faults} \end{cases}$$

$$\delta I_{max} = 1 \quad .$$

Figure 2 is a plot of the assumed fault sources in the Southern California region that are used in the example for seismic risk analysis in this report. There are a total of 29 line faults and one region of "diffused seismicity." Each of the 29 line faults is labeled by the corresponding fault number either at the "beginning" or at the "end" of the fault. Faults No. 7 and No. 29 have the same beginning and end, as can be seen from the figure. They correspond respectively to the north and south branches of the "San Andreas" fault from "Cajon" to "Imperial Valley." The diffused region is enclosed by the dashed lines. It ranges from 33°N to 35° 30'N and from 117° 30'W to 121°W. Within this region the earthquakes can occur at any point with uniform probability and with frequency according to the data in Table II, and for Y = 50 years.

The scaling equations which relate PSV amplitudes at a given period of motion further require one to specify the "depth" of sediments beneath the station (Trifunac and Lee, 1985b). Using the maps of Yerkes et al. (1965) as a general guide we have developed our idealized model of the depth of sediments. It is presented, in tabular form, in Table III for a rectangular mesh with spacing of 5'. It is seen from Table III that the depth of sediments in our model ranges from 0 to 31,000 feet (at 118° 10' W and 33° 55' N). From Table III the depth at other intermediate coordinates has been interpreted to provide the data for computations at the grid spacing of one minute.

All spectral amplitudes presented in the maps in this report (Appendices A and B) represent Pseudo Relative Velocity Spectra (PSV) with 5% damping for horizontal ground shaking. The results can be corrected to vertical spectra by multiplying these amplitudes by the scaling factor shown in Figure 3, plotted versus period T.

The most recent presentation of the spectral scaling equations (Trifunac and Lee, 1985b) utilizes the frequency dependent attenuation of strong ground motion (Trifunac and Lee, 1985a) and for scaling in terms of the earthquake magnitude M uses the focal depth H. Since most earthquakes in Southern California, which have been recorded by strong motion accelerographs, have H in the range from 0 to about 25 km (Lee and Trifunac, 1987) for simplicity in this report we have assumed that all activity occurs at H = 5 km. While this assumption should lead to reasonable overall distribution of spectral amplitudes, it must be emphasized that in localized regions, close to active faults for which H is different from the assumed 5 km, the shape of the

TABLE III

Depth of sediments h, in thousands of feet at grid points with 5' spacing for greater Los Angeles metropolitan area (after Yerkes et al., 1965).

	30'	25'	20'	15'	10'	5'	118°00'	55'	50'	45'	40'
20'											
15'		0	0	0	0	0	0	0	0	0	0
10'	6	10	8.5	0	0	1	0	0	0	0	0
5'	0	0	7	9	4	7	10.5	8	2	0	2
34°00'	6	11	20	26	17	18	5	7	5.5	2.5	2
55'	5.5	7.5	11	21	31	25	17	18.5	16.5	5	5
50'	1	5	5.5	11	16	28	23	12	11	10	0
45'		2.5	0	8	10	15.5	18	15.5	8.5	8	5
40'			7.5	4.5	15	13.5	9.5	15	9.5	6	7
35'					9	8	8	6	13.5	8	9
30'										10.5	12

h in thousands of feet

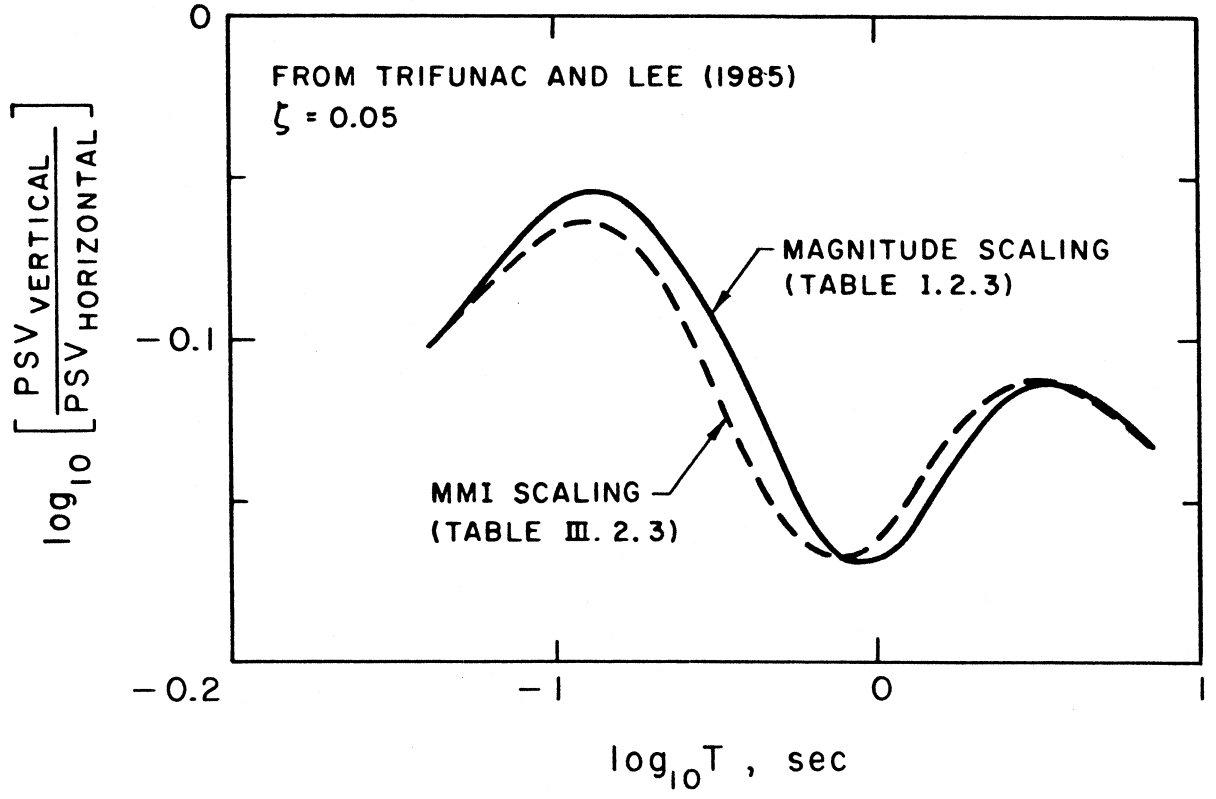
0
−0.1
−0.2
FROM TRIFUNAC AND LEE (1985)
ζ = 0.05
MAGNITUDE SCALING
(TABLE I.2.3)
MMI SCALING
(TABLE III. 2.3)
log10 [PSV VERTICAL / PSV HORIZONTAL]
−1
0
1
log10T , sec

Figure 3

Uniform Risk Spectra will be different from what is presented in this report. This effect is important for high frequency spectral amplitudes only.

Since 1977, when the concept of Uniform Risk Spectra had been proposed (Anderson and Trifunac, 1977), we have been developing and improving, in parallel, two independent scaling procedures, one using earthquake magnitude and the other based on the local site intensity (e.g. Trifunac, 1979). In all these analyses we continue to find certain advantages in using the local site intensity. These advantages result from greater simplicity and a smaller number of intermediate computational steps which are involved in scaling with MMI. Though the resulting URS computed with M and with MMI scaling are somewhat different in shape, their overall amplitudes agree very well (Figures 4 and 5).

The URS in Appendices A and B have been calculated from a consistent sequence of events at all adopted sources (Table II and Figure 2) i.e. we have assumed that an earthquake of magnitude M at source i corresponds to an earthquake of intensity I_o at the same source and we have computed I_o from equation (13). After this definition of the sources, the computation of URS in Appendices A and B follows completely independent paths and uses different empirical scaling relationships (4) and (6) developed for magnitude and intensity scaling relationships independently (Trifunac and Lee, 1985b). In Figures 4 and 5 we compare the two resulting spectra, one from Appendix A and one from Appendix B, for two sites, one on deep sediments (h = 25,000 feet) at 33° 55' N, 118° 5' W (Figure 4). In both figures the dashed lines represent the uniform risk PSV spectral amplitudes computed via MMI scaling relations.

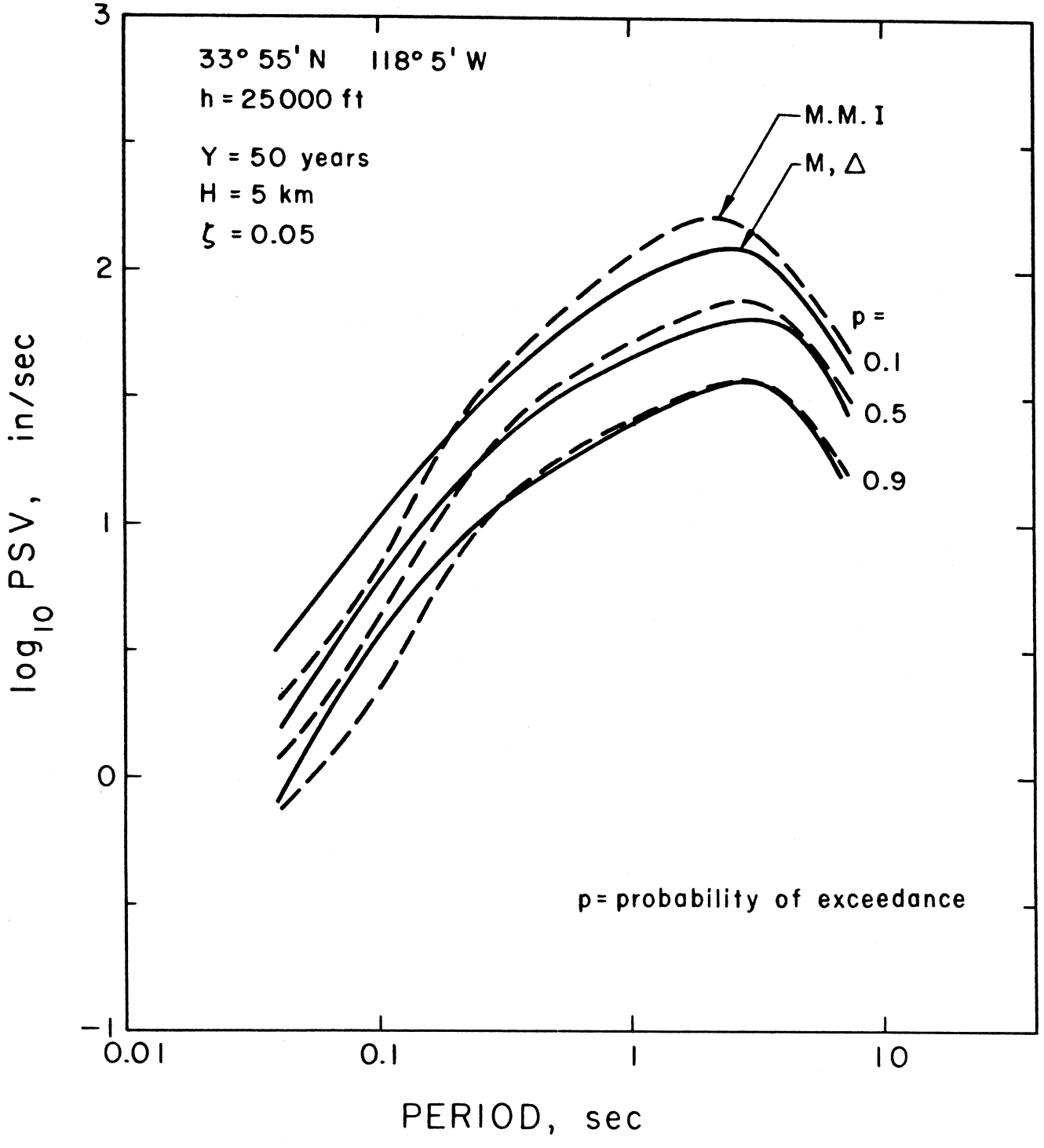
33° 55' N 118° 5' W
h = 25000 ft
Y = 50 years
H = 5 km
ζ = 0.05
M.M. I
M, Δ
p =
0.1
0.5
0.9
p = probability of exceedance
log10 PSV, in/sec
PERIOD, sec
3
2
1
0
−1
0.01
0.1
1
10

Figure 4

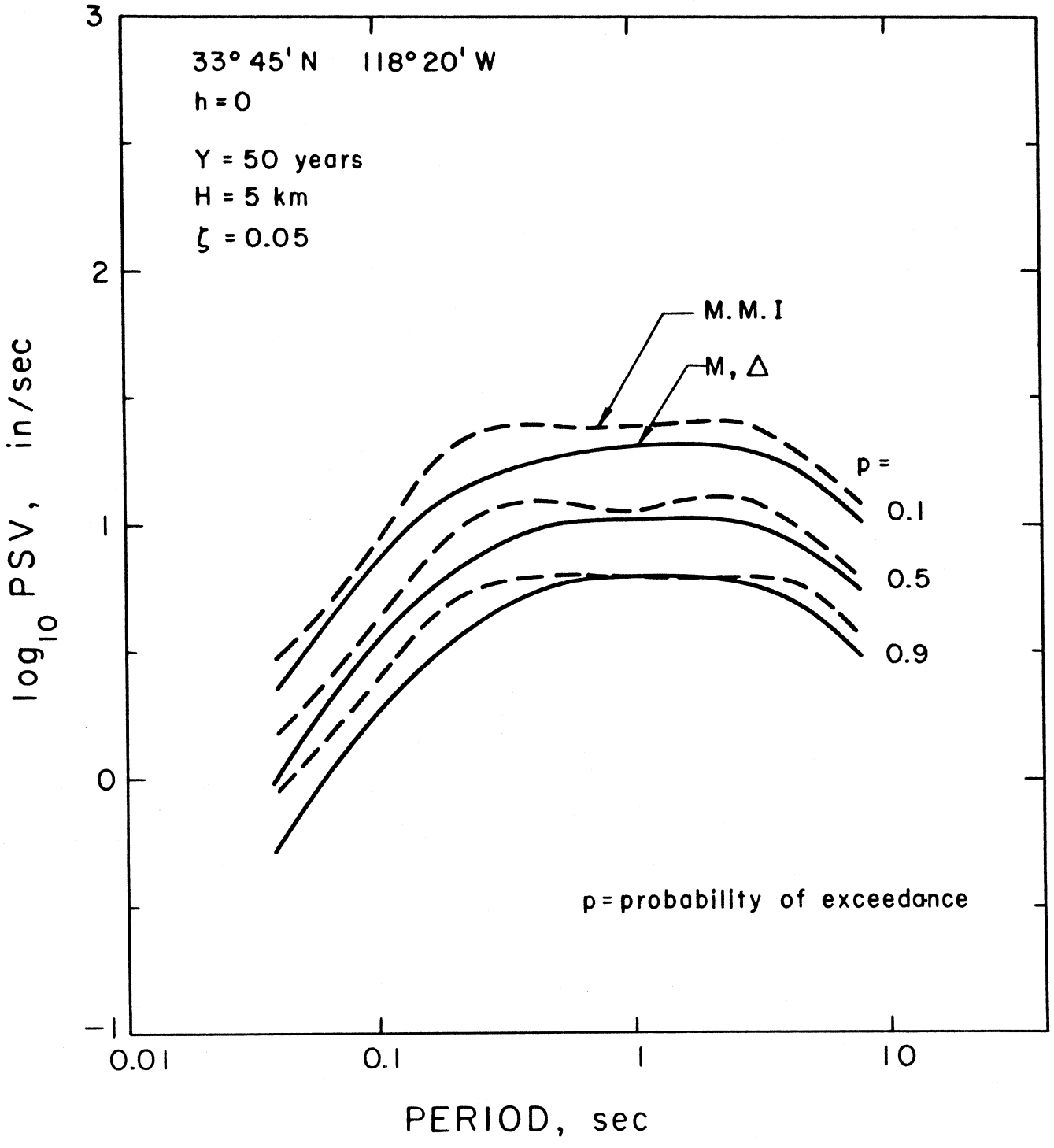
33° 45' N 118° 20' W
h = 0
Y = 50 years
H = 5 km
ζ = 0.05
M.M.I
M, Δ
p =
0.1
0.5
0.9
p = probability of exceedance
log10 PSV, in/sec
PERIOD, sec
3
2
1
0
−1
0.01
0.1
1
10

Figure 5

The three solid lines represent the same spectra for the probabilities of exceedance p = 0.90, 0.50 and 0.1, computed from magnitude scaling, and for the same seismicity model. It is seen that the two methods of calculation agree remarkably well. For short periods, shapes of the two estimates are slightly different because the magnitude scaling model assumes the overall average depth of all sources contributing to this URS to be H = 5 km, while the scaling in terms of MMI averages over all source depths, by not considering the source depth explicitly. We did not make an attempt to compute the most representative H for the magnitude scaling model, to achieve better agreement of the two spectra at high frequencies, because this is not the aim of this example and because the reader can judge about the quality of the MMI scaling model and its narrow distribution of amplitudes from the examples in Figures 4 and 5 as presented here, and without this refinement.

The Figures representing maps of URS for selected probabilities of exceedance and for a chosen oscillator period T are presented in Appendices A and B. Table IV summarizes the figure numbers in Appendices A and B with respect to T and P.

There are many different ways in which the results from Appendices A and B can be viewed. One of the most direct ways has already been illustrated in Figures 4 and 5 which have been plotted by interpolating from amplitudes at eleven natural periods at (33° 55' N, 118° 5' W) and (33° 45' N, 118° 20' W) from Figures B2.1 to B2.11 and B4.1 through B4.11 and from Figures A2.1 through A2.11, A3.1 through A3.11 and A4.1 through A4.11. By themselves the figures in Appendixes A and B show the geographical distribution of horizontal PSV amplitudes, for 5% damping,

TABLE IV

Figure numbers $A_{i,j}$ presenting $\log_{10}$ (PSV) in in/sec for T = 0.04, 0.065, 0.11, 0.19, 0.34, 0.5, 0.9, 1.6, 2.8, 4.4 and 7.5 sec, for damping ζ = 0.05 in terms of magnitude scaling, for H = 5 km and Y = 50 years, are presented in Appendix A as follows:

p= \ T=	0.04	0.065	0.11	0.19	0.34	0.50	0.90	1.6	2.8	4.4	7.5
.99	A1.1	A1.2	A1.3	A1.4	A1.5	A1.6	A1.7	A1.8	A1.9	A1.10	A1.11
.90	A2.1	A2.2	A2.3	A2.4	A2.5	A2.6	A2.7	A2.8	A2.9	A2.10	A2.11
.50	A3.1	A3.2	A3.3	A3.4	A3.5	A3.6	A3.7	A3.8	A3.9	A3.10	A3.11
.10	A4.1	A4.2	A4.3	A4.4	A4.5	A4.6	A4.7	A4.8	A4.9	A4.10	A4.11
.01	A5.1	A5.2	A5.3	A5.4	A5.5	A5.6	A5.7	A5.8	A5.9	A5.10	A5.11

Figure numbers $B_{i,j}$ presenting $\log_{10}$ (PSV) in in/sec for T = 0.04, 0.065,...7.5 sec, for damping ζ = 0.05, in terms of Modified Mercalli scaling, for Y = 50 years and for probabilities of exceedance P = 0.99, 0.9, 0.5, 0.1 and 0.01 are presented in Appendix C as follows:

P= \ T=	0.04	0.065	0.11	0.19	0.34	0.50	0.90	1.6	2.8	4.4	7.5
.99	B1.1	B1.2	B1.3	B1.4	B1.5	B1.6	B1.7	B1.8	B1.9	B1.10	B1.11
.90	B2.1	B2.2	B2.3	B2.4	B2.5	B2.6	B2.7	B2.8	B2.9	B2.10	B2.11
.50	B3.1	B3.2	B3.3	B3.4	B3.5	B3.6	B3.7	B3.8	B3.9	B3.10	B3.11
.10	B4.1	B4.2	B4.3	B4.4	B4.5	B4.6	B4.7	B4.8	B4.9	B4.10	B4.11
.01	B5.1	B5.2	B5.3	B5.4	B5.5	B5.6	B5.7	B5.8	B5.9	B5.10	B5.11

for a given probability of exceedance during 50 years of exposure and for a given oscillator period T. It is seen that by and large the high frequency spectral amplitudes depend on the proximity of the site to "San Andreas" fault (Figure 2). At intermediate and long periods the deep sedimentary basin in the central region of the metropolitan area (Table III) amplifies the longer seismic waves for all probabilities of exceedance.

CONCLUSIONS

The main conclusions of this work can be summarized as follows:

1. The method involving uniform risk spectra (Anderson and Trifunac, 1977; Lee and Trifunac, 1985) can be used to construct maps of spectral amplitudes with constant probability of being exceeded, at least once in Y years. The method offers excellent means to account for all sources of seismicity and to combine all sources of uncertainty in a uniform and balanced way. It is most efficient in showing the relative significance of different sources,given the different epicentral distances, of the levels of source activity, of the largest magnitude (intensity) expected at each source, and of the local geologic conditions beneath the site.

2. For the seismicity model selected in the examples presented here, the results are dominated by the expected earthquake occurrence on the "San Andreas" fault. Its contribution to the risk overshadows all other faults in the metropolitan area.

3. In the central region of the metropolitan area, the assumed depth of sediments (Table III, up to 31,000 feet) significantly amplifies long period ground motion.

REFERENCES

Akademia Nauk SSSR (1980). Seismicheskoe Reionirovanie Teritorii SSSR, Izdatelstro "Nauka" Moskva 1980.

Allam, A. (1969). An Investigation Into the Nature of Microtremors, Ph.D. Thesis, Tokyo Univ.

Anderson, J. G. and M. D. Trifunac (1977). Uniform Risk Functionals for Characterization of Strong Earthquake Ground Motion, Dept. Civil Eng. Report No. 77-02, Univ. Southern Calif., Los Angeles, Calif.

Anderson, J. G. and M. D. Trifunac (1978a). Uniform Risk Functionals for Characterization of Strong Earthquake Ground Motion, Bull. Seism. Soc. Amer., 68, 205-218.

Anderson, J. G. and M. D. Trifunac (1978b). Application of Seismic Risk Procedures to Problems in Microzonation, Proc. Second Int. Conf. on Microzonation, Vol. I, 559-569, San Francisco, Calif.

Cornell, C. A. (1968). Engineering Seismic Risk Analysis, Bull. Seism. Soc. Amer., 58, 1583-1606.

Der Kiureghian, A. and A. H.-S. Ang (1975). A Line Source Model for Seismic Risk Analysis, Struct. Res. Series No. 419, Univ. Illinois, Urbana, Illinois.

Goto, H. and H. Kameda (1969). Statistical Reference of the Future Earthquake Ground Motion, 4th World Conf. Earthquake Engineering, Santiago, Chile, A-1, 39-54.

Gaus, M. P. and M. A. Sherif (1972). Zonation and Microzonation, in Proc. Microzonation Conference, Seattle, Washington, I, 3-7.

Herrera, I. and E. Rosenblueth (1965). Response Spectra in Stratified Soil, Proc. Third World Conf. Earthquake Eng., 1, 44-60.

International Association for Earthquake Engineering (1984). Earthquake Resistant Regulations, a World List - 1984.

Jennings, C. W. (1975). Fault Map of California, California Division of Mines and Geology, Sacramento, California.

Kanai, F. (1983). Engineering Seismology, Unif. Tokyo Press, Tokyo, Japan.

Karnik, V. (1972). Microzoning Programme Within the UNDP-UNESCO Survey of the Seismicity of the Balkan Region, Proc. Microzonation Conference, Seattle, Washington, I, 213-215.

Kiremidjian, A. S. (1977). Probabilistic Hazard Mapping in Development of Site Dependent Seismic Load Parameters, Ph. D. Thesis, Stanford Univ.

Kuroiwa, J. E., Deza, H. Jáen and J. Kogan (1973). Microzonation Methods and Techniques Used in Peru, Proc. Second International Conf. on Microzonation, Vol. I, 341-352, San Francisco, Calif.

Lee, V. W. and M. D. Trifunac (1985). Uniform Risk Spectra of Strong Earthquake Ground Motion, Dept. Civil Eng. Report No. 85-05, Univ. Southern Calif., Los Angeles, Calif.

Lee, V. W. and M. D. Trifunac (1987). Strong Earthquake Ground Motion Data in EQINFOS: Part 1, Dept. Civil Eng. Report No. 87-01, Univ. Southern Calif., Los Angeles, Calif.

Liao, Z. (1985). Seismic Microzonation in China, Institute of Engineering Mechanics, State Seismological Bureau, Research Report 1-37.

Lommnitz, C. (1974). Global Tectonics and Earthquake Risk, Elsevier Scientific Publishing Company, Amsterdam.

McGuire (1974). Seismic Structural Response Risk Analysis, Incorporating Peak Response Regressions on Earthquake Magnitude and Distance, R 74-51, Dept. Civil Eng. Mass. Inst. of Tech., Cambridge, Mass.

Medvedev, S. V. (1962). Inzenernaja Seizmologija, Akademia Nauk SSSR, Institut Fiziki Zemli Imeni O. Smidta, Moskva.

Osaki, Y. (1972). Japanese Microzonation Methods, Proc. Microzonation Conf., Seattle, Washington, I. 161-182.

Richter, C. F. (1959). Seismic Regionalization, Bull. Seism. Soc. Amer., 49, 123-162.

Roberts, E. B. and F. P. Ulrich (1951). Seismological Activities of the U.S. Coast and Geodetic Survey in 1949, Bull. Seism. Soc. Amer., 41, 205-220.

Steinbrugge, K. (1978). Earthquake Insurance and Microzonation, Proc. Microzonation Conference, San Francisco, California, I. 201-213.

Tenhaus, P. C. et al. (1980). Probabilistic Estimates of Maximum Seismic Horizontal Ground Motion on Rock in Coastal California and the Adjacent Outer Continental Shelf, U.S.G.S. Open File Report 80-924.

Thatcher, W. and T. C. Hanks (1973). Source Parameters of Southern California Earthquakes, J. Geophys. Res., 78, 8547-8576.

Trifunac, M. D. (1971). Surface Motion on a Semi-Cylindrical Alluvial Valley for Incident SH Waves, Bull. Seism. Soc. Amer., 61, 1739-1753.

Trifunac, M. D. (1973). Scattering of Plane SH Waves by a Semi-Cylindrical Canyon, Int. J. Earthquake Eng. and Struct. Dyn., 1, 267-281.

Trifunac, M. D. and A. G. Brady (1975). On the Correlation of Seismic Intensity Scales With the Peaks of Recorded Strong Ground Motion, Bull. Seism. Soc. Amer., 65, 139-162.

Trifunac, M. D. (1979). Preliminary Empirical Model for Scaling Fourier Amplitude Spectra of Strong Motion Acceleration in Terms of Modified Mercalli Intensity and Geologic Site Conditions, Int. J. Earthquake Eng. and Structural Dynamics, 7, 63-74.

Trifunac, M. D. and V. W. Lee (1985a). Preliminary Empirical Model for Scaling Fourier Amplitude Spactra of Strong Ground Acceleration in Terms of Earthquake Magnitude, Source to Station Distance, Site Intensity and Recording Site Conditions: Second Paper, Dept. Civil Eng. Report No. 85-03, Univ. Southern Calif., Los Angeles, Calif.

Trifunac, M. D. and V. W. Lee (1985b). Preliminary Empirical Model for Scaling Pseudo Relative Velocity Spectra of Strong Earthquake Acceleration in Terms of Magnitude, Distance, Site Intensity and Recording Site Conditions, Dept. of Civil Eng. Report No. 85-04, Univ. Southern Calif., Los Angeles, Calif.

Trifunac, M. D. and V. W. Lee (1985c). Frequency Dependent Attenuation of Strong Earthquake Ground Motion, Dept. of Civil Eng. Report No. 85-02, Univ. of Southern Calif., Los Angeles, Calif.

Udwadia, F. E. and M. D. Trifunac (1973). Comparison of Earthquake and Microtremor Ground Motions in El Centro, California, Bull. Seism. Soc. Amer., 63, No. 4, 1227-1253.

Wong, H. L. and M. D. Trifunac (1974). Surface Motion of a Semi-Elliptical Alluvial Valley for Incident Plane SH-Waves, Bull. Seism. Soc. Amer., 64, 1389-1408.

Yerkes, R. F., T. H. McCulloh, J. E. Schoellhamer and J. G. Vedder (1965). Geology of the Los Angeles Basin, California - an Introduction, U.S. Geological Survey Professional Paper 420-A.

APPENDIX A

In this appendix figures A1.1 through A5.11 present $\log_{10}$(PSV), in in/sec, for T = 0.04, 0.065, 0.11, 0.19, 0.34, 0.50, 0.90, 1.6, 2.8, 4.4 and 7.5 seconds periods, for damping ζ = 0.05, in terms of magnitude scaling (Trifunac and Lee, 1985b), for average focal depth of earthquakes H = 5 km, and for the exposure time of Y = 50 years as follows:

P= \ T=	0.04	0.065	0.11	0.19	0.34	0.50	0.90	1.6	2.8	4.4	7.5
.99	A1.1	A1.2	A1.3	A1.4	A1.5	A1.6	A1.7	A1.8	A1.9	A1.10	A1.11
.90	A2.1	A2.2	A2.3	A2.4	A2.5	A2.6	A2.7	A2.8	A2.9	A2.10	A2.11
.50	A3.1	A3.2	A3.3	A3.4	A3.5	A3.6	A3.7	A3.8	A3.9	A3.10	A3.11
.10	A4.1	A4.2	A4.3	A4.4	A4.5	A4.6	A4.7	A4.8	A4.9	A4.10	A4.11
.01	A5.1	A5.2	A5.3	A5.4	A5.5	A5.6	A5.7	A5.8	A5.9	A5.10	A5.11

P represents the probability of at least one exceedance in Y = 50 years. The logarithms of spectral amplitudes have been rounded to discrete amplitudes with resolution of 0.1, and are presented by printer-plots on the rectangular mesh with spacing of one minute. It is assumed that all sources result in Poissonian sequence of events in time.

PSEUDO RELATIVE VELOCITY, PSV (IN/SEC) AT T = .040 SEC
PROBABILITY OF EXCEEDANCE = .99 FOR 50 YEARS

CONTOUR LEVELS OF LOG(PSV):

1 -.8 : -.7 2 -.6 " -.5 3 -.4 : -.3 4 -.2 ; -.1 5 .0

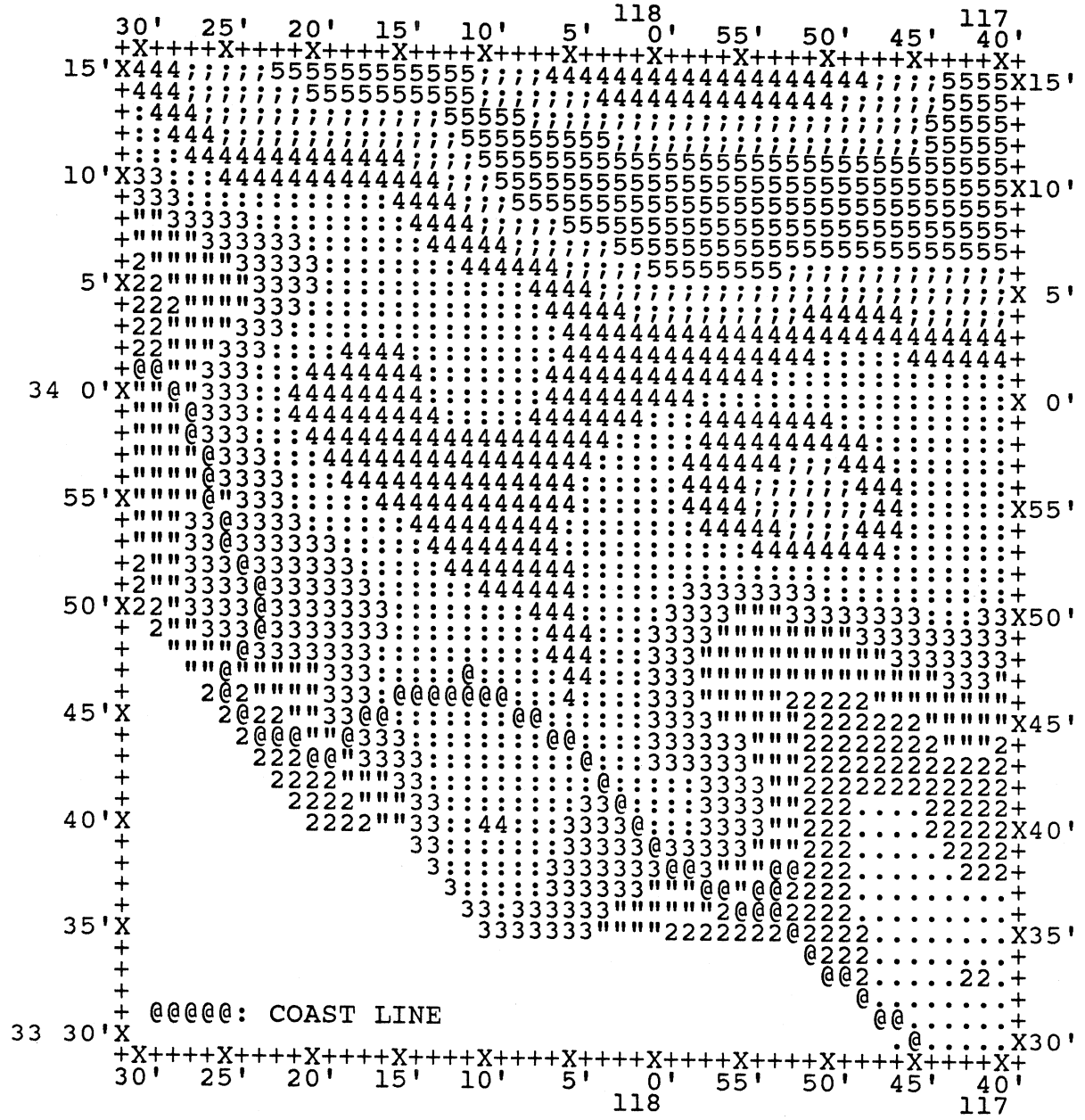

Figure A1.1

PSEUDO RELATIVE VELOCITY, PSV (IN/SEC) AT T = .065 SEC
PROBABILITY OF EXCEEDANCE = .99 FOR 50 YEARS

CONTOUR LEVELS OF LOG(PSV):

3 : 4 ; 5 | 6 -
-.4 -.3 -.2 -.1 .0 .1 .2 .3

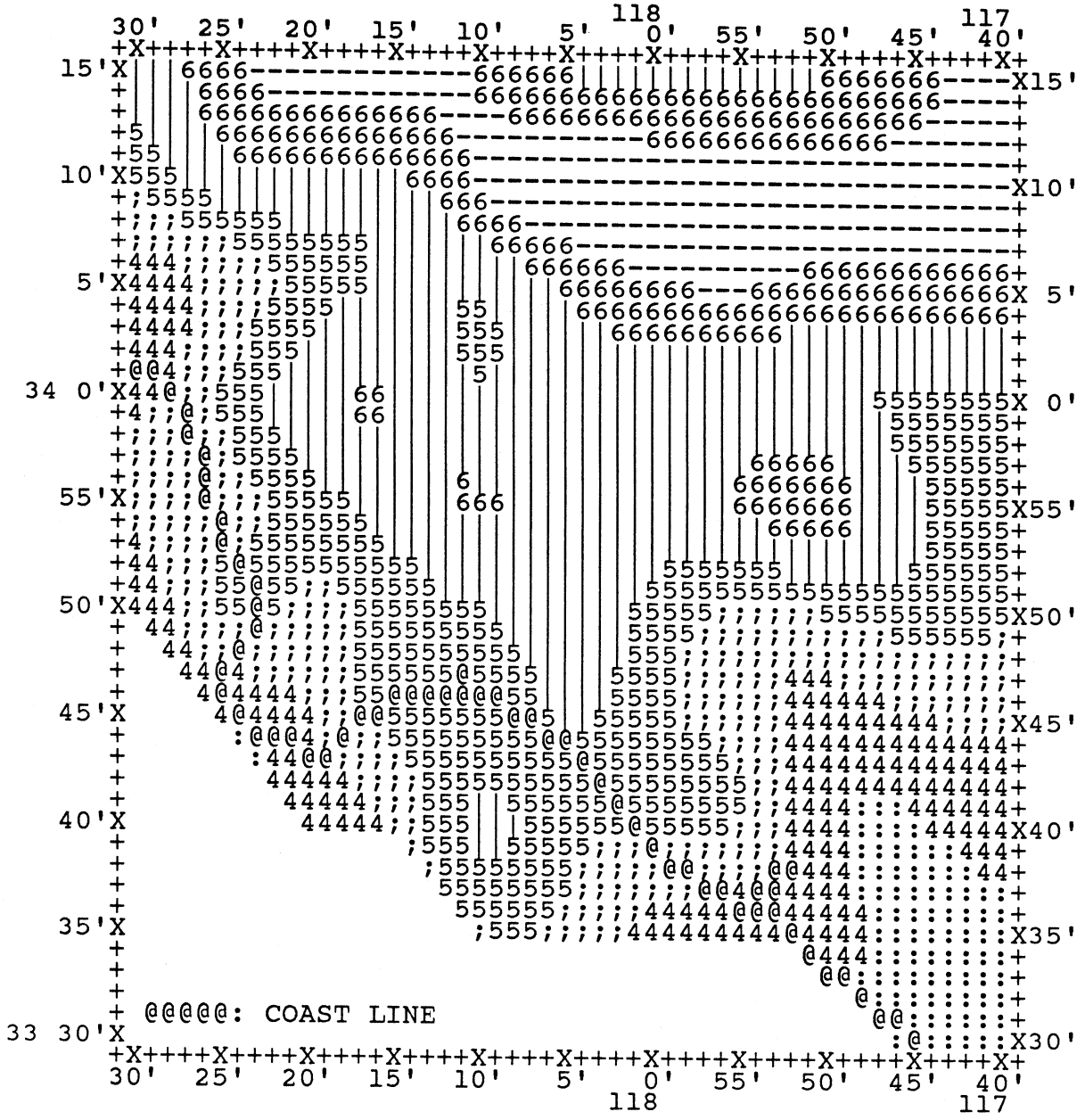

Figure A1.2

PSEUDO RELATIVE VELOCITY, PSV (IN/SEC) AT T = .110 SEC
PROBABILITY OF EXCEEDANCE = .99 FOR 50 YEARS

CONTOUR LEVELS OF LOG(PSV):

; -.1 5 .0 | .1 6 - .2 7 .3 / .4 8 .5 .6

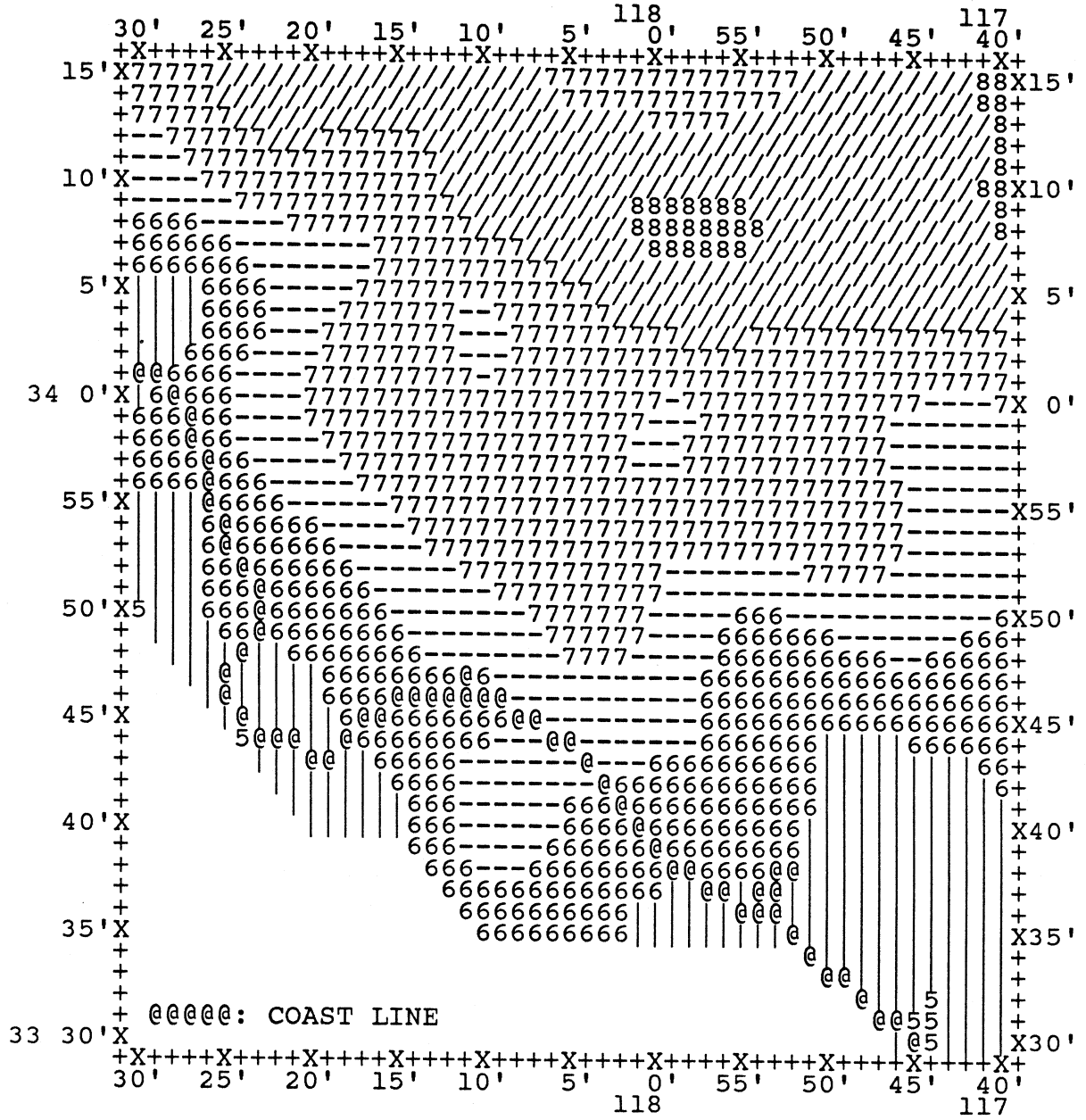

Figure A1.3

PSEUDO RELATIVE VELOCITY, PSV (IN/SEC) AT T = .190 SEC
PROBABILITY OF EXCEEDANCE = .99 FOR 50 YEARS

CONTOUR LEVELS OF LOG(PSV):

	6	-	7	/	8	~	9
.1	.2	.3	.4	.5	.6	.7	.8

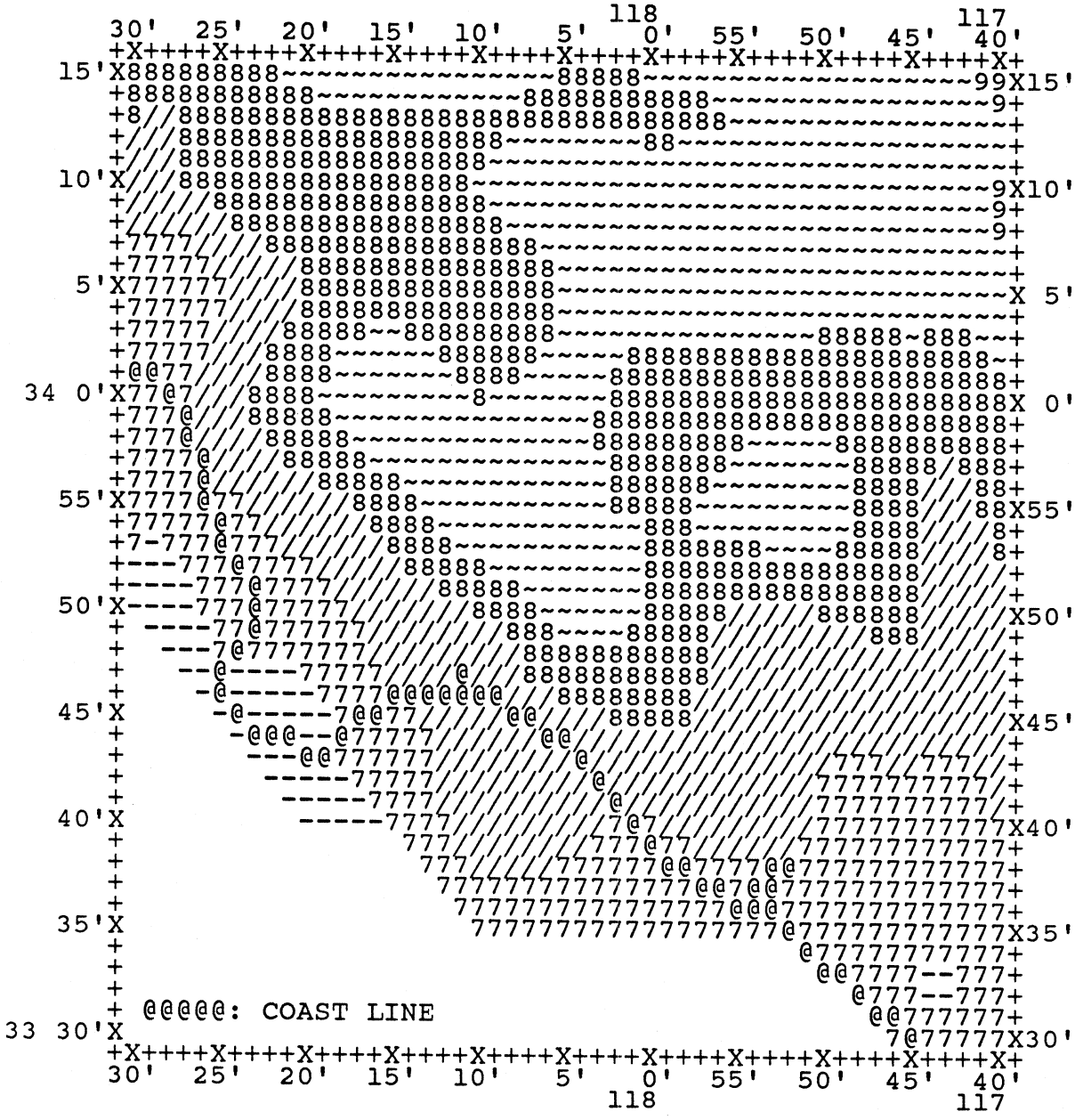

Figure A1.4

PSEUDO RELATIVE VELOCITY, PSV (IN/SEC) AT T = .340 SEC
PROBABILITY OF EXCEEDANCE = .99 FOR 50 YEARS

CONTOUR LEVELS OF LOG(PSV):

7	/	8	~	9	!	a
.4	.5	.6	.7	.8	.9	1.0

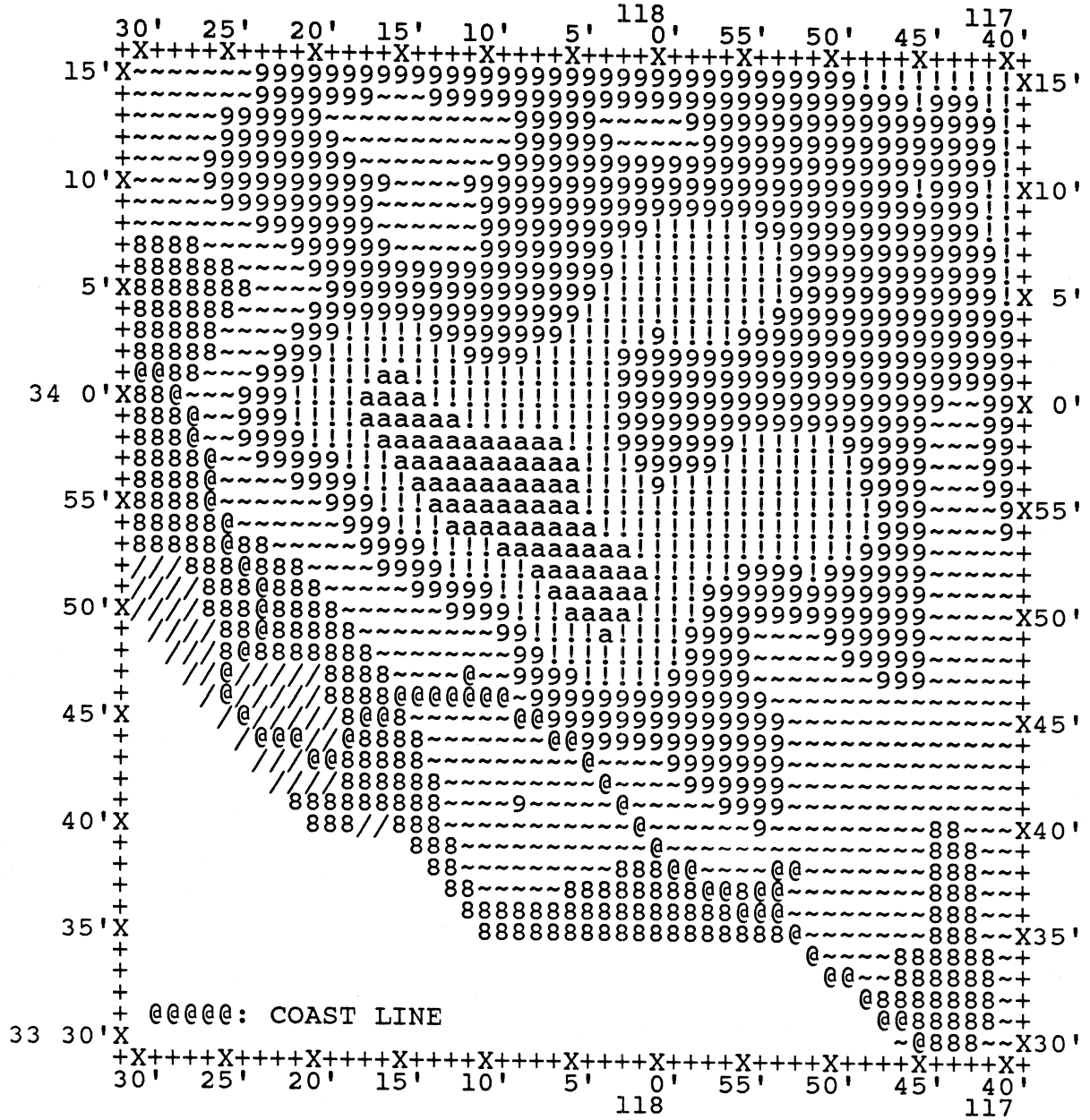

Figure A1.5

PSEUDO RELATIVE VELOCITY, PSV (IN/SEC) AT T = .500 SEC
PROBABILITY OF EXCEEDANCE = .99 FOR 50 YEARS

CONTOUR LEVELS OF LOG(PSV):

/	8	~	9	!	a	[
.5	.6	.7	.8	.9	1.0	1.1

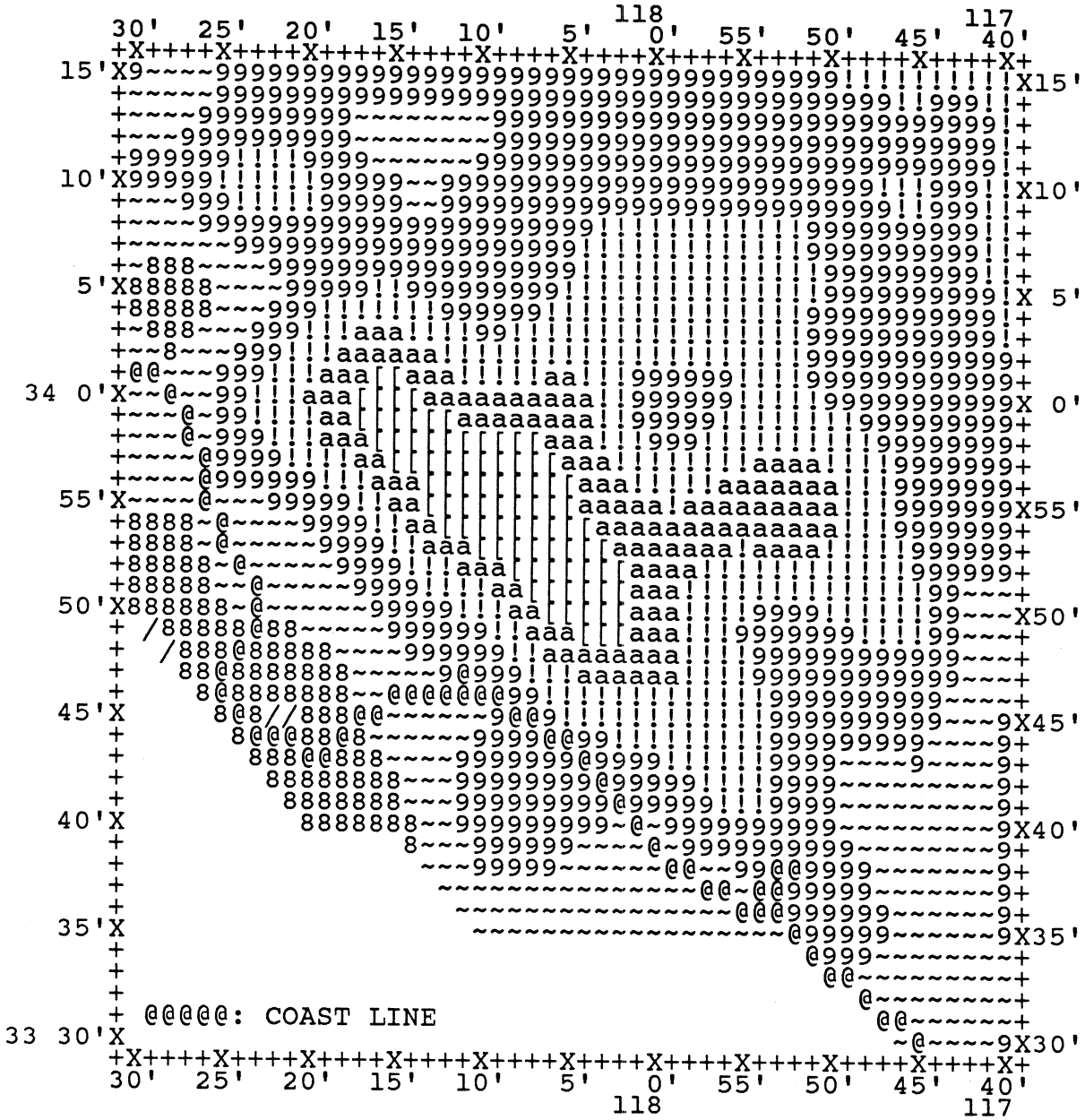

Figure A1.6

PSEUDO RELATIVE VELOCITY, PSV (IN/SEC) AT T = .900 SEC
PROBABILITY OF EXCEEDANCE = .99 FOR 50 YEARS

CONTOUR LEVELS OF LOG(PSV):

/	8	~	9	!	a	[	b	]
.5	.6	.7	.8	.9	1.0	1.1	1.2	1.3

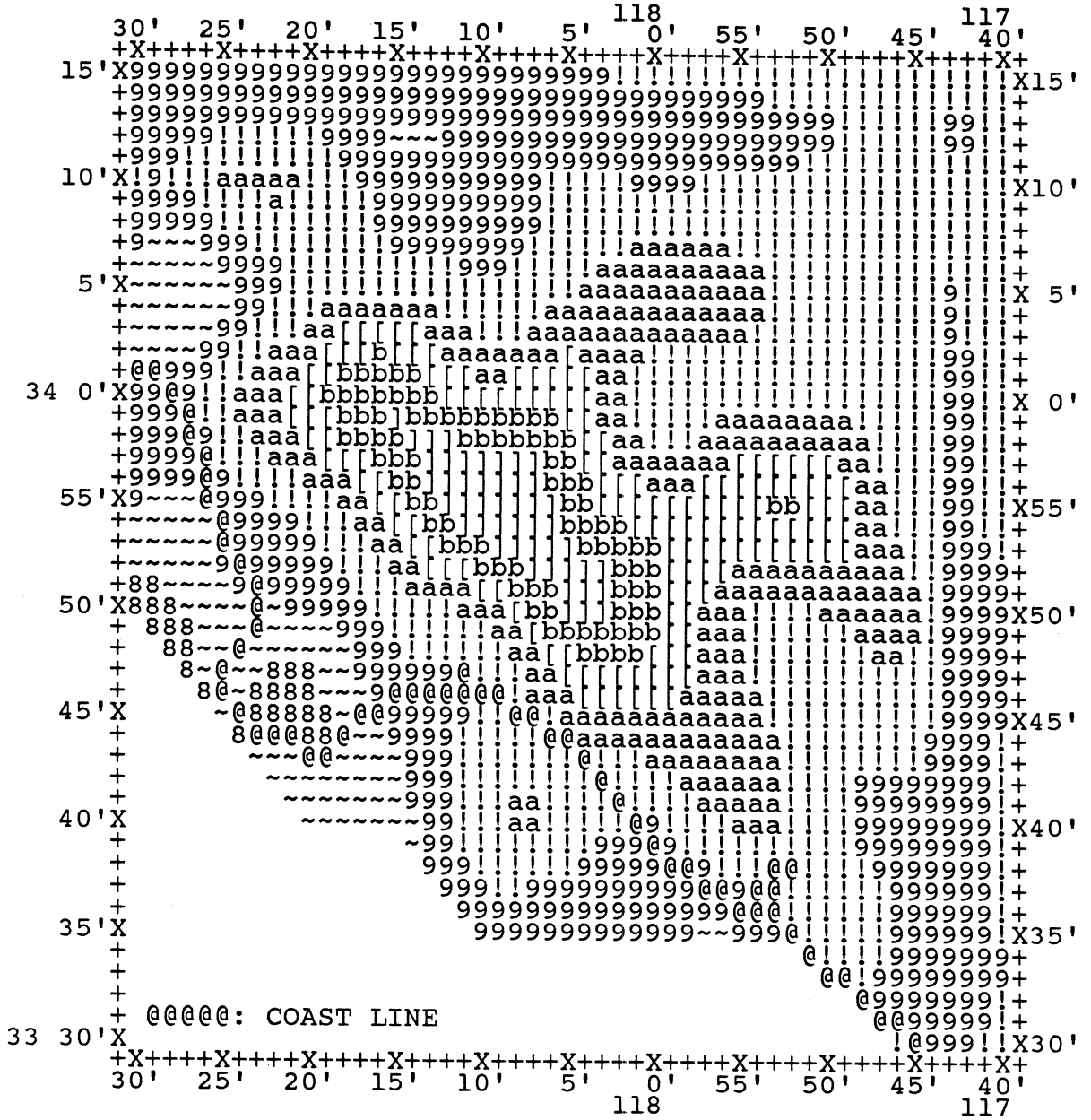

Figure A1.7

PSEUDO RELATIVE VELOCITY, PSV (IN/SEC) AT T = 1.600 SEC

PROBABILITY OF EXCEEDANCE = .99 FOR 50 YEARS

CONTOUR LEVELS OF LOG(PSV):

/	8	~	9	!	a	[	b	]	c
.5	.6	.7	.8	.9	1.0	1.1	1.2	1.3	1.4

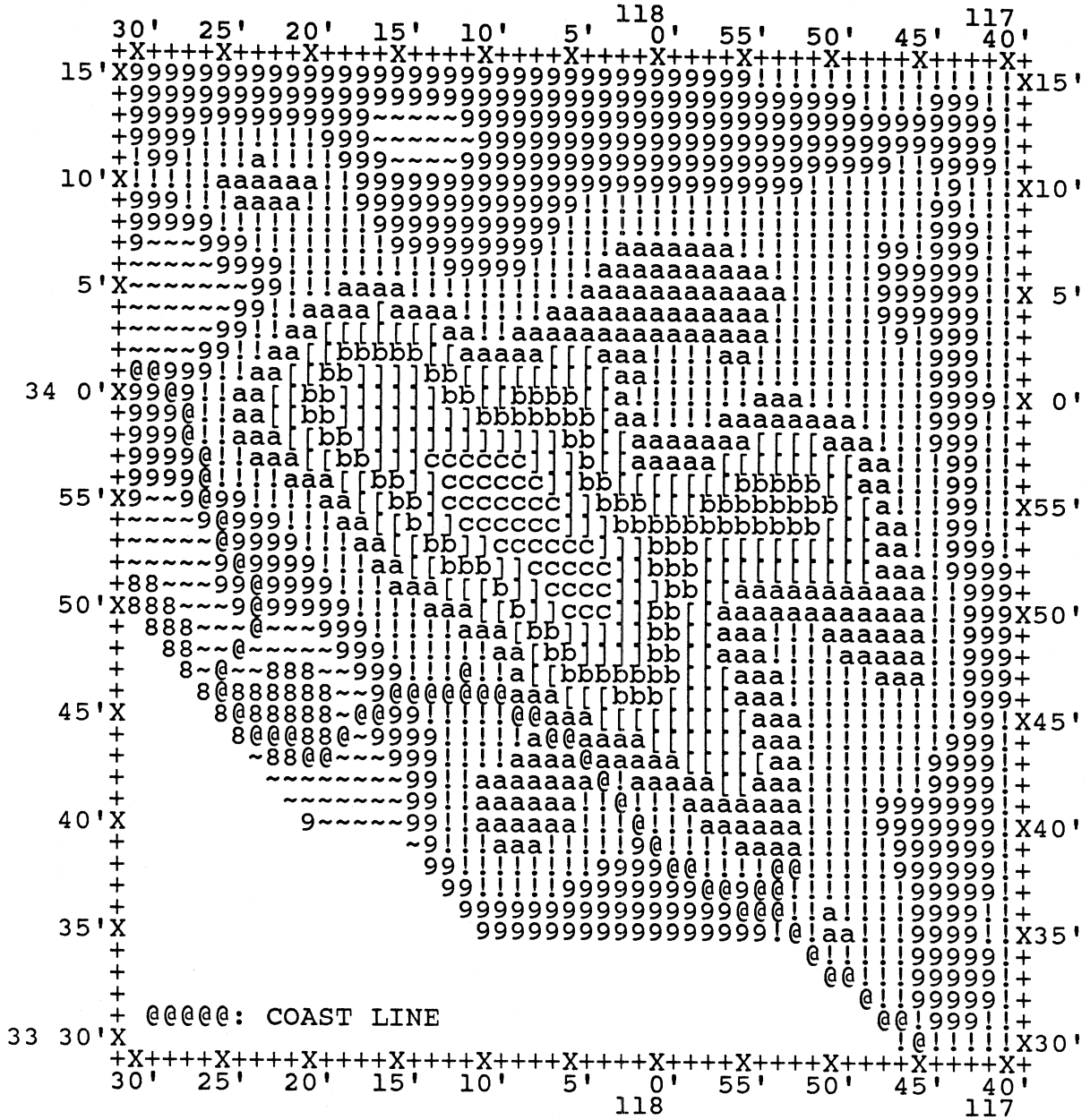

Figure A1.8

PSEUDO RELATIVE VELOCITY, PSV (IN/SEC) AT T = 2.800 SEC
PROBABILITY OF EXCEEDANCE = .99 FOR 50 YEARS

CONTOUR LEVELS OF LOG(PSV):

/	8	~	9	!	a	[	b	]	c	^
.5	.6	.7	.8	.9	1.0	1.1	1.2	1.3	1.4	1.5

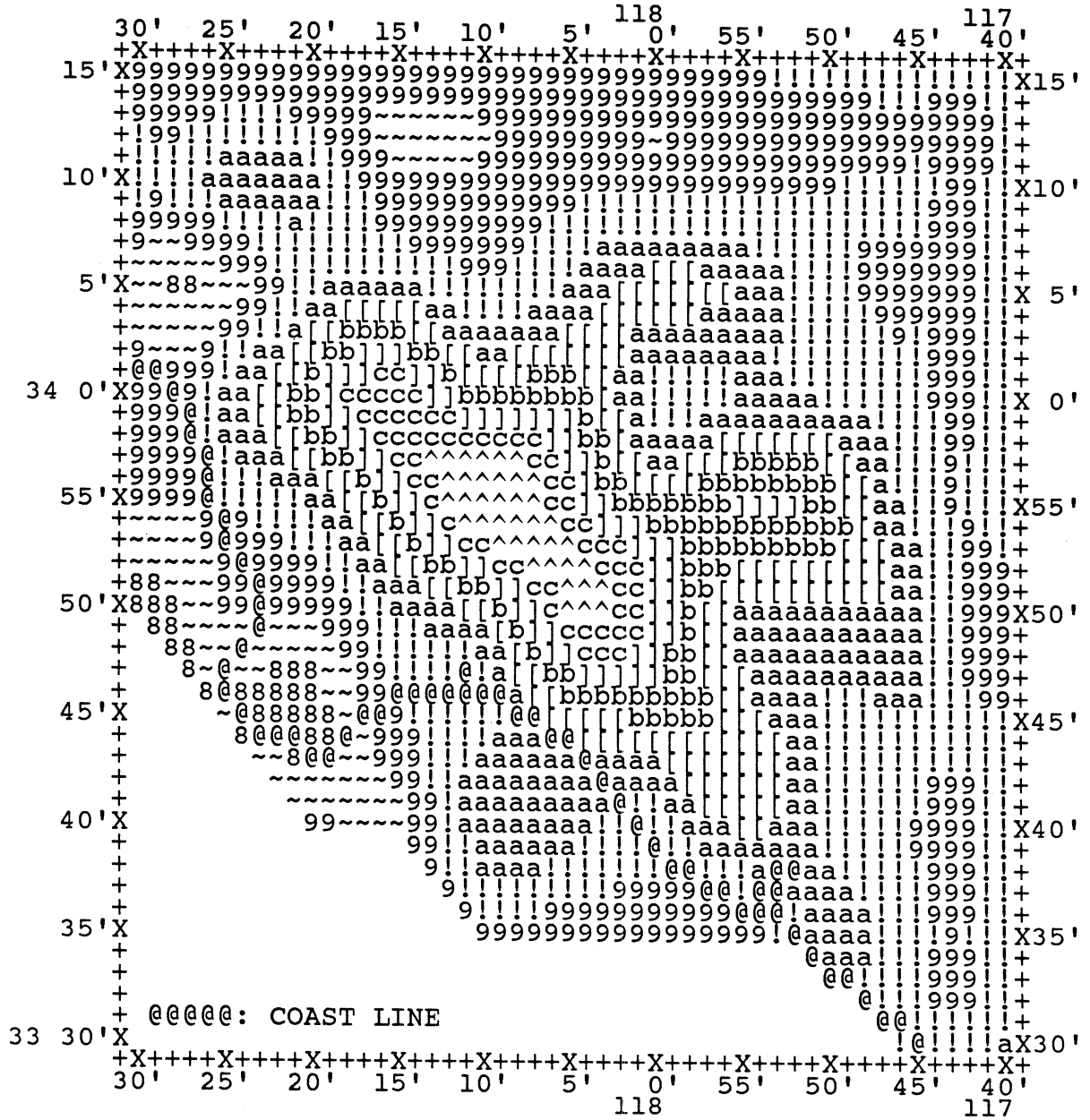

Figure A1.9

PSEUDO RELATIVE VELOCITY, PSV (IN/SEC) AT T = 4.400 SEC
PROBABILITY OF EXCEEDANCE = .99 FOR 50 YEARS

CONTOUR LEVELS OF LOG(PSV):

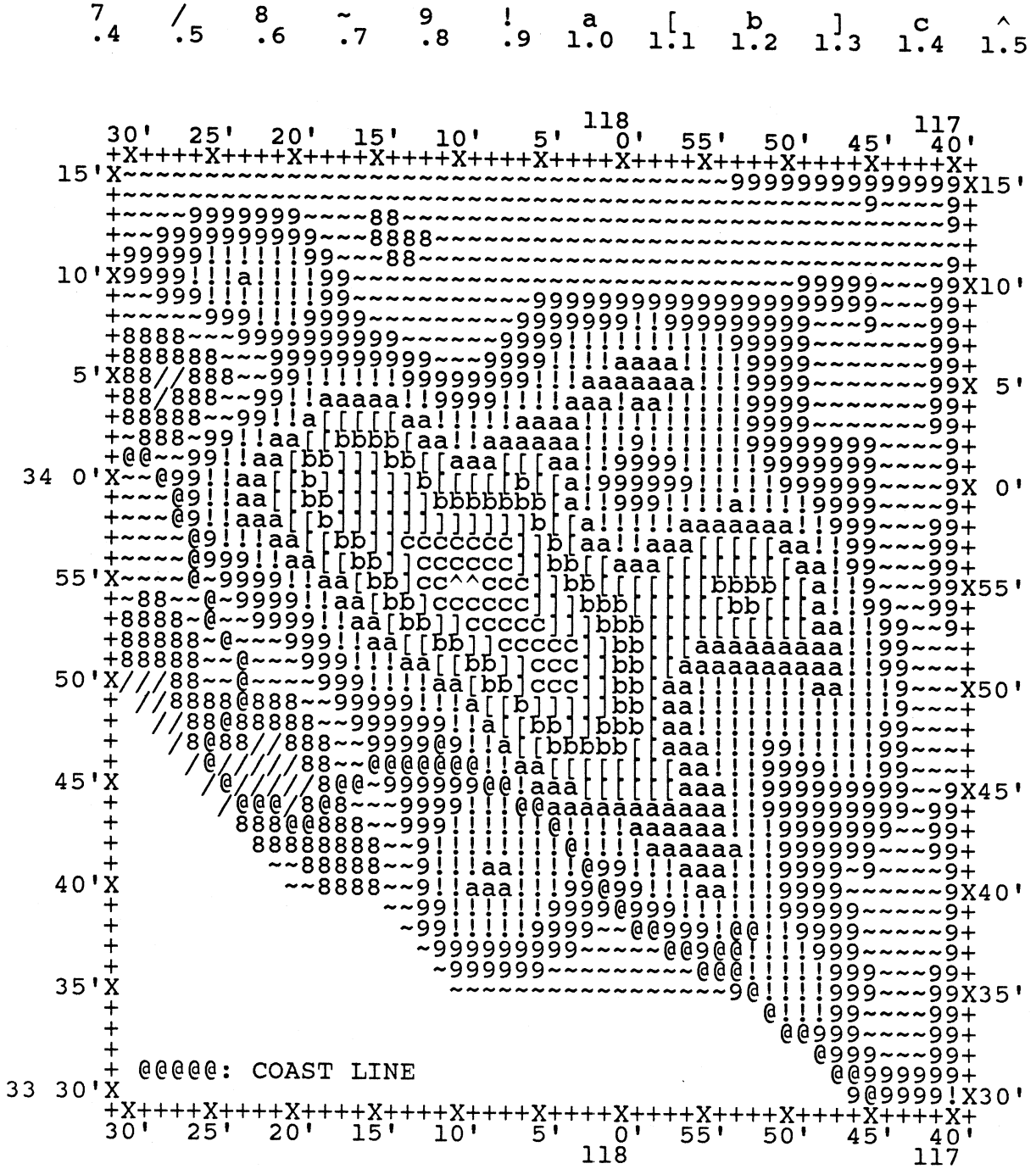

Figure A1.10

PSEUDO RELATIVE VELOCITY, PSV (IN/SEC) AT T = 7.500 SEC
PROBABILITY OF EXCEEDANCE = .99 FOR 50 YEARS

CONTOUR LEVELS OF LOG(PSV):

-	7	/	8	~	9	!	a	[	b
.3	.4	.5	.6	.7	.8	.9	1.0	1.1	1.2

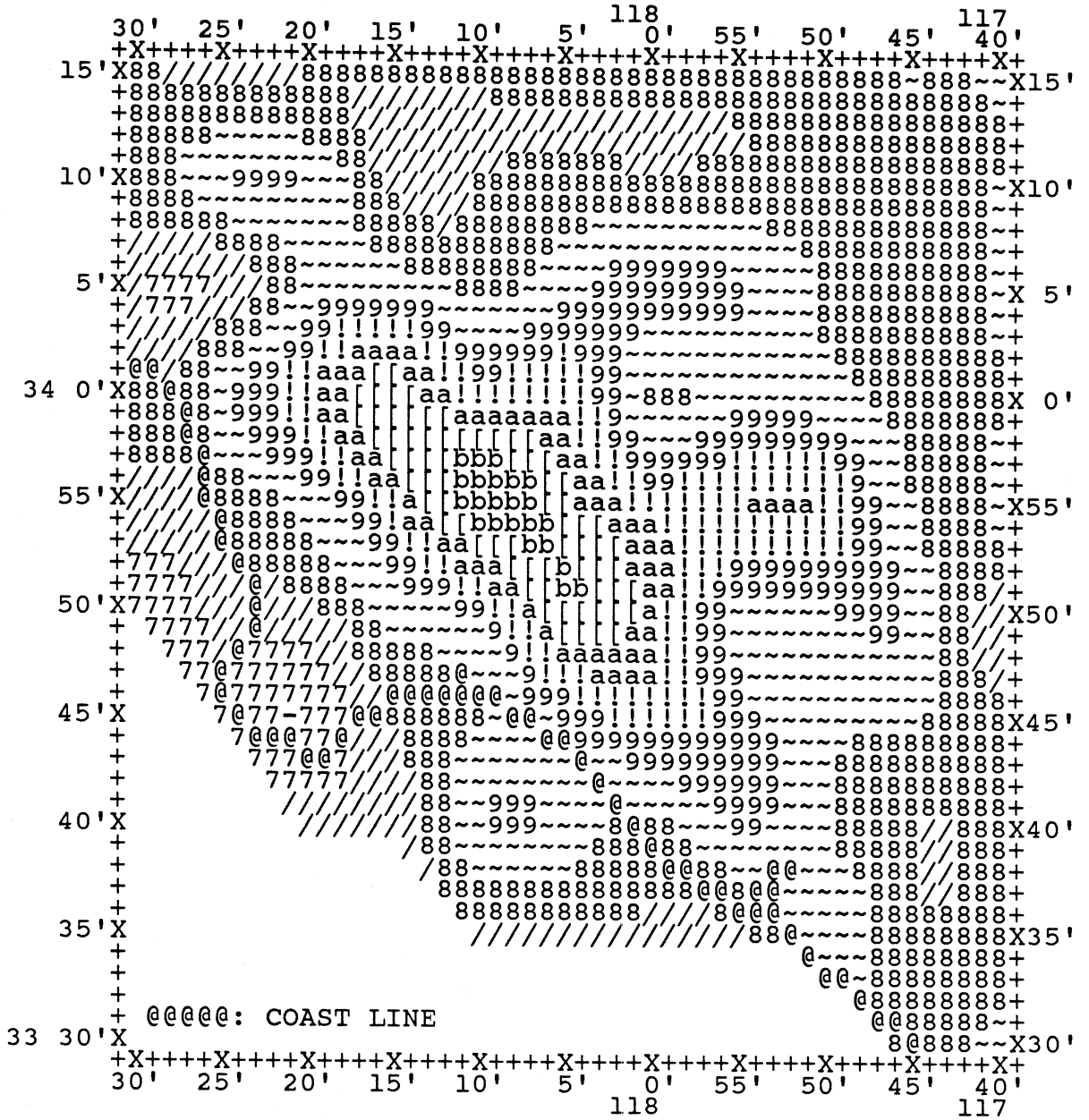

Figure A1.11

PSEUDO RELATIVE VELOCITY, PSV (IN/SEC) AT T = .040 SEC
PROBABILITY OF EXCEEDANCE = .90 FOR 50 YEARS

CONTOUR LEVELS OF LOG(PSV):

2 -.6 " -.5 3 -.4 : -.3 4 -.2 ; -.1 5 .0 | .1 6 .2

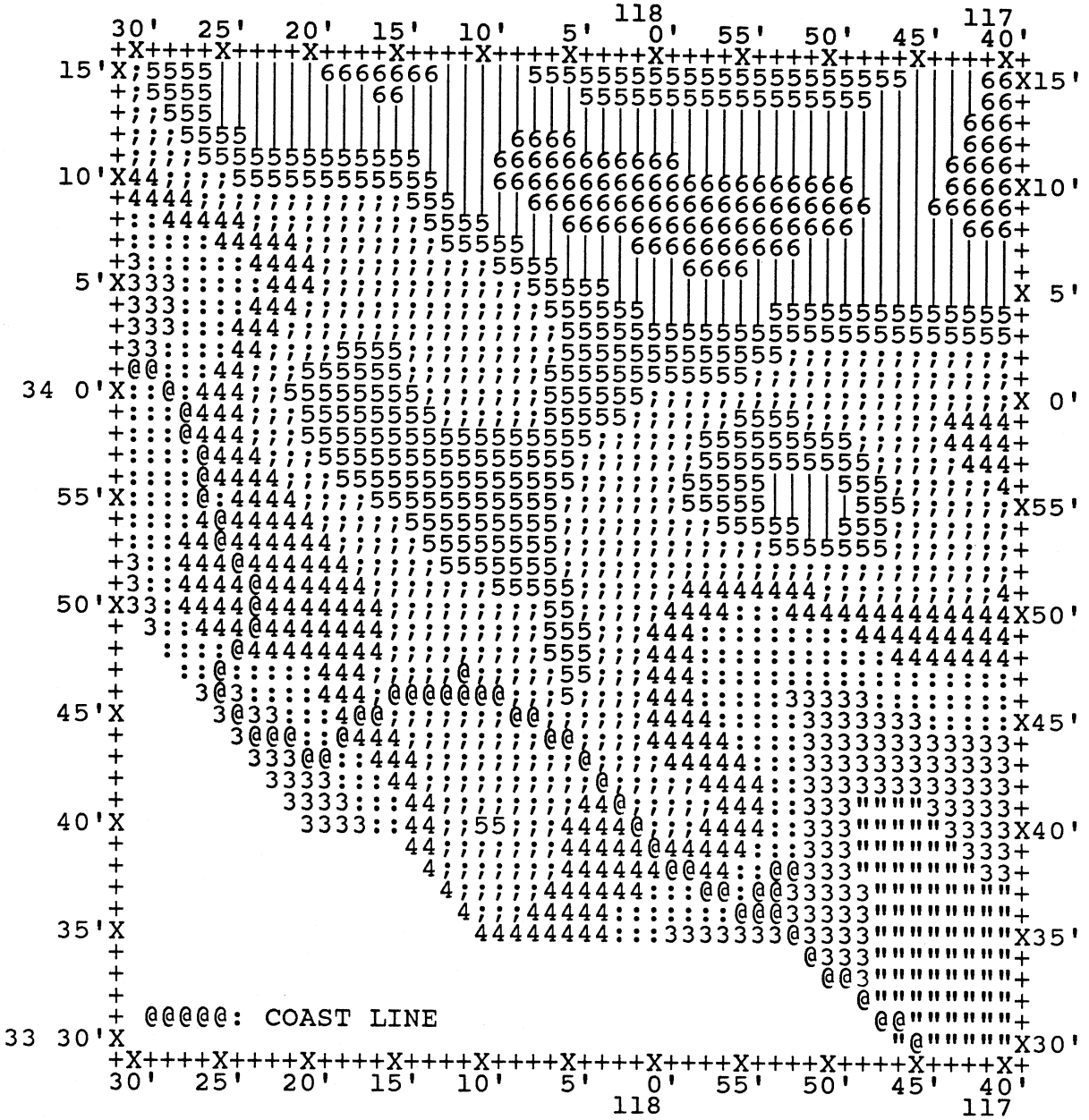

Figure A2.1

PSEUDO RELATIVE VELOCITY, PSV (IN/SEC) AT T = .065 SEC
PROBABILITY OF EXCEEDANCE = .90 FOR 50 YEARS

CONTOUR LEVELS OF LOG(PSV):

4 ; 5 | 6 - 7 /
-.2 -.1 .0 .1 .2 .3 .4 .5

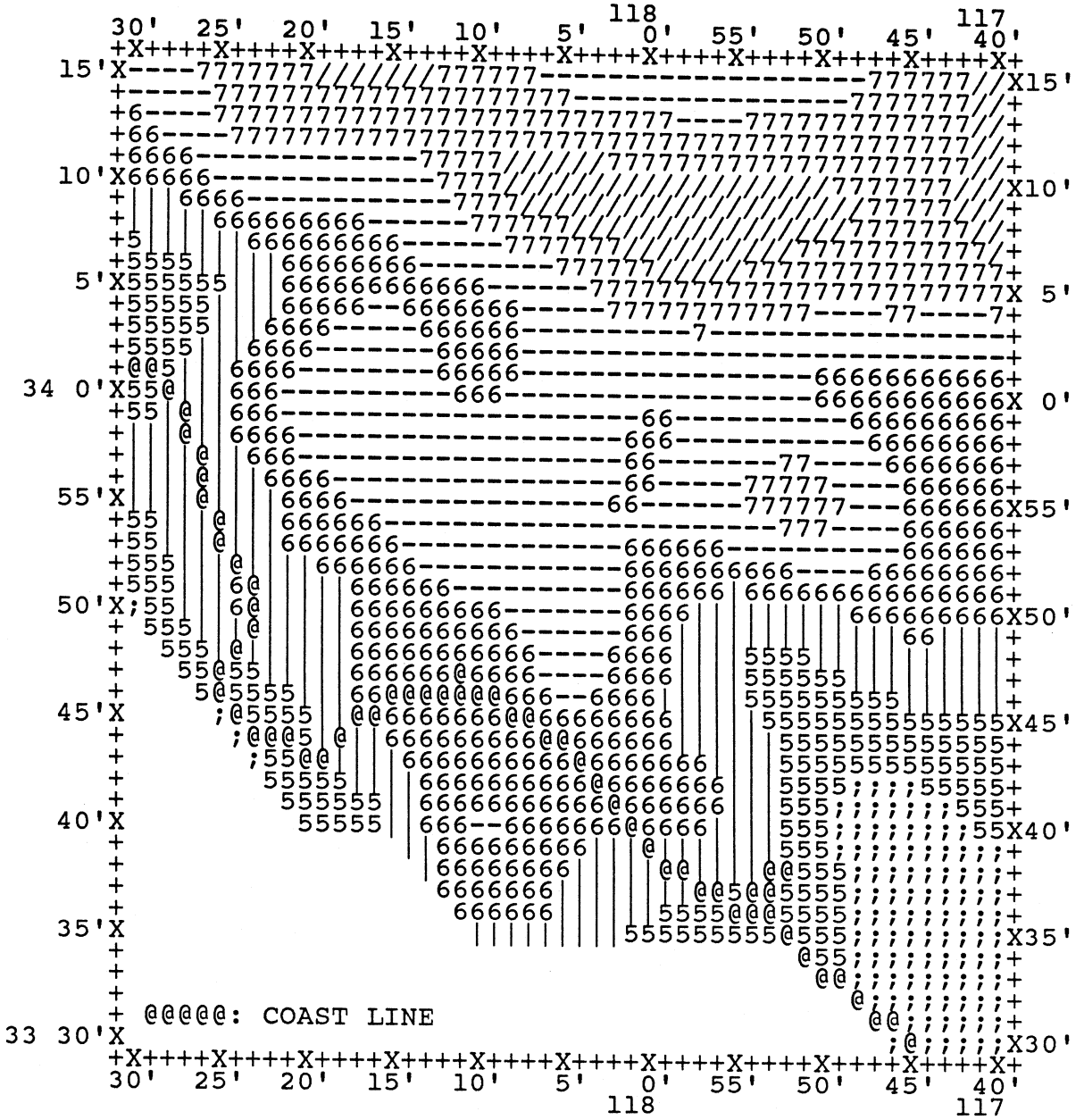

Figure A2.2

PSEUDO RELATIVE VELOCITY, PSV (IN/SEC) AT T = .110 SEC
PROBABILITY OF EXCEEDANCE = .90 FOR 50 YEARS

CONTOUR LEVELS OF LOG(PSV):

| 6 - 7 / 8 ~ 9
.1 .2 .3 .4 .5 .6 .7 .8

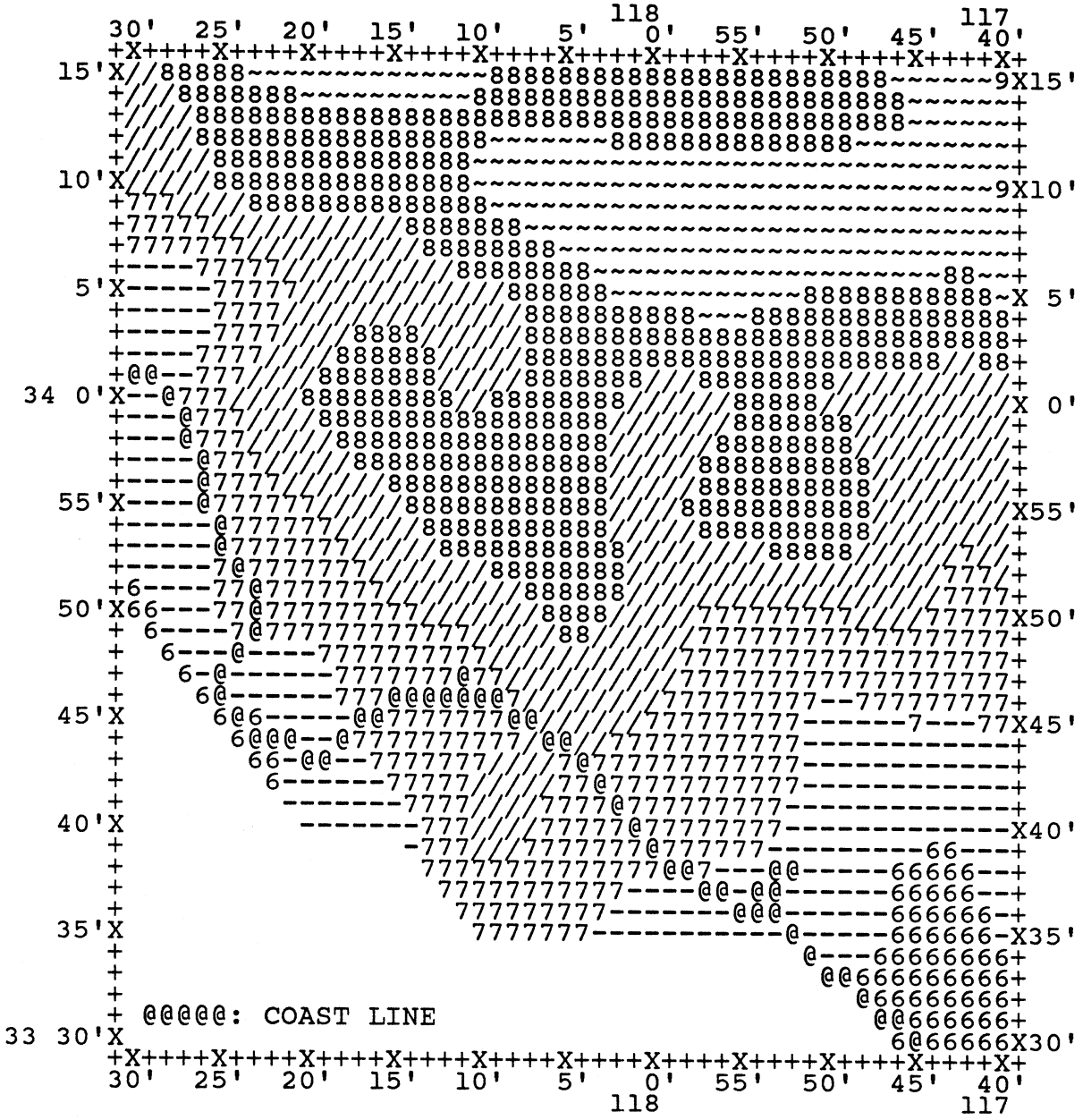

Figure A2.3

PSEUDO RELATIVE VELOCITY, PSV (IN/SEC) AT T = .190 SEC
PROBABILITY OF EXCEEDANCE = .90 FOR 50 YEARS

CONTOUR LEVELS OF LOG(PSV):

7	/	8	~	9	!	a
.4	.5	.6	.7	.8	.9	1.0

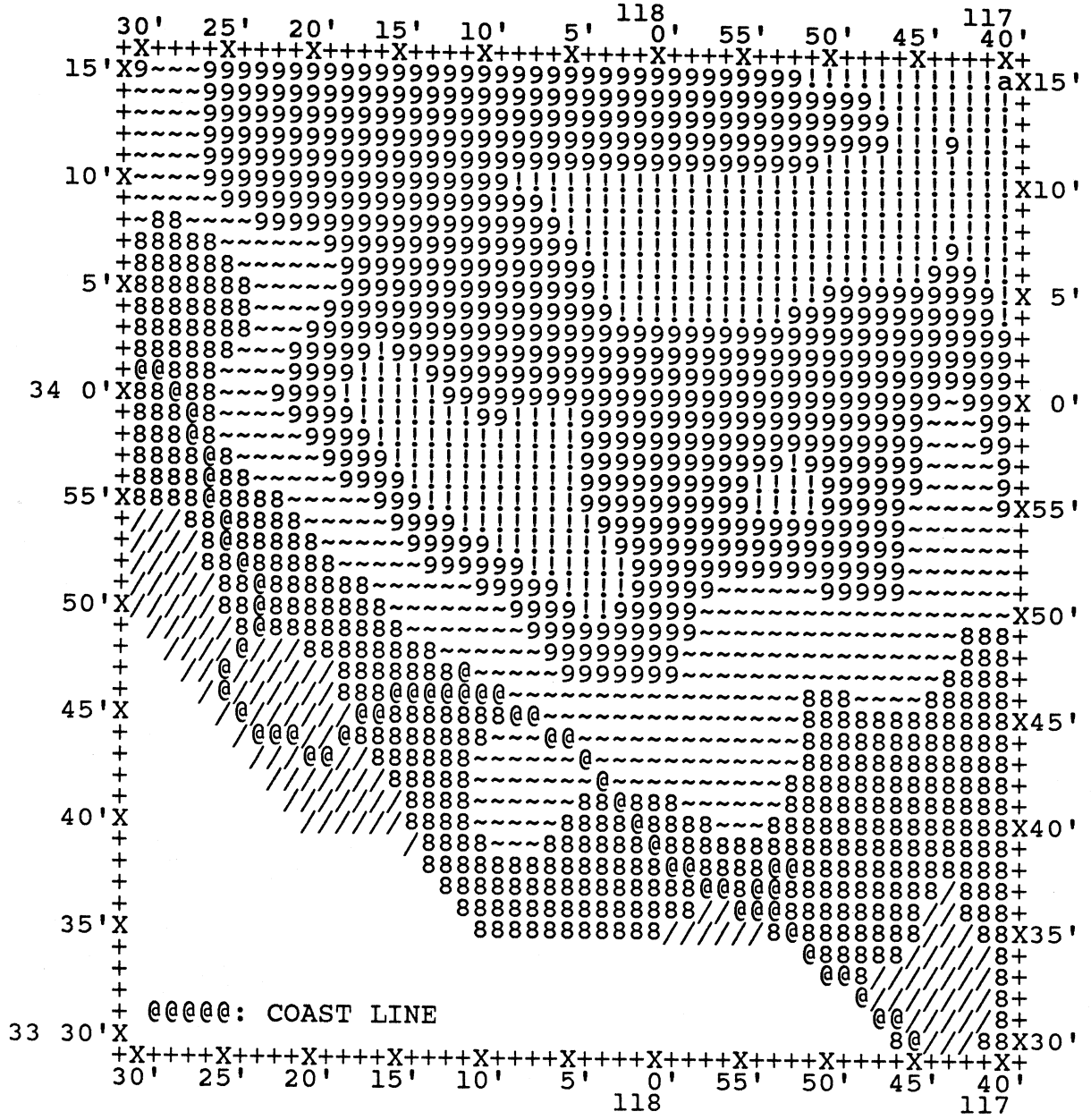

Figure A2.4

PSEUDO RELATIVE VELOCITY, PSV (IN/SEC) AT T = .340 SEC
PROBABILITY OF EXCEEDANCE = .90 FOR 50 YEARS

CONTOUR LEVELS OF LOG(PSV):

8	~	9	!	a	[	b
.6	.7	.8	.9	1.0	1.1	1.2

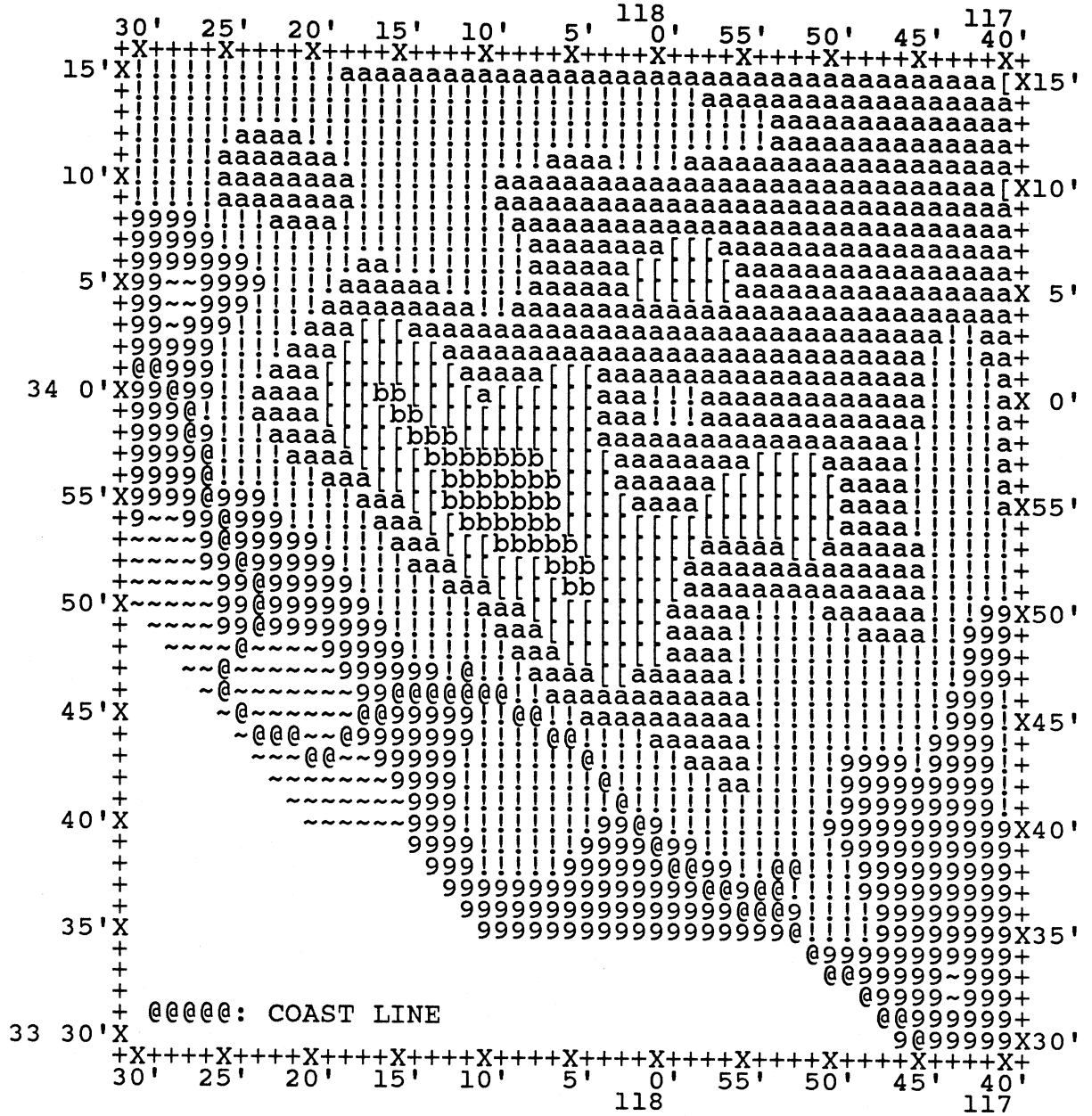

Figure A2.5

PSEUDO RELATIVE VELOCITY, PSV (IN/SEC) AT T = .500 SEC
PROBABILITY OF EXCEEDANCE = .90 FOR 50 YEARS

CONTOUR LEVELS OF LOG(PSV):

8	~	9	!	a	[	b	]
.6	.7	.8	.9	1.0	1.1	1.2	1.3

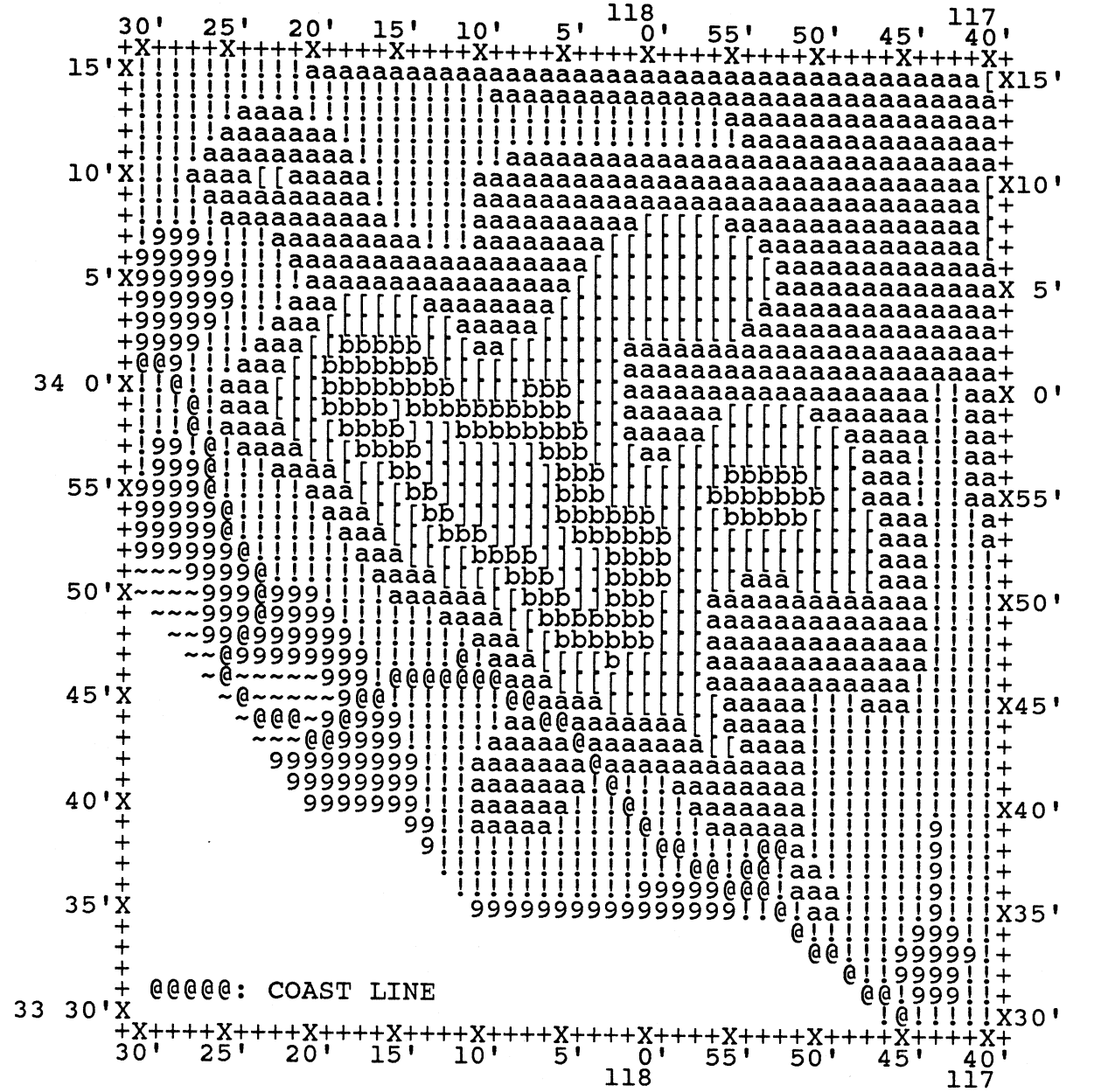

Figure A2.6

PSEUDO RELATIVE VELOCITY, PSV (IN/SEC) AT T = .900 SEC
PROBABILITY OF EXCEEDANCE = .90 FOR 50 YEARS

CONTOUR LEVELS OF LOG(PSV):

8	~	9	!	a	[	b	]	c	^
.6	.7	.8	.9	1.0	1.1	1.2	1.3	1.4	1.5

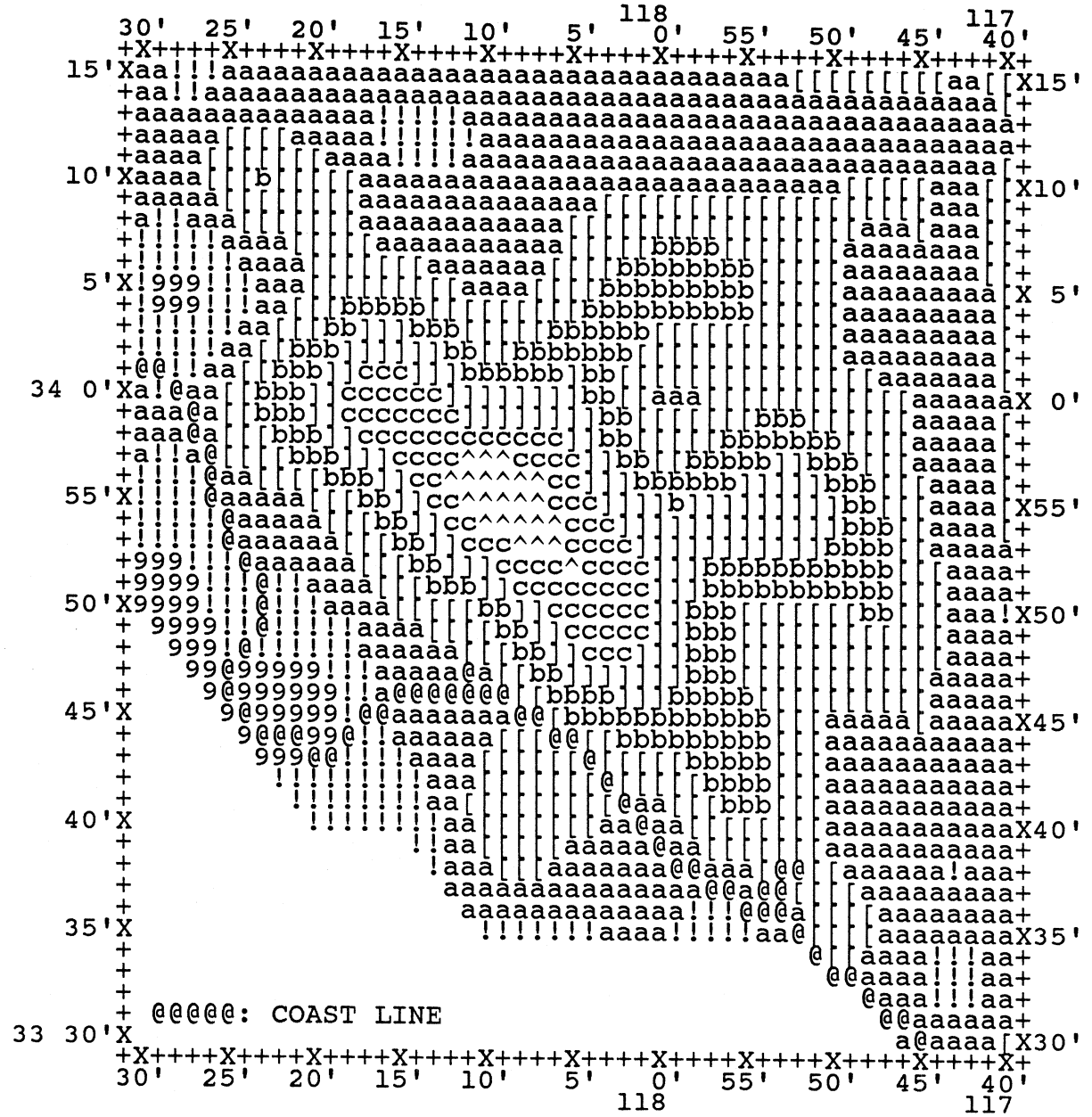

Figure A2.7

PSEUDO RELATIVE VELOCITY, PSV (IN/SEC) AT T = 1.600 SEC

PROBABILITY OF EXCEEDANCE = .90 FOR 50 YEARS

CONTOUR LEVELS OF LOG(PSV):

8	~	9	!	a	[	b	]	c	^	d
.6	.7	.8	.9	1.0	1.1	1.2	1.3	1.4	1.5	1.6

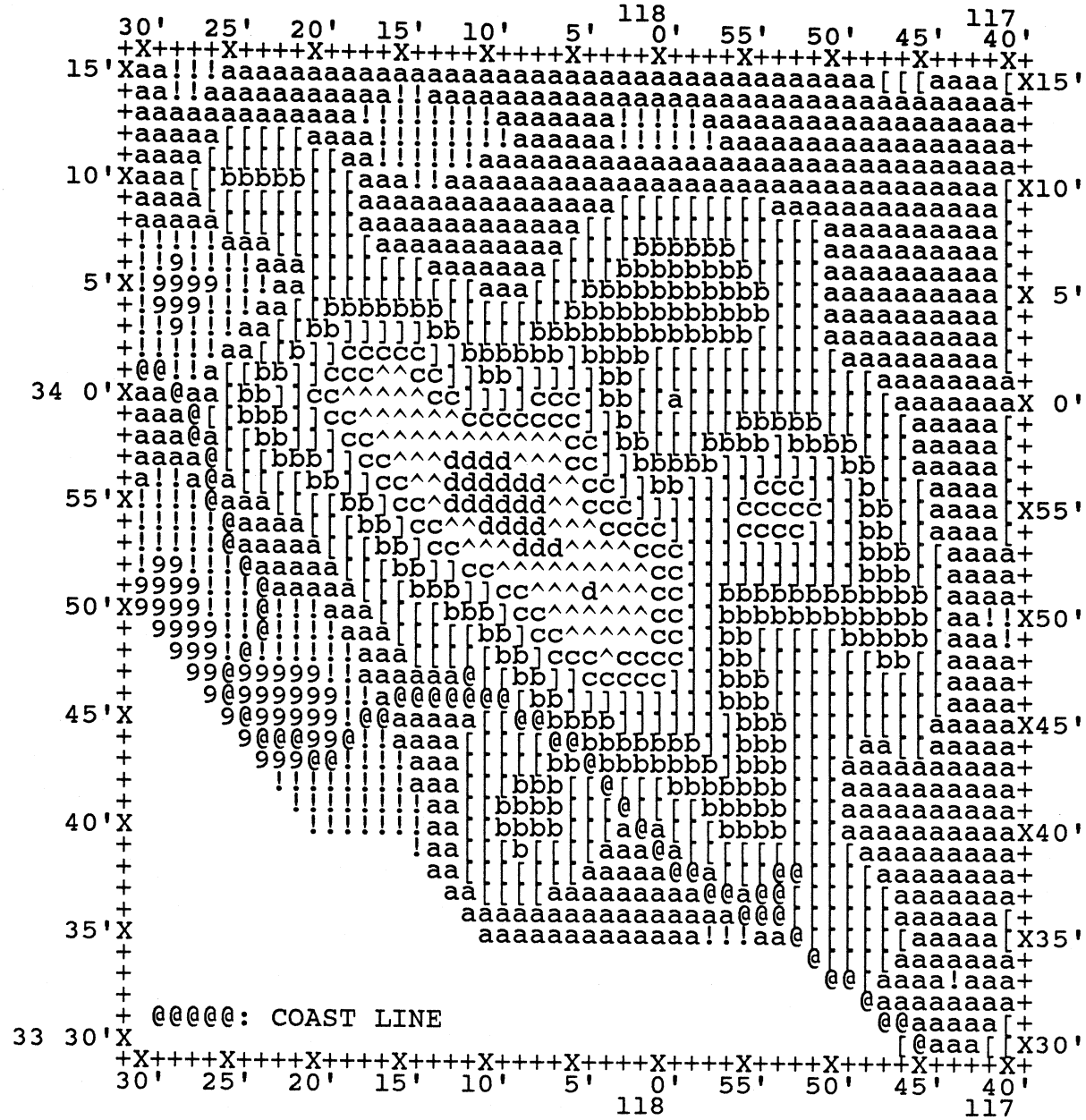

Figure A2.8

PSEUDO RELATIVE VELOCITY, PSV (IN/SEC) AT T = 2.800 SEC
PROBABILITY OF EXCEEDANCE = .90 FOR 50 YEARS

CONTOUR LEVELS OF LOG(PSV):

8	~	9	!	a	[	b	]	c	^	d	>
.6	.7	.8	.9	1.0	1.1	1.2	1.3	1.4	1.5	1.6	1.7

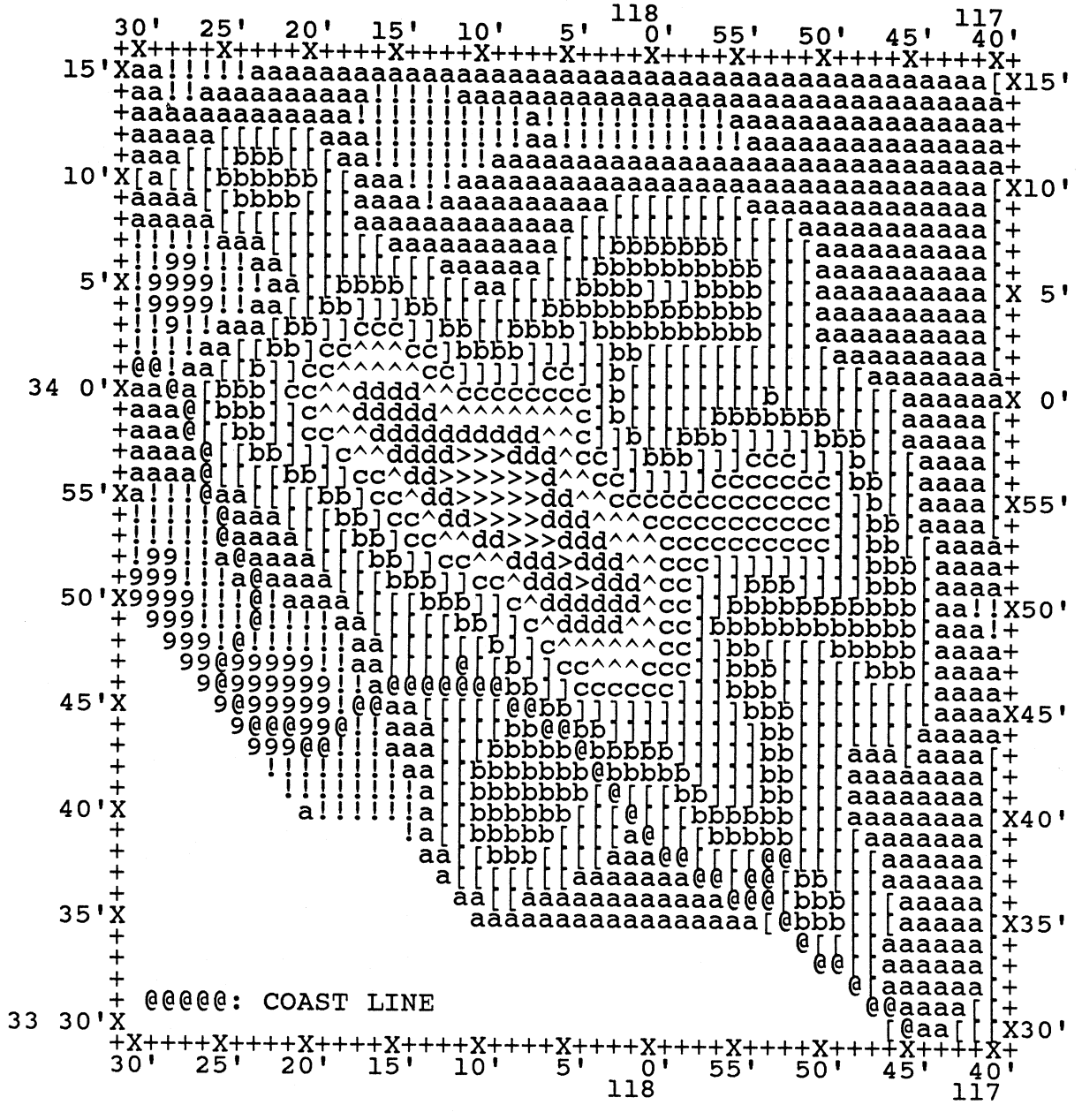

Figure A2.9

PSEUDO RELATIVE VELOCITY, PSV (IN/SEC) AT T = 4.400 SEC
PROBABILITY OF EXCEEDANCE = .90 FOR 50 YEARS

CONTOUR LEVELS OF LOG(PSV):

8	~	9	!	a	[	b	]	c	^	d
.6	.7	.8	.9	1.0	1.1	1.2	1.3	1.4	1.5	1.6

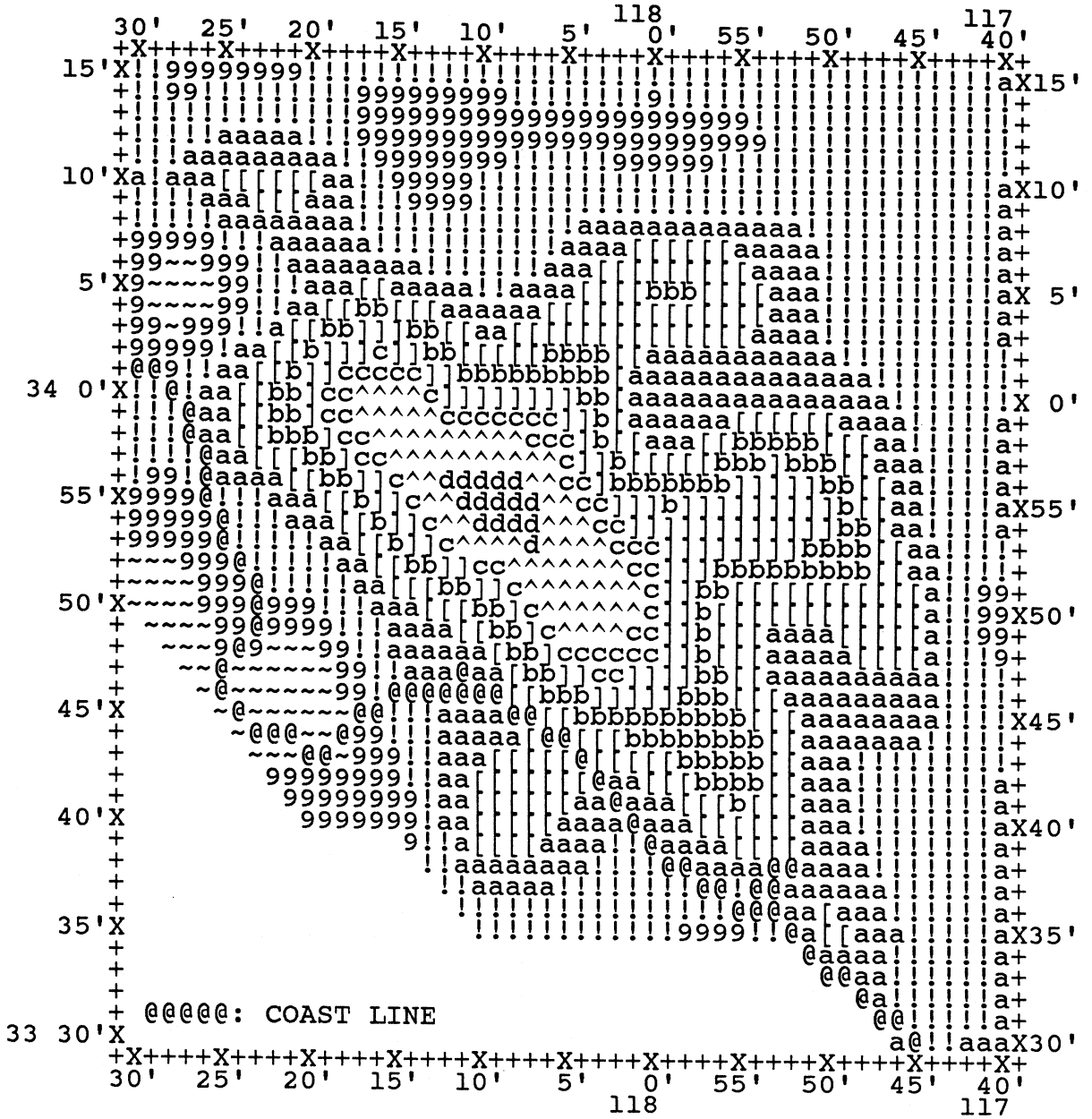

Figure A2.10

PSEUDO RELATIVE VELOCITY, PSV (IN/SEC) AT T = 7.500 SEC
PROBABILITY OF EXCEEDANCE = .90 FOR 50 YEARS

CONTOUR LEVELS OF LOG(PSV):

7	/	8	~	9	!	a	[	b	]	c
.4	.5	.6	.7	.8	.9	1.0	1.1	1.2	1.3	1.4

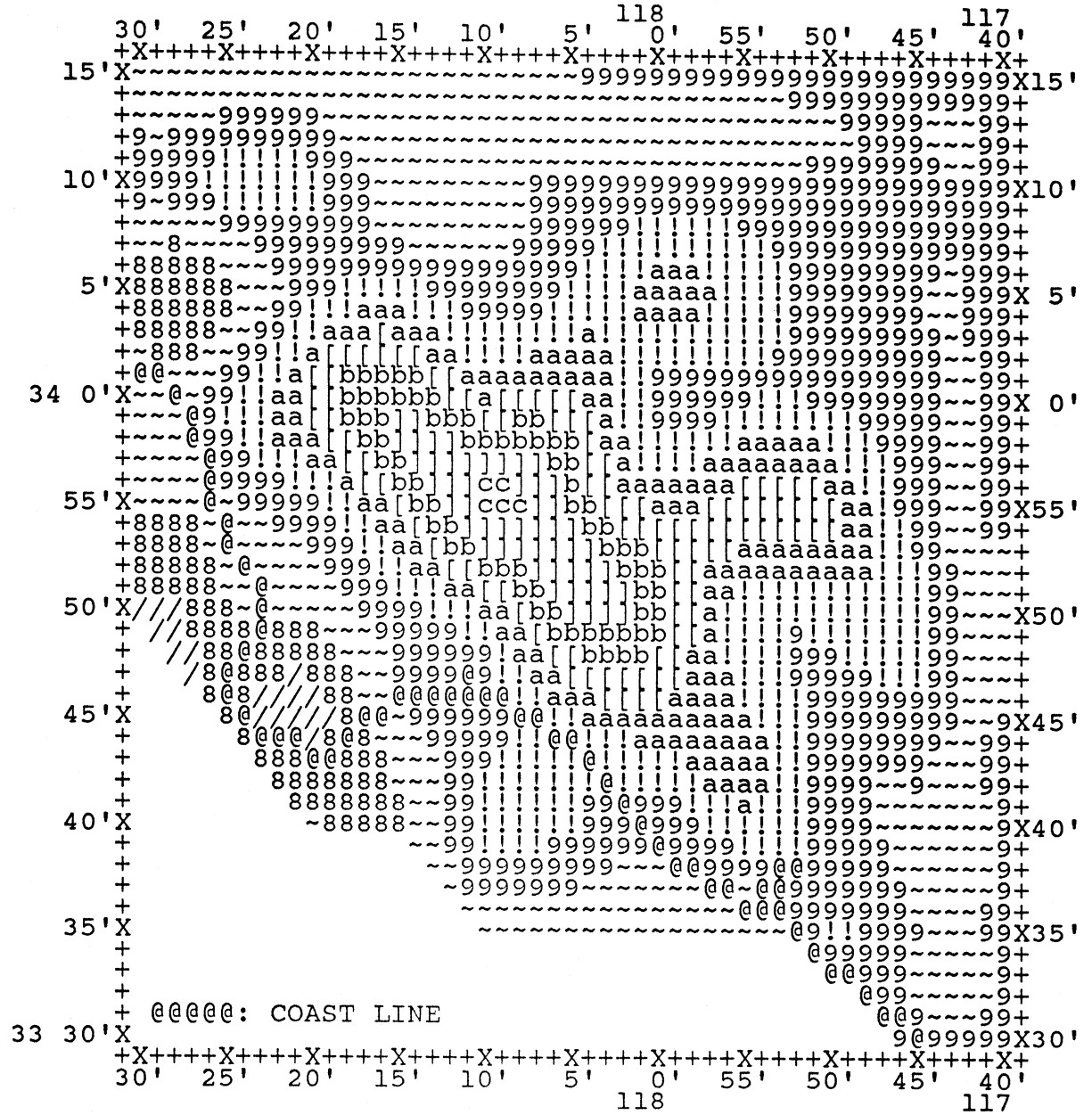

Figure A2.11

PSEUDO RELATIVE VELOCITY, PSV (IN/SEC) AT T = .040 SEC
PROBABILITY OF EXCEEDANCE = .50 FOR 50 YEARS

CONTOUR LEVELS OF LOG(PSV):

: -.3 4 -.2 ; -.1 5 .0 | .1 6 .2 - .3 7 .4

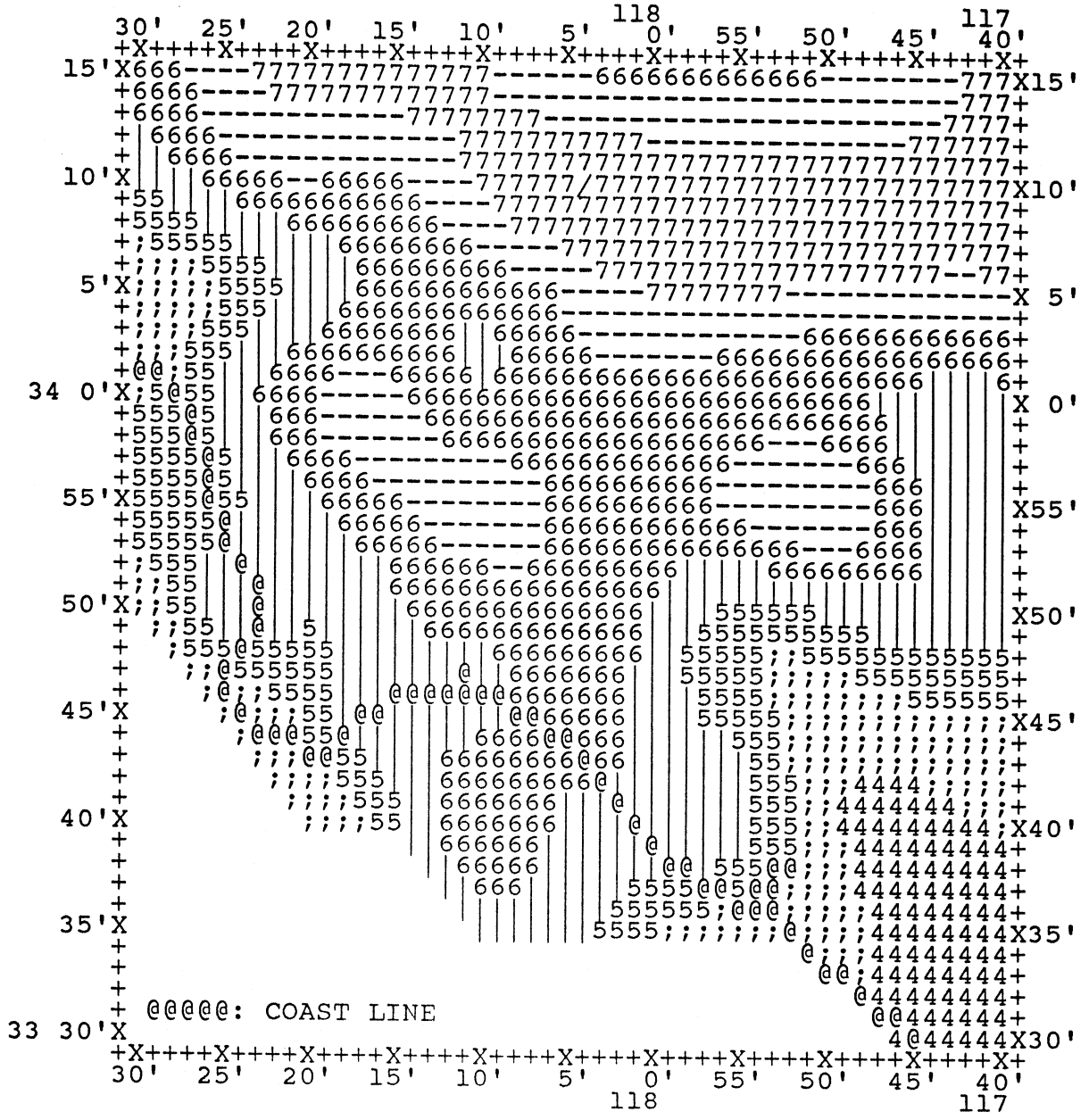

Figure A3.1

PSEUDO RELATIVE VELOCITY, PSV (IN/SEC) AT T = .065 SEC
PROBABILITY OF EXCEEDANCE = .50 FOR 50 YEARS

CONTOUR LEVELS OF LOG(PSV):

;	5	|	6	-	7	/	8	~
-.1	.0	.1	.2	.3	.4	.5	.6	.7

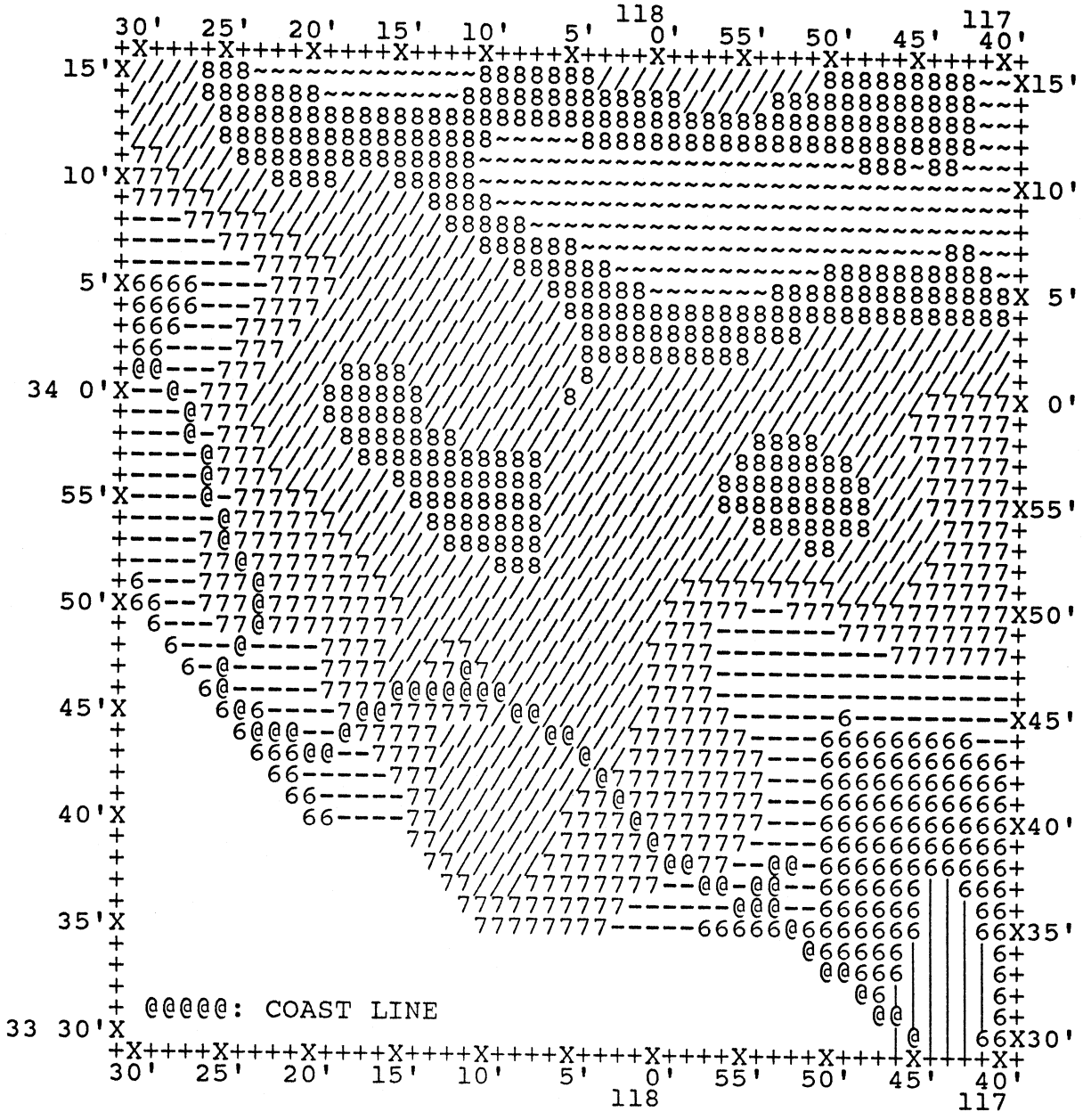

Figure A3.2

PSEUDO RELATIVE VELOCITY, PSV (IN/SEC) AT T = .110 SEC
PROBABILITY OF EXCEEDANCE = .50 FOR 50 YEARS

CONTOUR LEVELS OF LOG(PSV):

-	7	/	8	~	9	!	a
.3	.4	.5	.6	.7	.8	.9	1.0

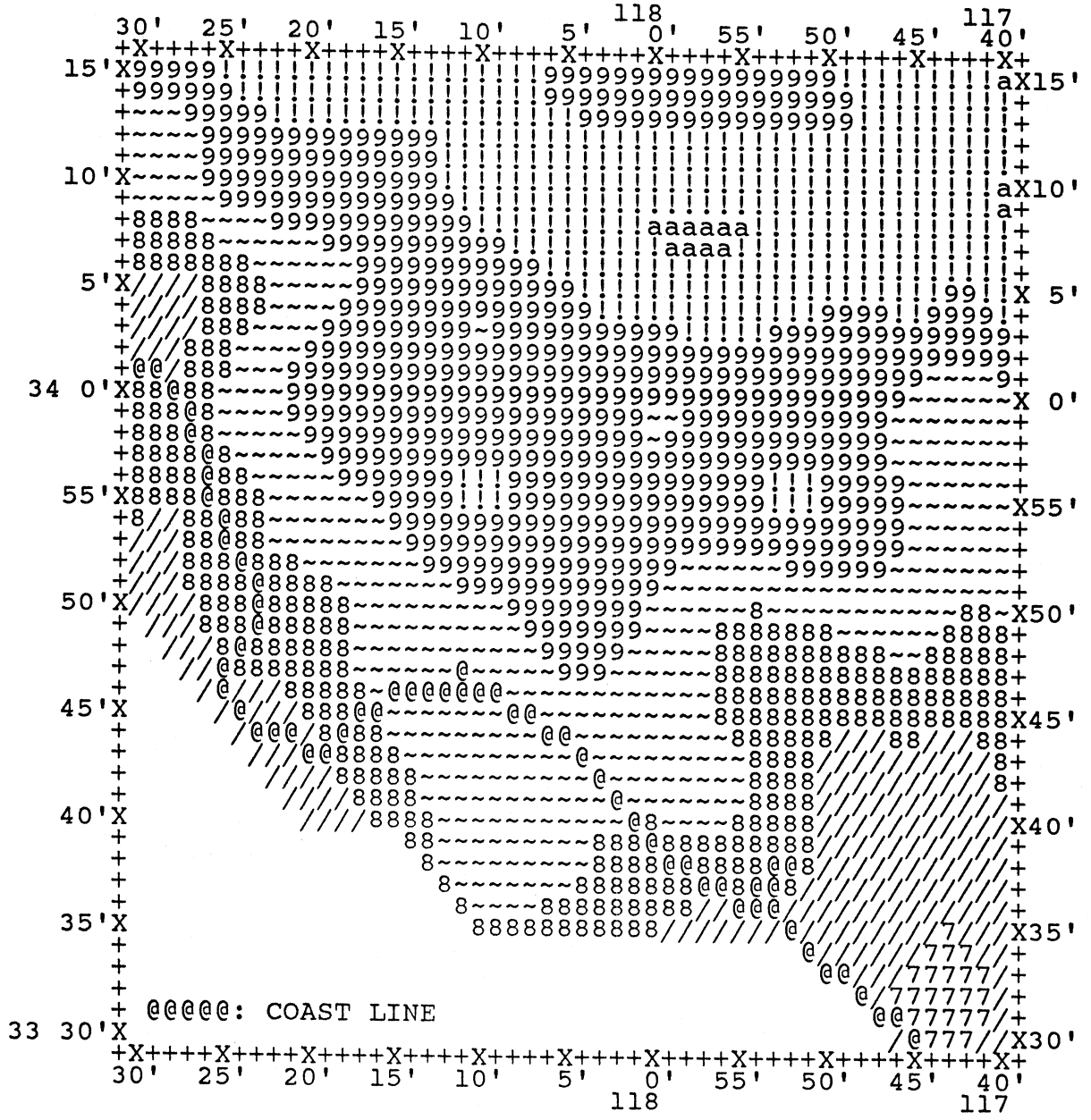

Figure A3.3

PSEUDO RELATIVE VELOCITY, PSV (IN/SEC) AT T = .190 SEC
PROBABILITY OF EXCEEDANCE = .50 FOR 50 YEARS

CONTOUR LEVELS OF LOG(PSV):

8	~	9	!	a	[	b
.6	.7	.8	.9	1.0	1.1	1.2

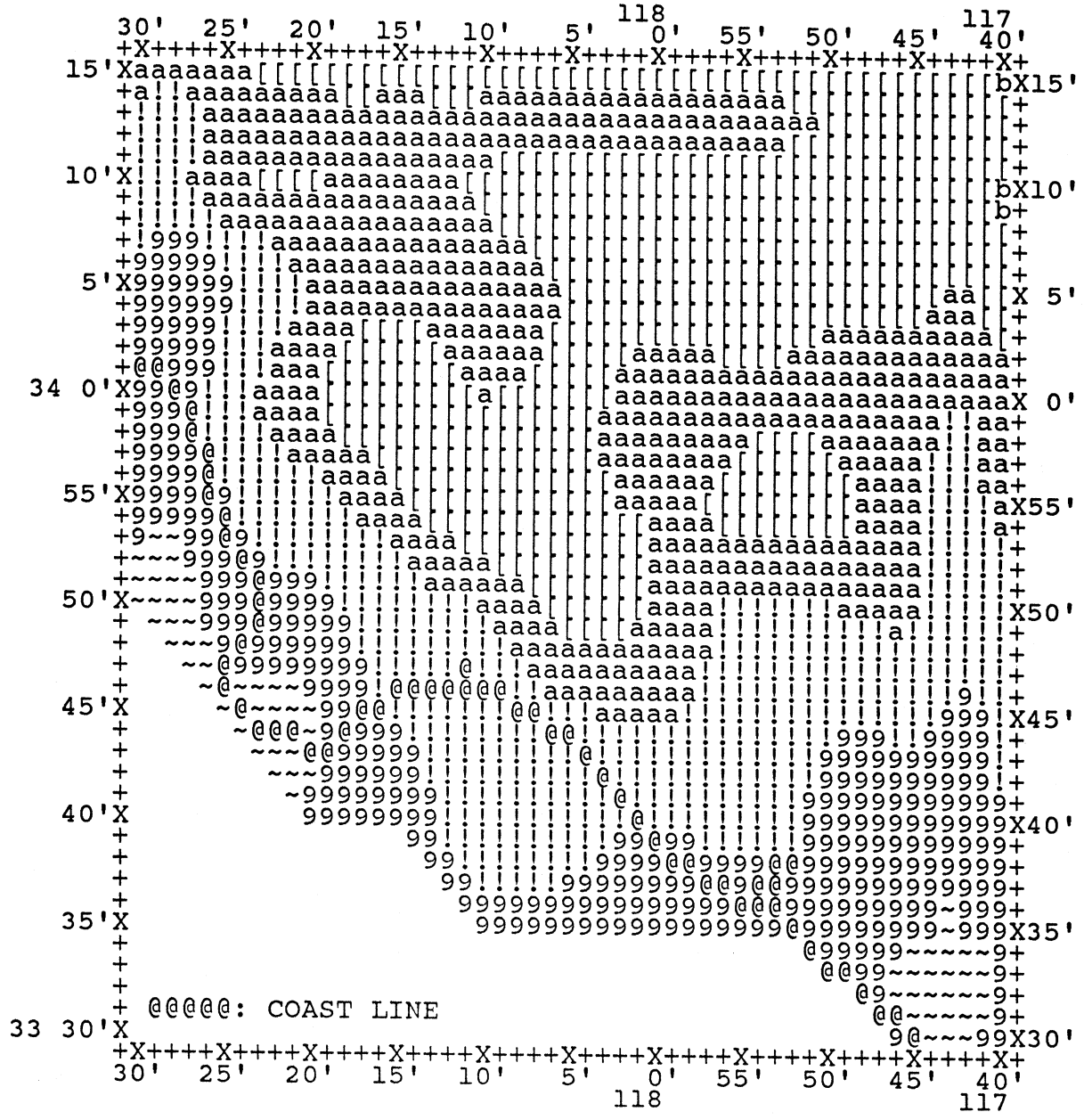

Figure A3.4

PSEUDO RELATIVE VELOCITY, PSV (IN/SEC) AT T = .340 SEC
PROBABILITY OF EXCEEDANCE = .50 FOR 50 YEARS

CONTOUR LEVELS OF LOG(PSV):

9	!	a	[	b	]	c
.8	.9	1.0	1.1	1.2	1.3	1.4

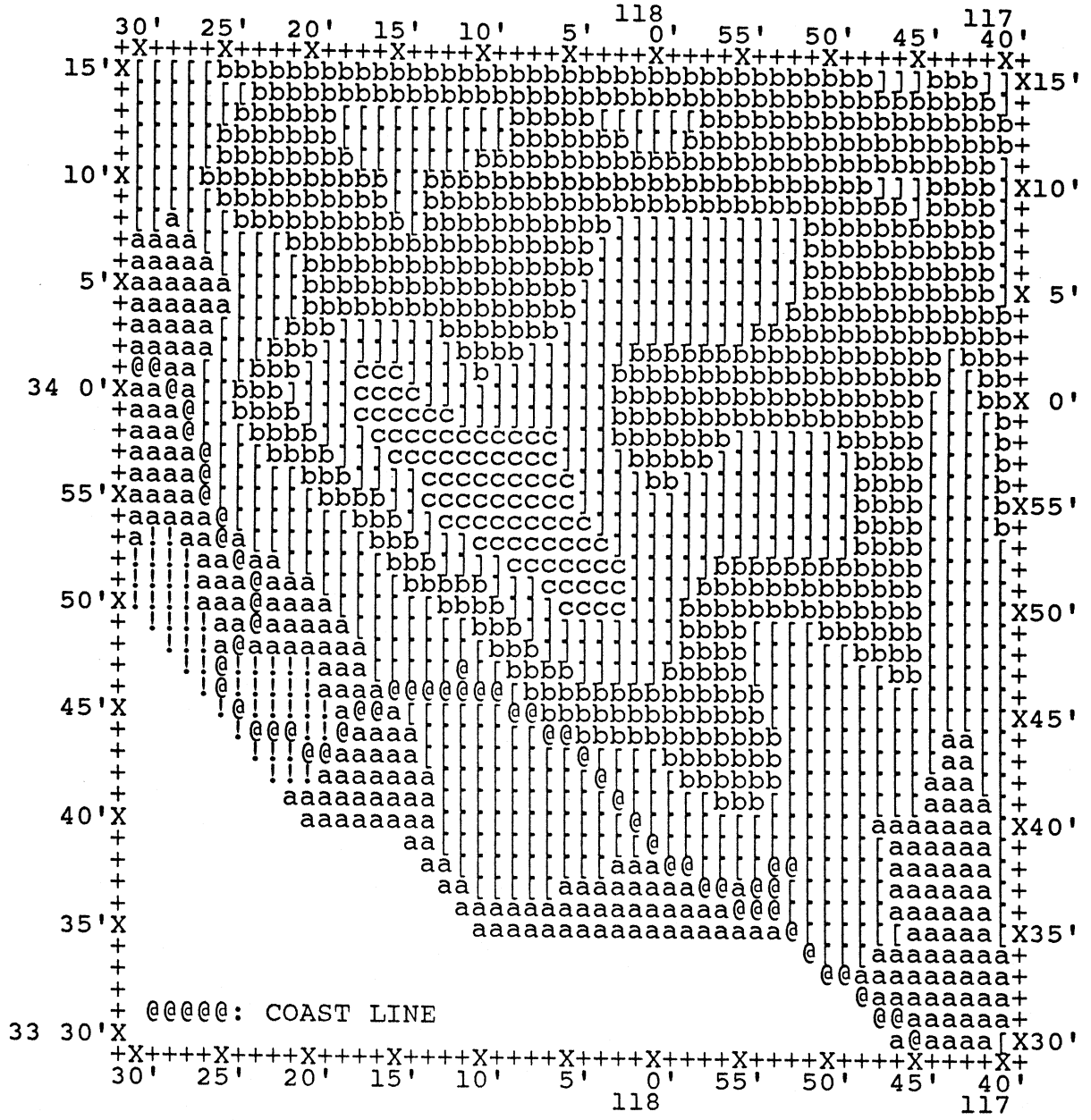

Figure A3.5

PSEUDO RELATIVE VELOCITY, PSV (IN/SEC) AT T = .500 SEC
PROBABILITY OF EXCEEDANCE = .50 FOR 50 YEARS

CONTOUR LEVELS OF LOG(PSV):

!	a	[	b	]	c	^
.9	1.0	1.1	1.2	1.3	1.4	1.5

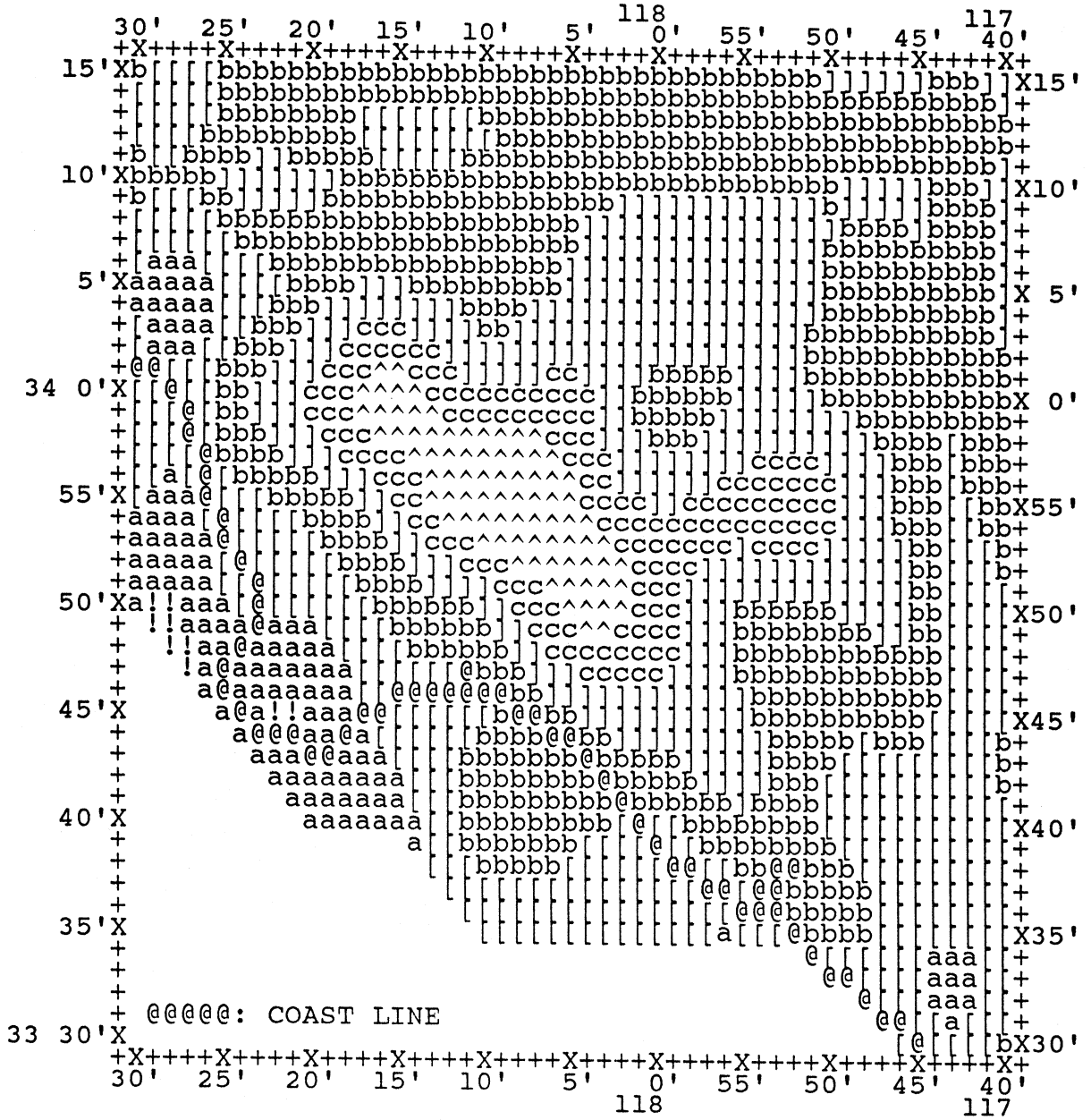

Figure A3.6

PSEUDO RELATIVE VELOCITY, PSV (IN/SEC) AT T = .900 SEC
PROBABILITY OF EXCEEDANCE = .50 FOR 50 YEARS

CONTOUR LEVELS OF LOG(PSV):

!	a	[	b	]	c	^	d	>
.9	1.0	1.1	1.2	1.3	1.4	1.5	1.6	1.7

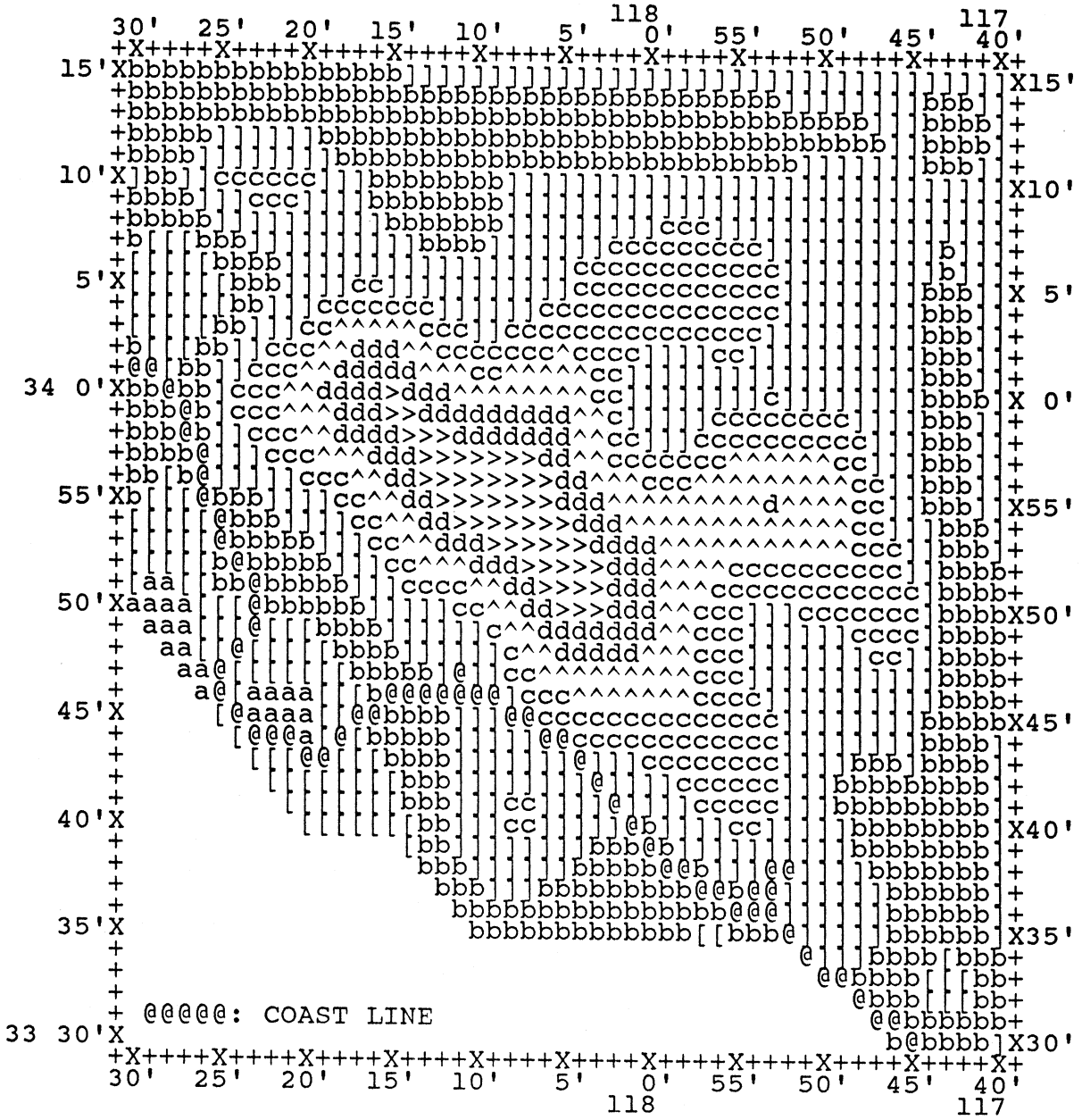

Figure A3.7

PSEUDO RELATIVE VELOCITY, PSV (IN/SEC) AT T = 1.600 SEC
PROBABILITY OF EXCEEDANCE = .50 FOR 50 YEARS

CONTOUR LEVELS OF LOG(PSV):

! .9 a 1.0 [1.1 b 1.2] 1.3 c 1.4 ^ 1.5 d 1.6 > 1.7 e 1.8

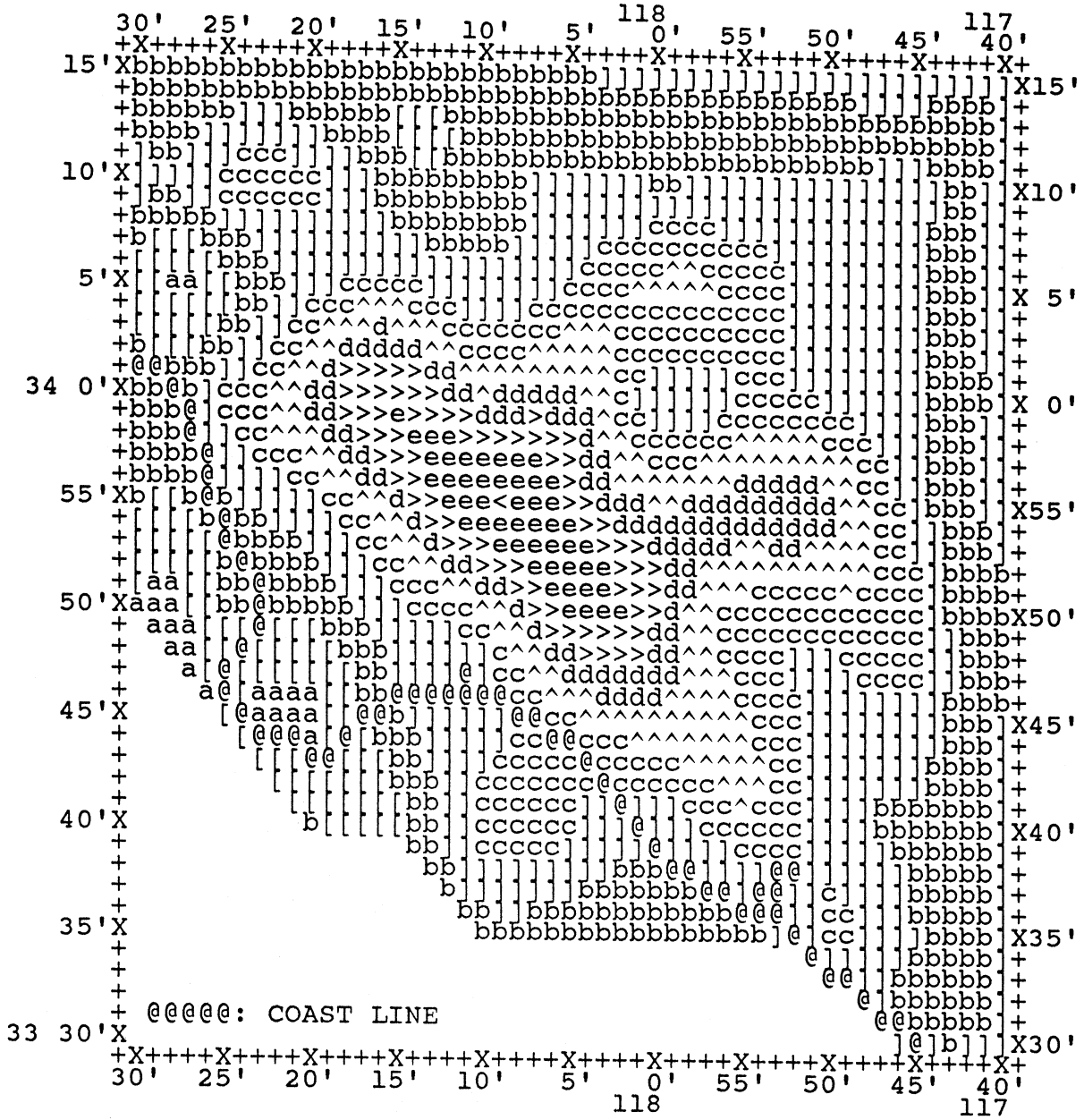

Figure A3.8

PSEUDO RELATIVE VELOCITY, PSV (IN/SEC) AT T = 2.800 SEC
PROBABILITY OF EXCEEDANCE = .50 FOR 50 YEARS

CONTOUR LEVELS OF LOG(PSV):

!	a	[	b	]	c	^	d	>	e	<
.9	1.0	1.1	1.2	1.3	1.4	1.5	1.6	1.7	1.8	1.9

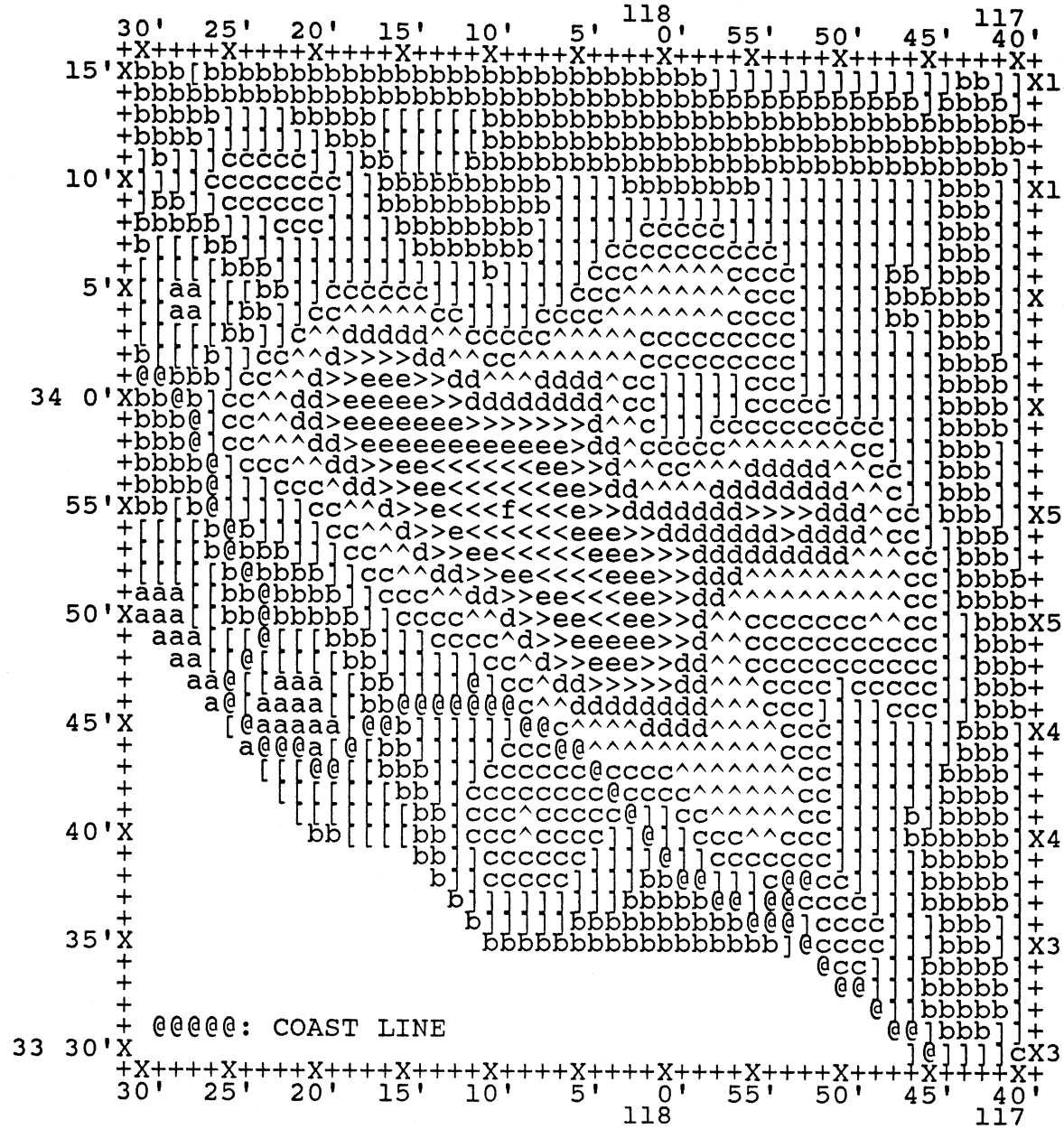

Figure A3.9

PSEUDO RELATIVE VELOCITY, PSV (IN/SEC) AT T = 4.400 SEC
PROBABILITY OF EXCEEDANCE = .50 FOR 50 YEARS

CONTOUR LEVELS OF LOG(PSV):

9	!	a	[	b	]	c	^	d	>	e
.8	.9	1.0	1.1	1.2	1.3	1.4	1.5	1.6	1.7	1.8

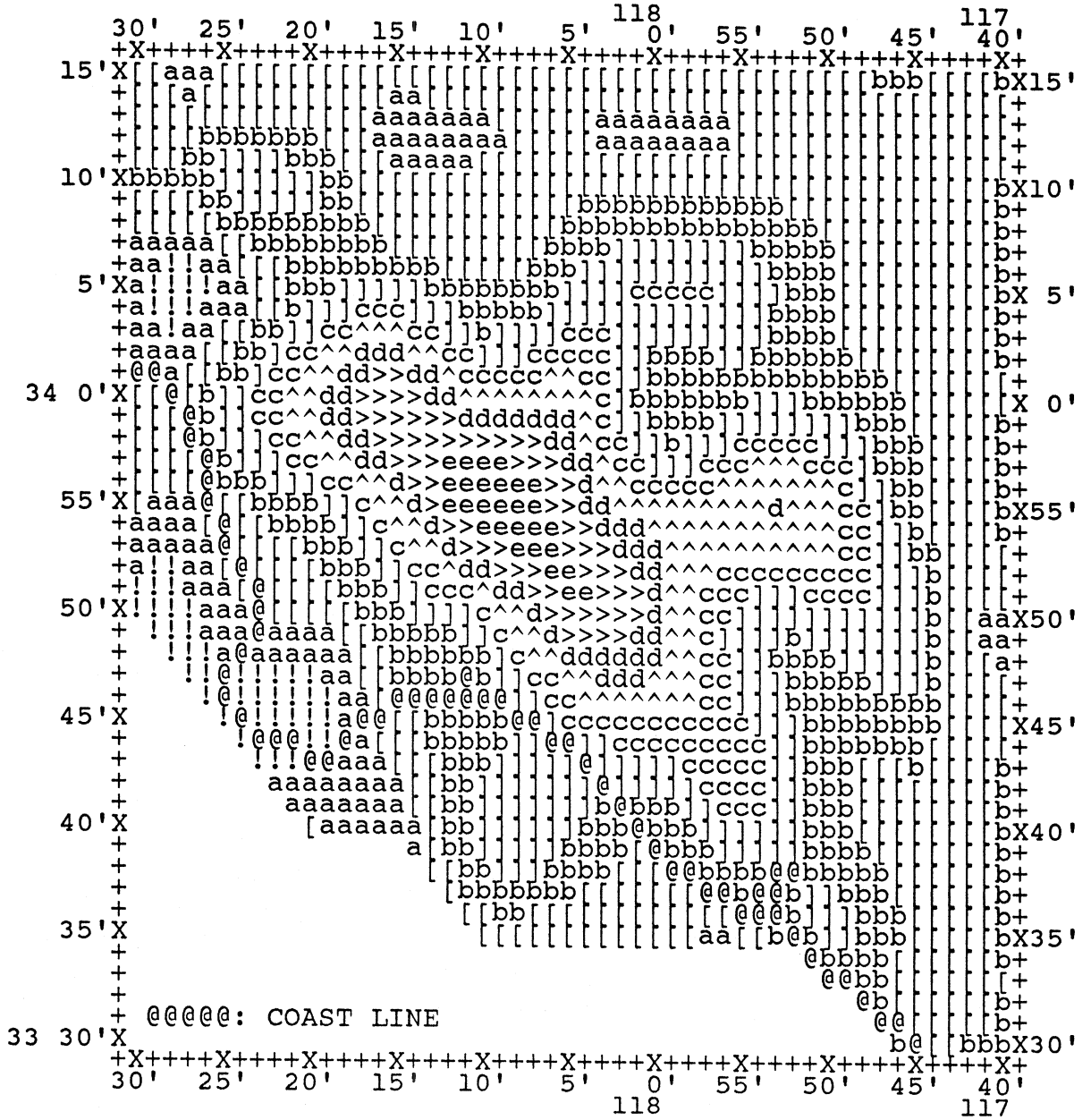

Figure A3.10

PSEUDO RELATIVE VELOCITY, PSV (IN/SEC) AT T = 7.500 SEC
PROBABILITY OF EXCEEDANCE = .50 FOR 50 YEARS

CONTOUR LEVELS OF LOG(PSV):

8	~	9	!	a	[	b	]	c	^	d
.6	.7	.8	.9	1.0	1.1	1.2	1.3	1.4	1.5	1.6

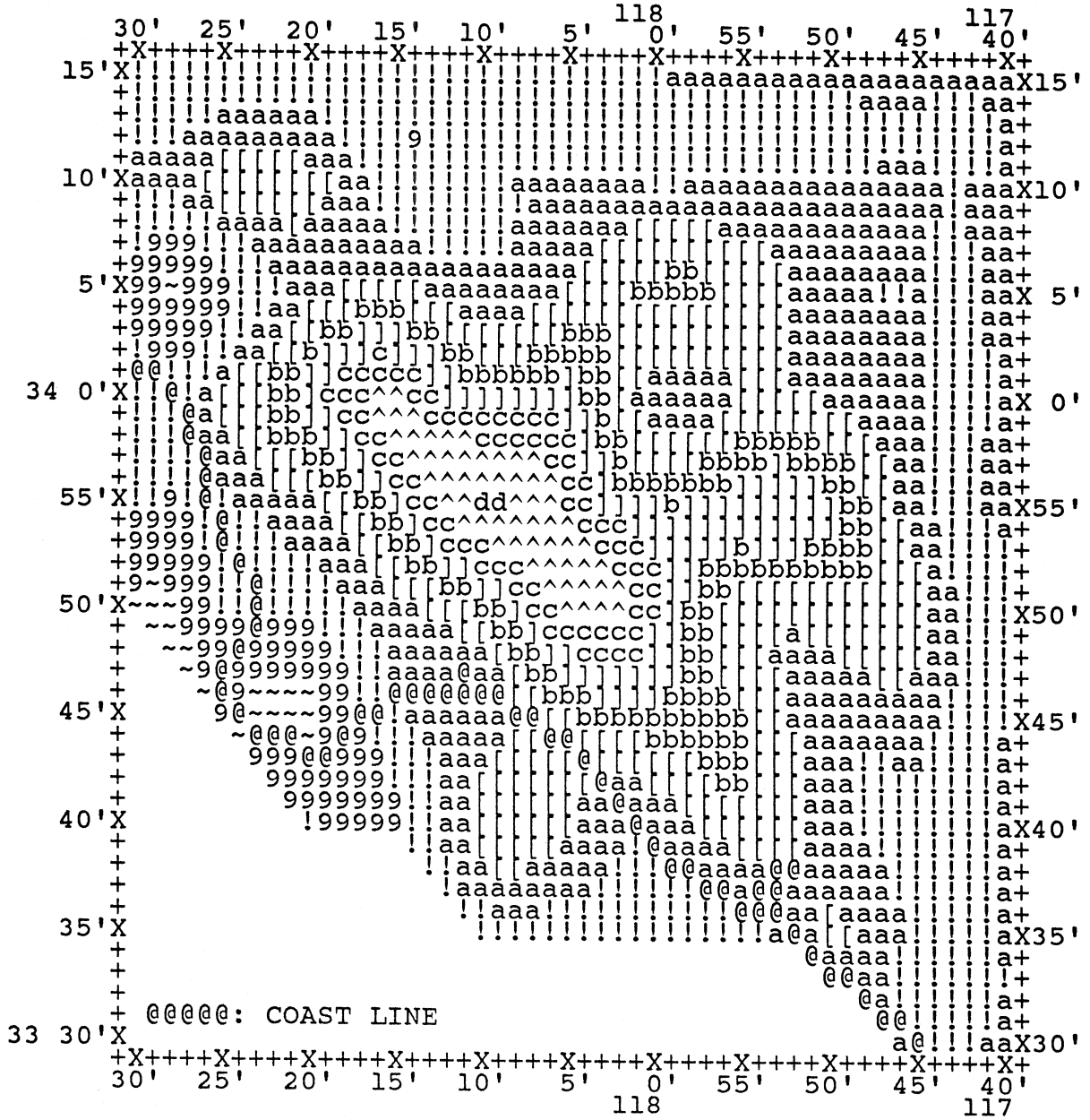

Figure A3.11

PSEUDO RELATIVE VELOCITY, PSV (IN/SEC) AT T = .040 SEC
PROBABILITY OF EXCEEDANCE = .10 FOR 50 YEARS

CONTOUR LEVELS OF LOG(PSV):

; -.1 5 .0 | .1 6 - .2 .3 7 / .4 .5 8 ~ .6 .7

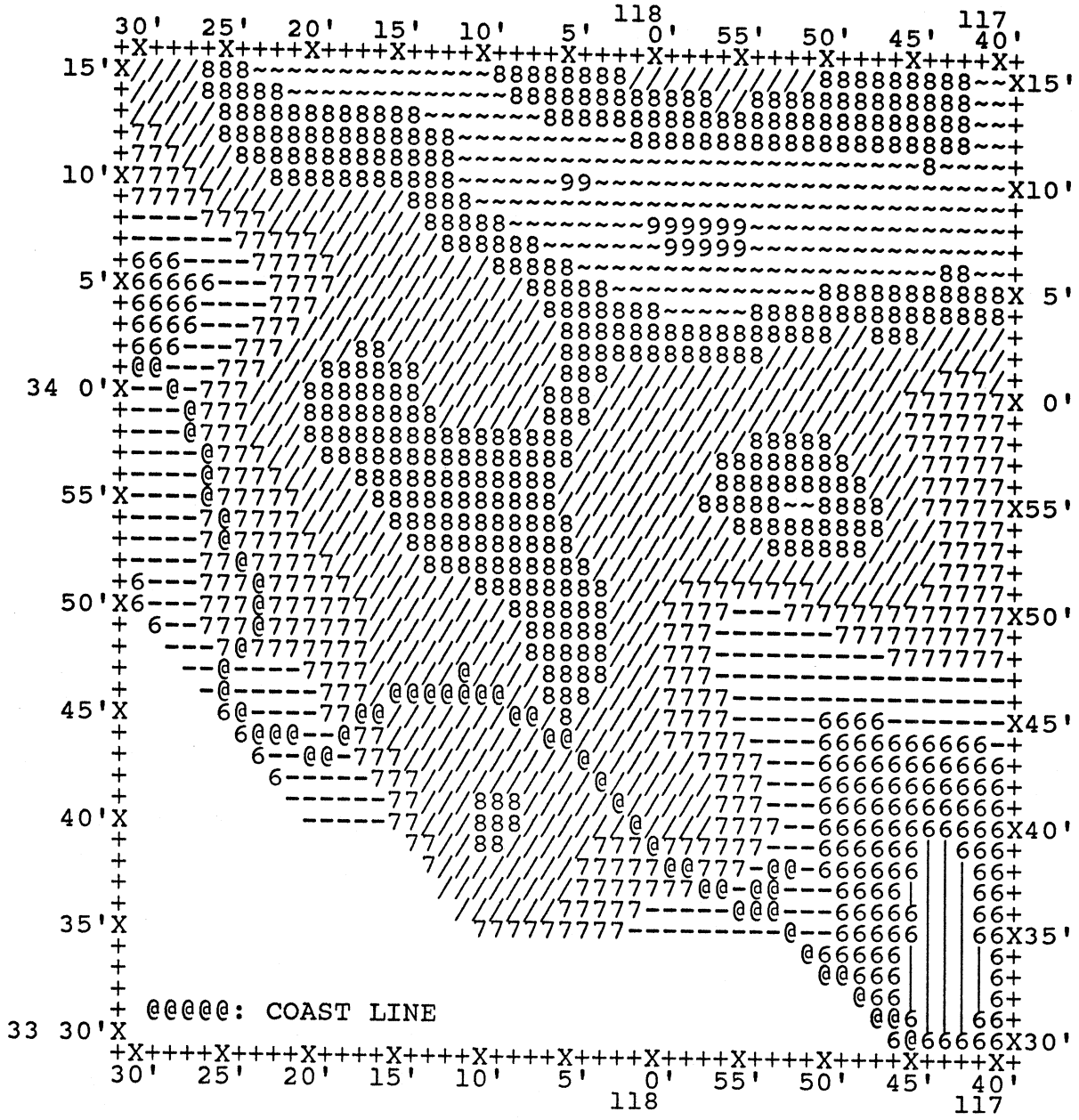

Figure A4.1

PSEUDO RELATIVE VELOCITY, PSV (IN/SEC) AT T = .065 SEC
PROBABILITY OF EXCEEDANCE = .10 FOR 50 YEARS

CONTOUR LEVELS OF LOG(PSV):

7	/	8	~	9	!	a
.4	.5	.6	.7	.8	.9	1.0

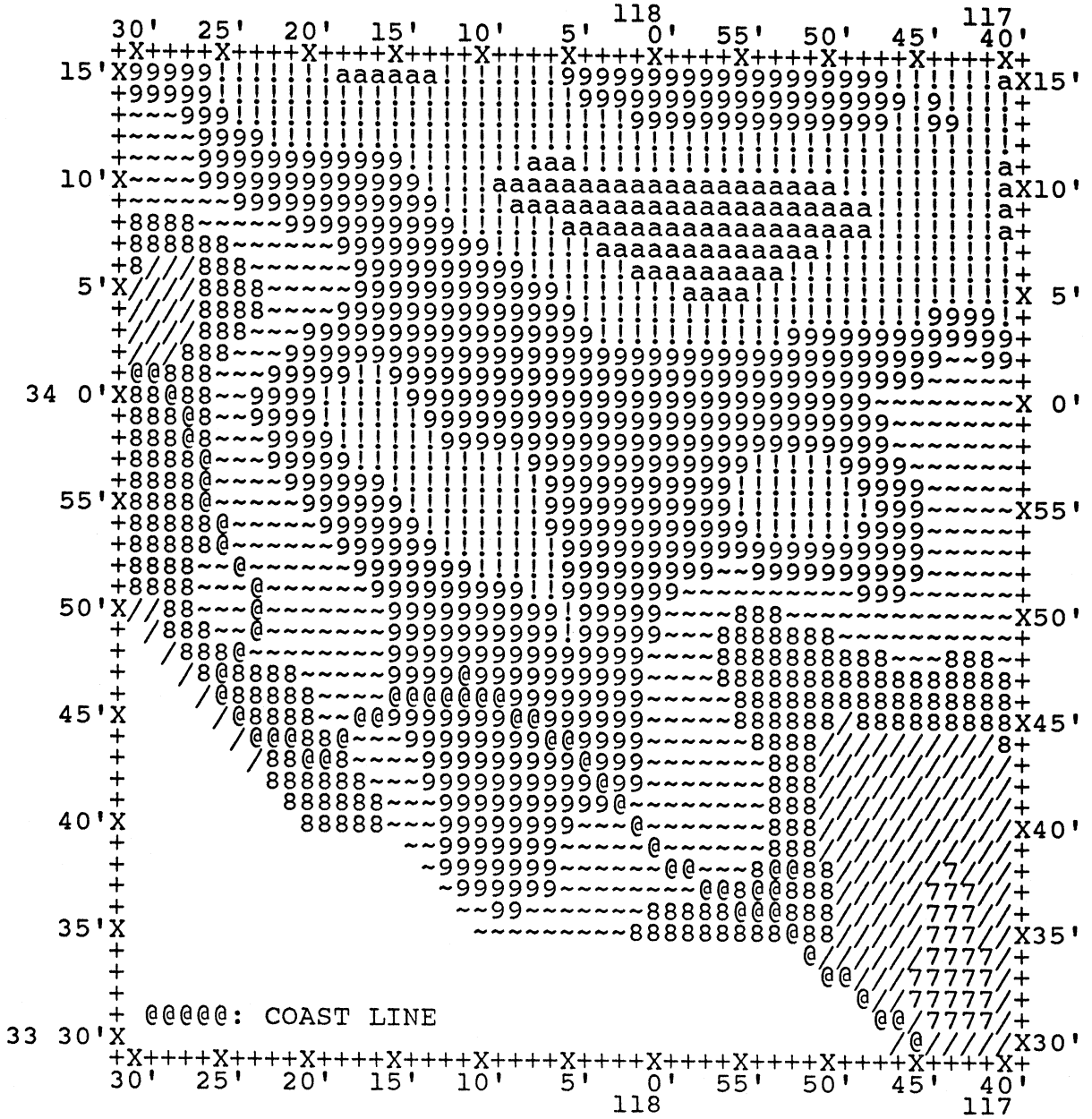

Figure A4.2

PSEUDO RELATIVE VELOCITY, PSV (IN/SEC) AT T = .110 SEC
PROBABILITY OF EXCEEDANCE = .10 FOR 50 YEARS

CONTOUR LEVELS OF LOG(PSV):

8	~	9	!	a	[	b
.6	.7	.8	.9	1.0	1.1	1.2

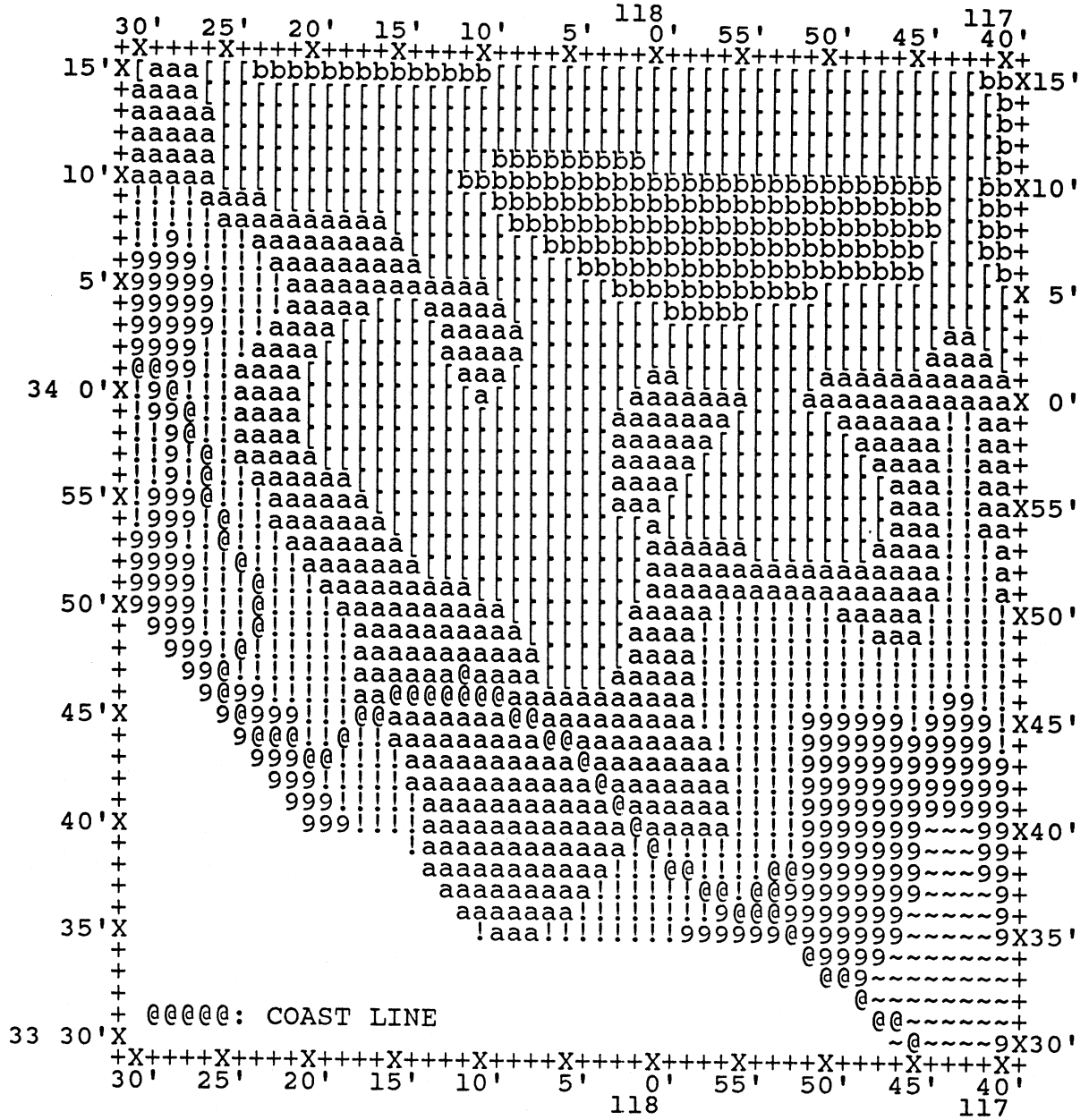

Figure A4.3

PSEUDO RELATIVE VELOCITY, PSV (IN/SEC) AT T = .190 SEC
PROBABILITY OF EXCEEDANCE = .10 FOR 50 YEARS

CONTOUR LEVELS OF LOG(PSV):

!	a	[	b	]	c
.9	1.0	1.1	1.2	1.3	1.4

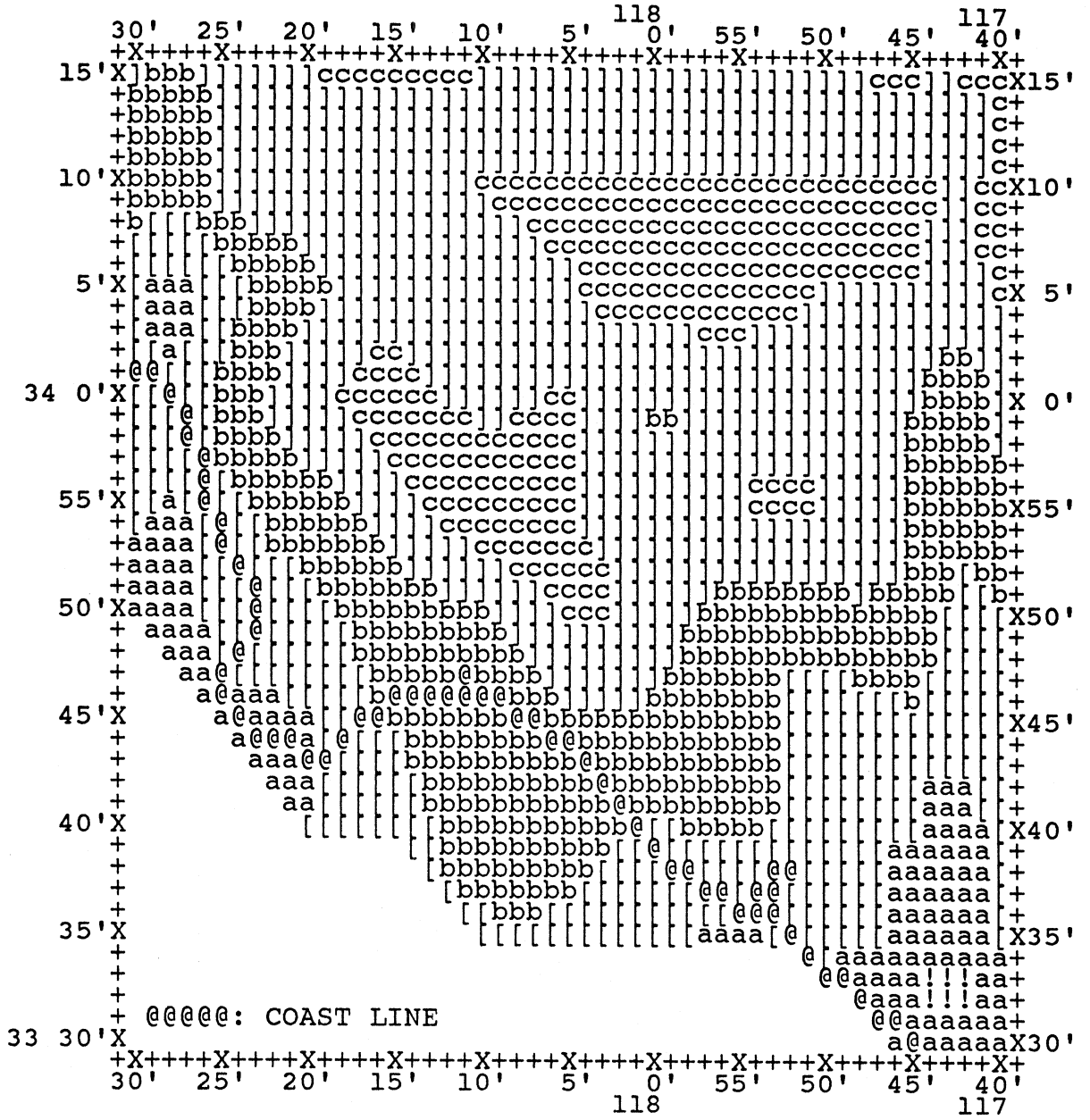

Figure A4.4

PSEUDO RELATIVE VELOCITY, PSV (IN/SEC) AT T = .340 SEC
PROBABILITY OF EXCEEDANCE = .10 FOR 50 YEARS

CONTOUR LEVELS OF LOG(PSV):

[1.1 b 1.2] 1.3 c 1.4 ^ 1.5 d 1.6 > 1.7

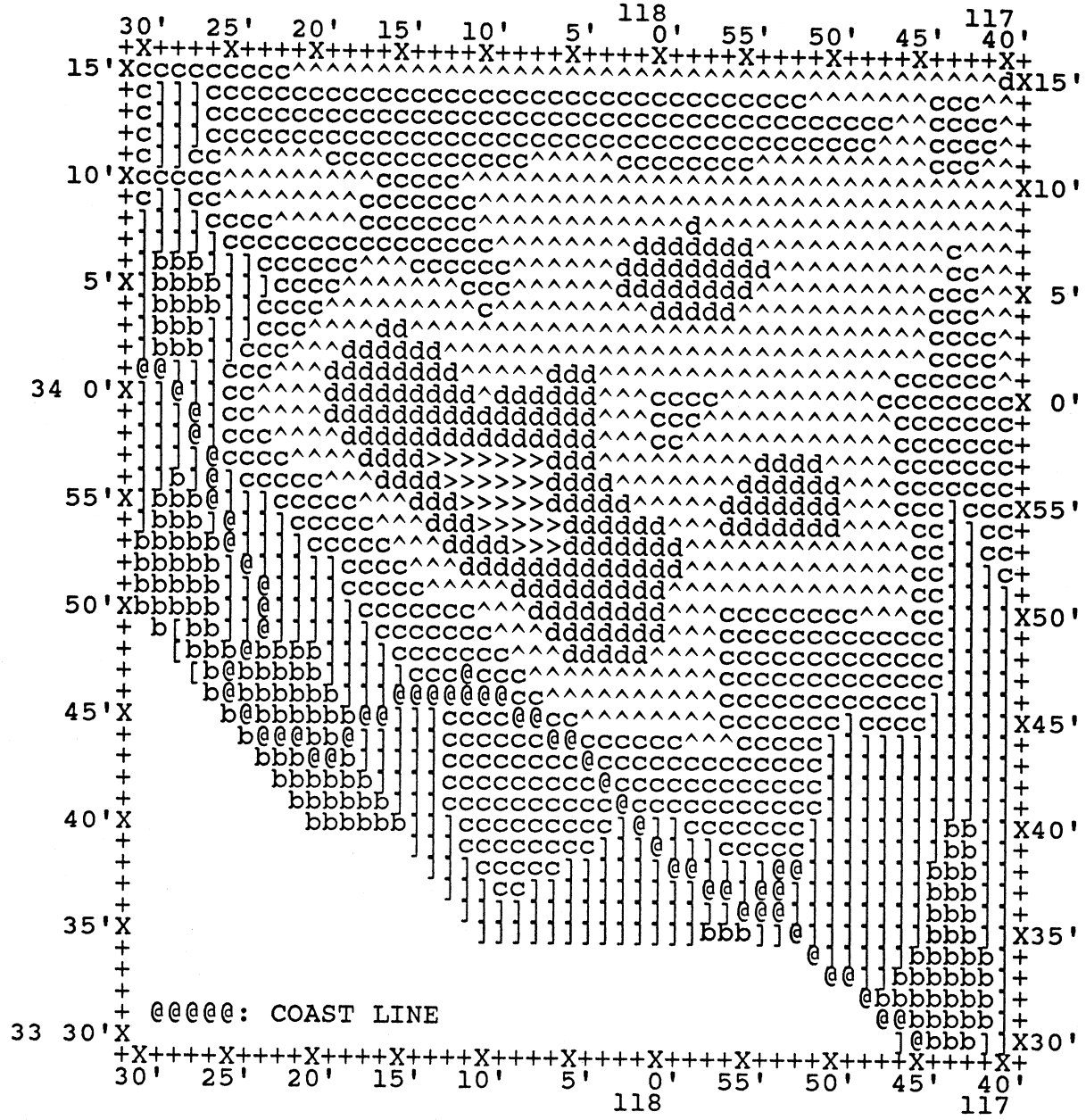

Figure A4.5

PSEUDO RELATIVE VELOCITY, PSV (IN/SEC) AT T = .500 SEC
PROBABILITY OF EXCEEDANCE = .10 FOR 50 YEARS

CONTOUR LEVELS OF LOG(PSV):

[1.1 b 1.2] 1.3 c 1.4 ^ 1.5 d 1.6 > 1.7 e 1.8

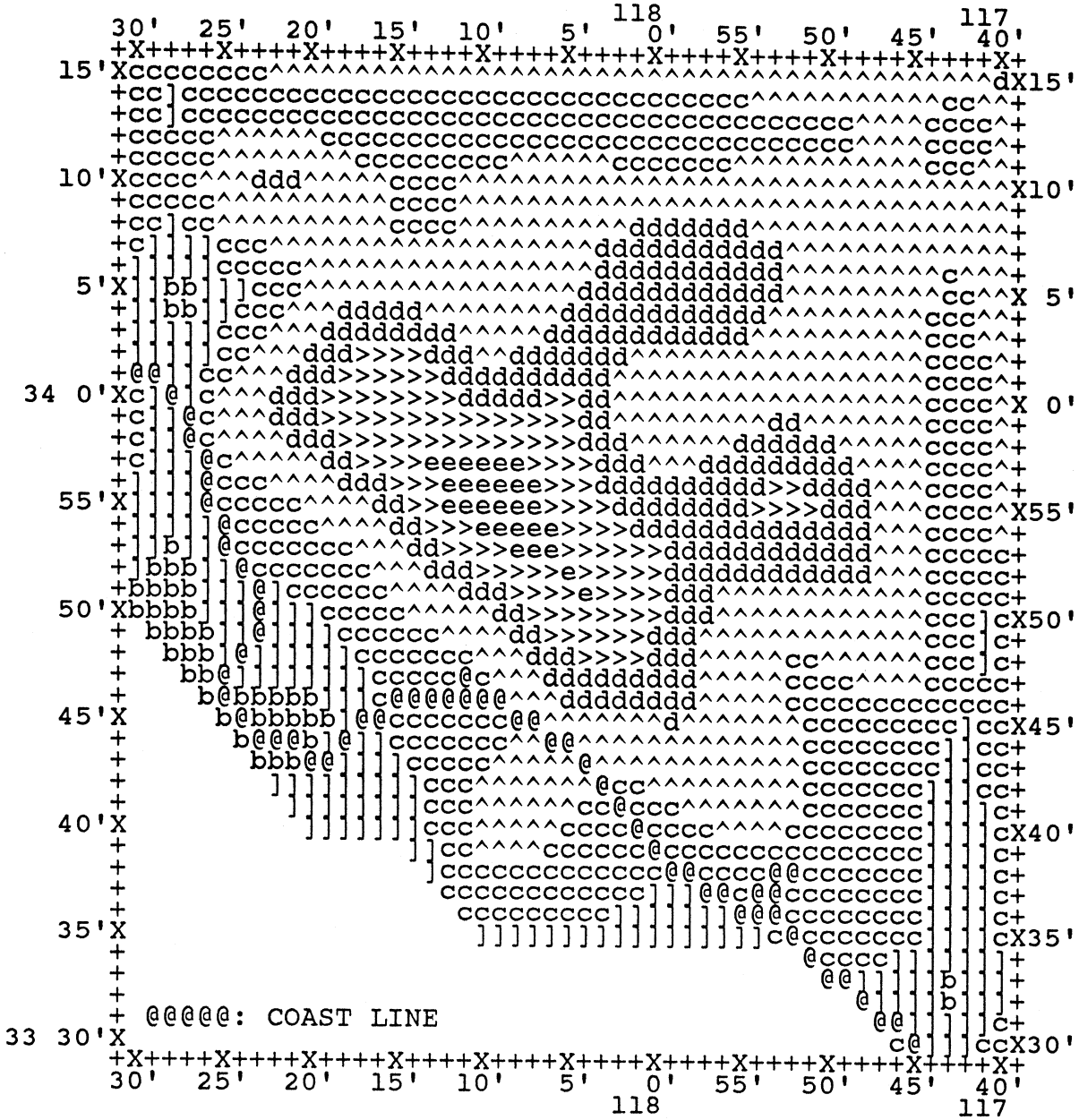

Figure A4.6

PSEUDO RELATIVE VELOCITY, PSV (IN/SEC) AT T = .900 SEC
PROBABILITY OF EXCEEDANCE = .10 FOR 50 YEARS

CONTOUR LEVELS OF LOG(PSV):

b 1.2] 1.3 c 1.4 ^ 1.5 d 1.6 > 1.7 e 1.8 < 1.9 f 2.0

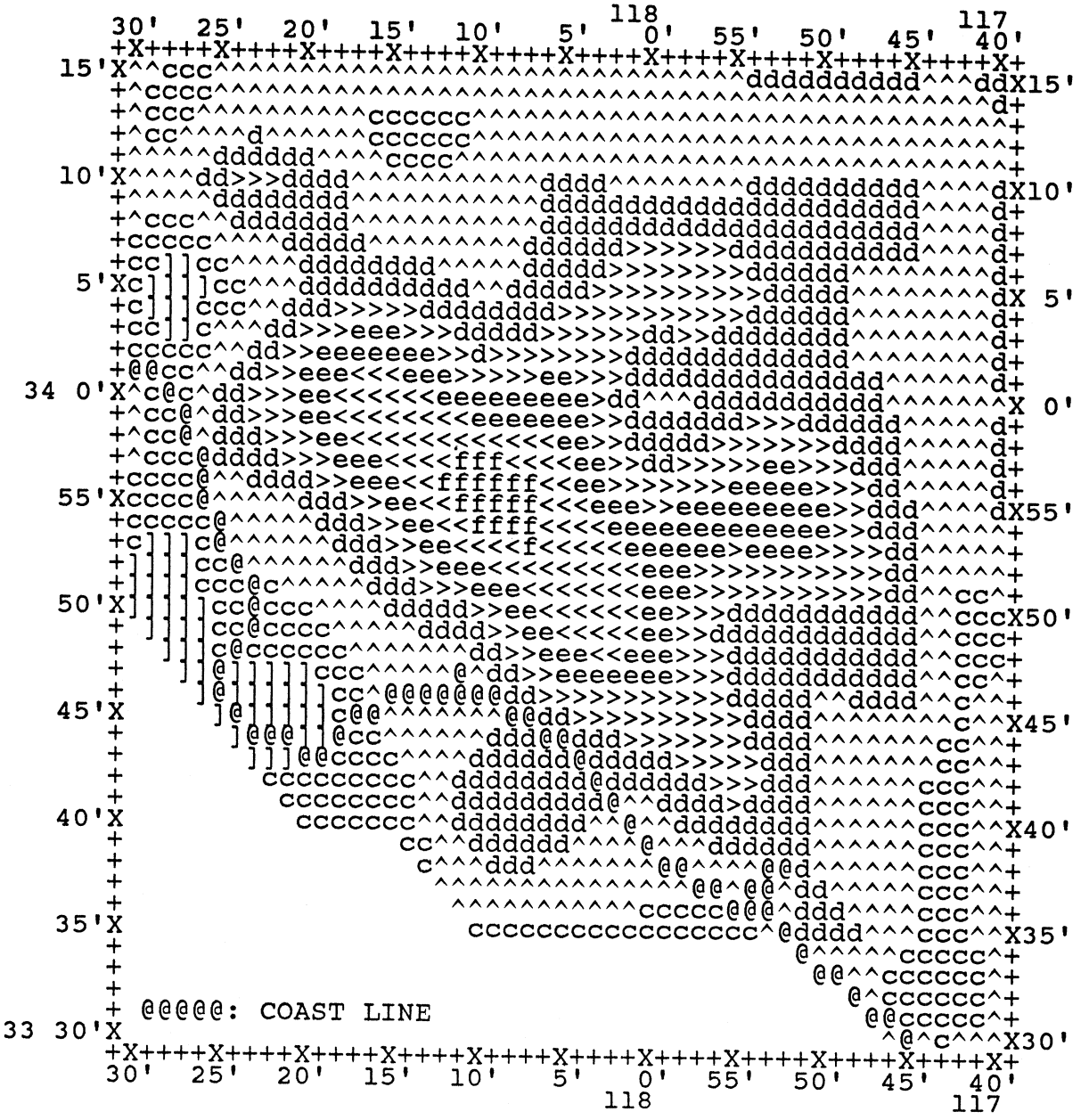

Figure A4.7

PSEUDO RELATIVE VELOCITY, PSV (IN/SEC) AT T = 1.600 SEC
PROBABILITY OF EXCEEDANCE = .10 FOR 50 YEARS

CONTOUR LEVELS OF LOG(PSV):

b	]	c	^	d	>	e	<	f	\
1.2	1.3	1.4	1.5	1.6	1.7	1.8	1.9	2.0	2.1

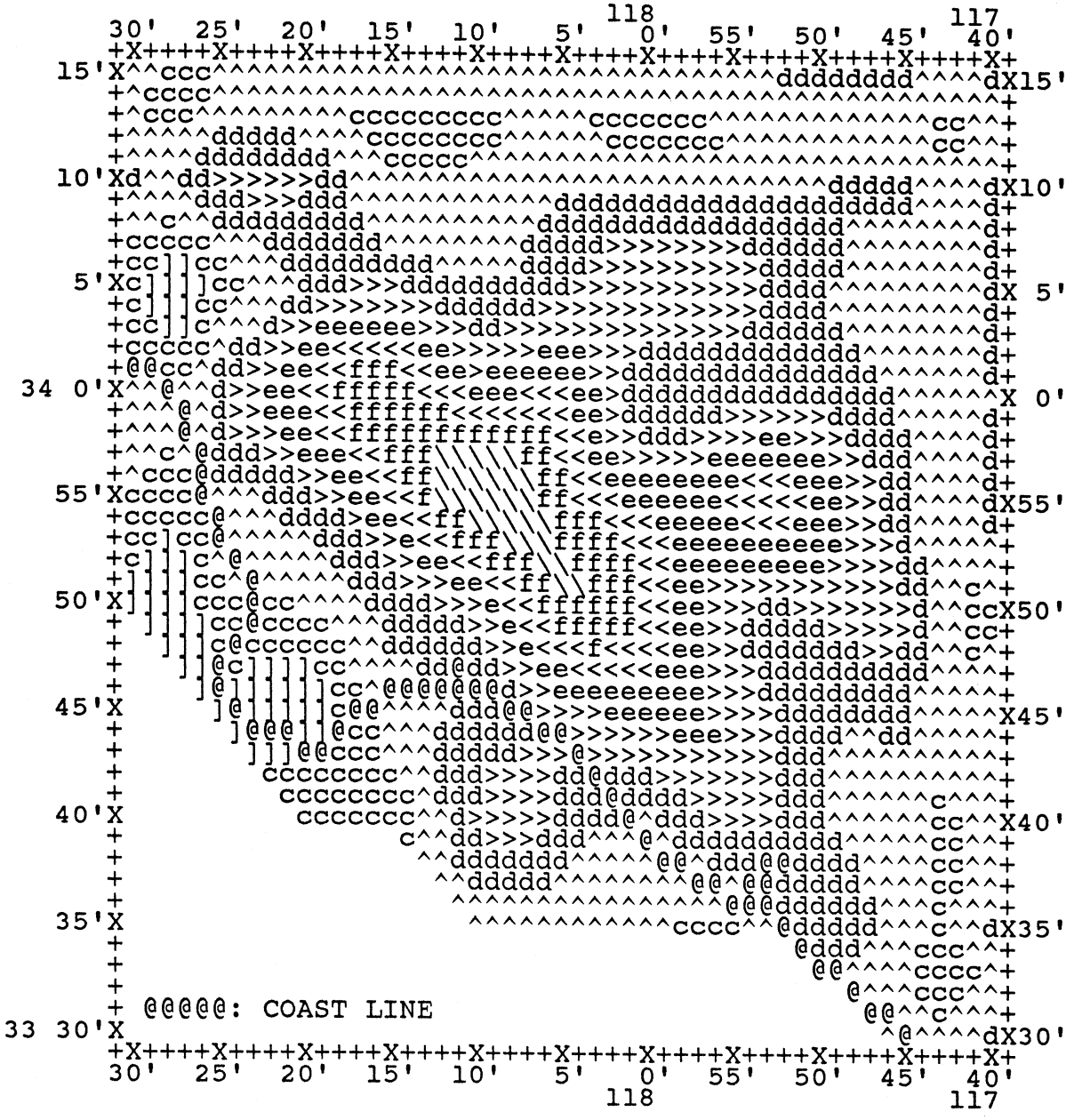

Figure A4.8

PSEUDO RELATIVE VELOCITY, PSV (IN/SEC) AT T = 2.800 SEC
PROBABILITY OF EXCEEDANCE = .10 FOR 50 YEARS

CONTOUR LEVELS OF LOG(PSV):

b 1.2] 1.3 c 1.4 ^ 1.5 d 1.6 > 1.7 e 1.8 < 1.9 f 2.0 \ 2.1 g 2.2

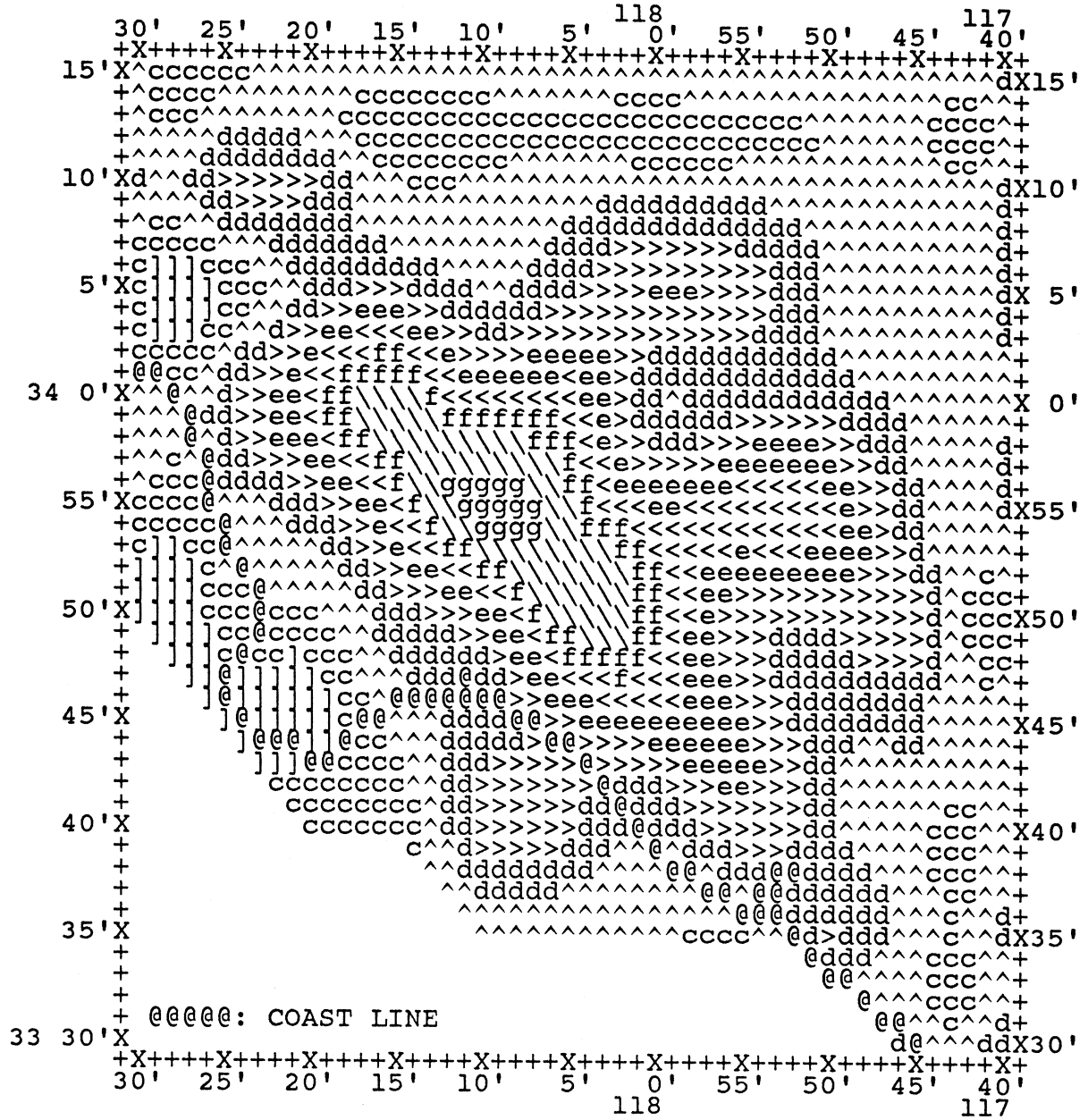

Figure A4.9

PSEUDO RELATIVE VELOCITY, PSV (IN/SEC) AT T = 4.400 SEC
PROBABILITY OF EXCEEDANCE = .10 FOR 50 YEARS

CONTOUR LEVELS OF LOG(PSV):

a 1.0 [1.1 b 1.2] 1.3 c 1.4 ^ 1.5 d 1.6 > 1.7 e 1.8 < 1.9 f 2.0 \ 2.1

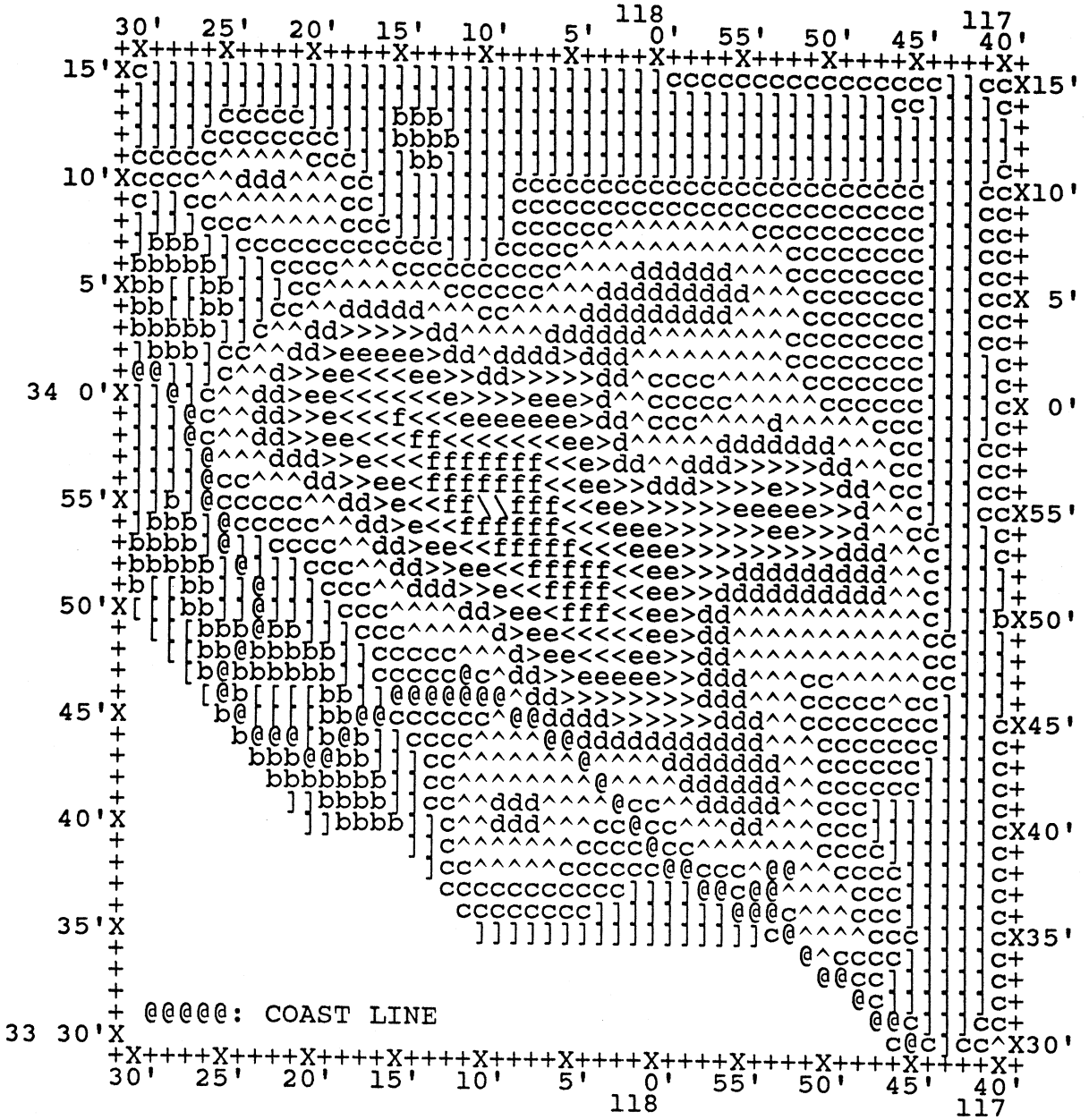

Figure A4.10

PSEUDO RELATIVE VELOCITY, PSV (IN/SEC) AT T = 7.500 SEC
PROBABILITY OF EXCEEDANCE = .10 FOR 50 YEARS

CONTOUR LEVELS OF LOG(PSV):

9	!	a	[	b	]	c	^	d	>	e
.8	.9	1.0	1.1	1.2	1.3	1.4	1.5	1.6	1.7	1.8

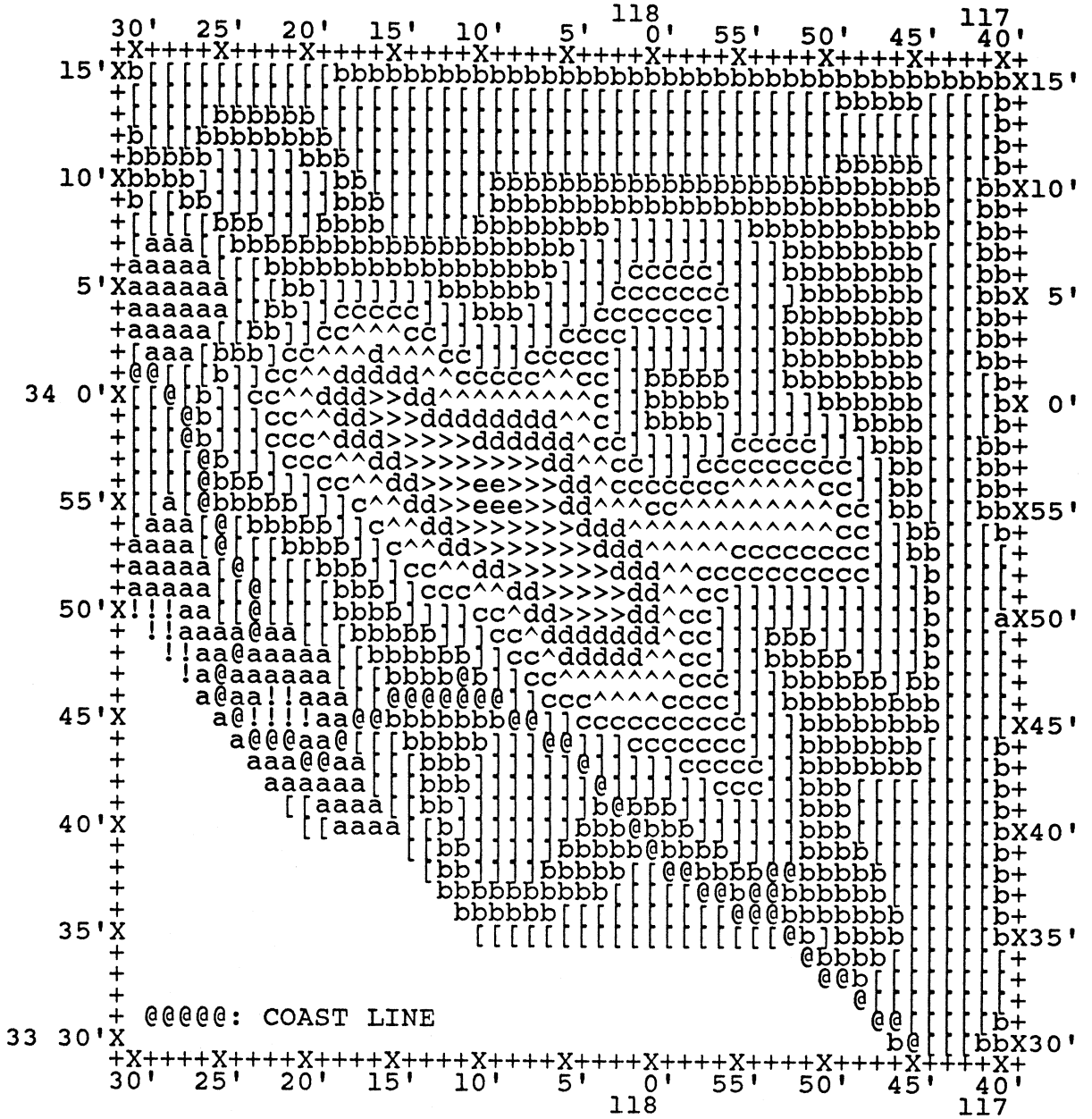

Figure A4.11

PSEUDO RELATIVE VELOCITY, PSV (IN/SEC) AT T = .040 SEC
PROBABILITY OF EXCEEDANCE = .01 FOR 50 YEARS

CONTOUR LEVELS OF LOG(PSV):

7	/	8	~	9	!	a	[
.4	.5	.6	.7	.8	.9	1.0	1.1

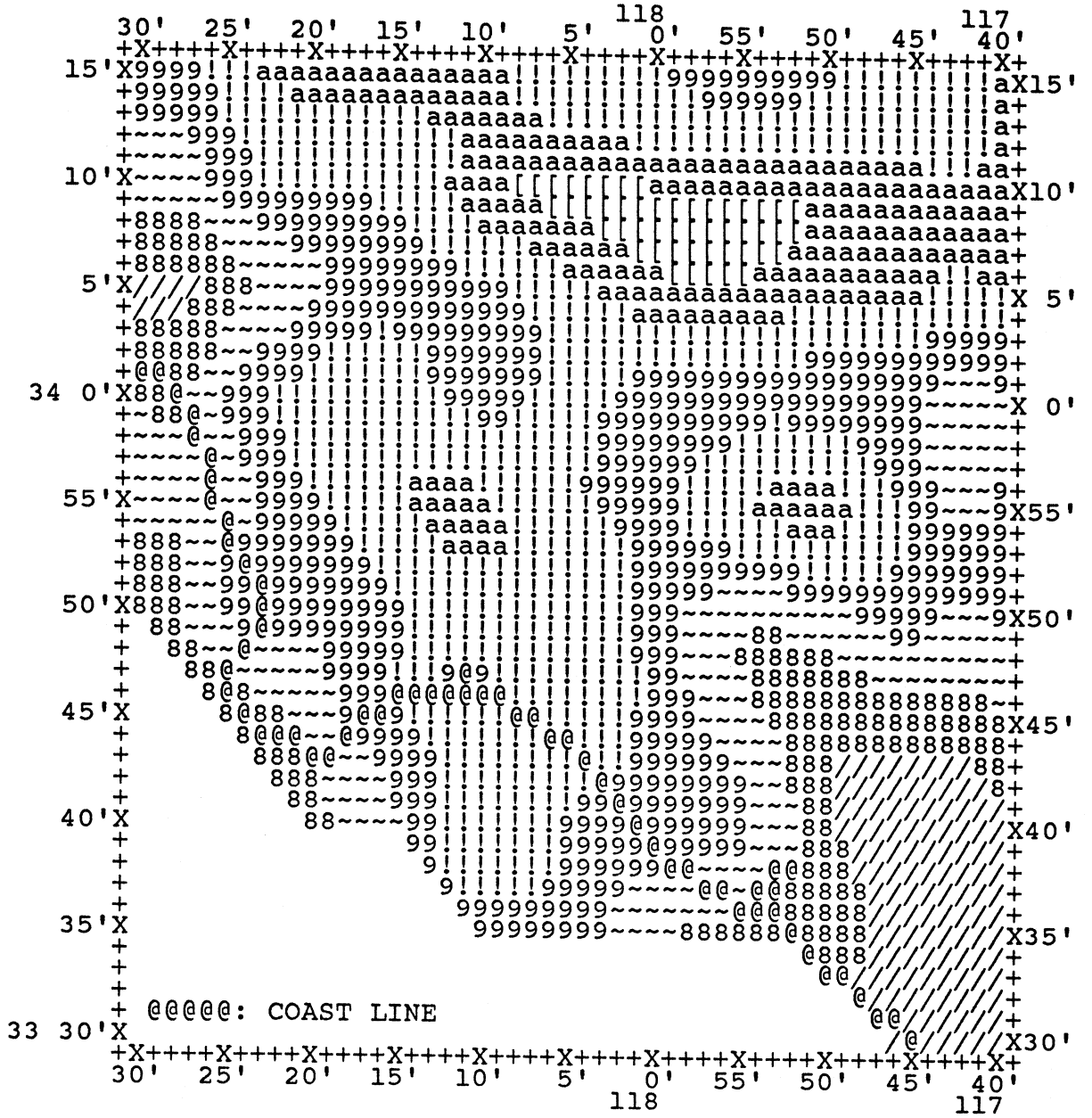

Figure A5.1

PSEUDO RELATIVE VELOCITY, PSV (IN/SEC) AT T = .065 SEC
PROBABILITY OF EXCEEDANCE = .01 FOR 50 YEARS

CONTOUR LEVELS OF LOG(PSV):

8	~	9	!	a	[	b	]
.6	.7	.8	.9	1.0	1.1	1.2	1.3

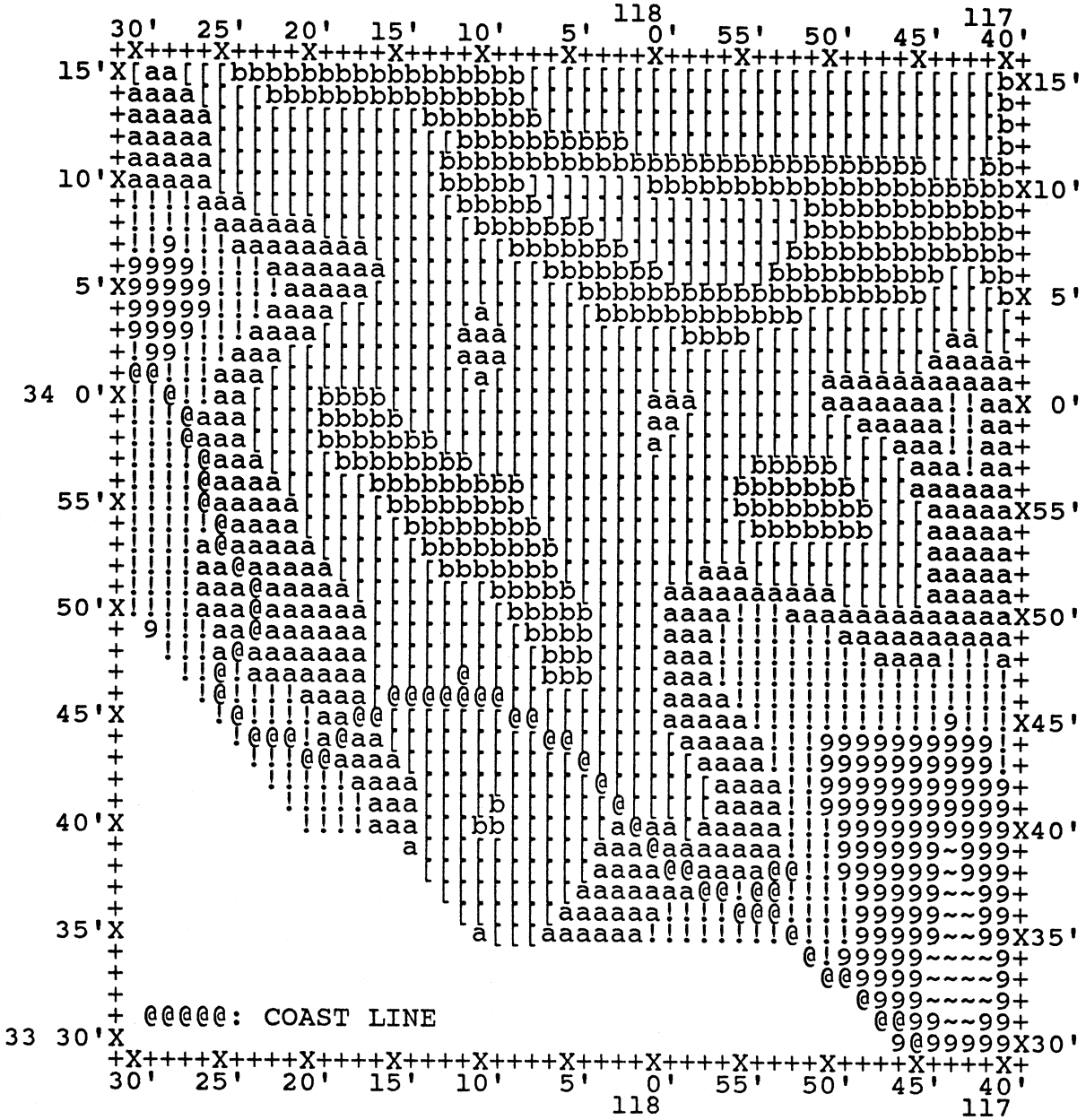

Figure A5.2

PSEUDO RELATIVE VELOCITY, PSV (IN/SEC) AT T = .110 SEC
PROBABILITY OF EXCEEDANCE = .01 FOR 50 YEARS

CONTOUR LEVELS OF LOG(PSV):

!	a	[	b	]	c	^
.9	1.0	1.1	1.2	1.3	1.4	1.5

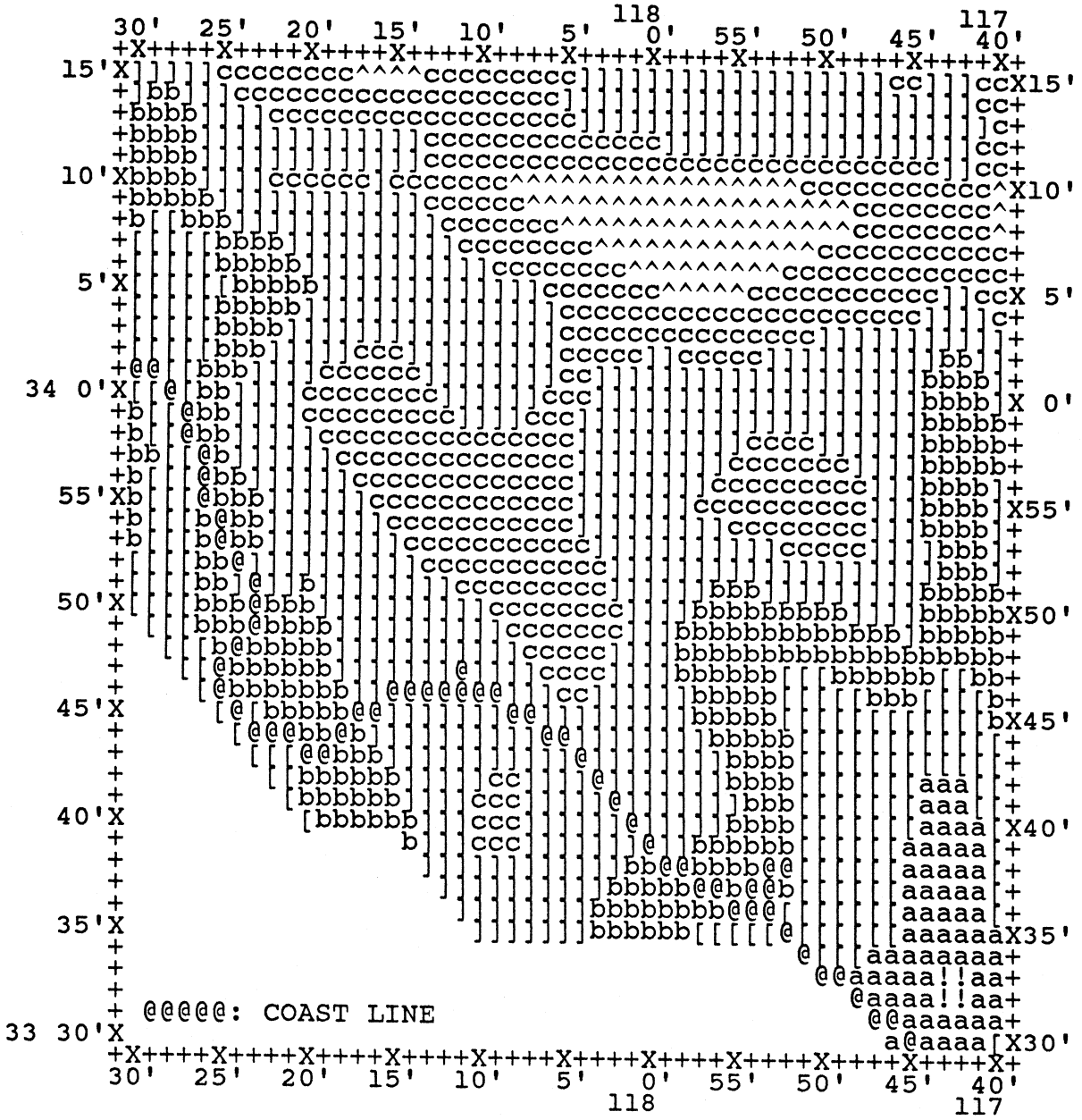

Figure A5.3

PSEUDO RELATIVE VELOCITY, PSV (IN/SEC) AT T = .190 SEC
PROBABILITY OF EXCEEDANCE = .01 FOR 50 YEARS

CONTOUR LEVELS OF LOG(PSV):

b	]	c	^	d	>
1.2	1.3	1.4	1.5	1.6	1.7

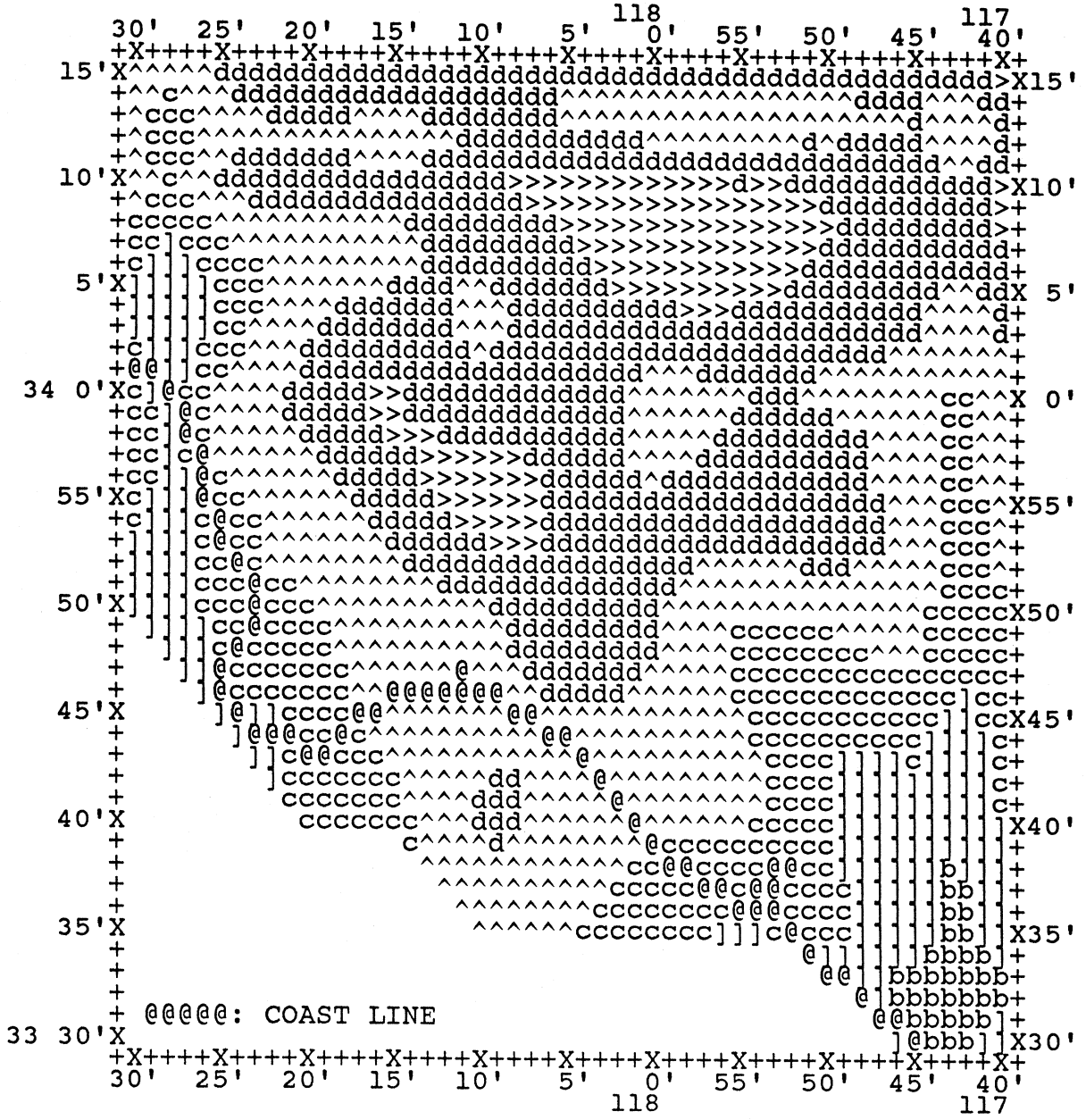

Figure A5.4

PSEUDO RELATIVE VELOCITY, PSV (IN/SEC) AT T = .340 SEC
PROBABILITY OF EXCEEDANCE = .01 FOR 50 YEARS

CONTOUR LEVELS OF LOG(PSV):

c	^	d	>	e	<
1.4	1.5	1.6	1.7	1.8	1.9

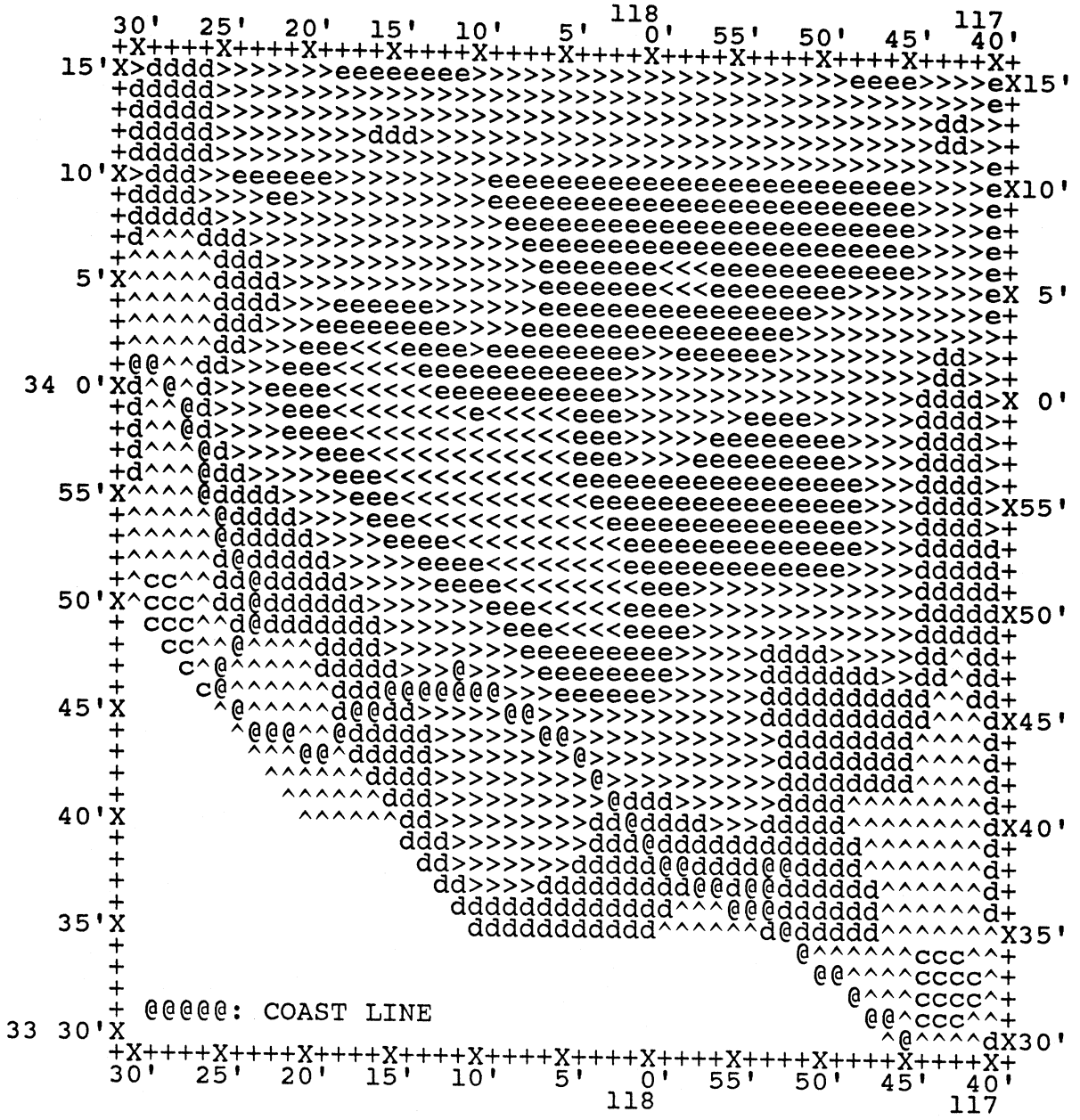

Figure A5.5

PSEUDO RELATIVE VELOCITY, PSV (IN/SEC) AT T = .500 SEC
PROBABILITY OF EXCEEDANCE = .01 FOR 50 YEARS

CONTOUR LEVELS OF LOG(PSV):

c	^	d	>	e	<	f
1.4	1.5	1.6	1.7	1.8	1.9	2.0

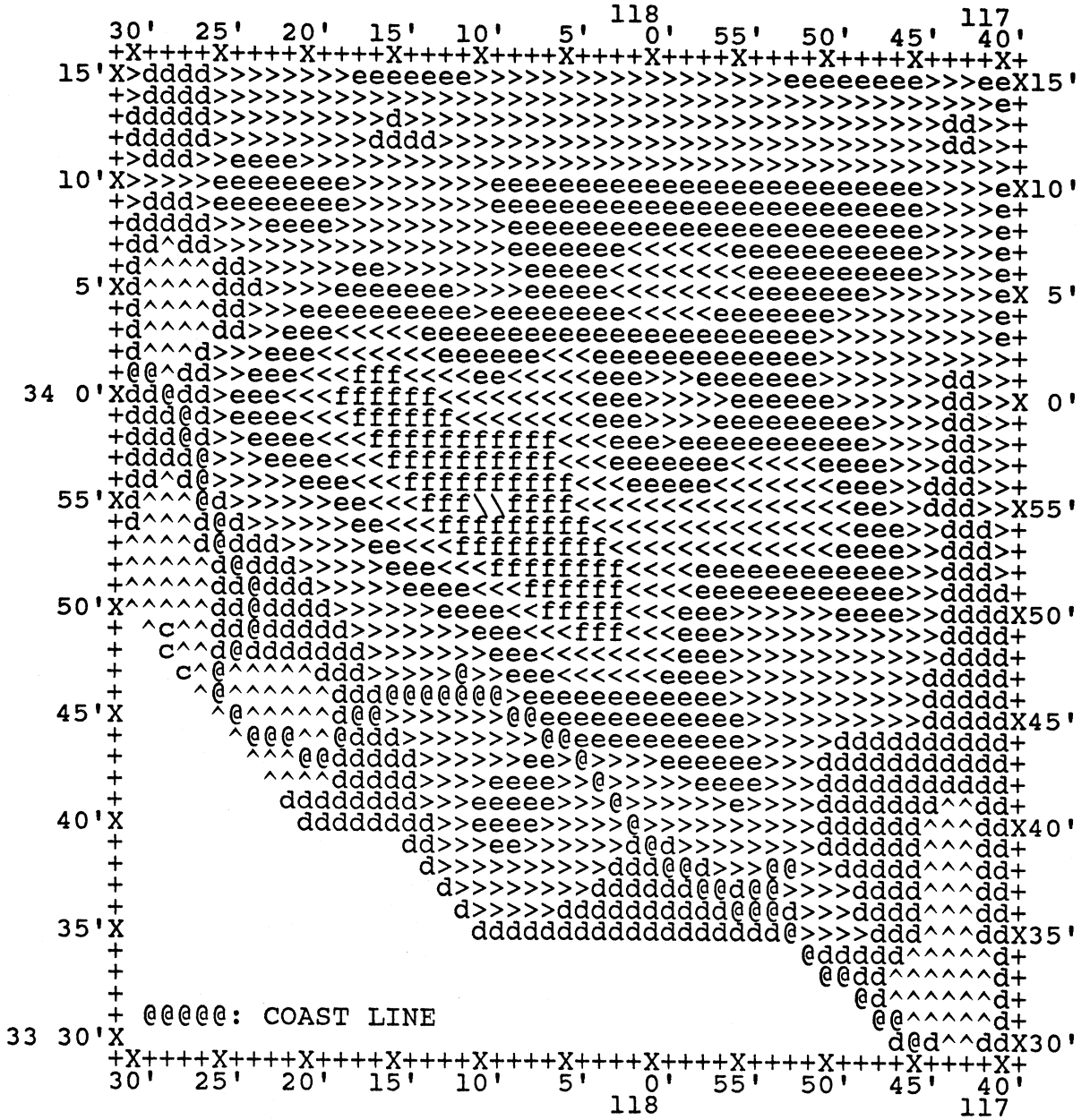

Figure A5.6

PSEUDO RELATIVE VELOCITY, PSV (IN/SEC) AT T = .900 SEC
PROBABILITY OF EXCEEDANCE = .01 FOR 50 YEARS

CONTOUR LEVELS OF LOG(PSV):

^	d	>	e	<	f	\	g
1.5	1.6	1.7	1.8	1.9	2.0	2.1	2.2

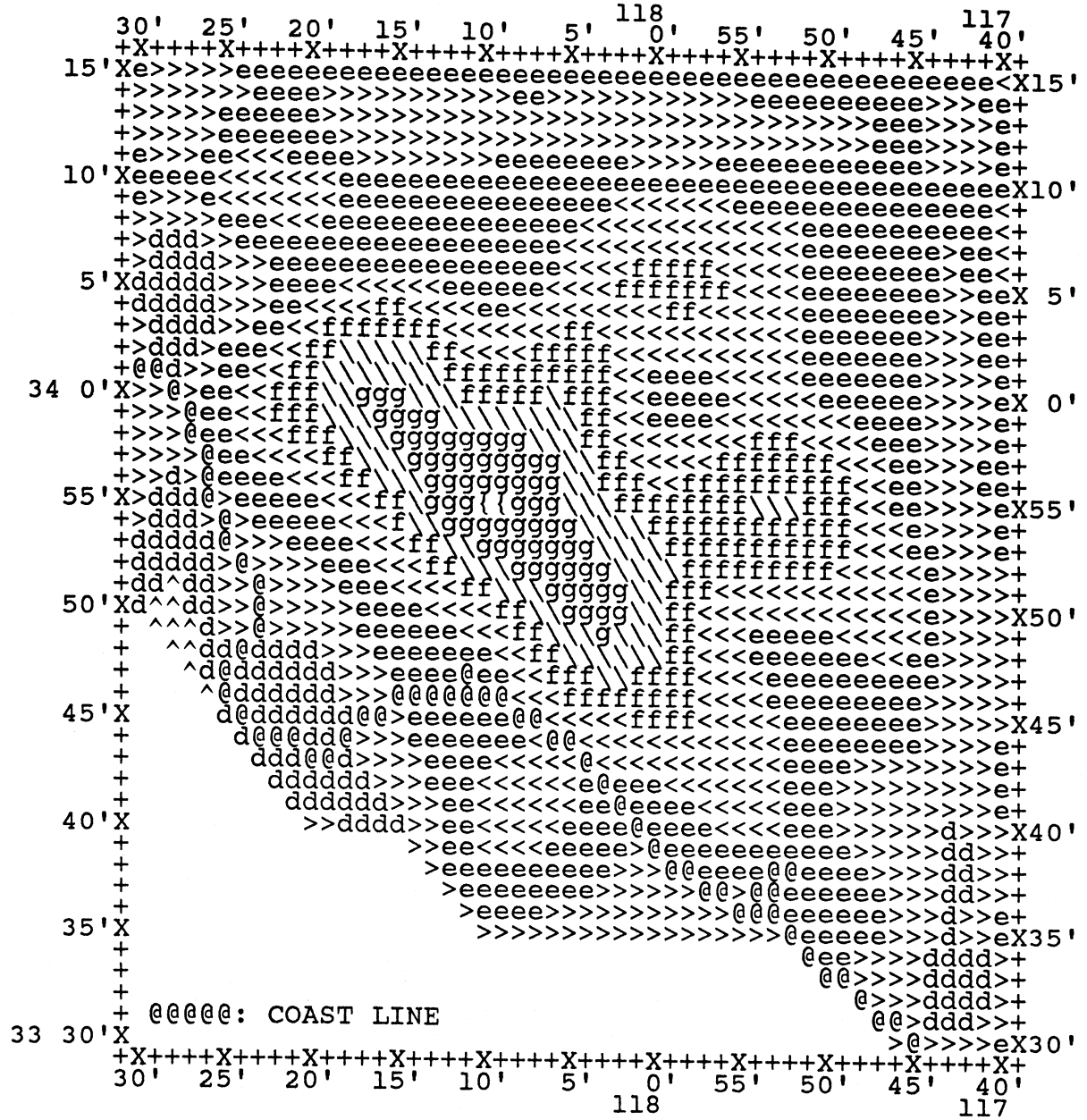

Figure A5.7

PSEUDO RELATIVE VELOCITY, PSV (IN/SEC) AT T = 1.600 SEC
PROBABILITY OF EXCEEDANCE = .01 FOR 50 YEARS

CONTOUR LEVELS OF LOG(PSV):

^	d	>	e	<	f	\	g	{	h
1.5	1.6	1.7	1.8	1.9	2.0	2.1	2.2	2.3	2.4

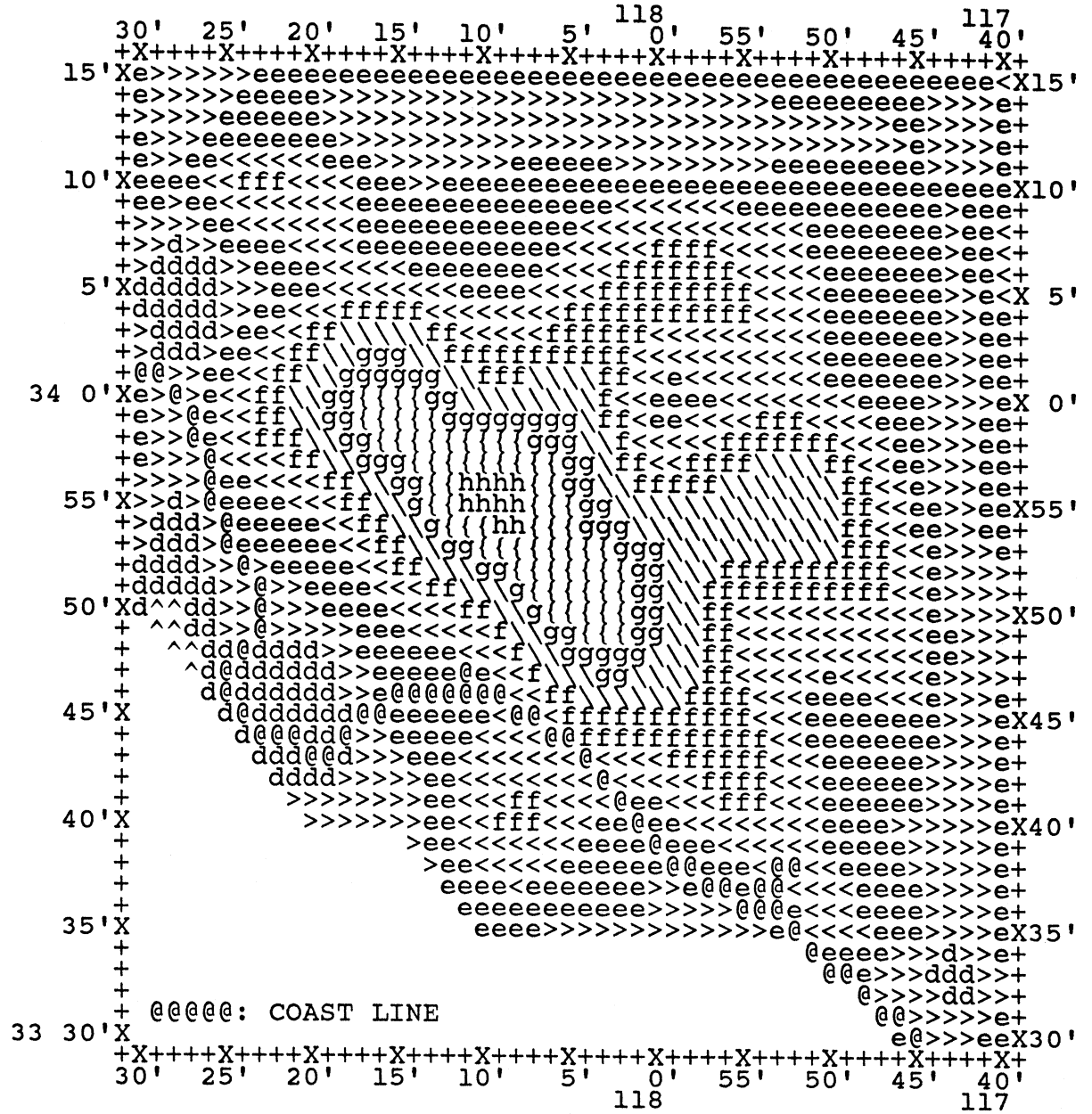

Figure A5.8

PSEUDO RELATIVE VELOCITY, PSV (IN/SEC) AT T = 2.800 SEC
PROBABILITY OF EXCEEDANCE = .01 FOR 50 YEARS

CONTOUR LEVELS OF LOG(PSV):

c	^	d	>	e	<	f	\	g	{	h	}
1.4	1.5	1.6	1.7	1.8	1.9	2.0	2.1	2.2	2.3	2.4	2.5

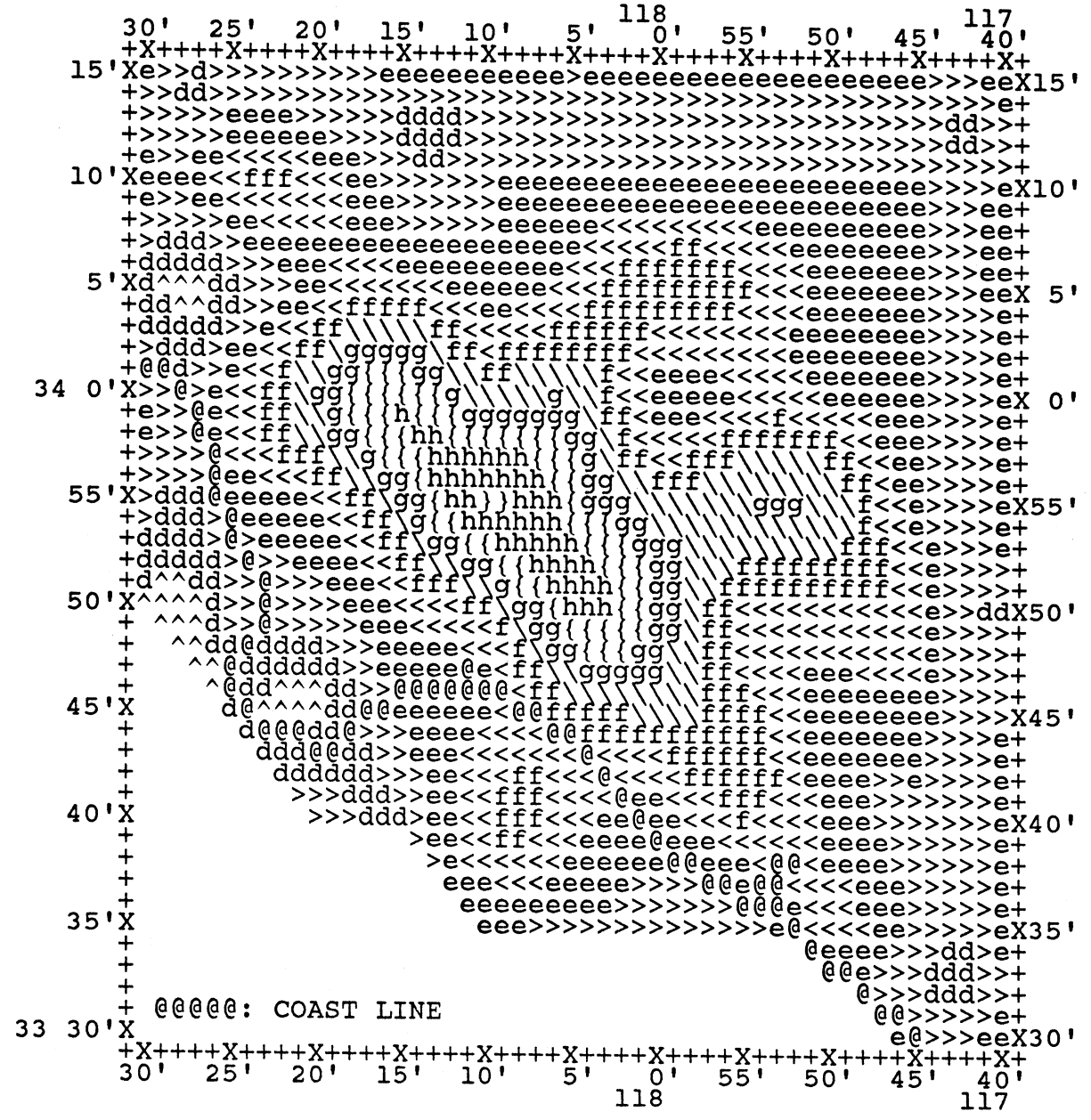

Figure A5.9

PSEUDO RELATIVE VELOCITY, PSV (IN/SEC) AT T = 4.400 SEC
PROBABILITY OF EXCEEDANCE = .01 FOR 50 YEARS

CONTOUR LEVELS OF LOG(PSV):

b 1.2] 1.3 c 1.4 ^ 1.5 d 1.6 > 1.7 e 1.8 < 1.9 f 2.0 \ 2.1 g 2.2 { 2.3

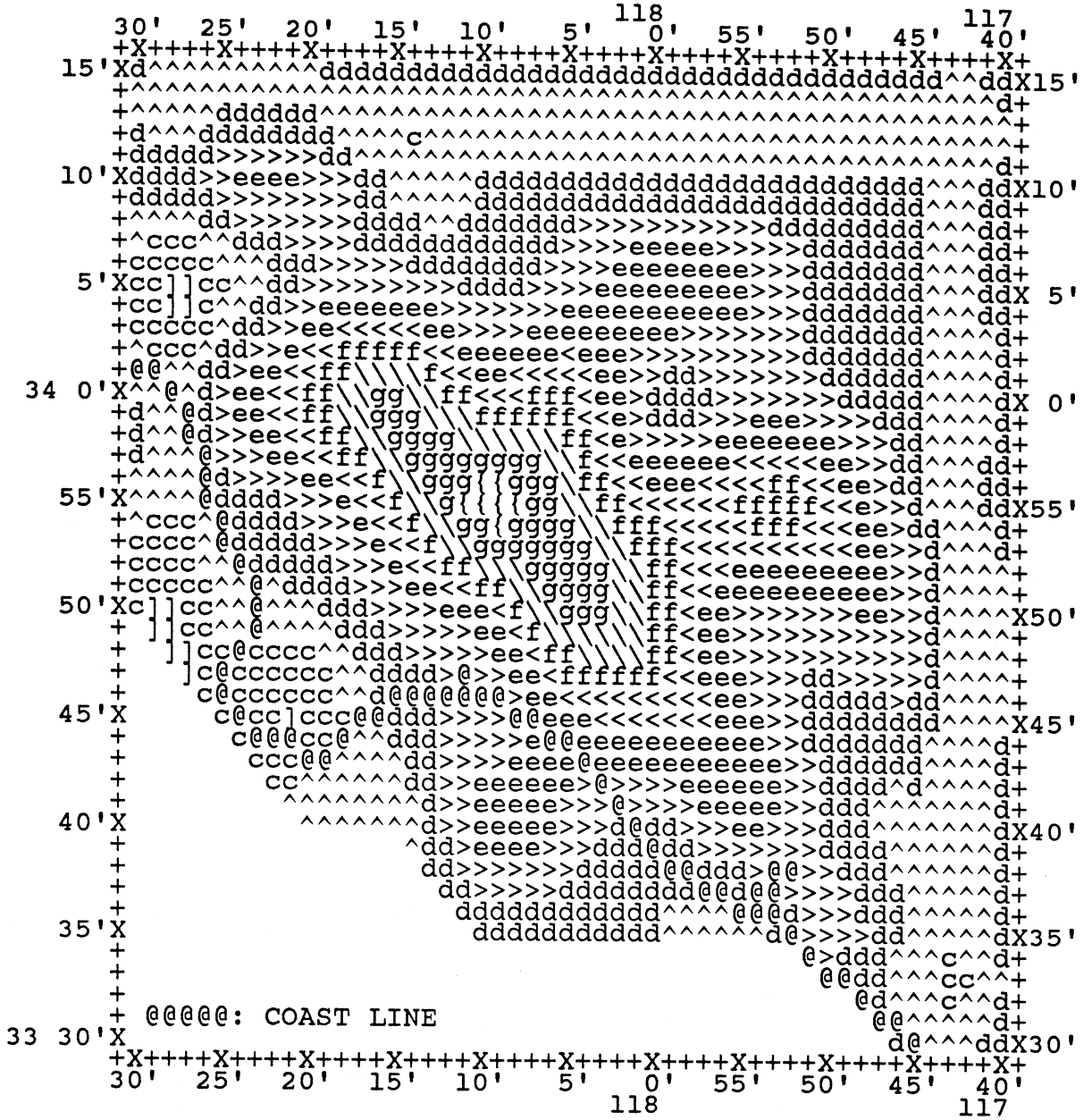

Figure A5.10

PSEUDO RELATIVE VELOCITY, PSV (IN/SEC) AT T = 7.500 SEC
PROBABILITY OF EXCEEDANCE = .01 FOR 50 YEARS

CONTOUR LEVELS OF LOG(PSV):

a	[	b	]	c	^	d	>	e	<
1.0	1.1	1.2	1.3	1.4	1.5	1.6	1.7	1.8	1.9

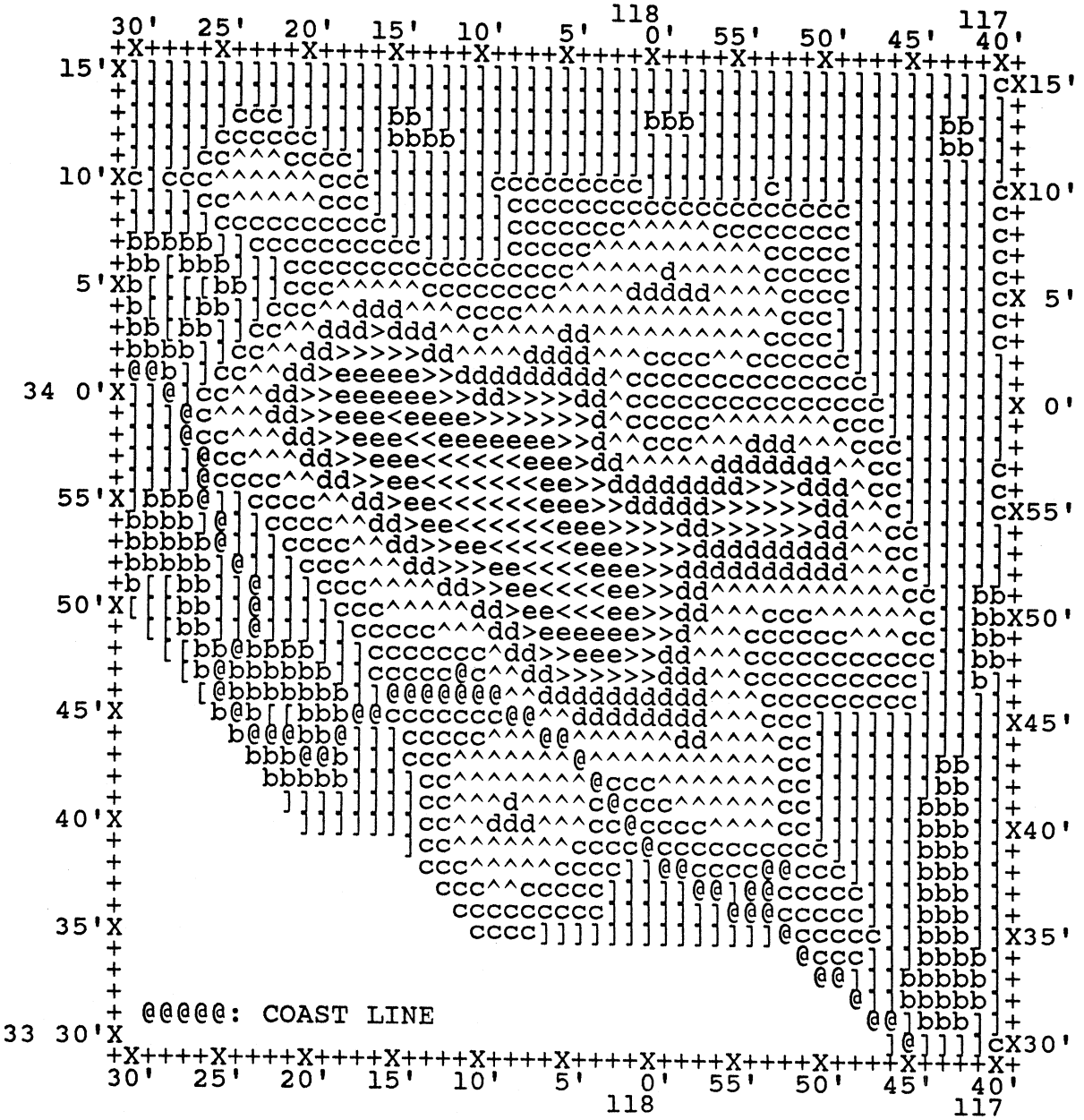

Figure A5.11

APPENDIX B

In this appendix Figures B1.1 through B5.11 present $\log_{10}$(PSV) in in/sec for T = 0.04, 0.65, 0.11, 0.19, 0.34, 0.50, 0.90, 1.6, 2.8, 4.4 and 7.5 second periods, for damping ζ = 0.05, in terms of Modified Mercalli Intensity (MMI) scaling (Trifunac and Lee, 1985b), and for the exposure time of Y = 50 years as follows:

P= \ T=	0.04	0.065	0.11	0.19	0.34	0.50	0.90	1.6	2.8	4.4	7.5
.99	B1.1	B1.2	B1.3	B1.4	B1.5	B1.6	B1.7	B1.8	B1.9	B1.10	B1.11
.90	B2.1	B2.2	B2.3	B2.4	B2.5	B2.6	B2.7	B2.8	B2.9	B2.10	B2.11
.50	B3.1	B3.2	B3.3	B3.4	B3.5	B3.6	B3.7	B3.8	B3.9	B3.10	B3.11
.10	B4.1	B4.2	B4.3	B4.4	B4.5	B4.6	B4.7	B4.8	B4.9	B4.10	B4.11
.01	B5.1	B5.2	B5.3	B5.4	B5.5	B5.6	B5.7	B5.8	B5.9	B5.10	B5.11

P represents the probability of at least one exceedance in Y = 50 years. The logarithms of spectral amplitudes have been rounded to discrete amplitudes with resolution of 0.1, and are presented by printer-plots on the rectangular mesh with spacing of one minute. It is assumed that all sources result in Poissonian sequence of events in time.

PSEUDO RELATIVE VELOCITY, PSV (IN/SEC) AT T = .040 SEC

PROBABILITY OF EXCEEDANCE = .99 FOR 50 YEARS
CALCULATED FROM ESTIMATED M.M.I. LEVELS AT SITES

CONTOUR LEVELS OF LOG(PSV):

3	:	4	;	5	|
-.4	-.3	-.2	-.1	.0	.1

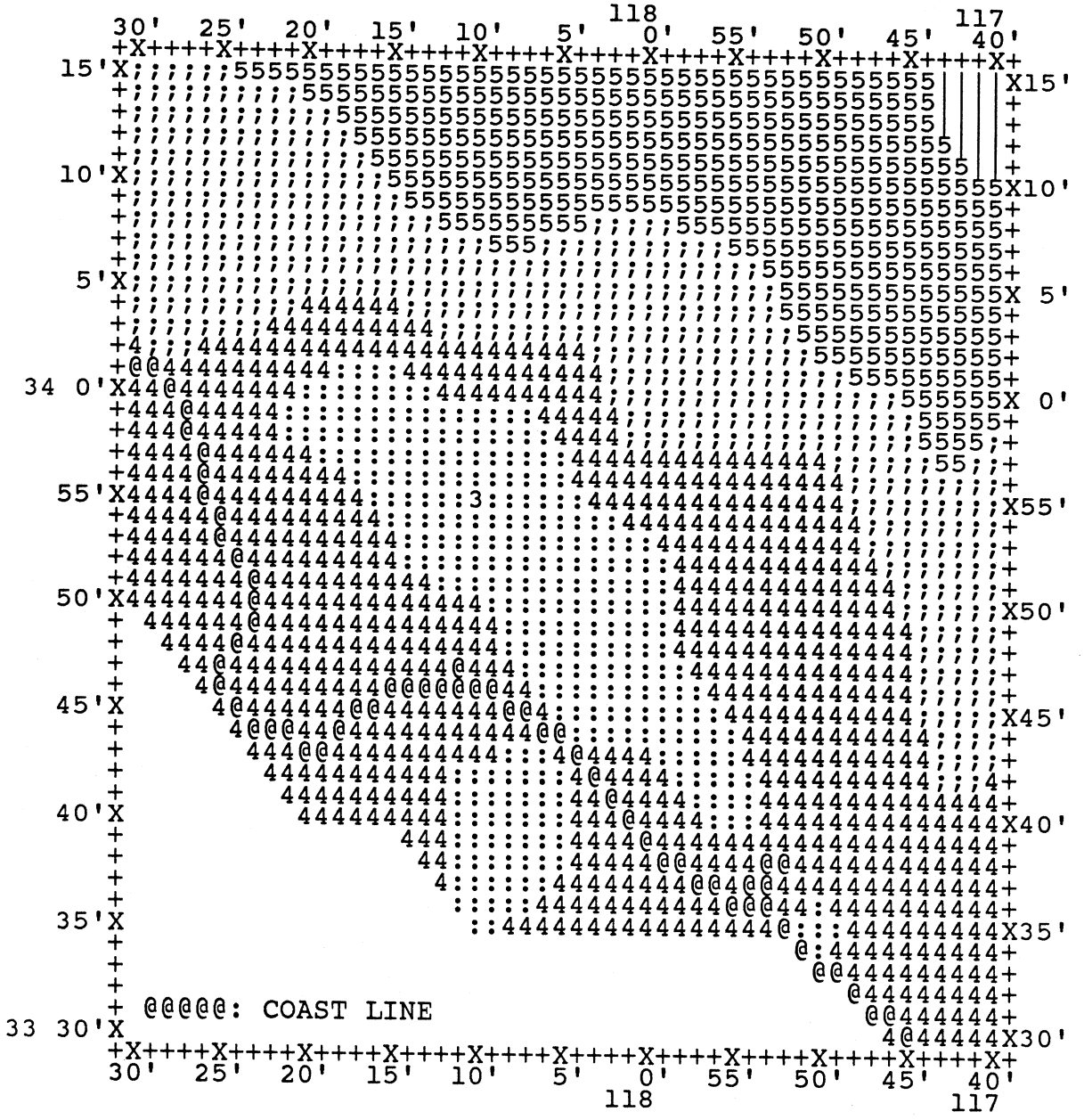

Figure B1.1

PSEUDO RELATIVE VELOCITY, PSV (IN/SEC) AT T = .065 SEC

PROBABILITY OF EXCEEDANCE = .99 FOR 50 YEARS
CALCULATED FROM ESTIMATED M.M.I. LEVELS AT SITES

CONTOUR LEVELS OF LOG(PSV):

4 ; 5 | 6 -
-.2 -.1 .0 .1 .2 .3

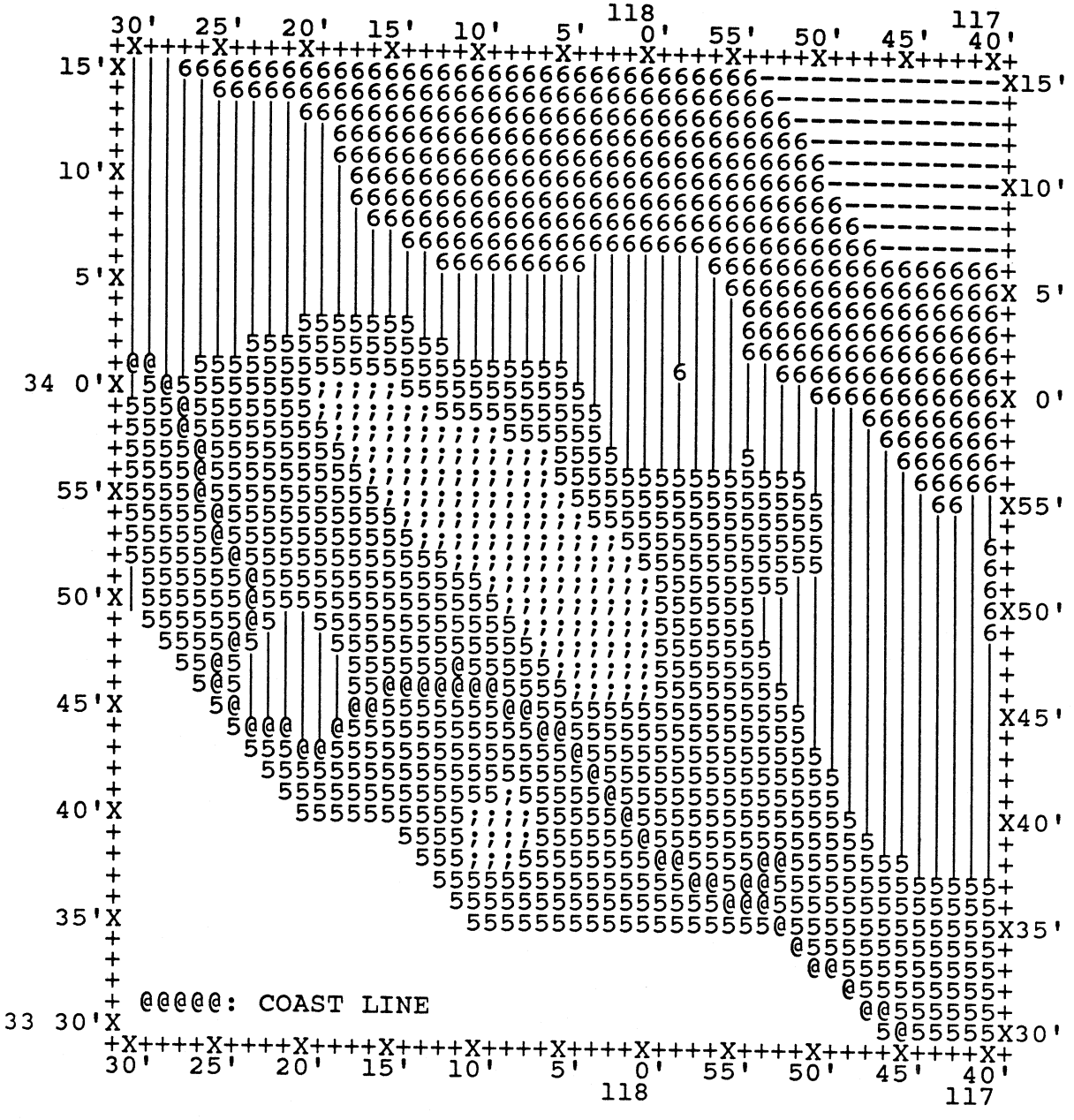

Figure B1.2

PSEUDO RELATIVE VELOCITY, PSV (IN/SEC) AT T = .110 SEC

PROBABILITY OF EXCEEDANCE = .99 FOR 50 YEARS
CALCULATED FROM ESTIMATED M.M.I. LEVELS AT SITES

CONTOUR LEVELS OF LOG(PSV):

6	-	7	/	8
.1	.2	.3	.4	.5	.6

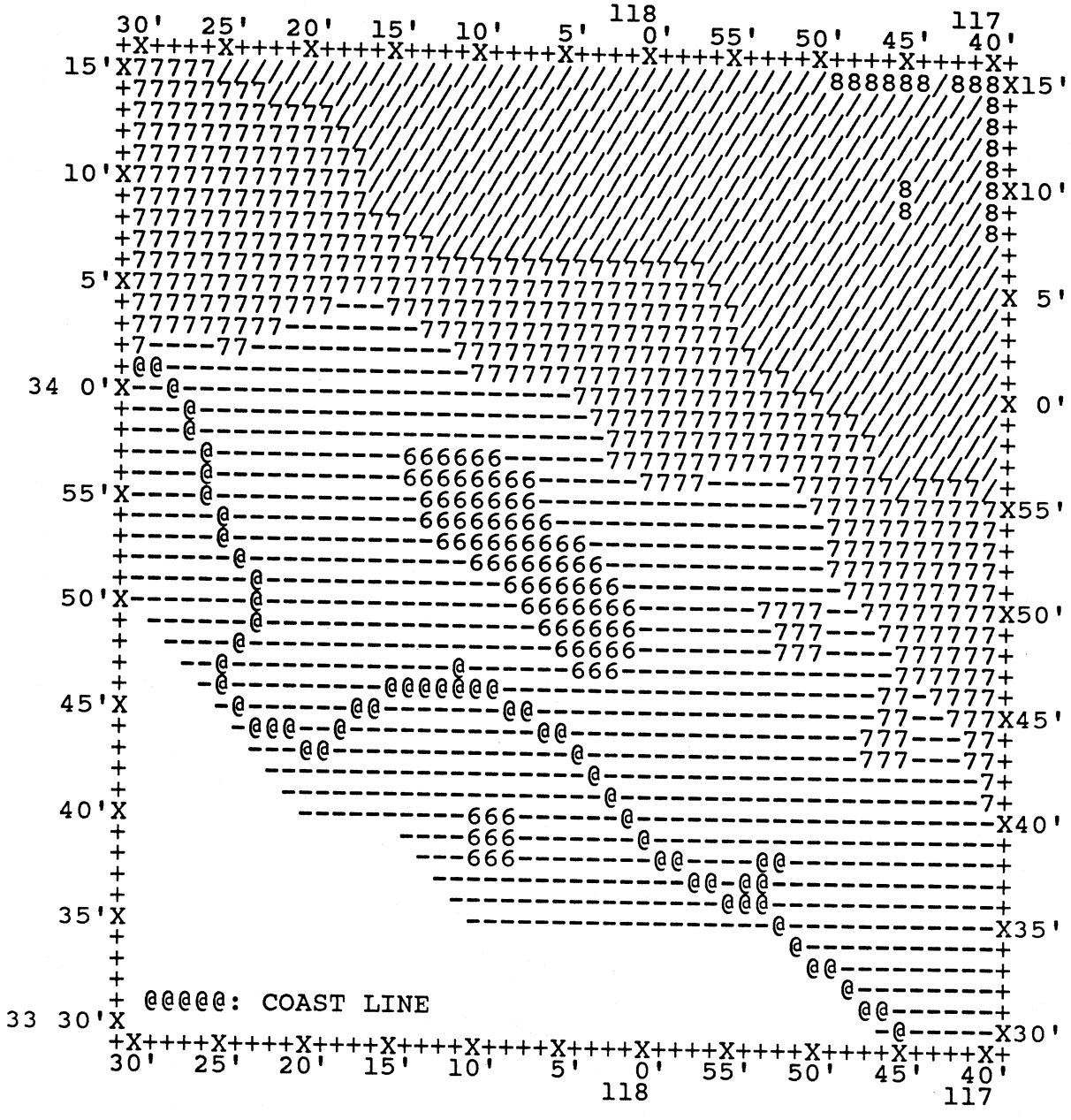

Figure B1.3

PSEUDO RELATIVE VELOCITY, PSV (IN/SEC) AT T = .190 SEC

PROBABILITY OF EXCEEDANCE = .99 FOR 50 YEARS
CALCULATED FROM ESTIMATED M.M.I. LEVELS AT SITES

CONTOUR LEVELS OF LOG(PSV):

7 / 8 ~ 9
.4 .5 .6 .7 .8

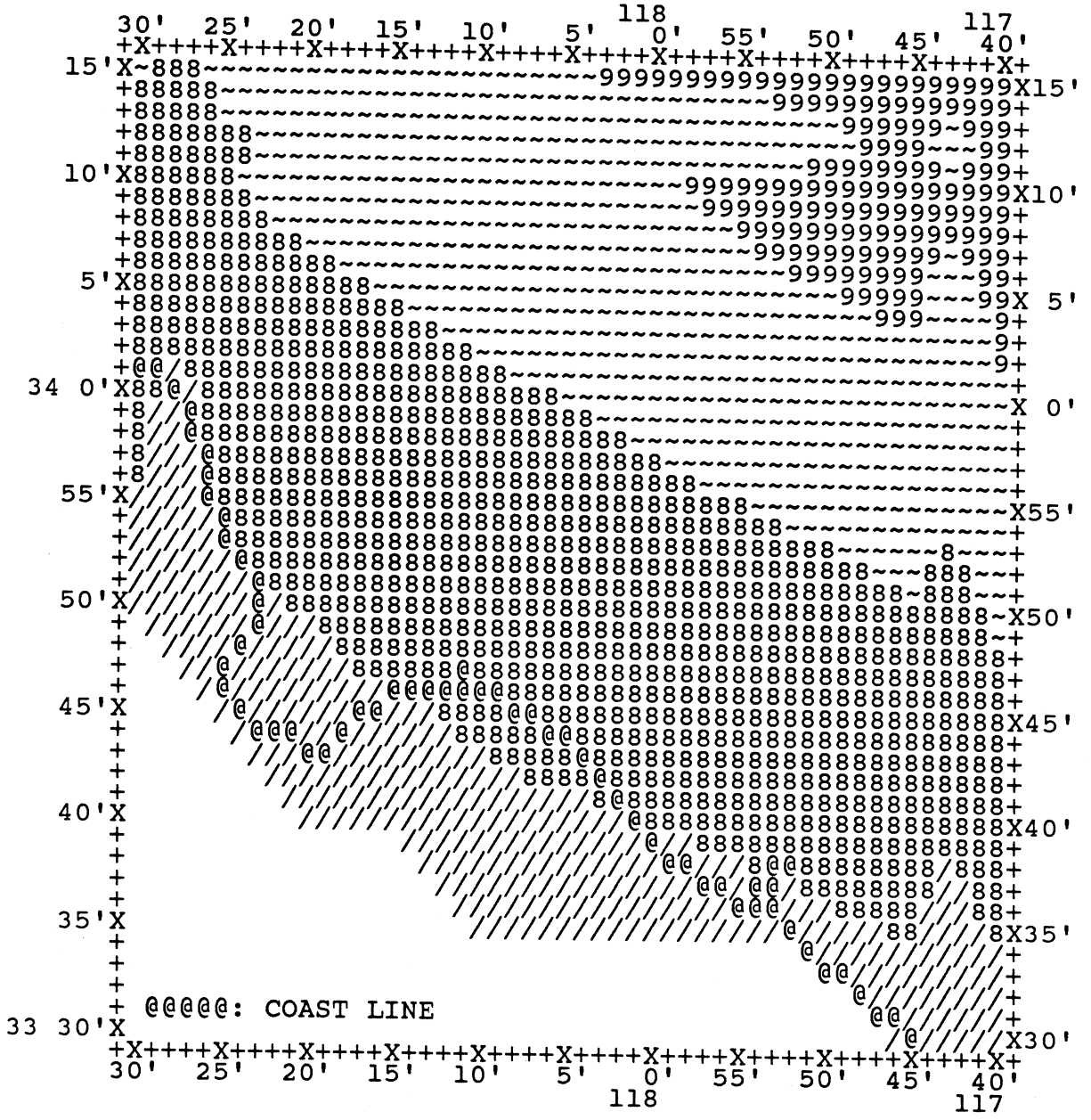

Figure B1.4

PSEUDO RELATIVE VELOCITY, PSV (IN/SEC) AT T = .340 SEC

PROBABILITY OF EXCEEDANCE = .99 FOR 50 YEARS
CALCULATED FROM ESTIMATED M.M.I. LEVELS AT SITES

CONTOUR LEVELS OF LOG(PSV):

/ .5 8 .6 ~ .7 9 .8 ! .9 a 1.0

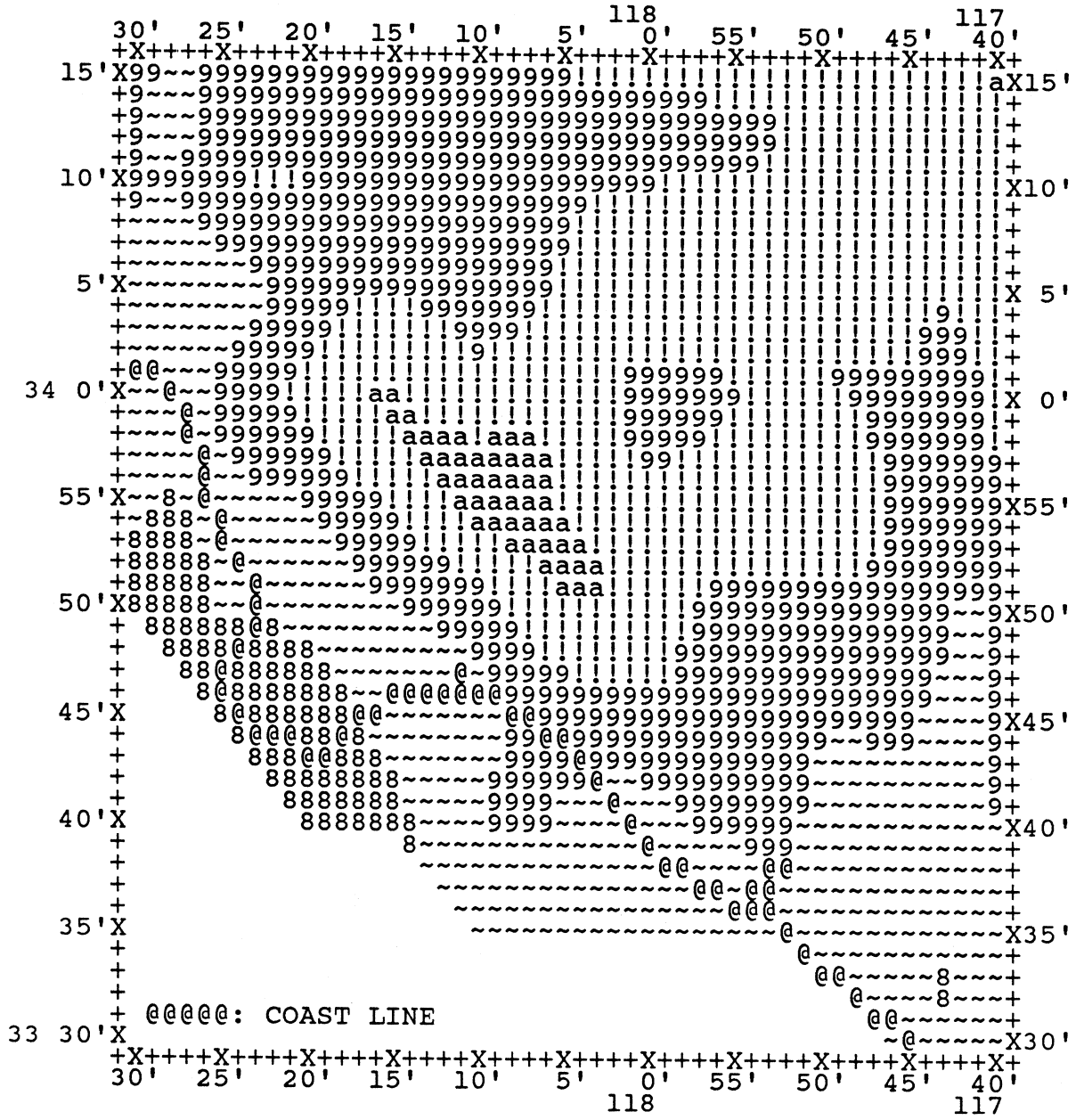

Figure B1.5

PSEUDO RELATIVE VELOCITY, PSV (IN/SEC) AT T = .500 SEC

PROBABILITY OF EXCEEDANCE = .99 FOR 50 YEARS
CALCULATED FROM ESTIMATED M.M.I. LEVELS AT SITES

CONTOUR LEVELS OF LOG(PSV):

/ .5 8 .6 ~ .7 9 .8 ! .9 a 1.0 [1.1

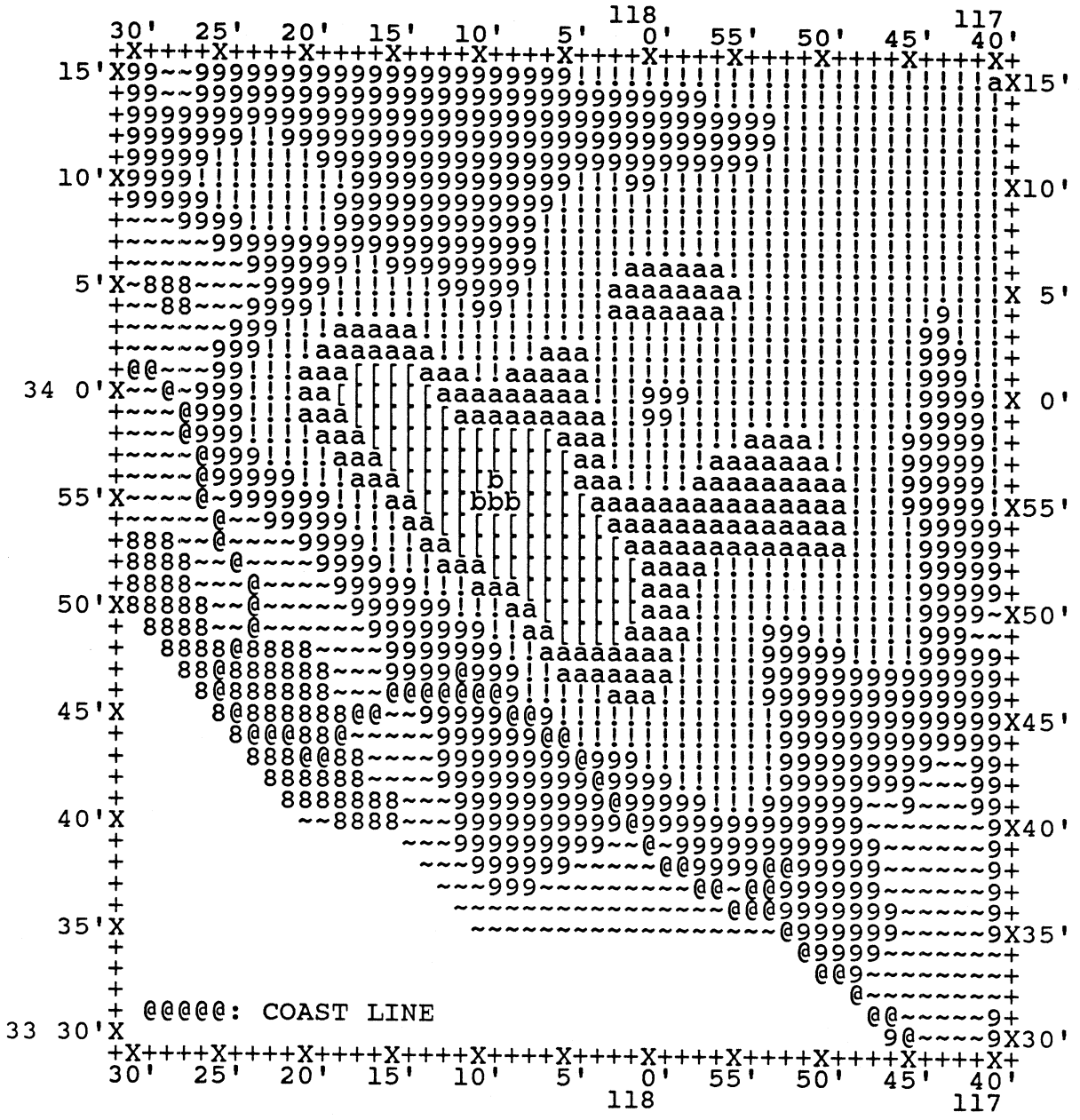

Figure B1.6

PSEUDO RELATIVE VELOCITY, PSV (IN/SEC) AT T = .900 SEC

PROBABILITY OF EXCEEDANCE = .99 FOR 50 YEARS
CALCULATED FROM ESTIMATED M.M.I. LEVELS AT SITES

CONTOUR LEVELS OF LOG(PSV):

/	8	~	9	!	a	[	b	]
.5	.6	.7	.8	.9	1.0	1.1	1.2	1.3

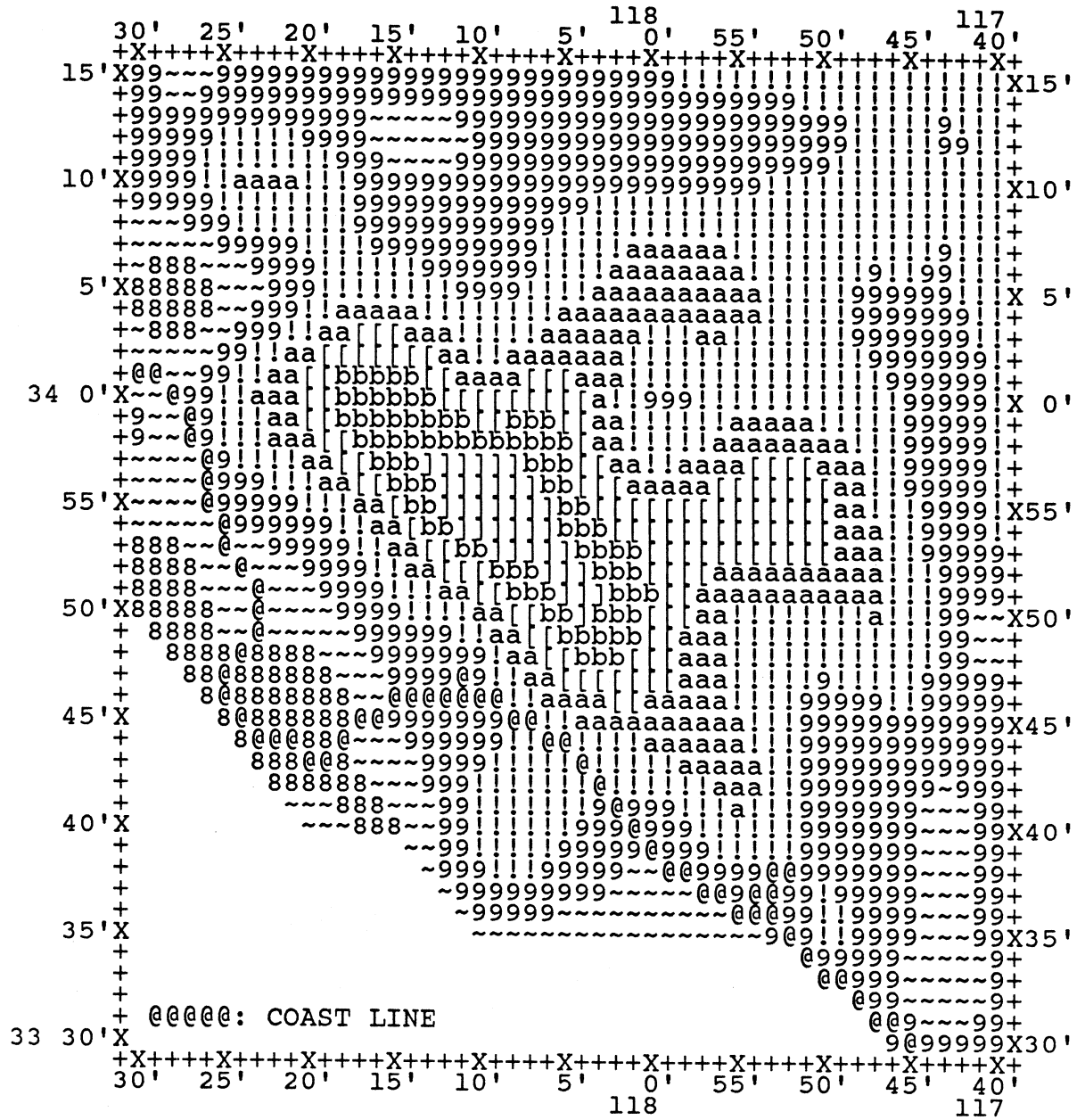

Figure B1.7

PSEUDO RELATIVE VELOCITY, PSV (IN/SEC) AT T = 1.600 SEC

PROBABILITY OF EXCEEDANCE = .99 FOR 50 YEARS
CALCULATED FROM ESTIMATED M.M.I. LEVELS AT SITES

CONTOUR LEVELS OF LOG(PSV):

/	8	~	9	!	a	[	b	]	c	^
.5	.6	.7	.8	.9	1.0	1.1	1.2	1.3	1.4	1.5

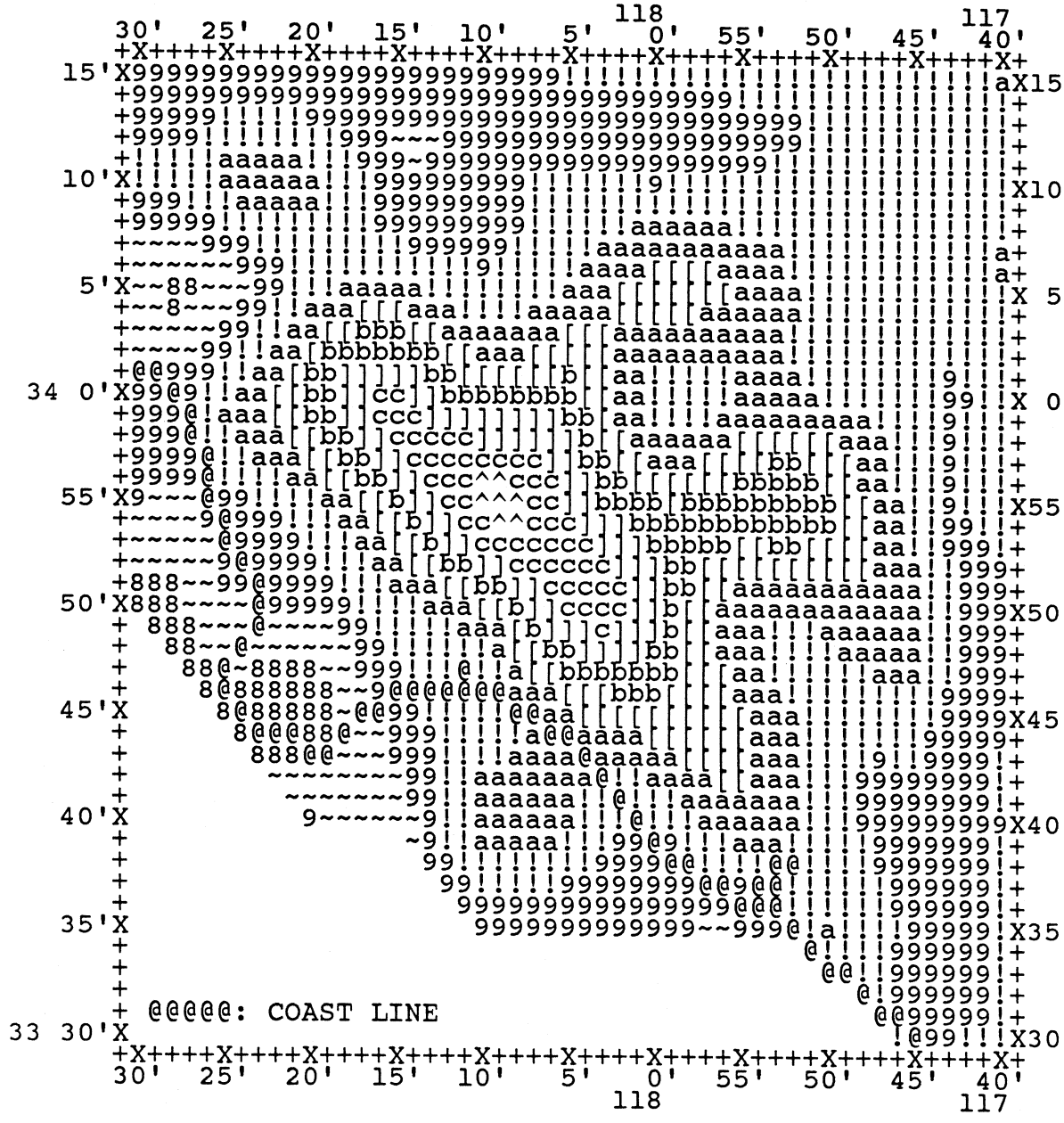

Figure B1.8

PSEUDO RELATIVE VELOCITY, PSV (IN/SEC) AT T = 2.800 SEC

PROBABILITY OF EXCEEDANCE = .99 FOR 50 YEARS
CALCULATED FROM ESTIMATED M.M.I. LEVELS AT SITES

CONTOUR LEVELS OF LOG(PSV):

/	8	~	9	!	a	[	b	]	c	^	d
.5	.6	.7	.8	.9	1.0	1.1	1.2	1.3	1.4	1.5	1.6

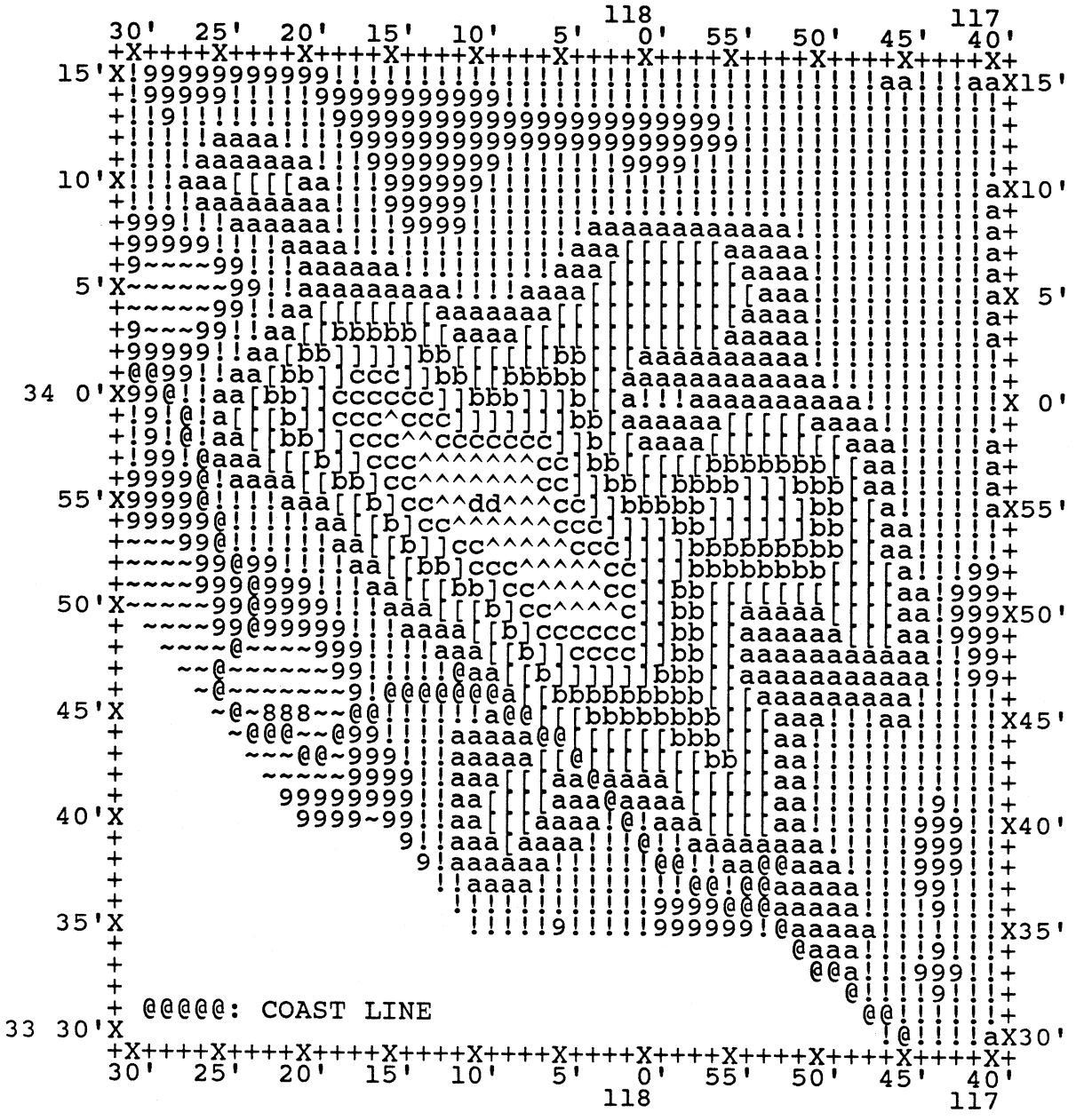

Figure B1.9

PSEUDO RELATIVE VELOCITY, PSV (IN/SEC) AT T = 4.400 SEC

PROBABILITY OF EXCEEDANCE = .99 FOR 50 YEARS
CALCULATED FROM ESTIMATED M.M.I. LEVELS AT SITES

CONTOUR LEVELS OF LOG(PSV):

/	8	~	9	!	a	[	b	]	c	^
.5	.6	.7	.8	.9	1.0	1.1	1.2	1.3	1.4	1.5

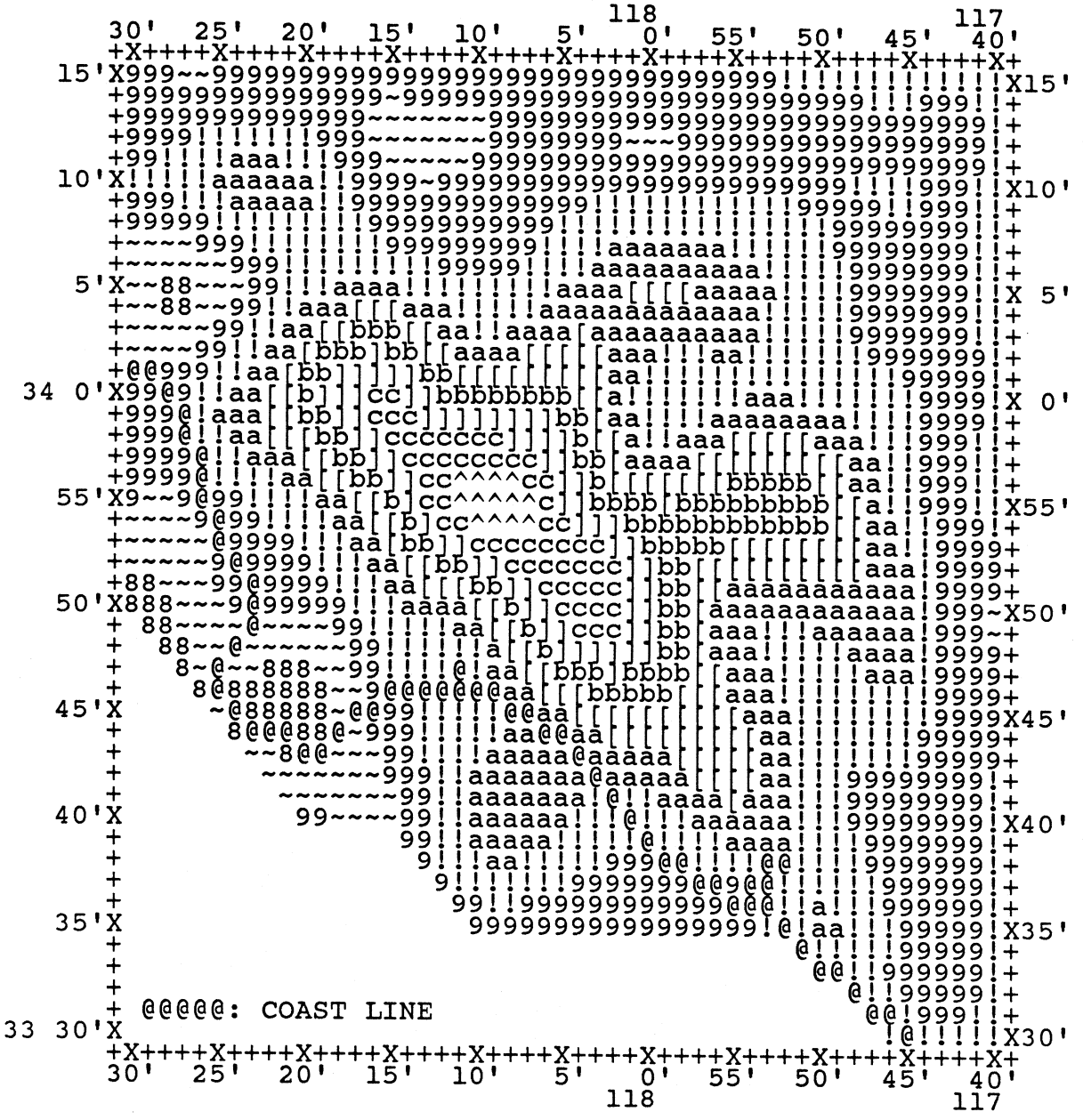

Figure B1.10

PSEUDO RELATIVE VELOCITY, PSV (IN/SEC) AT T = 7.500 SEC

PROBABILITY OF EXCEEDANCE = .99 FOR 50 YEARS
CALCULATED FROM ESTIMATED M.M.I. LEVELS AT SITES

CONTOUR LEVELS OF LOG(PSV):

7	/	8	~	9	!	a	[	b
.4	.5	.6	.7	.8	.9	1.0	1.1	1.2

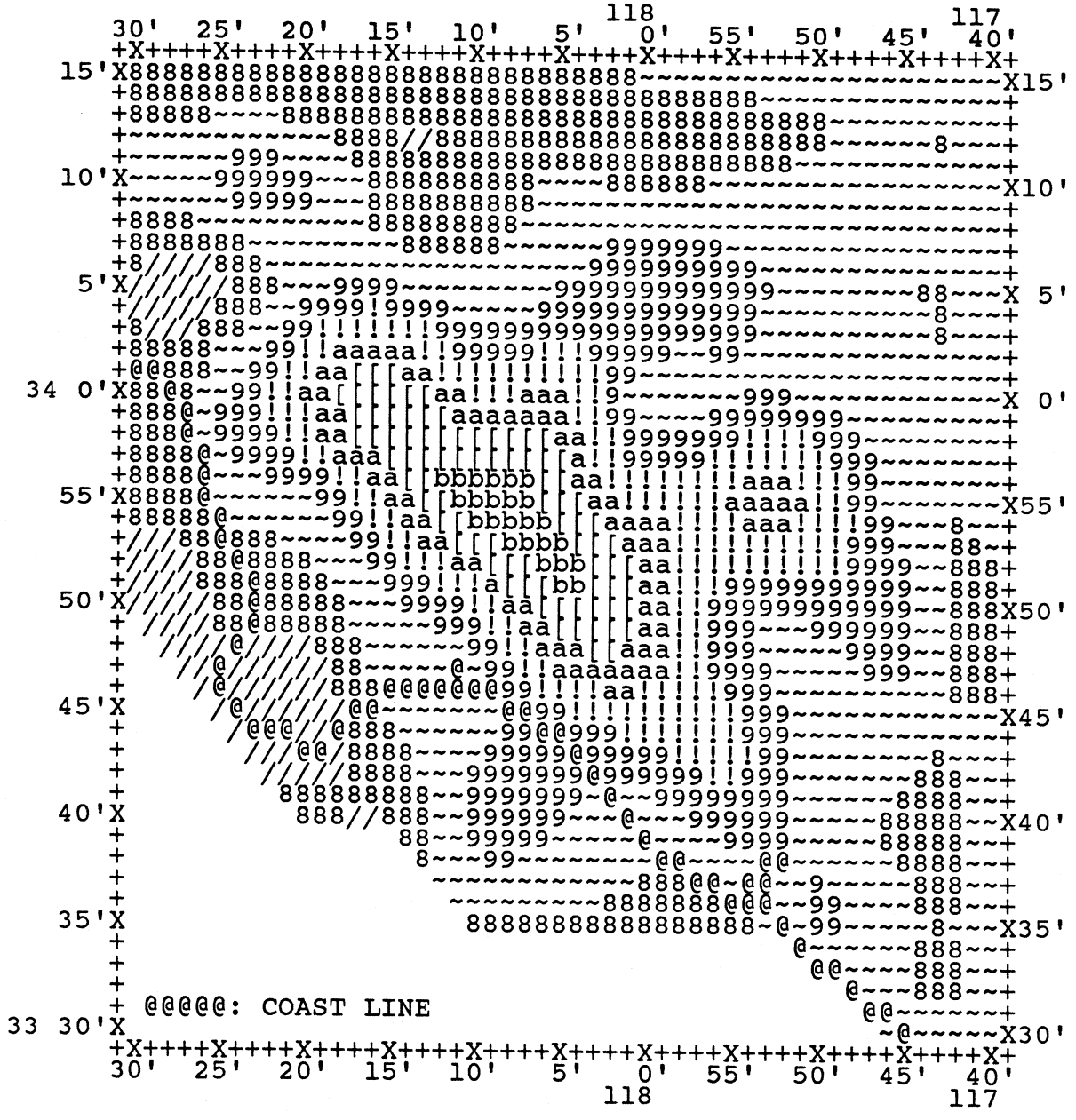

Figure B1.11

PSEUDO RELATIVE VELOCITY, PSV (IN/SEC) AT T = .040 SEC

PROBABILITY OF EXCEEDANCE = .90 FOR 50 YEARS
CALCULATED FROM ESTIMATED M.M.I. LEVELS AT SITES

CONTOUR LEVELS OF LOG(PSV):

: 3 4 2 ; 1 5 0 | 1 6 2

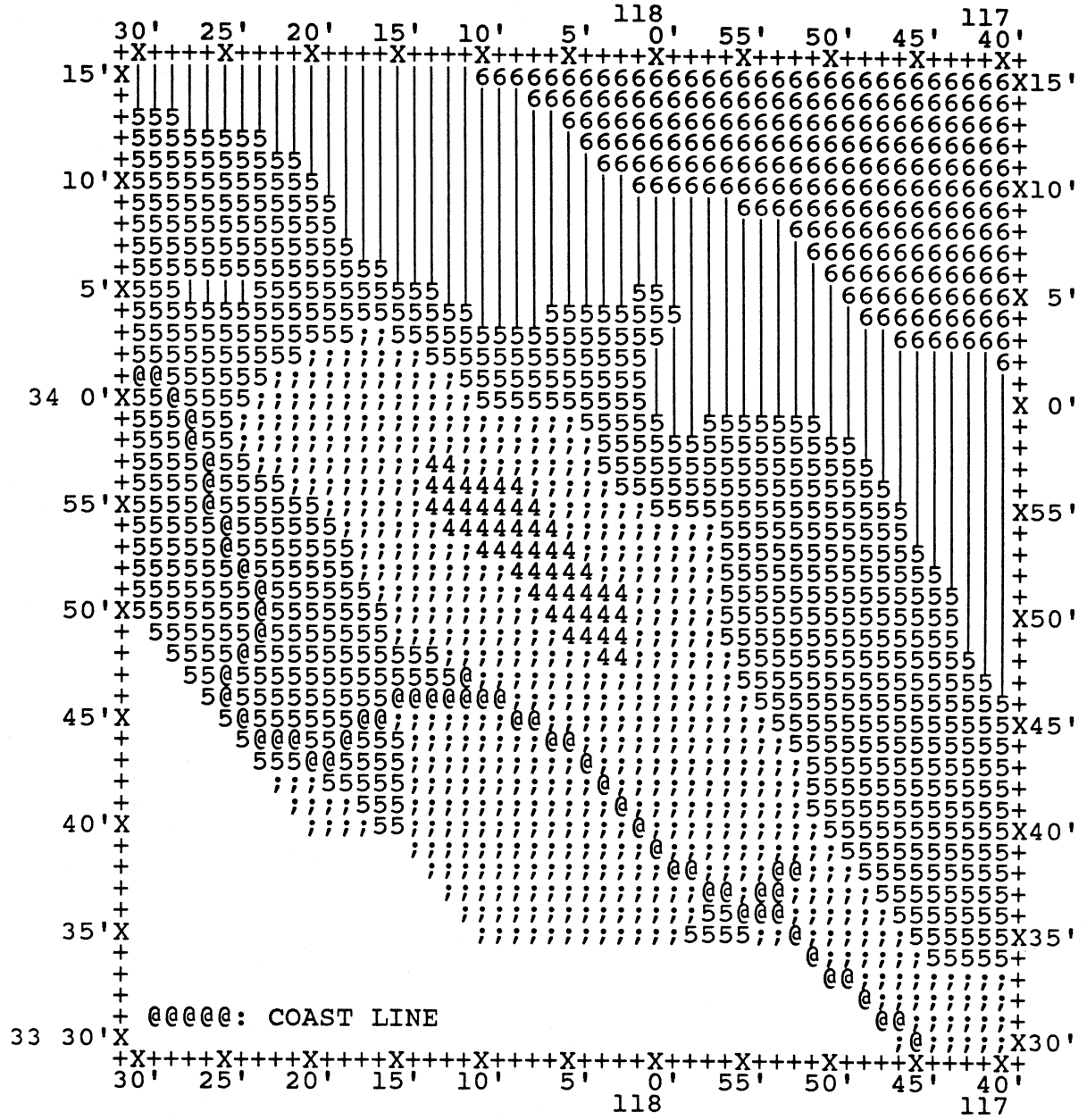

Figure B2.1

PSEUDO RELATIVE VELOCITY, PSV (IN/SEC) AT T = .065 SEC

PROBABILITY OF EXCEEDANCE = .90 FOR 50 YEARS
CALCULATED FROM ESTIMATED M.M.I. LEVELS AT SITES

CONTOUR LEVELS OF LOG(PSV):

; 5 | 6 - 7
-.1 .0 .1 .2 .3 .4

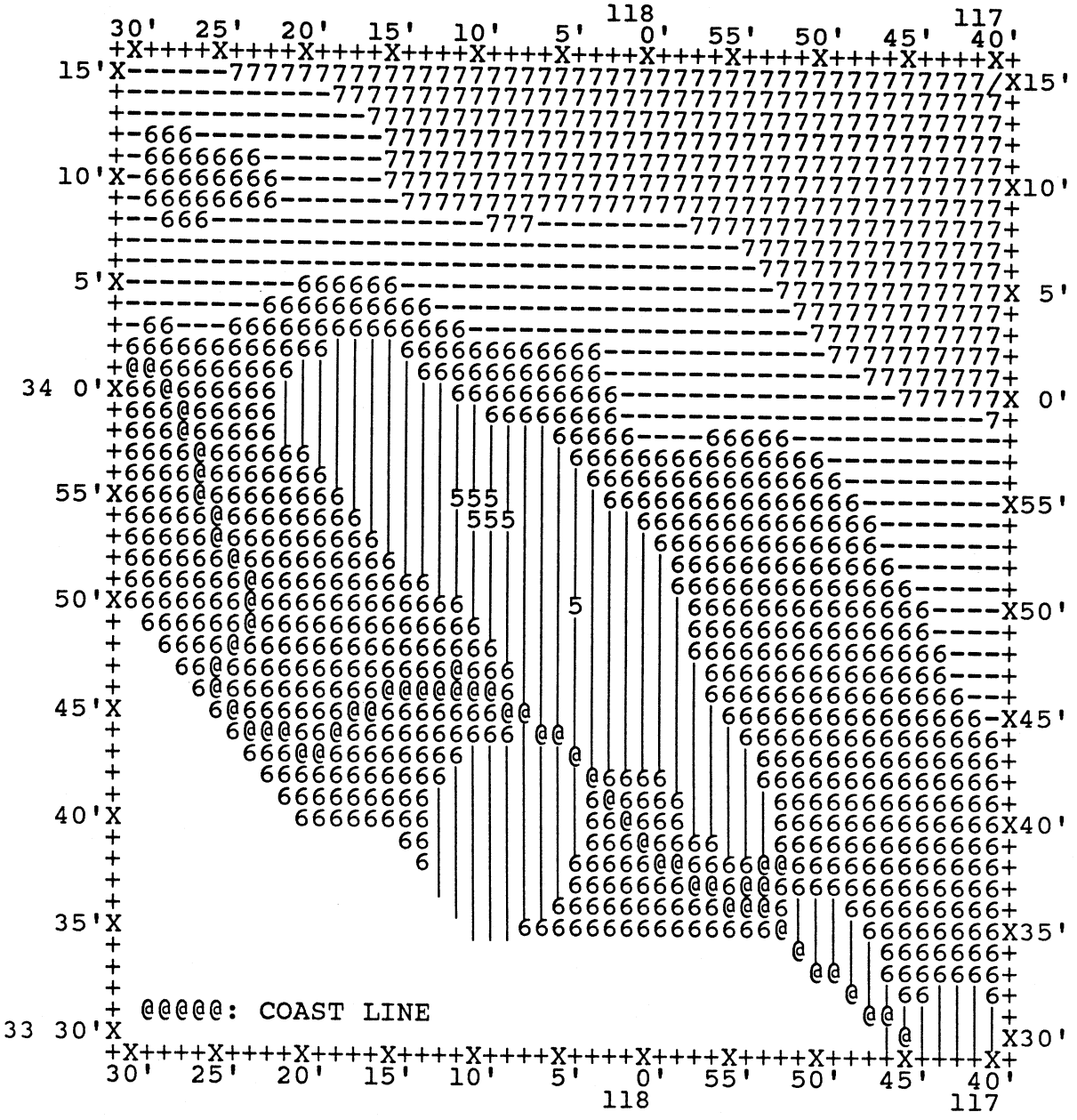

Figure B2.2

PSEUDO RELATIVE VELOCITY, PSV (IN/SEC) AT T = .110 SEC

PROBABILITY OF EXCEEDANCE = .90 FOR 50 YEARS
CALCULATED FROM ESTIMATED M.M.I. LEVELS AT SITES

CONTOUR LEVELS OF LOG(PSV):

-	7	/	8	~	9
.3	.4	.5	.6	.7	.8

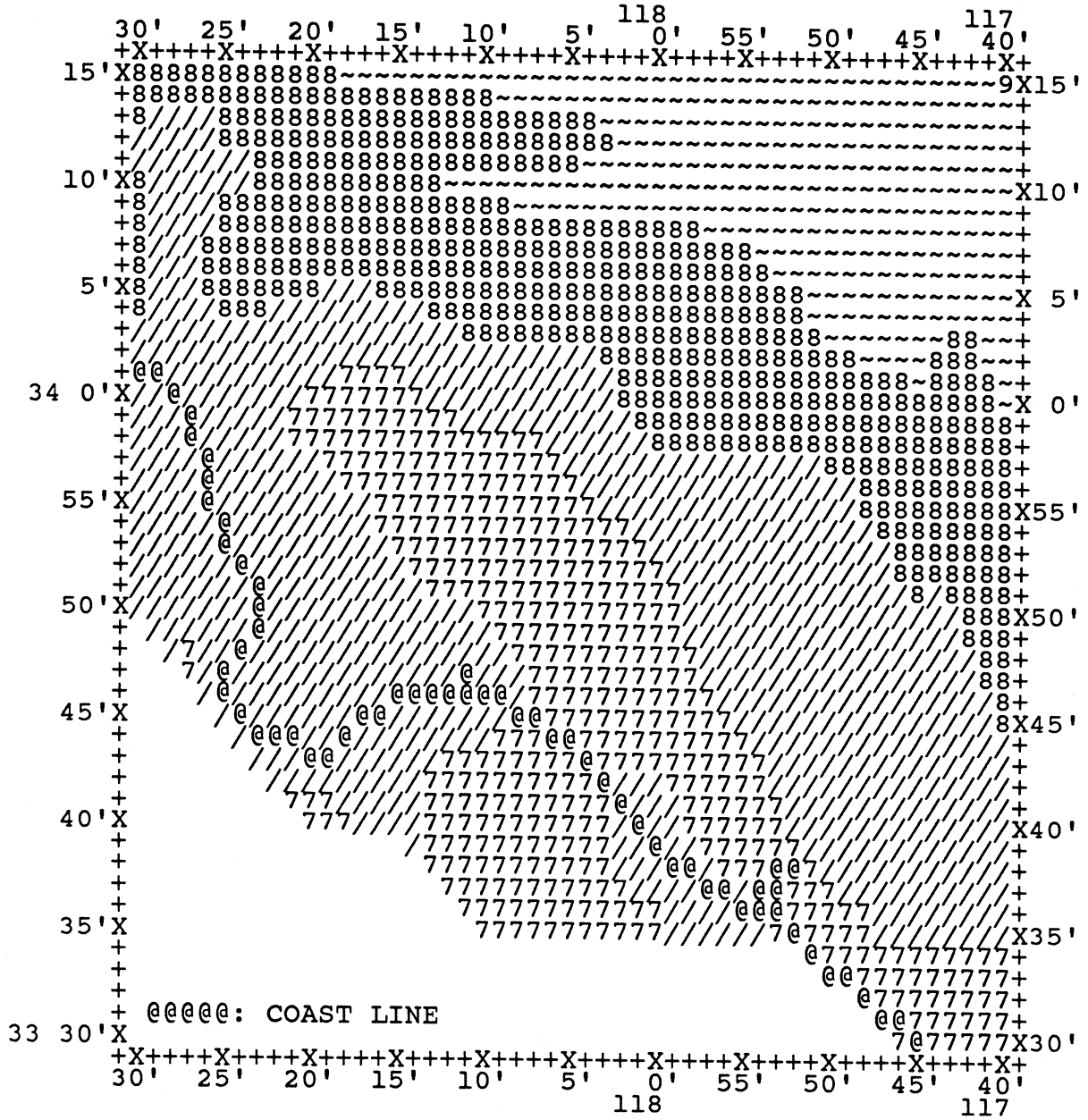

Figure B2.3

PSEUDO RELATIVE VELOCITY, PSV (IN/SEC) AT T = .190 SEC

PROBABILITY OF EXCEEDANCE = .90 FOR 50 YEARS
CALCULATED FROM ESTIMATED M.M.I. LEVELS AT SITES

CONTOUR LEVELS OF LOG(PSV):

8	~	9	!	a
.6	.7	.8	.9	1.0

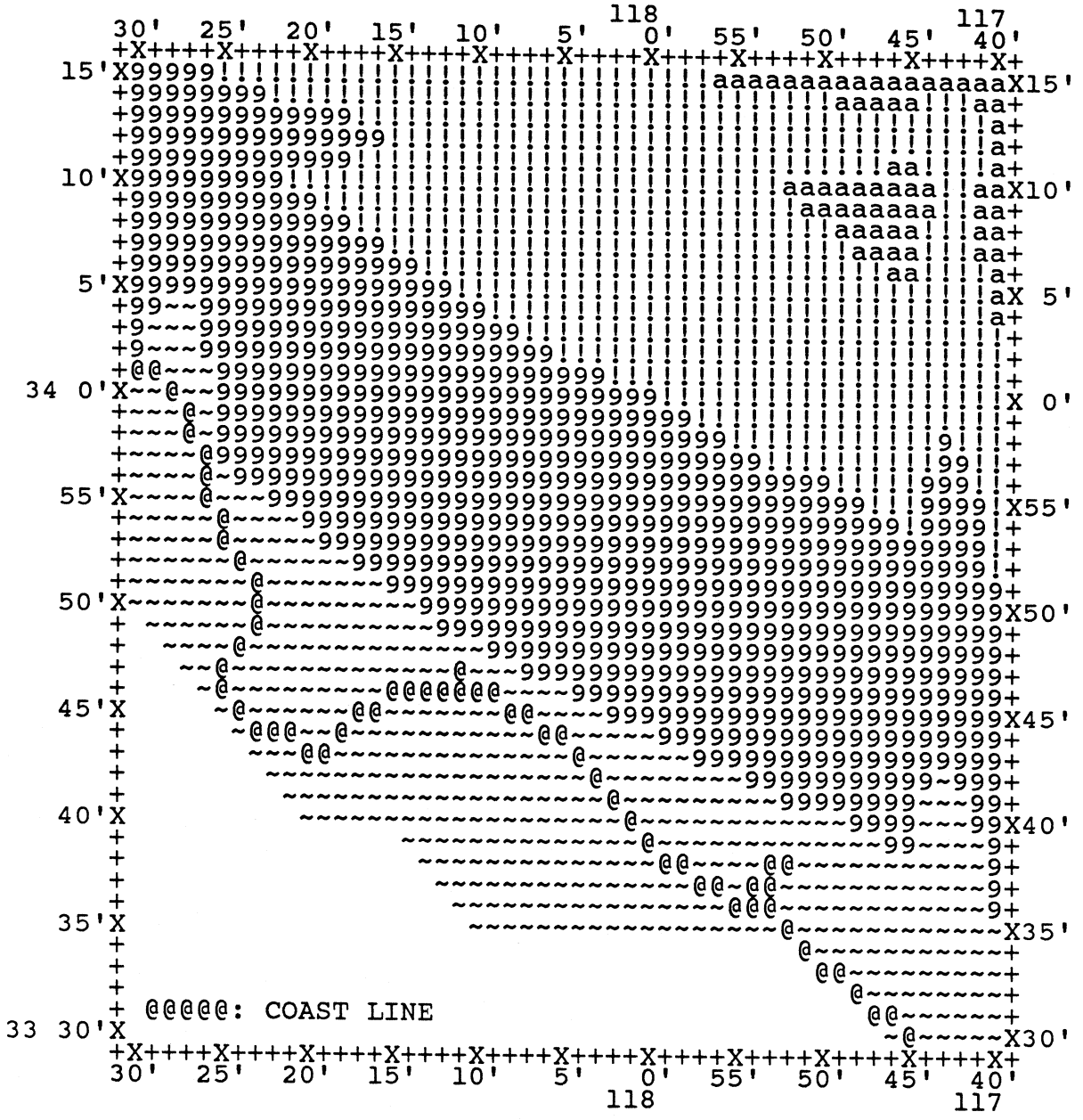

Figure B2.4

PSEUDO RELATIVE VELOCITY, PSV (IN/SEC) AT T = .340 SEC

PROBABILITY OF EXCEEDANCE = .90 FOR 50 YEARS
CALCULATED FROM ESTIMATED M.M.I. LEVELS AT SITES

CONTOUR LEVELS OF LOG(PSV):

8	~	9	!	a	[	b
.6	.7	.8	.9	1.0	1.1	1.2

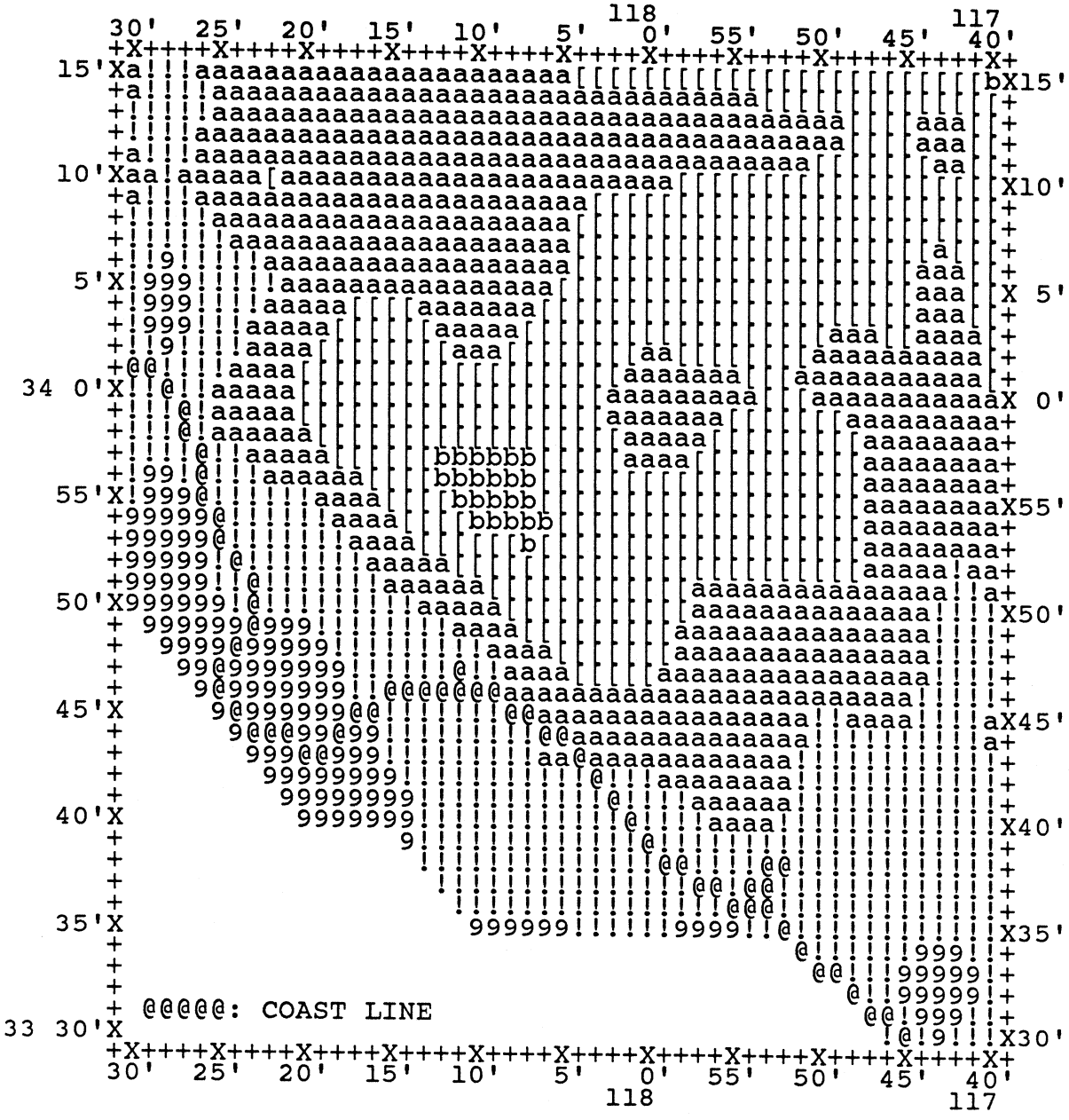

Figure B2.5

PSEUDO RELATIVE VELOCITY, PSV (IN/SEC) AT T = .500 SEC

PROBABILITY OF EXCEEDANCE = .90 FOR 50 YEARS
CALCULATED FROM ESTIMATED M.M.I. LEVELS AT SITES

CONTOUR LEVELS OF LOG(PSV):

8	~	9	!	a	[	b	]
.6	.7	.8	.9	1.0	1.1	1.2	1.3

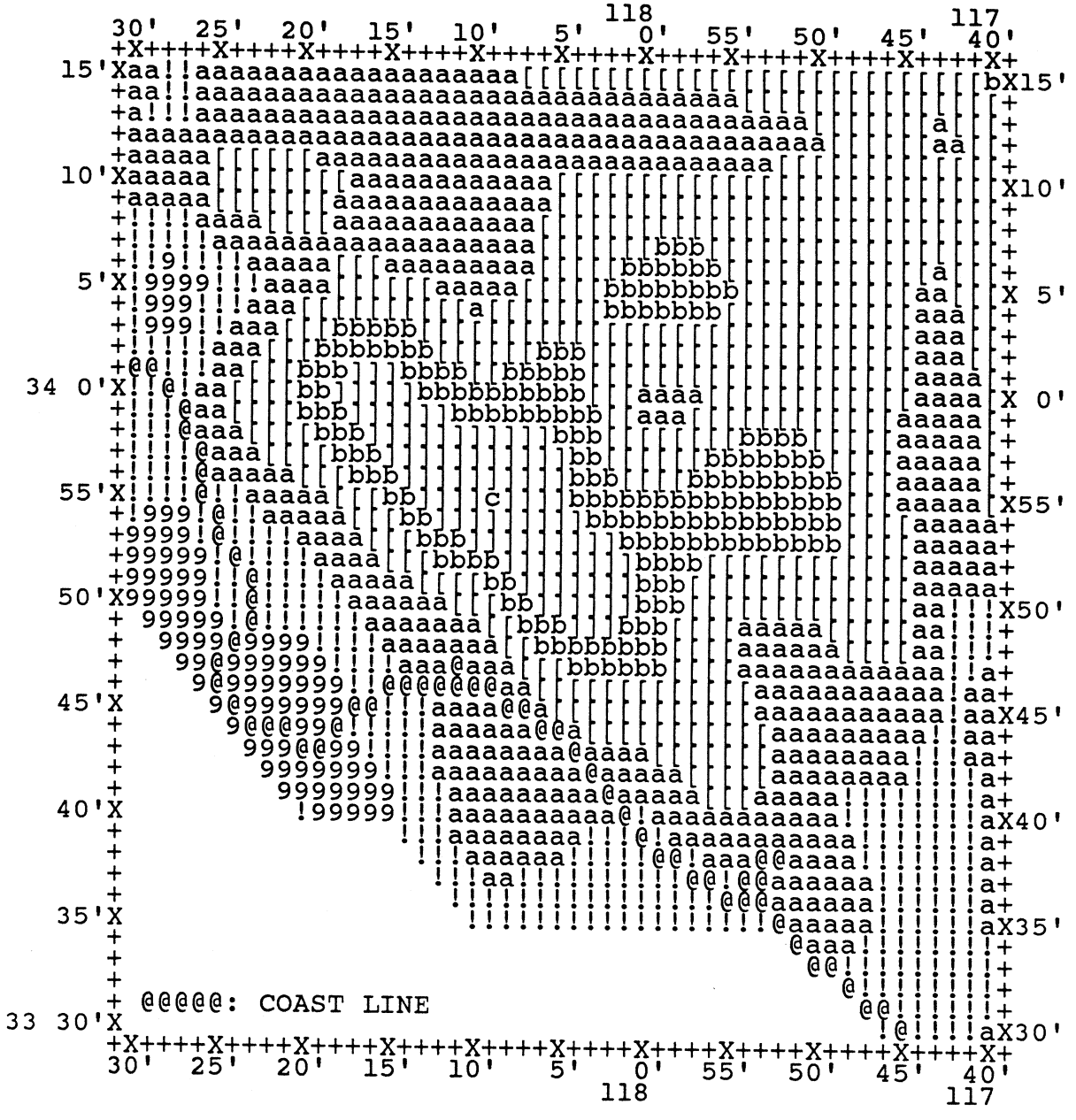

Figure B2.6

PSEUDO RELATIVE VELOCITY, PSV (IN/SEC) AT T = .900 SEC

PROBABILITY OF EXCEEDANCE = .90 FOR 50 YEARS
CALCULATED FROM ESTIMATED M.M.I. LEVELS AT SITES

CONTOUR LEVELS OF LOG(PSV):

8	~	9	!	a	[	b	]	c	^
.6	.7	.8	.9	1.0	1.1	1.2	1.3	1.4	1.5

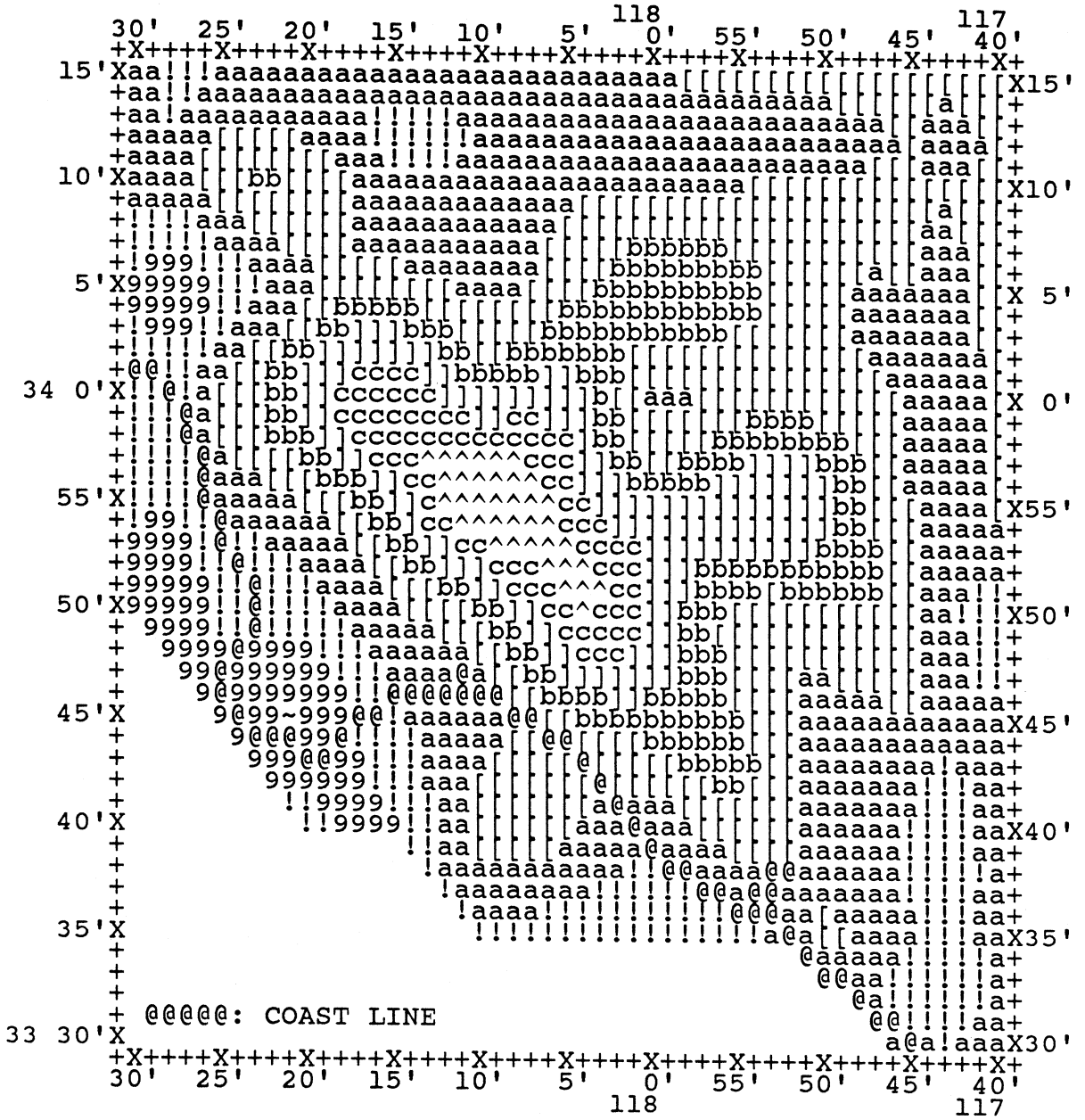

Figure B2.7

PSEUDO RELATIVE VELOCITY, PSV (IN/SEC) AT T = 1.600 SEC

PROBABILITY OF EXCEEDANCE = .90 FOR 50 YEARS
CALCULATED FROM ESTIMATED M.M.I. LEVELS AT SITES

CONTOUR LEVELS OF LOG(PSV):

8	~	9	!	a	[	b	]	c	^	d	>
.6	.7	.8	.9	1.0	1.1	1.2	1.3	1.4	1.5	1.6	1.7

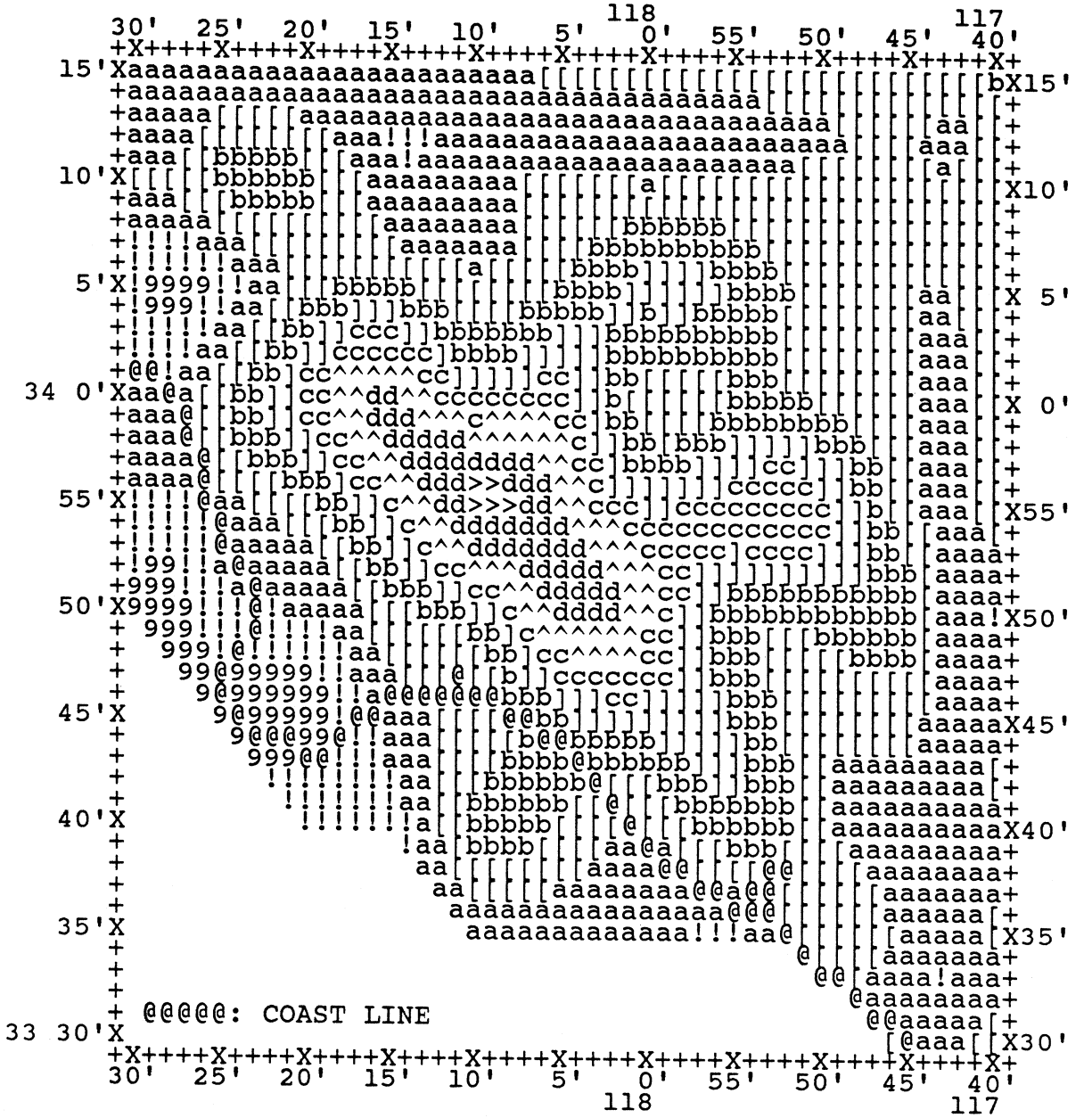

Figure B2.8

PSEUDO RELATIVE VELOCITY, PSV (IN/SEC) AT T = 2.800 SEC

PROBABILITY OF EXCEEDANCE = .90 FOR 50 YEARS
CALCULATED FROM ESTIMATED M.M.I. LEVELS AT SITES

CONTOUR LEVELS OF LOG(PSV):

8	~	9	!	a	[	b	]	c	^	d	>
.6	.7	.8	.9	1.0	1.1	1.2	1.3	1.4	1.5	1.6	1.7

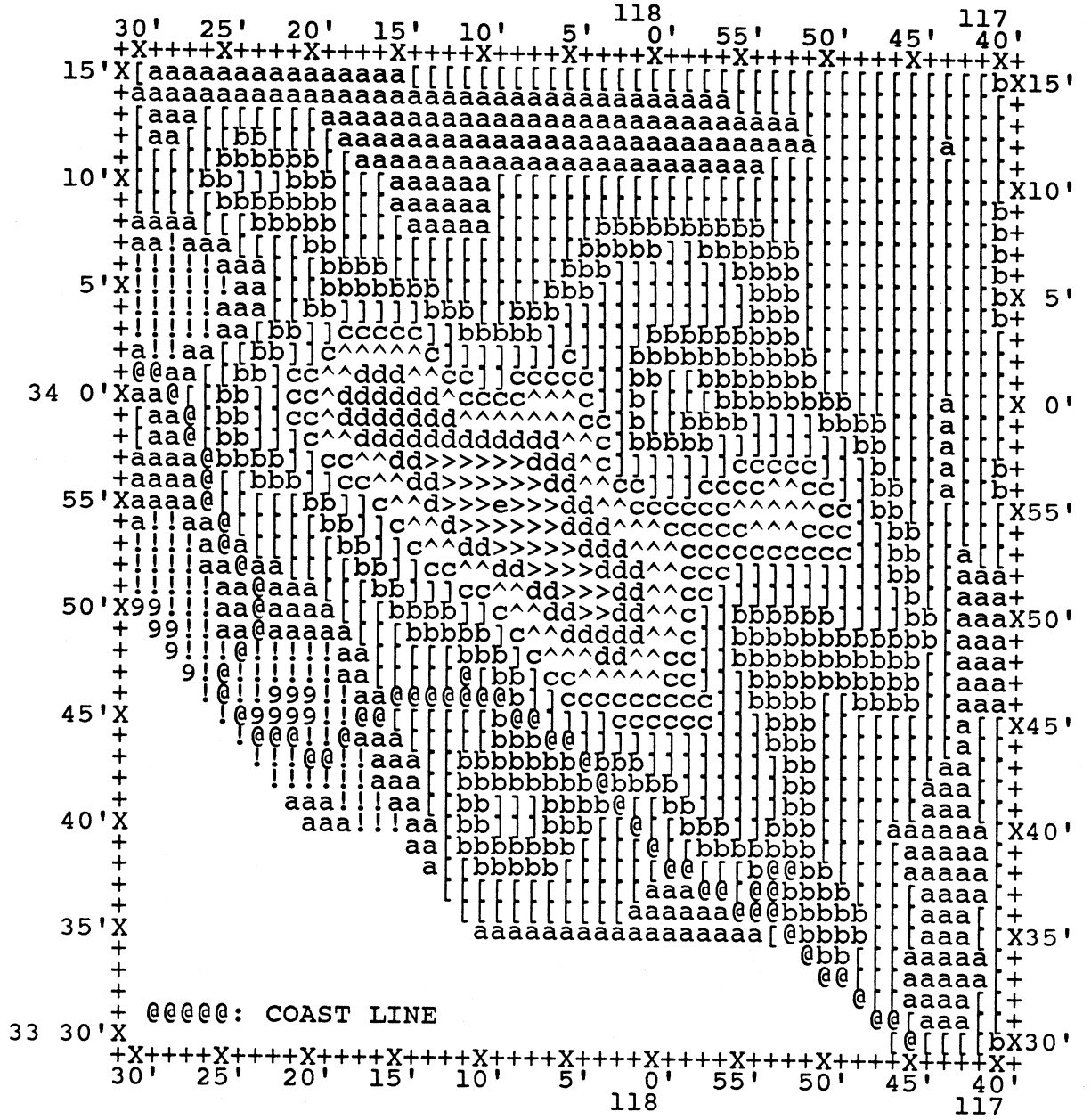

Figure B2.9

PSEUDO RELATIVE VELOCITY, PSV (IN/SEC) AT T = 4.400 SEC

PROBABILITY OF EXCEEDANCE = .90 FOR 50 YEARS
CALCULATED FROM ESTIMATED M.M.I. LEVELS AT SITES

CONTOUR LEVELS OF LOG(PSV):

8	~	9	!	a	[	b	]	c	^	d	>
.6	.7	.8	.9	1.0	1.1	1.2	1.3	1.4	1.5	1.6	1.7

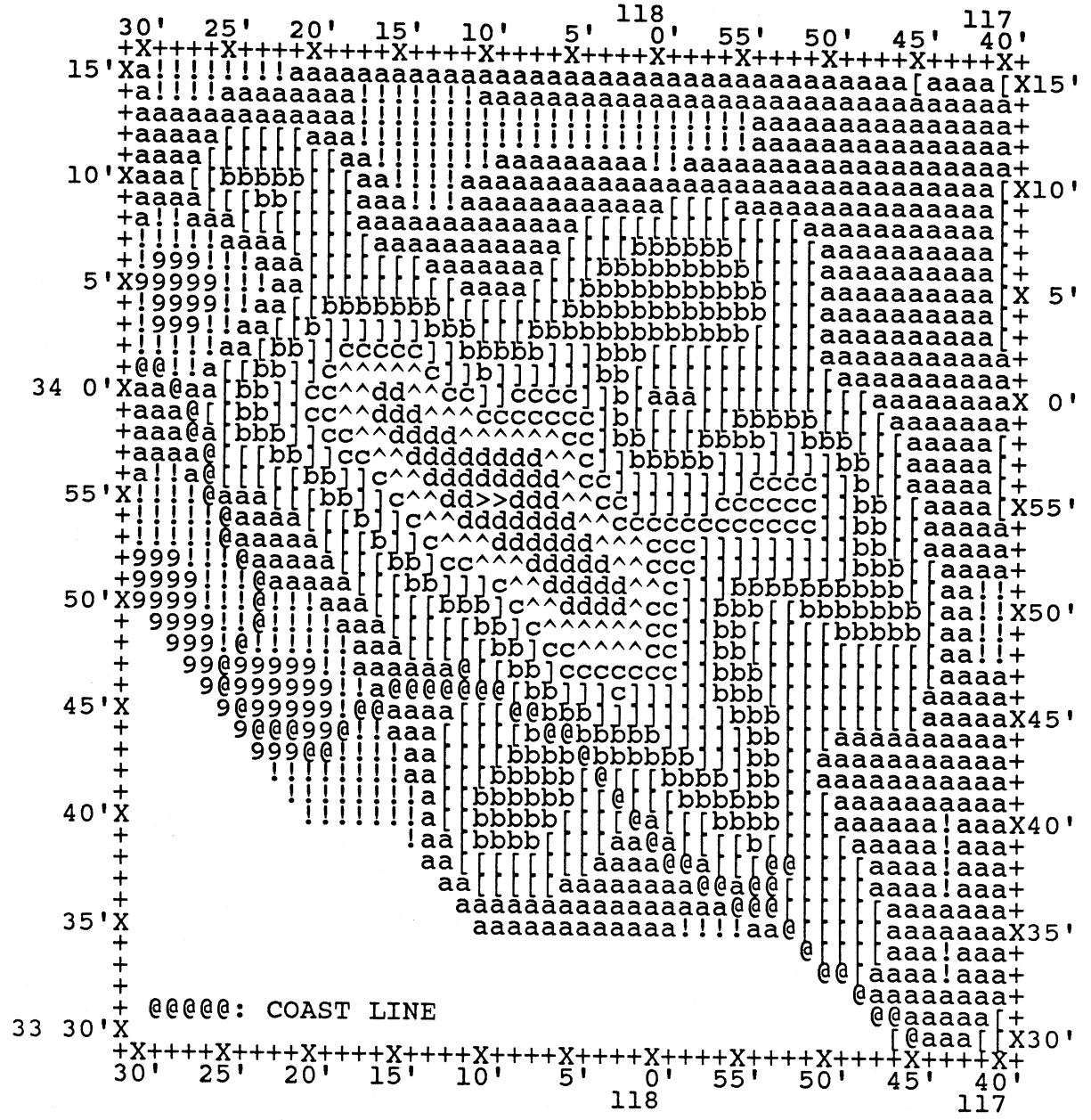

Figure B2.10

PSEUDO RELATIVE VELOCITY, PSV (IN/SEC) AT T = 7.500 SEC

PROBABILITY OF EXCEEDANCE = .90 FOR 50 YEARS
CALCULATED FROM ESTIMATED M.M.I. LEVELS AT SITES

CONTOUR LEVELS OF LOG(PSV):

/	8	~	9	!	a	[	b	]	c
.5	.6	.7	.8	.9	1.0	1.1	1.2	1.3	1.4

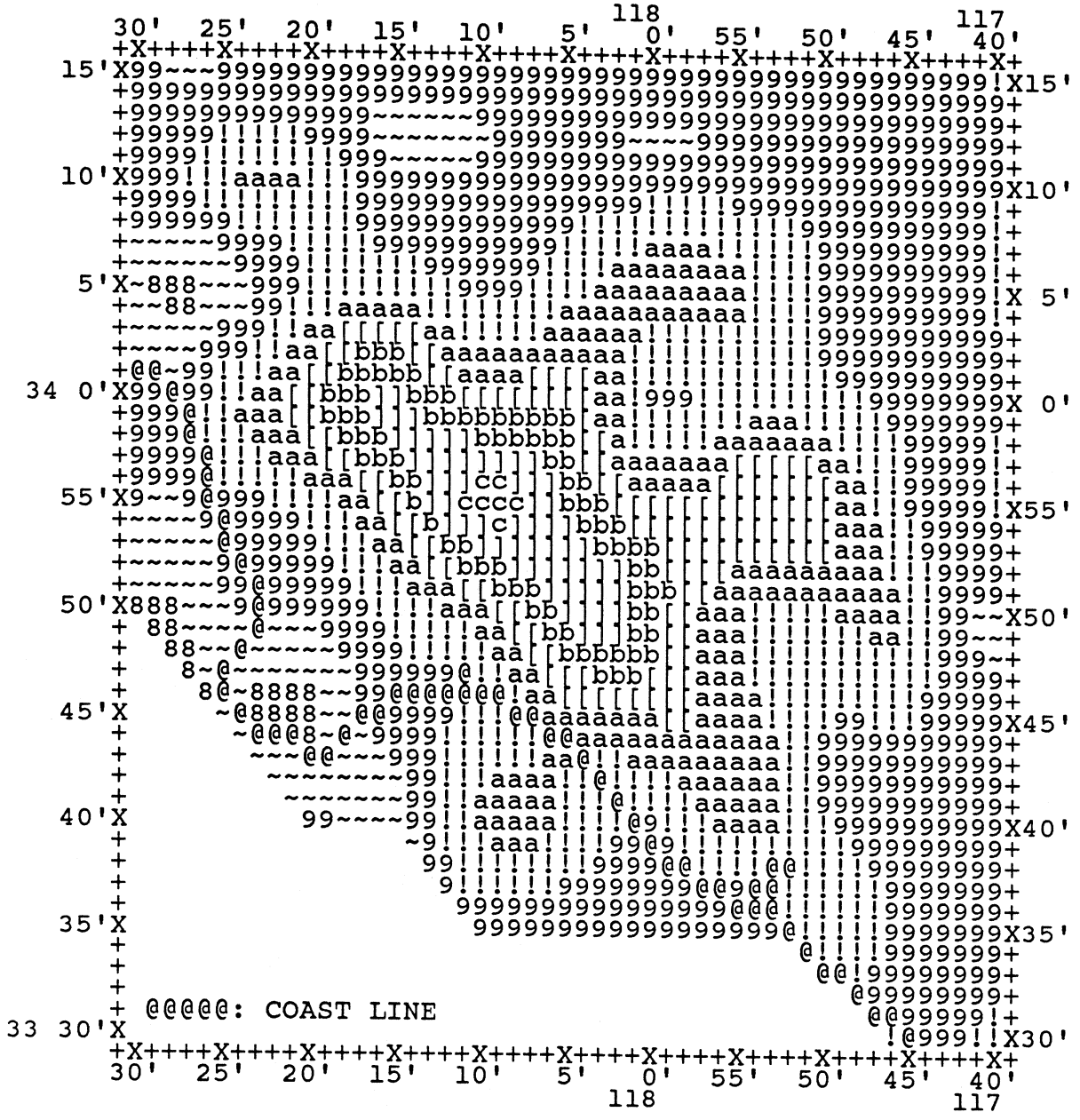

Figure B2.11

PSEUDO RELATIVE VELOCITY, PSV (IN/SEC) AT T = .040 SEC

PROBABILITY OF EXCEEDANCE = .50 FOR 50 YEARS
CALCULATED FROM ESTIMATED M.M.I. LEVELS AT SITES

CONTOUR LEVELS OF LOG(PSV):

; 5 | 6 - 7
-.1 .0 .1 .2 .3 .4

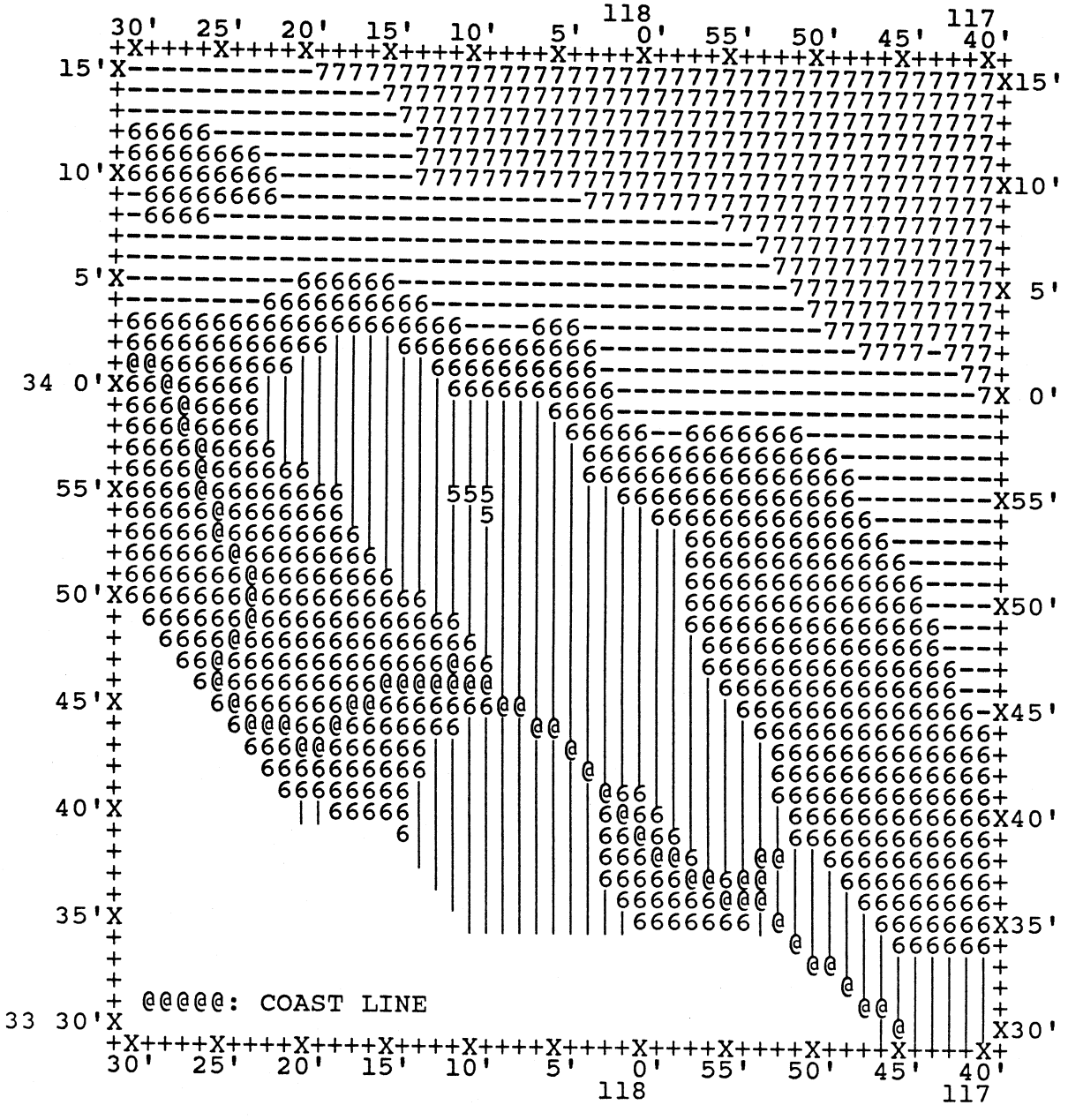

Figure B3.1

PSEUDO RELATIVE VELOCITY, PSV (IN/SEC) AT T = .065 SEC

PROBABILITY OF EXCEEDANCE = .50 FOR 50 YEARS
CALCULATED FROM ESTIMATED M.M.I. LEVELS AT SITES

CONTOUR LEVELS OF LOG(PSV):

	6	-	7	/	8	~
.1	.2	.3	.4	.5	.6	.7

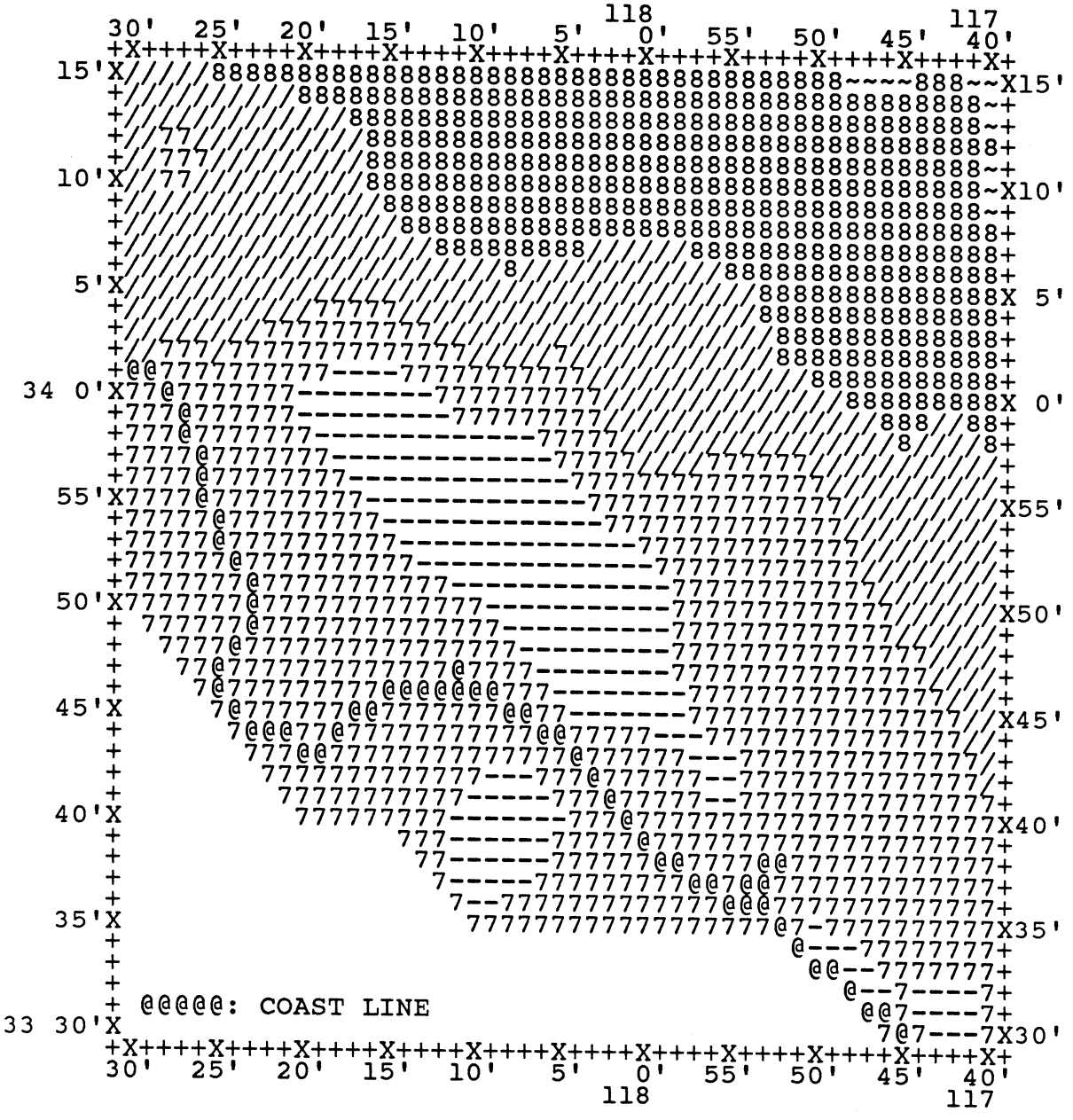

Figure B3.2

PSEUDO RELATIVE VELOCITY, PSV (IN/SEC) AT T = .110 SEC

PROBABILITY OF EXCEEDANCE = .50 FOR 50 YEARS
CALCULATED FROM ESTIMATED M.M.I. LEVELS AT SITES

CONTOUR LEVELS OF LOG(PSV):

/ .5 8 .6 ~ .7 9 .8 ! .9 a 1.0

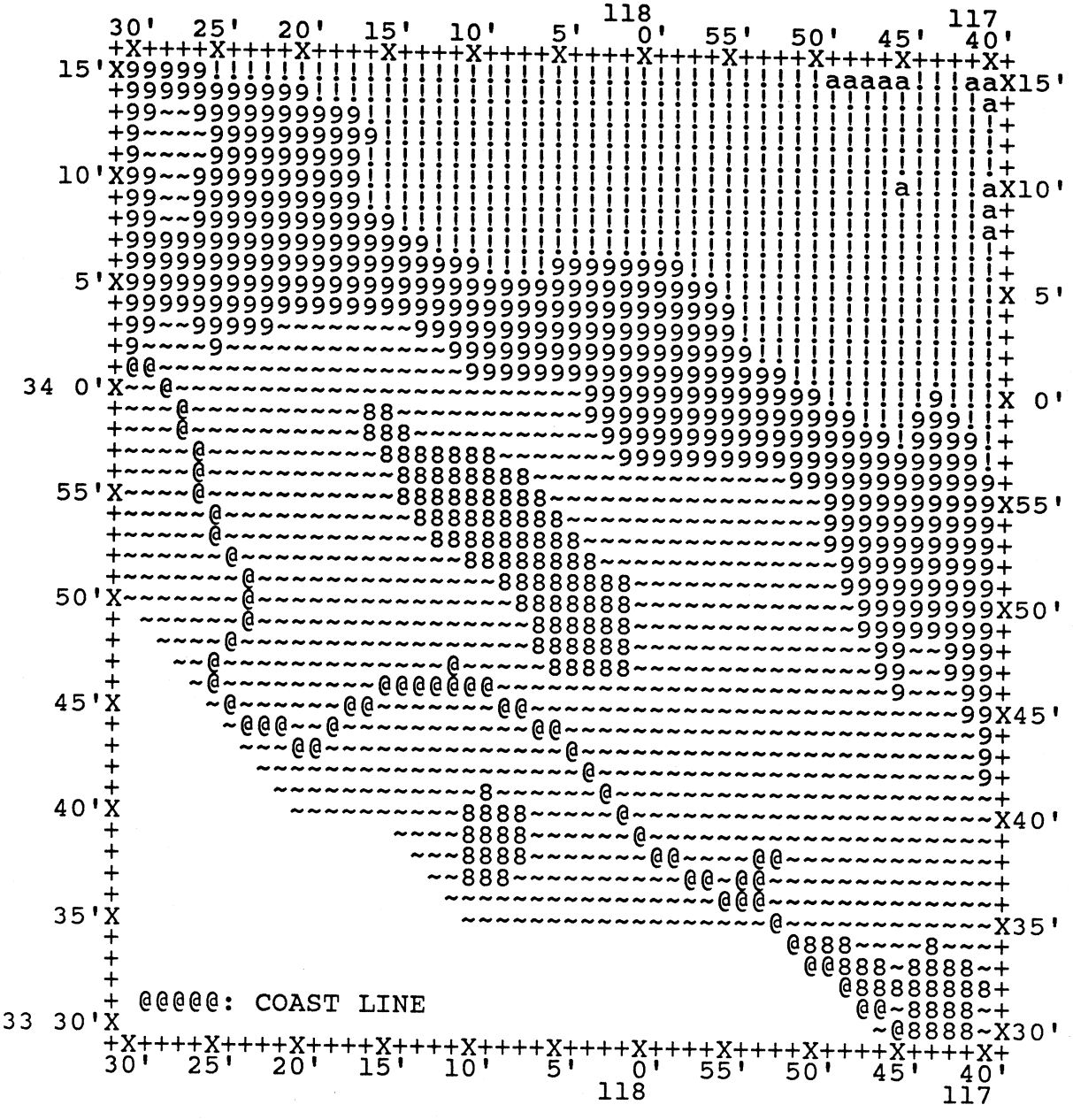

Figure B3.3

PSEUDO RELATIVE VELOCITY, PSV (IN/SEC) AT T = .190 SEC

PROBABILITY OF EXCEEDANCE = .50 FOR 50 YEARS
CALCULATED FROM ESTIMATED M.M.I. LEVELS AT SITES

CONTOUR LEVELS OF LOG(PSV):

9	!	a	[	b	]
.8	.9	1.0	1.1	1.2	1.3

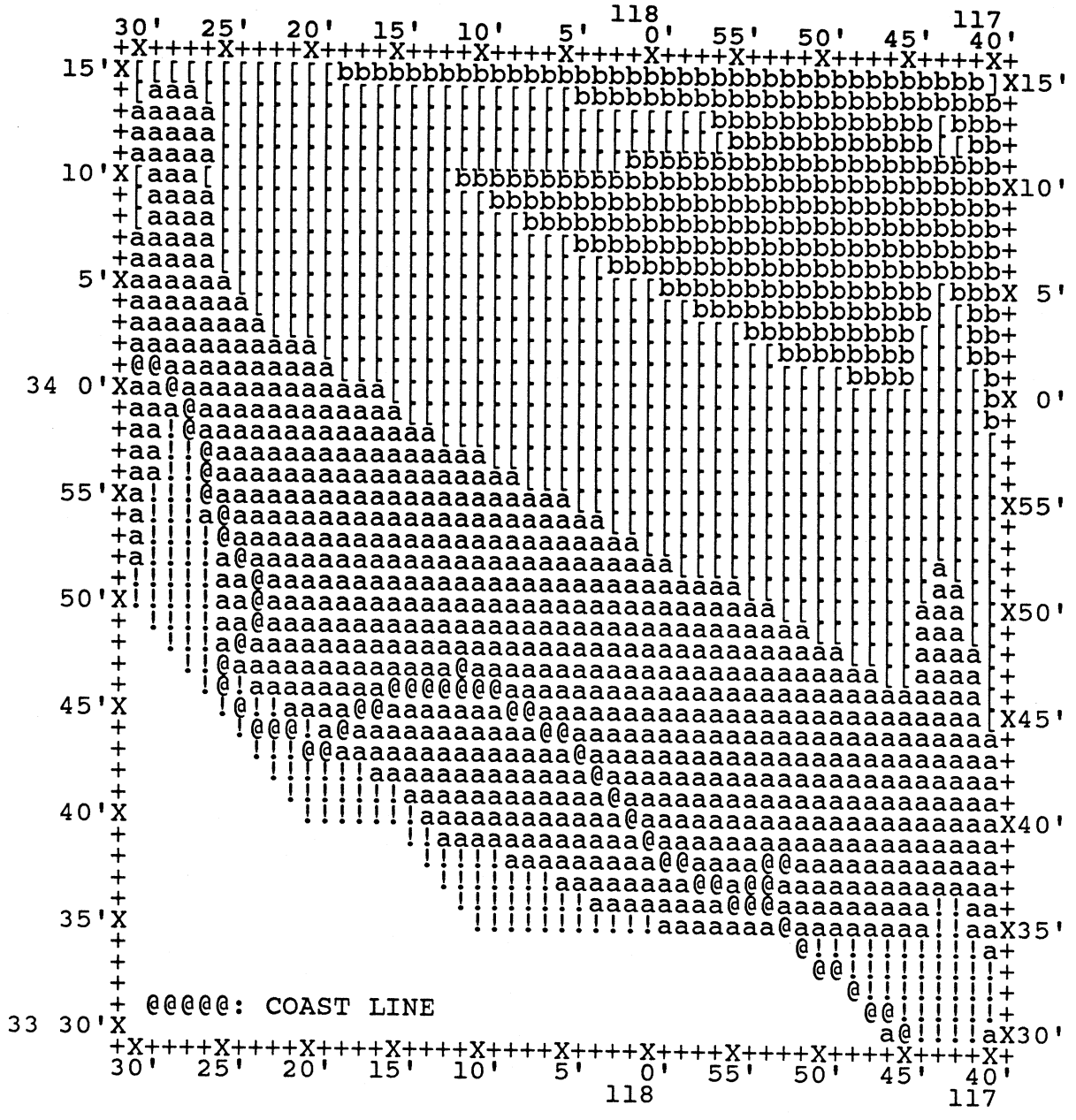

Figure B3.4

PSEUDO RELATIVE VELOCITY, PSV (IN/SEC) AT T = .340 SEC

PROBABILITY OF EXCEEDANCE = .50 FOR 50 YEARS
CALCULATED FROM ESTIMATED M.M.I. LEVELS AT SITES

CONTOUR LEVELS OF LOG(PSV):

a [b] c
1.0 1.1 1.2 1.3 1.4

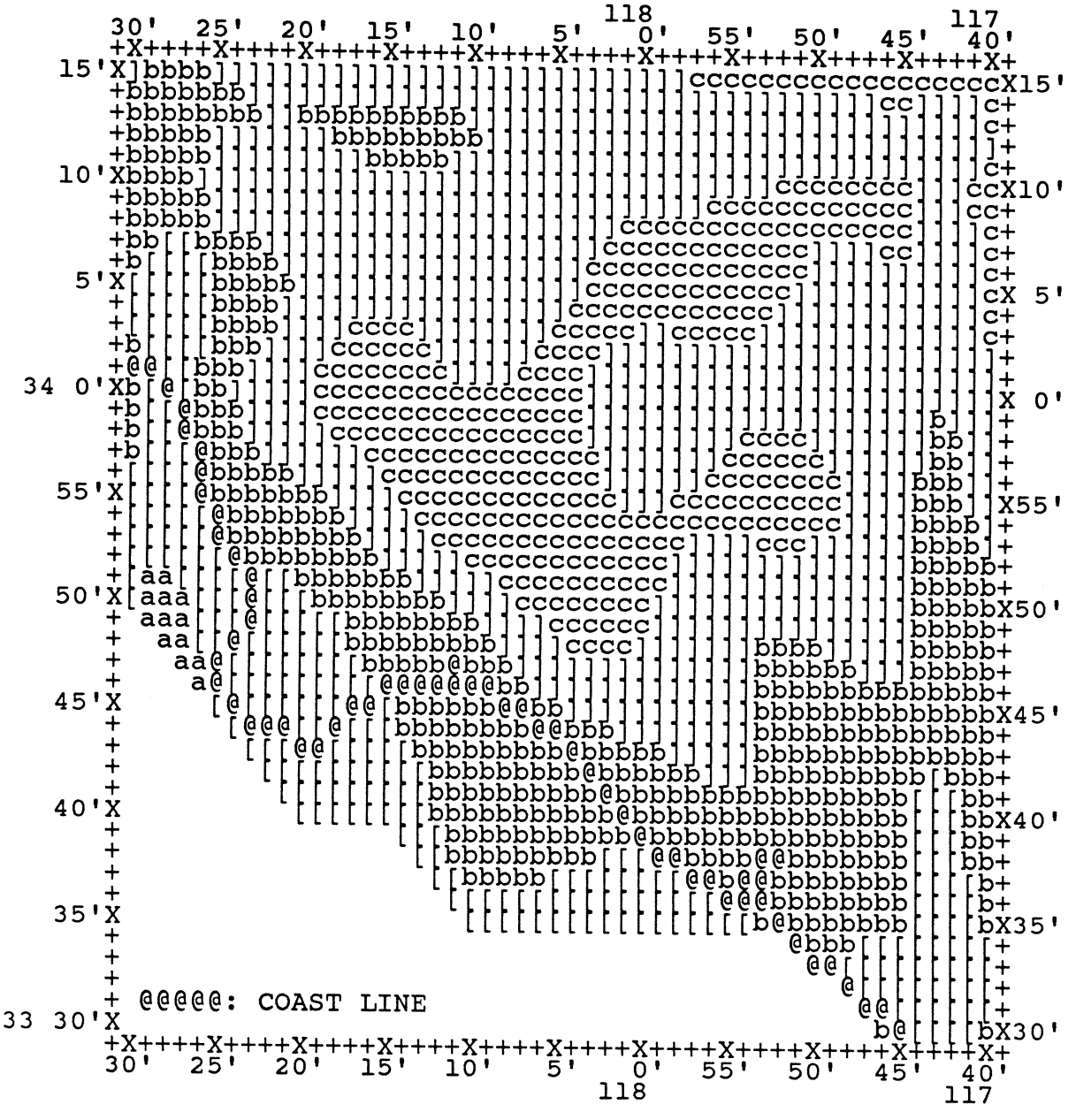

Figure B3.5

PSEUDO RELATIVE VELOCITY, PSV (IN/SEC) AT T = .500 SEC

PROBABILITY OF EXCEEDANCE = .50 FOR 50 YEARS
CALCULATED FROM ESTIMATED M.M.I. LEVELS AT SITES

CONTOUR LEVELS OF LOG(PSV):

a 1.0 [1.1 b 1.2] 1.3 c 1.4 ^ 1.5 d 1.6

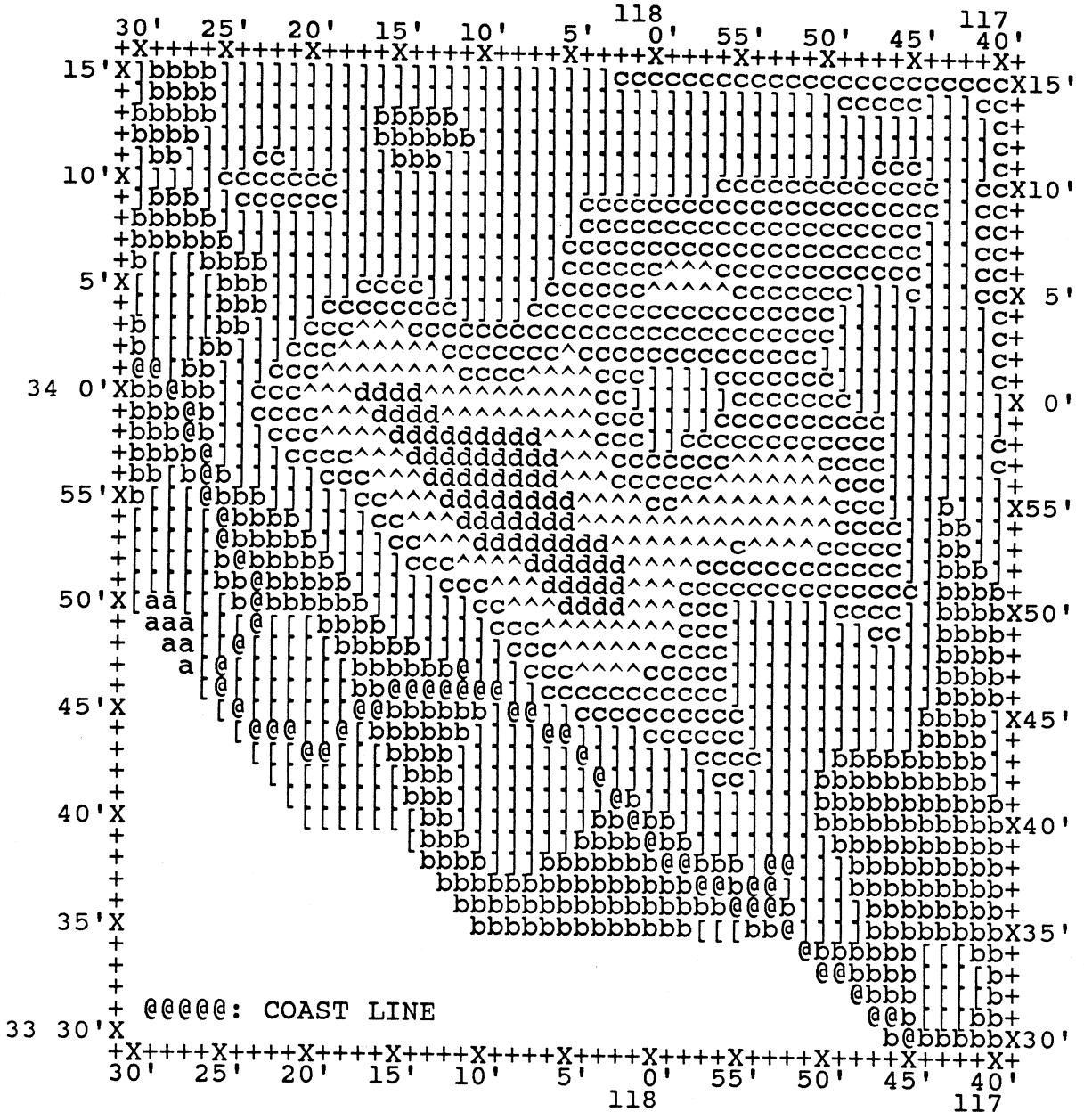

Figure B3.6

PSEUDO RELATIVE VELOCITY, PSV (IN/SEC) AT T = .900 SEC

PROBABILITY OF EXCEEDANCE = .50 FOR 50 YEARS
CALCULATED FROM ESTIMATED M.M.I. LEVELS AT SITES

CONTOUR LEVELS OF LOG(PSV):

!	a	[	b	]	c	^	d	>	e
.9	1.0	1.1	1.2	1.3	1.4	1.5	1.6	1.7	1.8

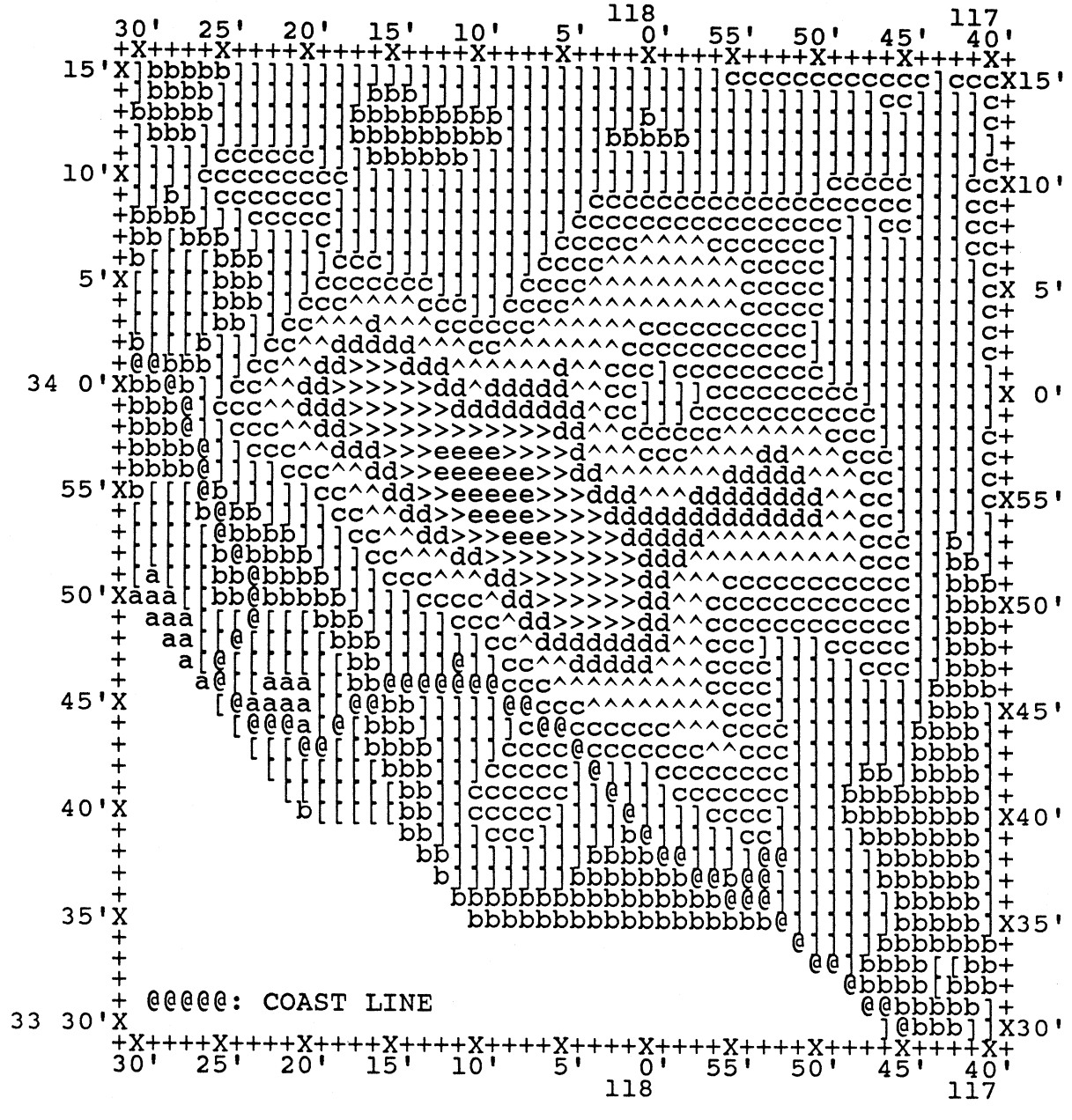

Figure B3.7

PSEUDO RELATIVE VELOCITY, PSV (IN/SEC) AT T = 1.600 SEC

PROBABILITY OF EXCEEDANCE = .50 FOR 50 YEARS
CALCULATED FROM ESTIMATED M.M.I. LEVELS AT SITES

CONTOUR LEVELS OF LOG(PSV):

a	[	b	]	c	^	d	>	e	<
1.0	1.1	1.2	1.3	1.4	1.5	1.6	1.7	1.8	1.9

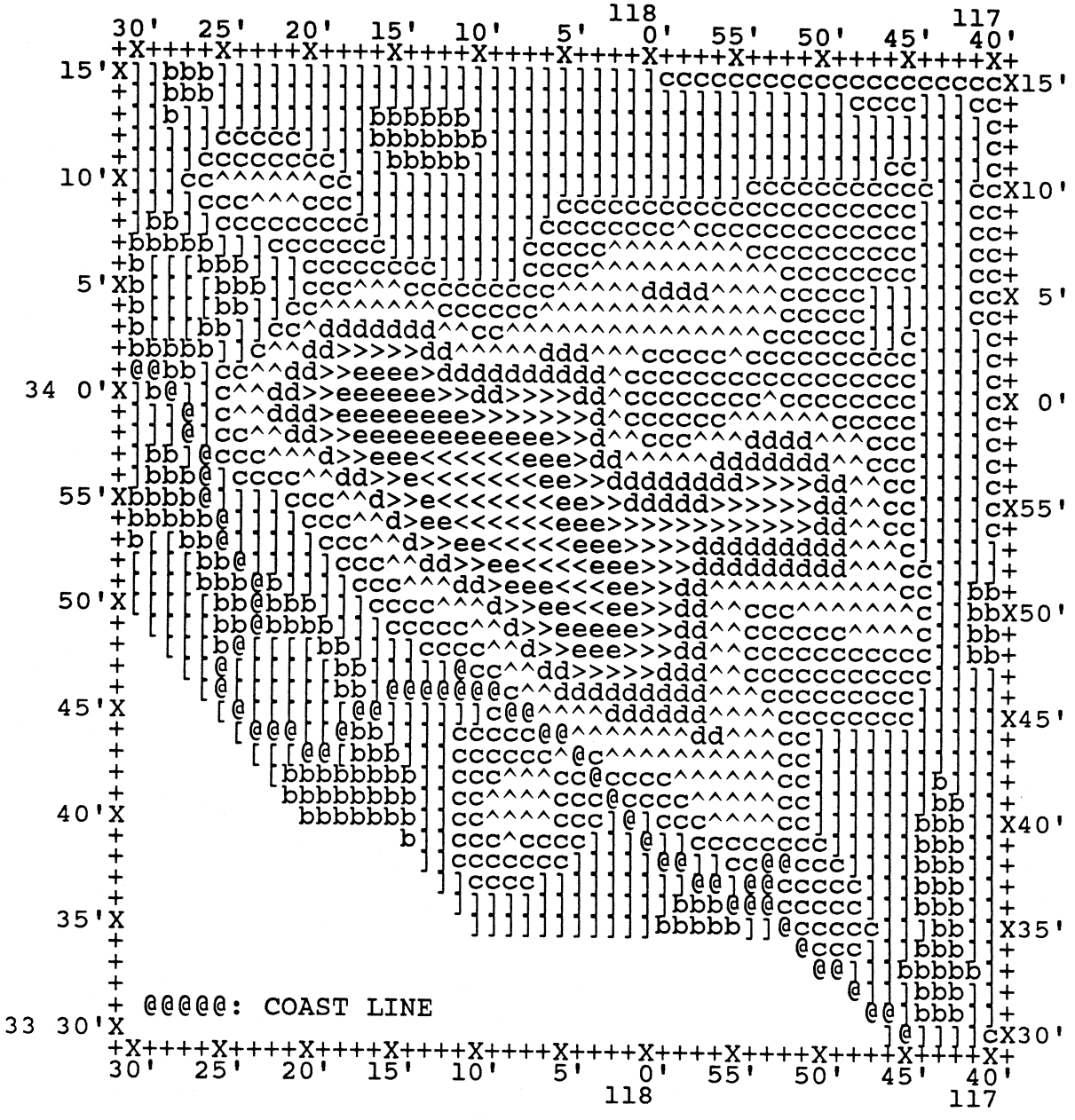

Figure B3.8

PSEUDO RELATIVE VELOCITY, PSV (IN/SEC) AT T = 2.800 SEC

PROBABILITY OF EXCEEDANCE = .50 FOR 50 YEARS
CALCULATED FROM ESTIMATED M.M.I. LEVELS AT SITES

CONTOUR LEVELS OF LOG(PSV):

a	[	b	]	c	^	d	>	e	<	f
1.0	1.1	1.2	1.3	1.4	1.5	1.6	1.7	1.8	1.9	2.0

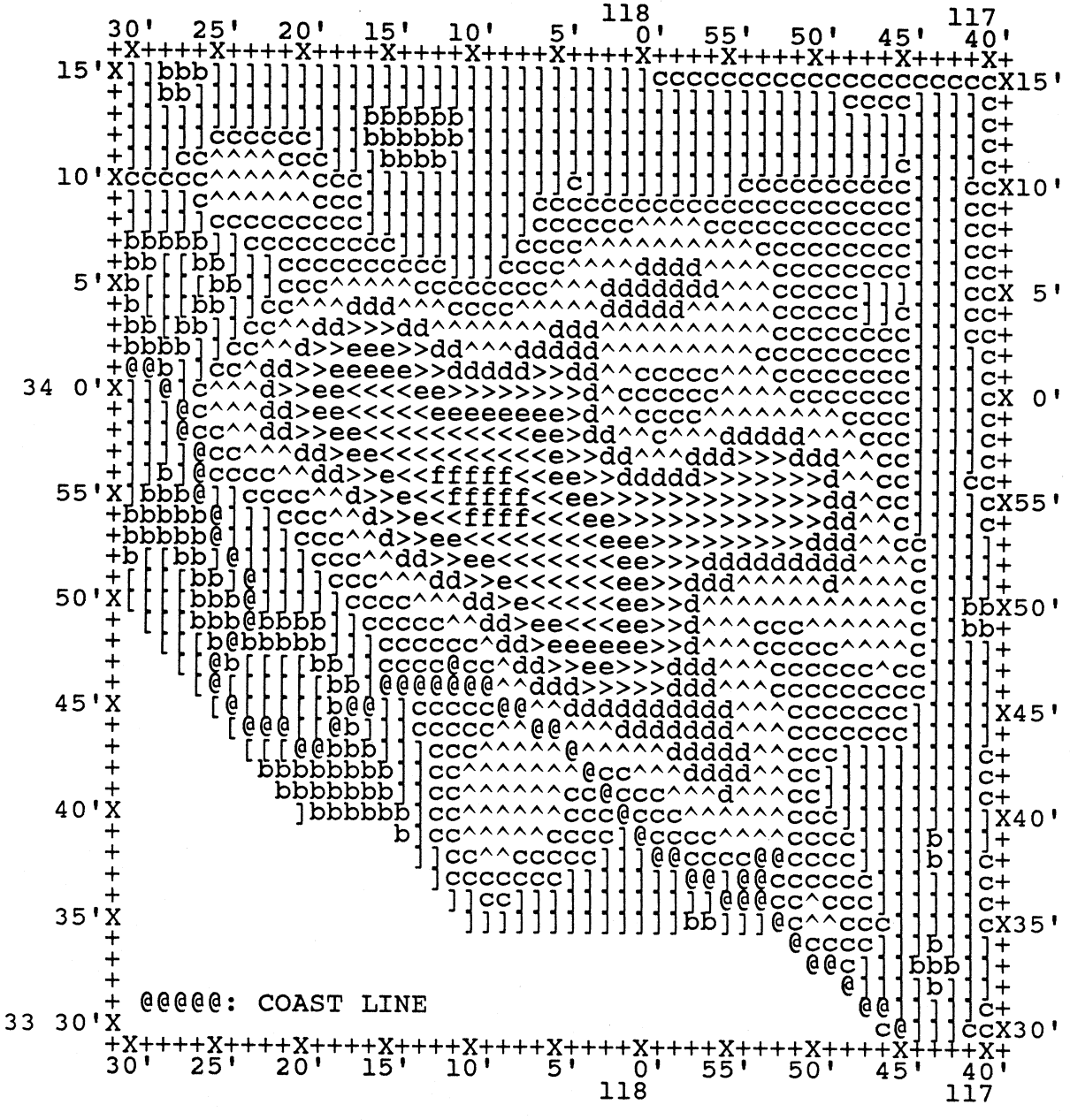

Figure B3.9

PSEUDO RELATIVE VELOCITY, PSV (IN/SEC) AT T = 4.400 SEC

PROBABILITY OF EXCEEDANCE = .50 FOR 50 YEARS
CALCULATED FROM ESTIMATED M.M.I. LEVELS AT SITES

CONTOUR LEVELS OF LOG(PSV):

!	a	[	b	]	c	^	d	>	e	<
.9	1.0	1.1	1.2	1.3	1.4	1.5	1.6	1.7	1.8	1.9

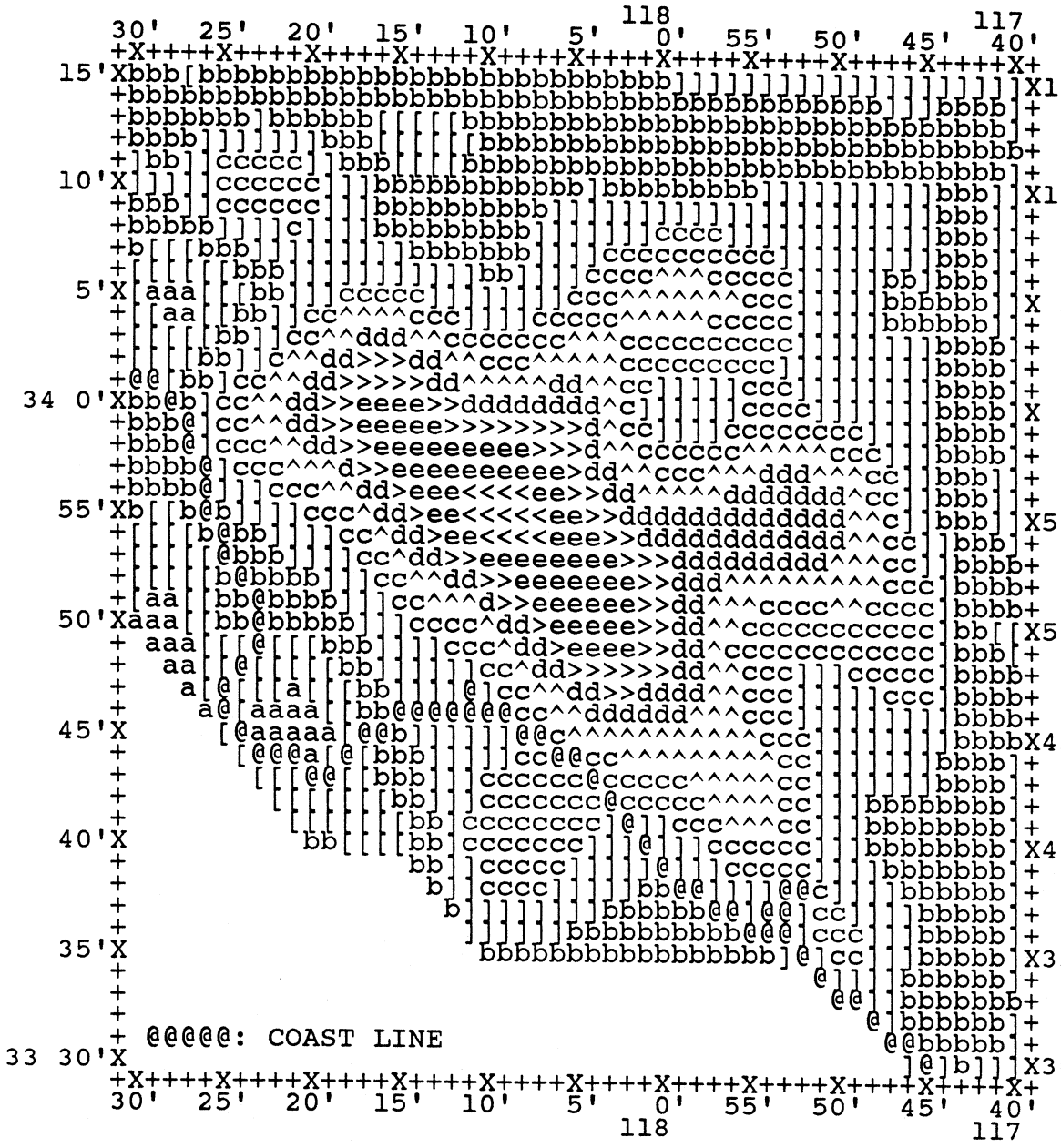

Figure B3.10

PSEUDO RELATIVE VELOCITY, PSV (IN/SEC) AT T = 7.500 SEC

PROBABILITY OF EXCEEDANCE = .50 FOR 50 YEARS
CALCULATED FROM ESTIMATED M.M.I. LEVELS AT SITES

CONTOUR LEVELS OF LOG(PSV):

8	~	9	!	a	[	b	]	c	^	d
.6	.7	.8	.9	1.0	1.1	1.2	1.3	1.4	1.5	1.6

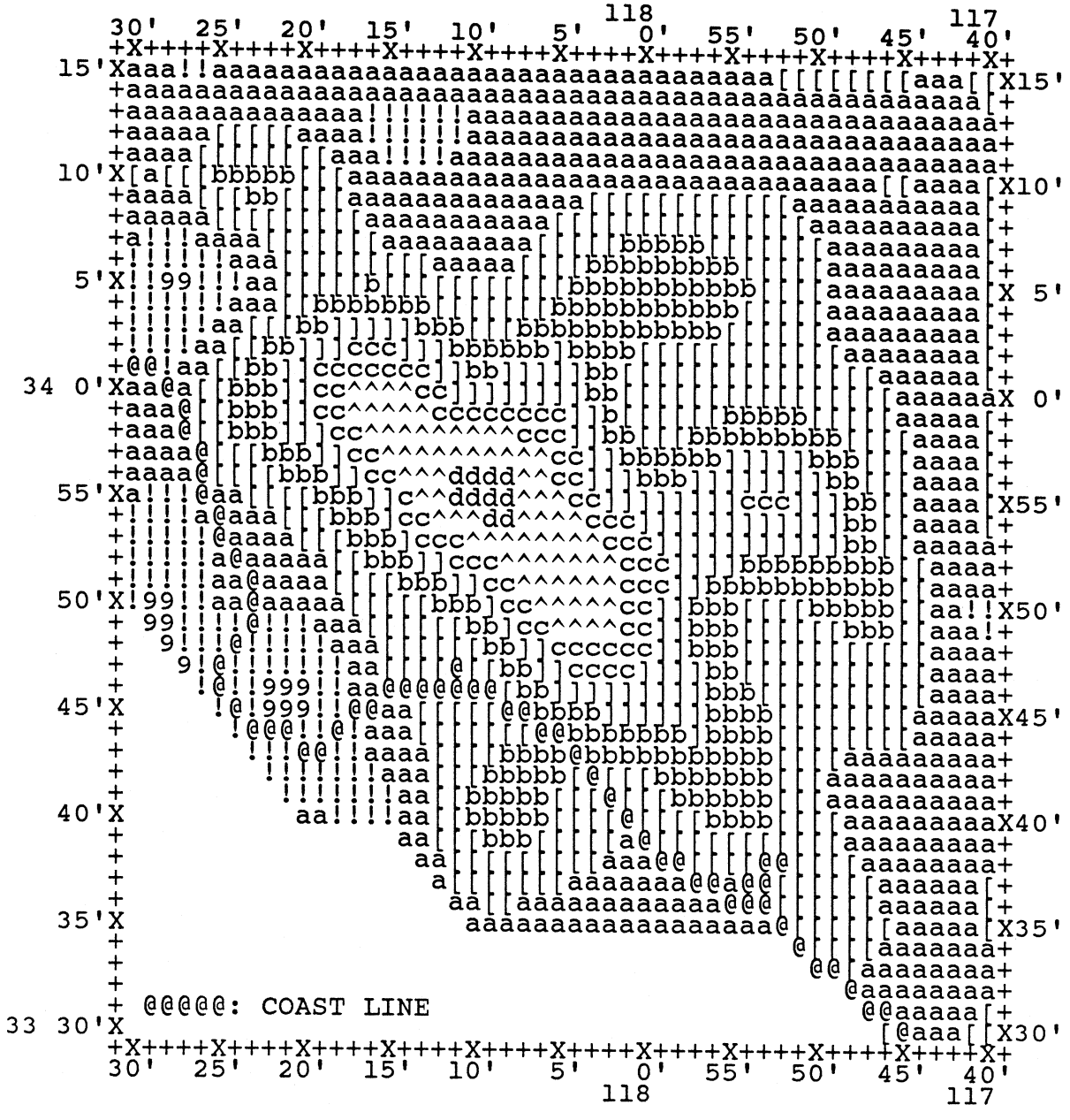

Figure B3.11

PSEUDO RELATIVE VELOCITY, PSV (IN/SEC) AT T = .040 SEC

PROBABILITY OF EXCEEDANCE = .10 FOR 50 YEARS
CALCULATED FROM ESTIMATED M.M.I. LEVELS AT SITES

CONTOUR LEVELS OF LOG(PSV):

	6	-	7	/	8	~
.1	.2	.3	.4	.5	.6	.7

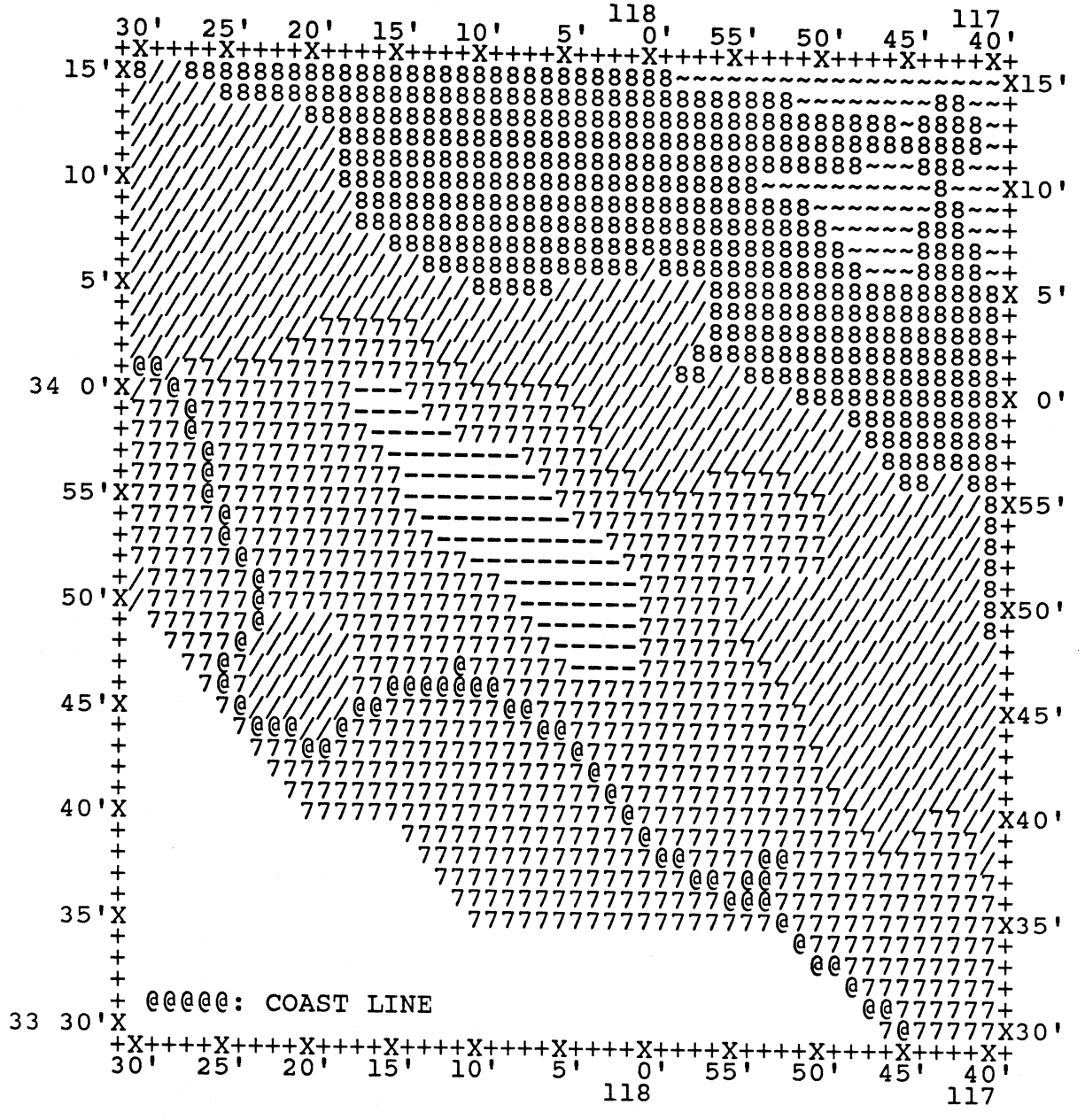

Figure B4.1

PSEUDO RELATIVE VELOCITY, PSV (IN/SEC) AT T = .065 SEC

PROBABILITY OF EXCEEDANCE = .10 FOR 50 YEARS
CALCULATED FROM ESTIMATED M.M.I. LEVELS AT SITES

CONTOUR LEVELS OF LOG(PSV):

7 / 8 ~ 9 !
.4 .5 .6 .7 .8 .9

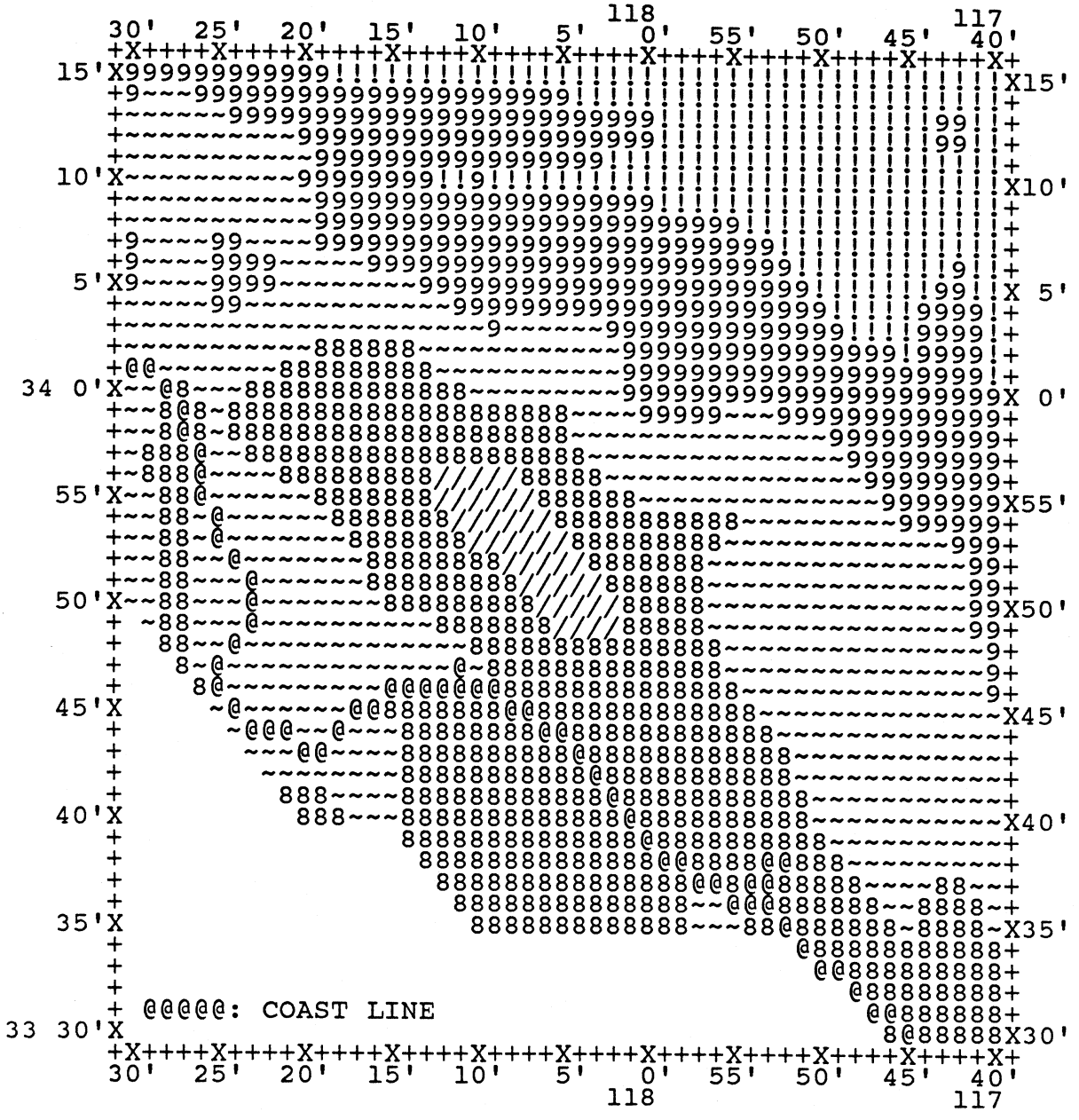

Figure B4.2

PSEUDO RELATIVE VELOCITY, PSV (IN/SEC) AT T = .110 SEC

PROBABILITY OF EXCEEDANCE = .10 FOR 50 YEARS
CALCULATED FROM ESTIMATED M.M.I. LEVELS AT SITES

CONTOUR LEVELS OF LOG(PSV):

9	!	a	[	b	]
.8	.9	1.0	1.1	1.2	1.3

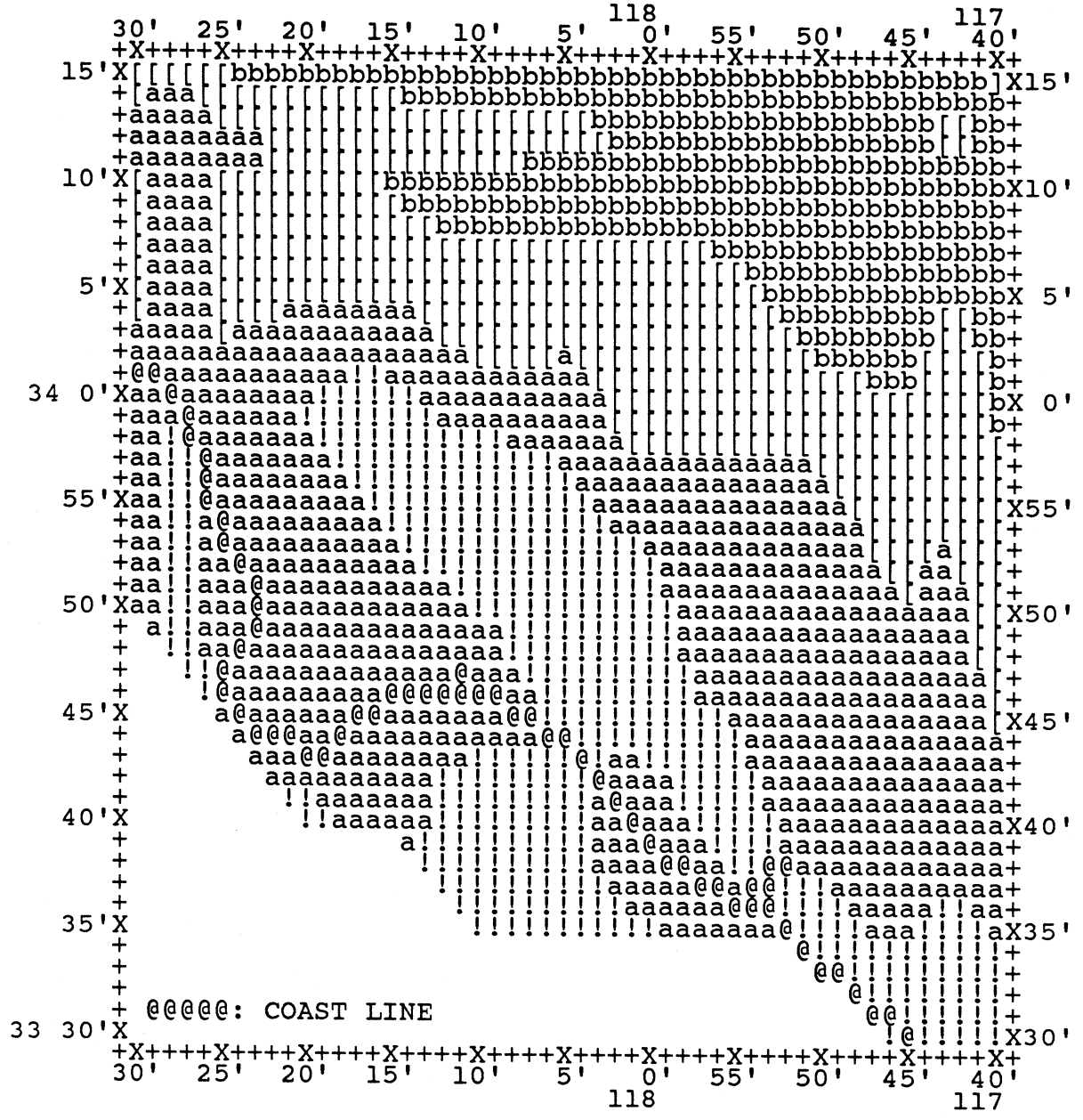

Figure B4.3

PSEUDO RELATIVE VELOCITY, PSV (IN/SEC) AT T = .190 SEC

PROBABILITY OF EXCEEDANCE = .10 FOR 50 YEARS
CALCULATED FROM ESTIMATED M.M.I. LEVELS AT SITES

CONTOUR LEVELS OF LOG(PSV):

[1.1 b 1.2] 1.3 c 1.4 ^ 1.5 d 1.6

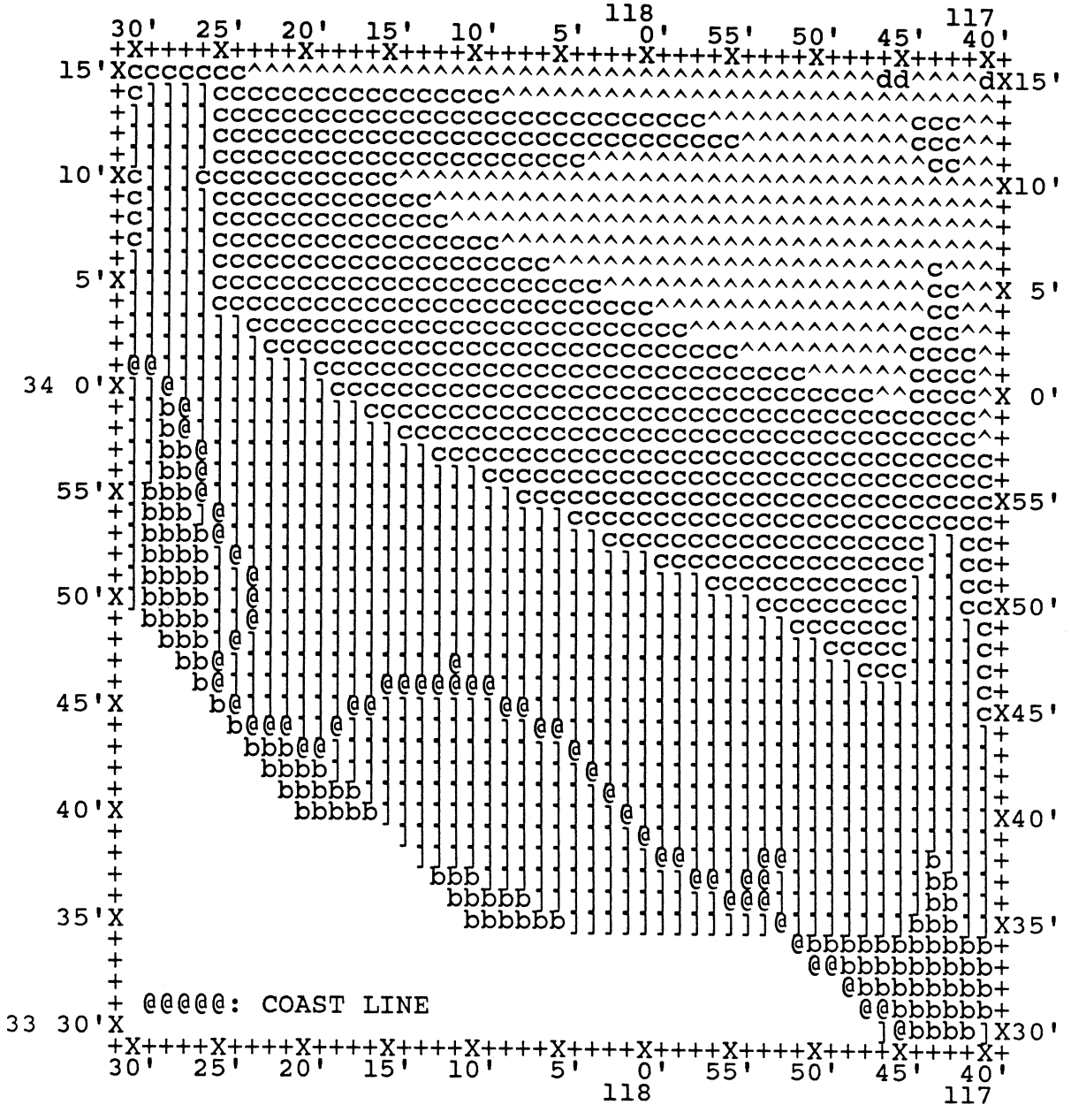

Figure B4.4

PSEUDO RELATIVE VELOCITY, PSV (IN/SEC) AT T = .340 SEC

PROBABILITY OF EXCEEDANCE = .10 FOR 50 YEARS
CALCULATED FROM ESTIMATED M.M.I. LEVELS AT SITES

CONTOUR LEVELS OF LOG(PSV):

]	c	^	d	>	e
1.3	1.4	1.5	1.6	1.7	1.8

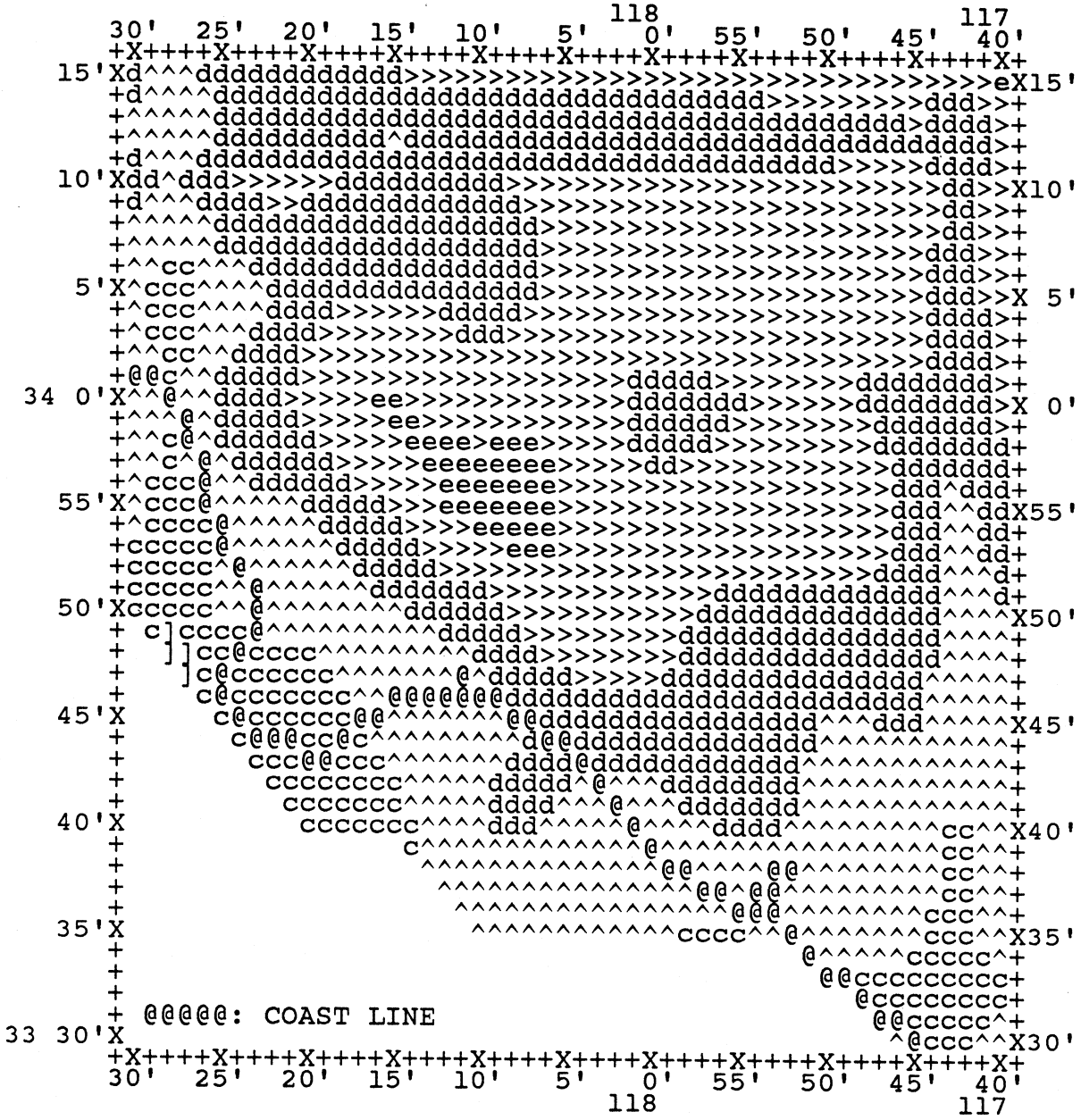

Figure B4.5

PSEUDO RELATIVE VELOCITY, PSV (IN/SEC) AT T = .500 SEC

PROBABILITY OF EXCEEDANCE = .10 FOR 50 YEARS
CALCULATED FROM ESTIMATED M.M.I. LEVELS AT SITES

CONTOUR LEVELS OF LOG(PSV):

]	c	^	d	>	e	<	f
1.3	1.4	1.5	1.6	1.7	1.8	1.9	2.0

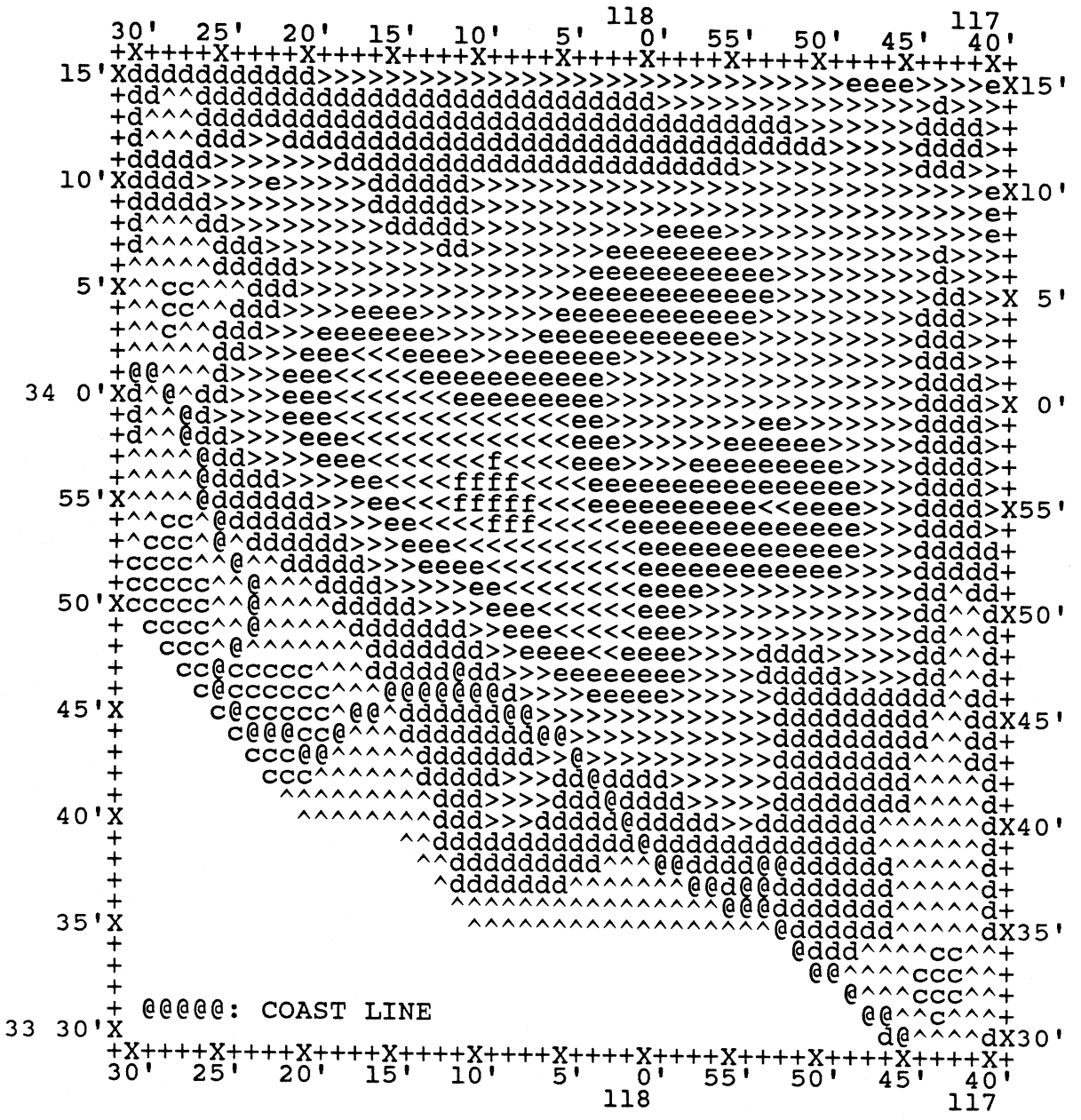

Figure B4.6

PSEUDO RELATIVE VELOCITY, PSV (IN/SEC) AT T = .900 SEC

PROBABILITY OF EXCEEDANCE = .10 FOR 50 YEARS
CALCULATED FROM ESTIMATED M.M.I. LEVELS AT SITES

CONTOUR LEVELS OF LOG(PSV):

]	c	^	d	>	e	<	f	\	g
1.3	1.4	1.5	1.6	1.7	1.8	1.9	2.0	2.1	2.2

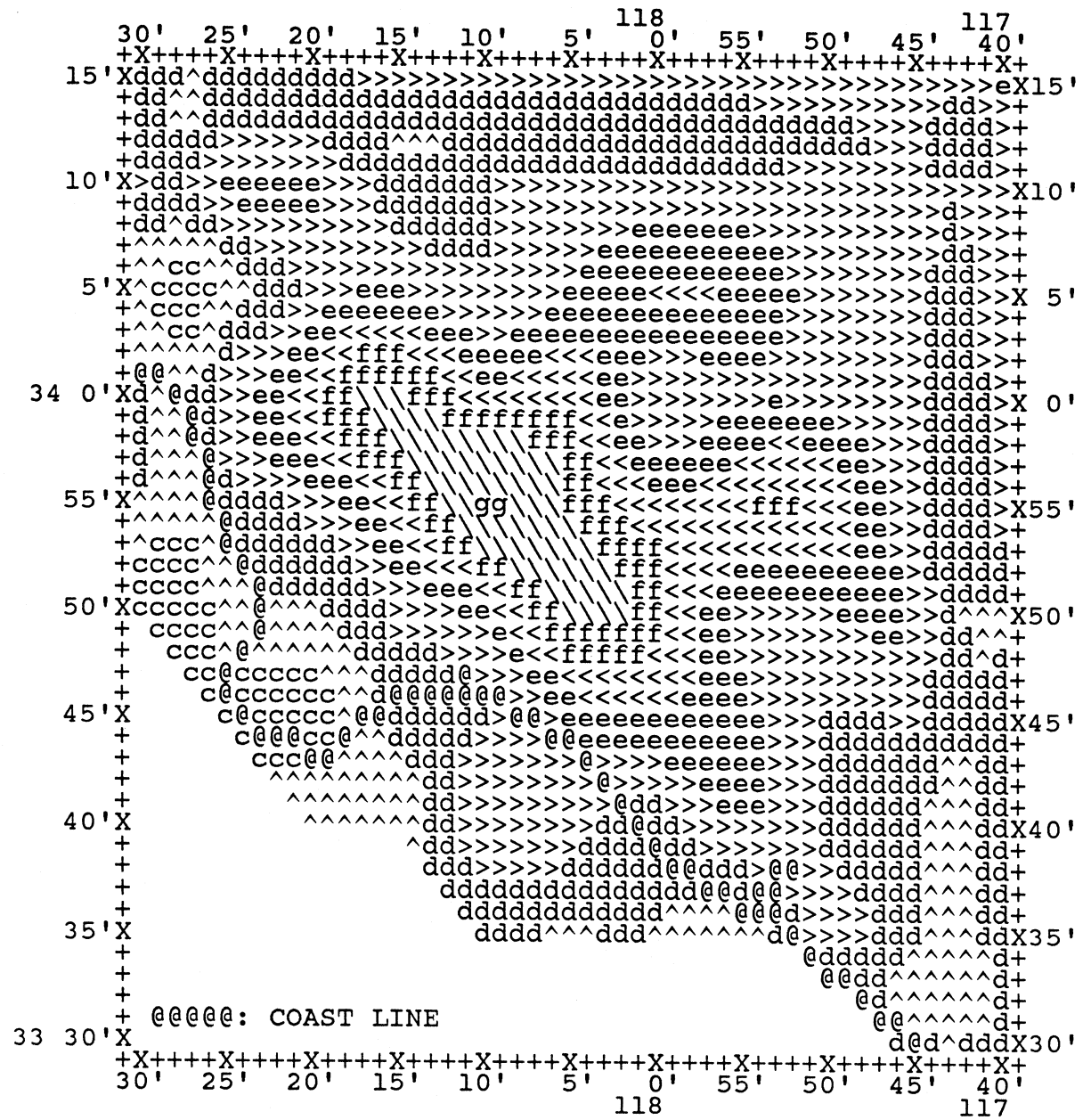

Figure B4.7

PSEUDO RELATIVE VELOCITY, PSV (IN/SEC) AT T = 1.600 SEC

PROBABILITY OF EXCEEDANCE = .10 FOR 50 YEARS
CALCULATED FROM ESTIMATED M.M.I. LEVELS AT SITES

CONTOUR LEVELS OF LOG(PSV):

] 1.3 c 1.4 ^ 1.5 d 1.6 > 1.7 e 1.8 < 1.9 f 2.0 \ 2.1 g 2.2 { 2.3

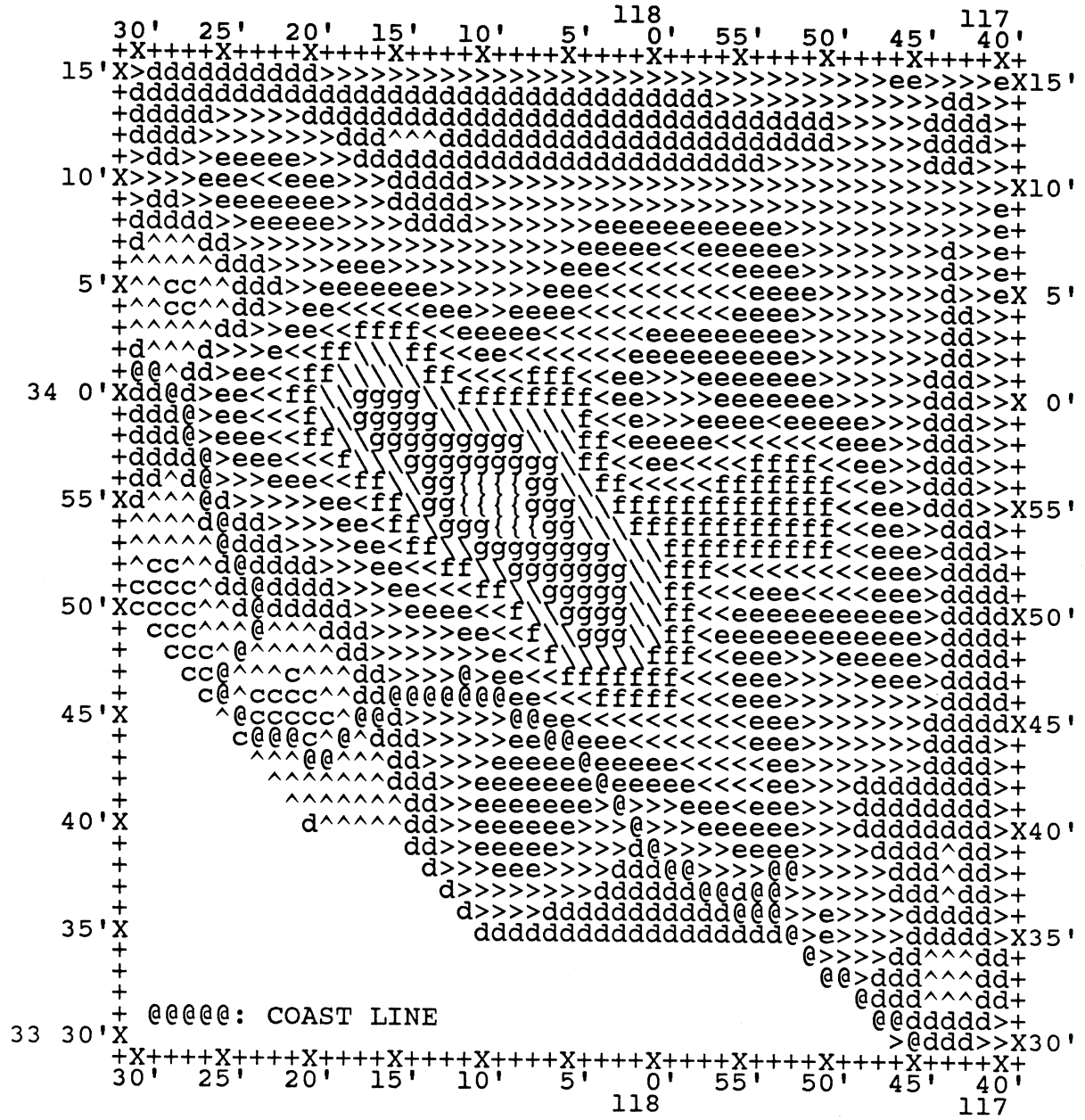

Figure B4.8

PSEUDO RELATIVE VELOCITY, PSV (IN/SEC) AT T = 2.800 SEC

PROBABILITY OF EXCEEDANCE = .10 FOR 50 YEARS
CALCULATED FROM ESTIMATED M.M.I. LEVELS AT SITES

CONTOUR LEVELS OF LOG(PSV):

```
  ]     c     ^     d     >     e     <     f     \     g     {
1.3   1.4   1.5   1.6   1.7   1.8   1.9   2.0   2.1   2.2   2.3
```

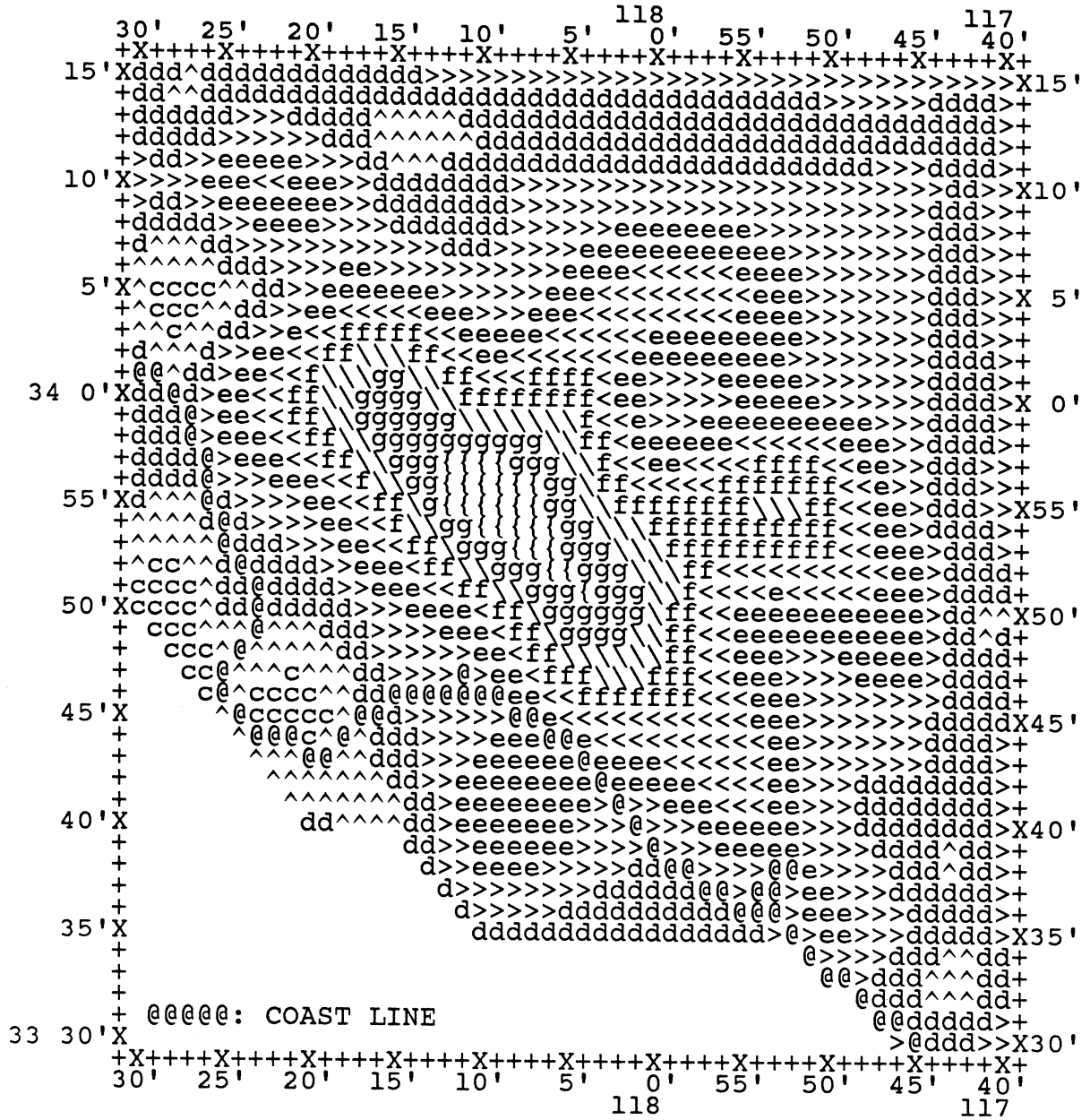

Figure B4.9

PSEUDO RELATIVE VELOCITY, PSV (IN/SEC) AT T = 4.400 SEC

PROBABILITY OF EXCEEDANCE = .10 FOR 50 YEARS
CALCULATED FROM ESTIMATED M.M.I. LEVELS AT SITES

CONTOUR LEVELS OF LOG(PSV):

b	]	c	^	d	>	e	<	f	\	g
1.2	1.3	1.4	1.5	1.6	1.7	1.8	1.9	2.0	2.1	2.2

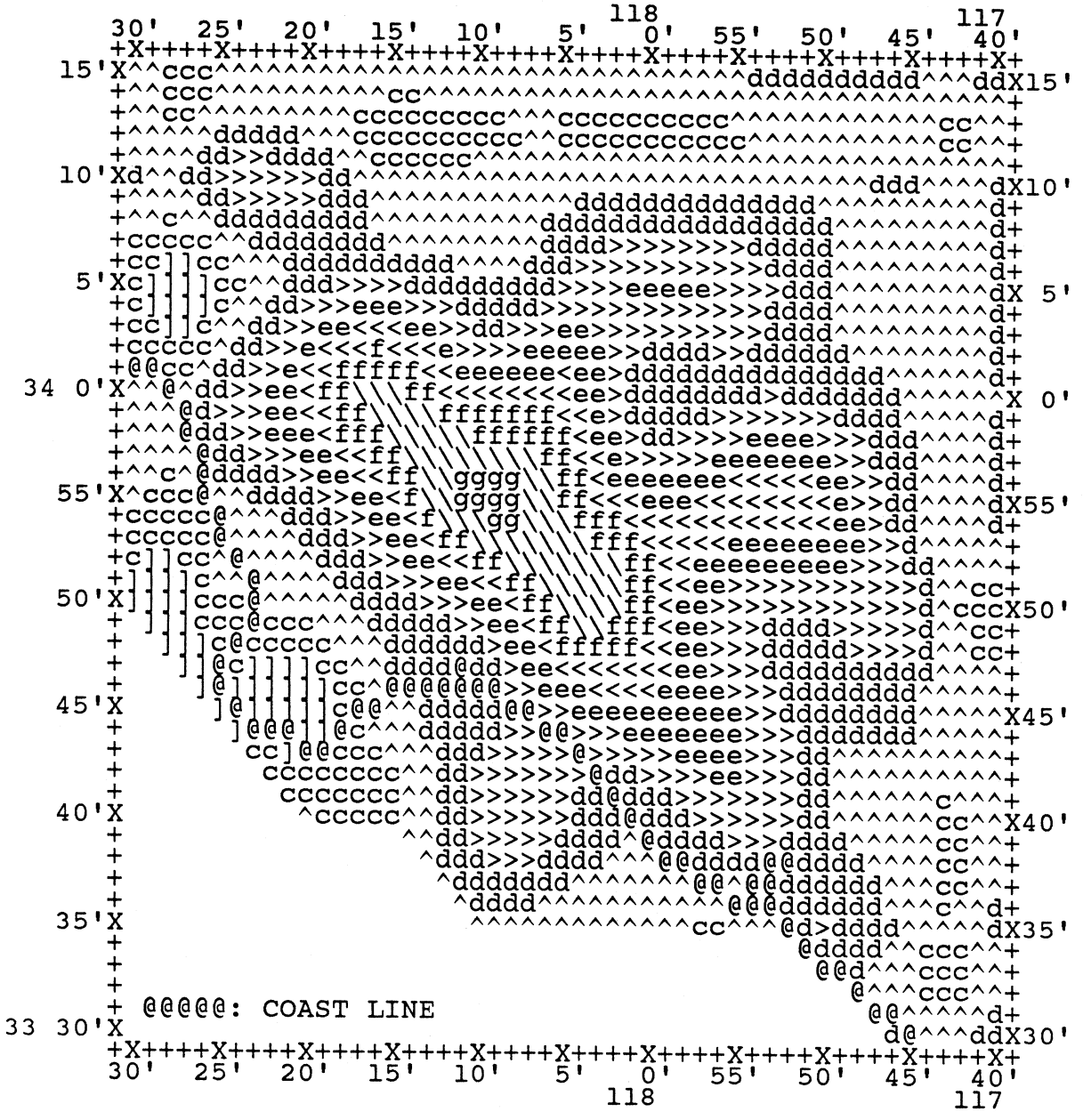

Figure B4.10

PSEUDO RELATIVE VELOCITY, PSV (IN/SEC) AT T = 7.500 SEC

PROBABILITY OF EXCEEDANCE = .10 FOR 50 YEARS
CALCULATED FROM ESTIMATED M.M.I. LEVELS AT SITES

CONTOUR LEVELS OF LOG(PSV):

a	[	b	]	c	^	d	>	e
1.0	1.1	1.2	1.3	1.4	1.5	1.6	1.7	1.8

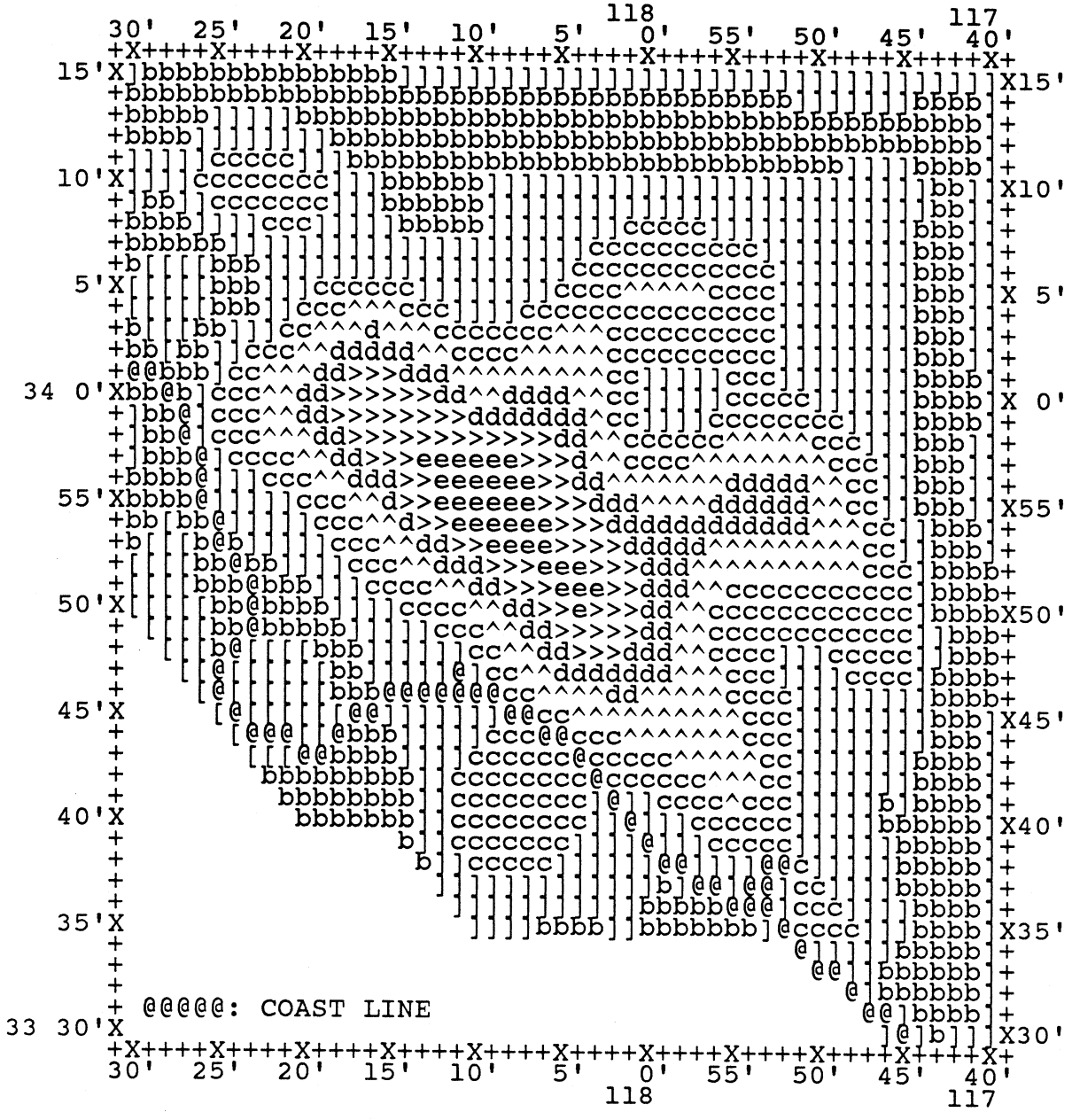

Figure B4.11

PSEUDO RELATIVE VELOCITY, PSV (IN/SEC) AT T = .040 SEC

PROBABILITY OF EXCEEDANCE = .01 FOR 50 YEARS
CALCULATED FROM ESTIMATED M.M.I. LEVELS AT SITES

CONTOUR LEVELS OF LOG(PSV):

/ .5 8 .6 ~ .7 9 .8 ! .9 a 1.0

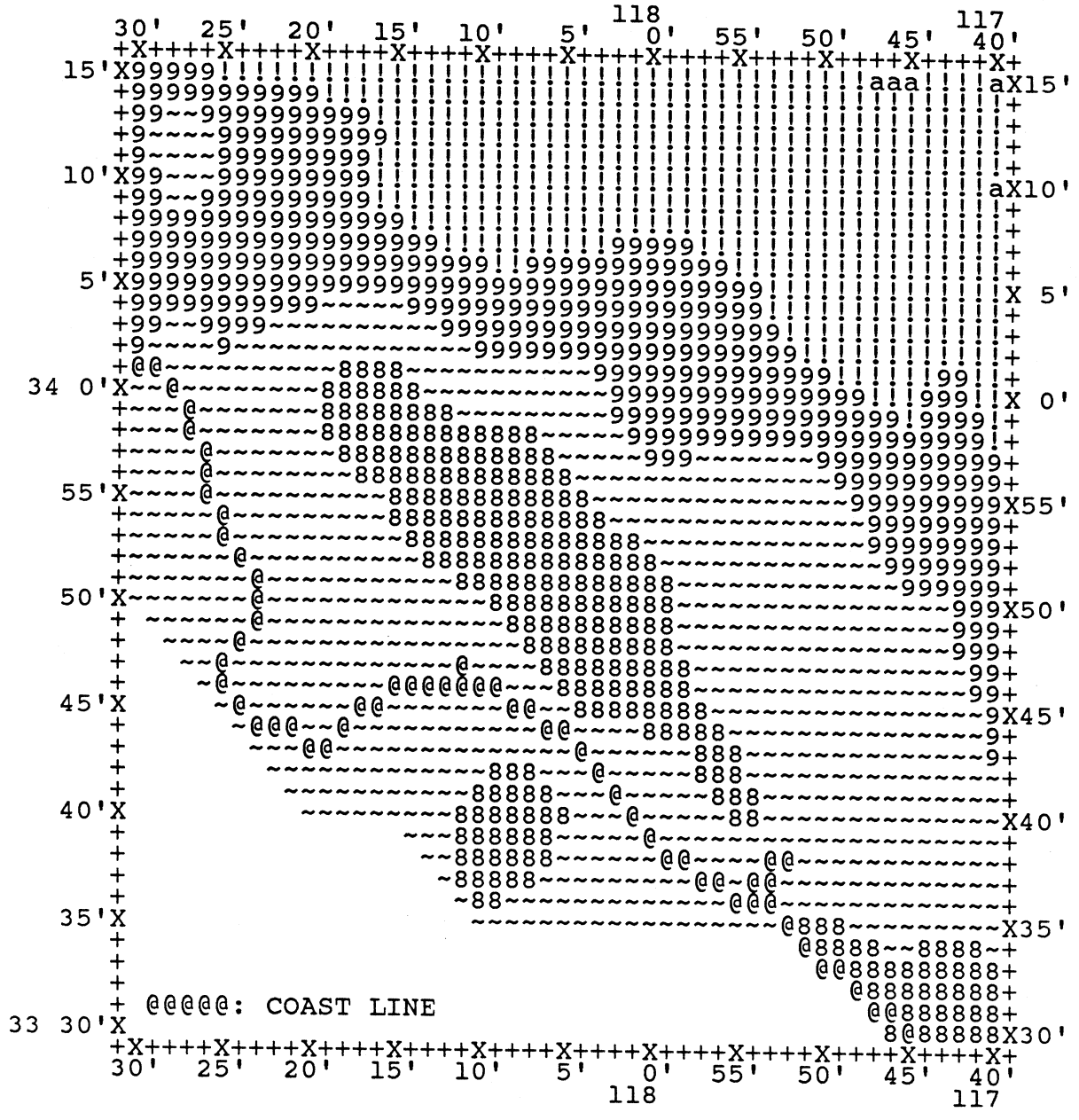

Figure B5.1

PSEUDO RELATIVE VELOCITY, PSV (IN/SEC) AT T = .065 SEC

PROBABILITY OF EXCEEDANCE = .01 FOR 50 YEARS
CALCULATED FROM ESTIMATED M.M.I. LEVELS AT SITES

CONTOUR LEVELS OF LOG(PSV):

8	~	9	!	a	[	b
.6	.7	.8	.9	1.0	1.1	1.2

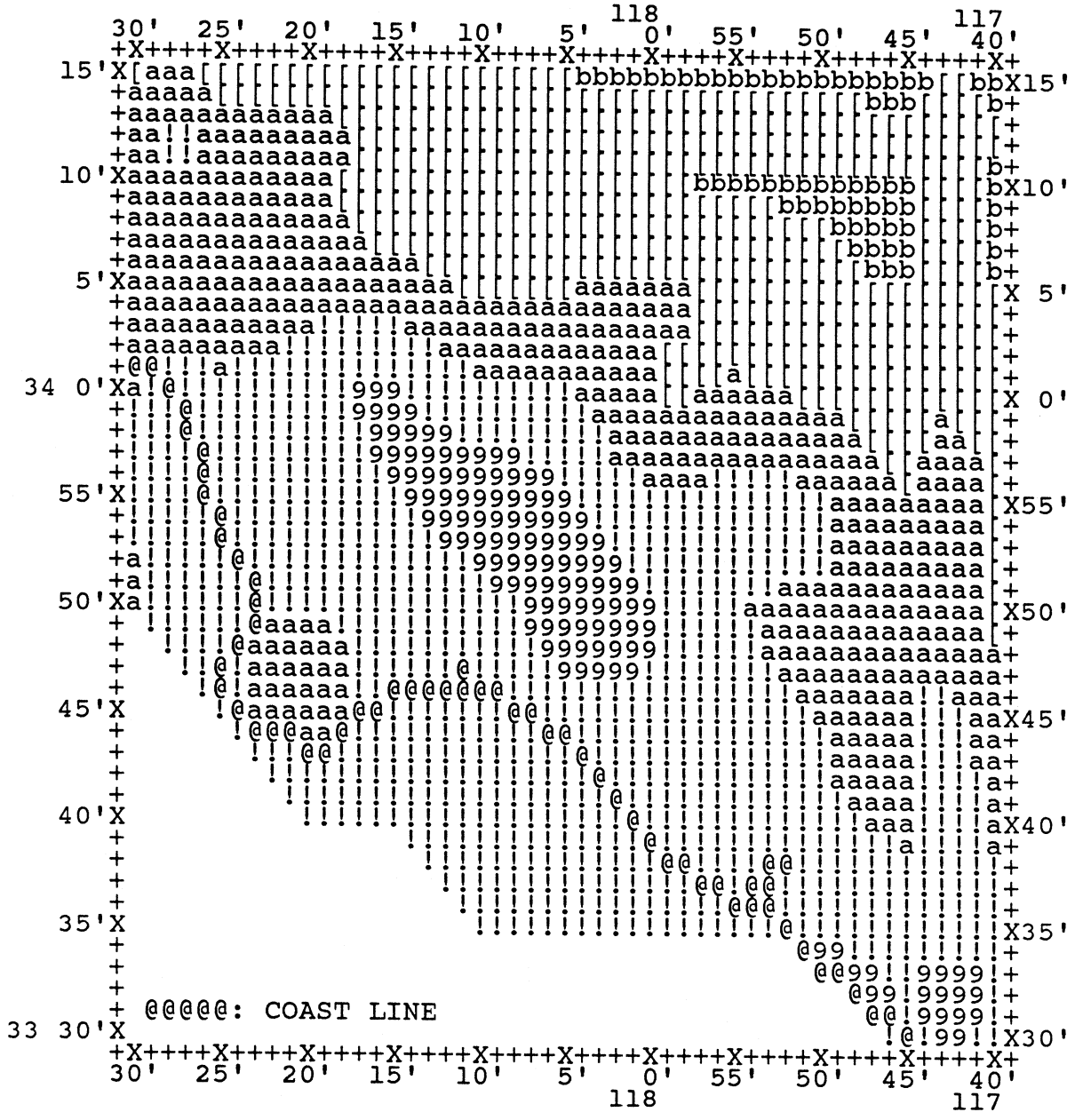

Figure B5.2

PSEUDO RELATIVE VELOCITY, PSV (IN/SEC) AT T = .110 SEC

PROBABILITY OF EXCEEDANCE = .01 FOR 50 YEARS
CALCULATED FROM ESTIMATED M.M.I. LEVELS AT SITES

CONTOUR LEVELS OF LOG(PSV):

[b] c ^
1.1 1.2 1.3 1.4 1.5

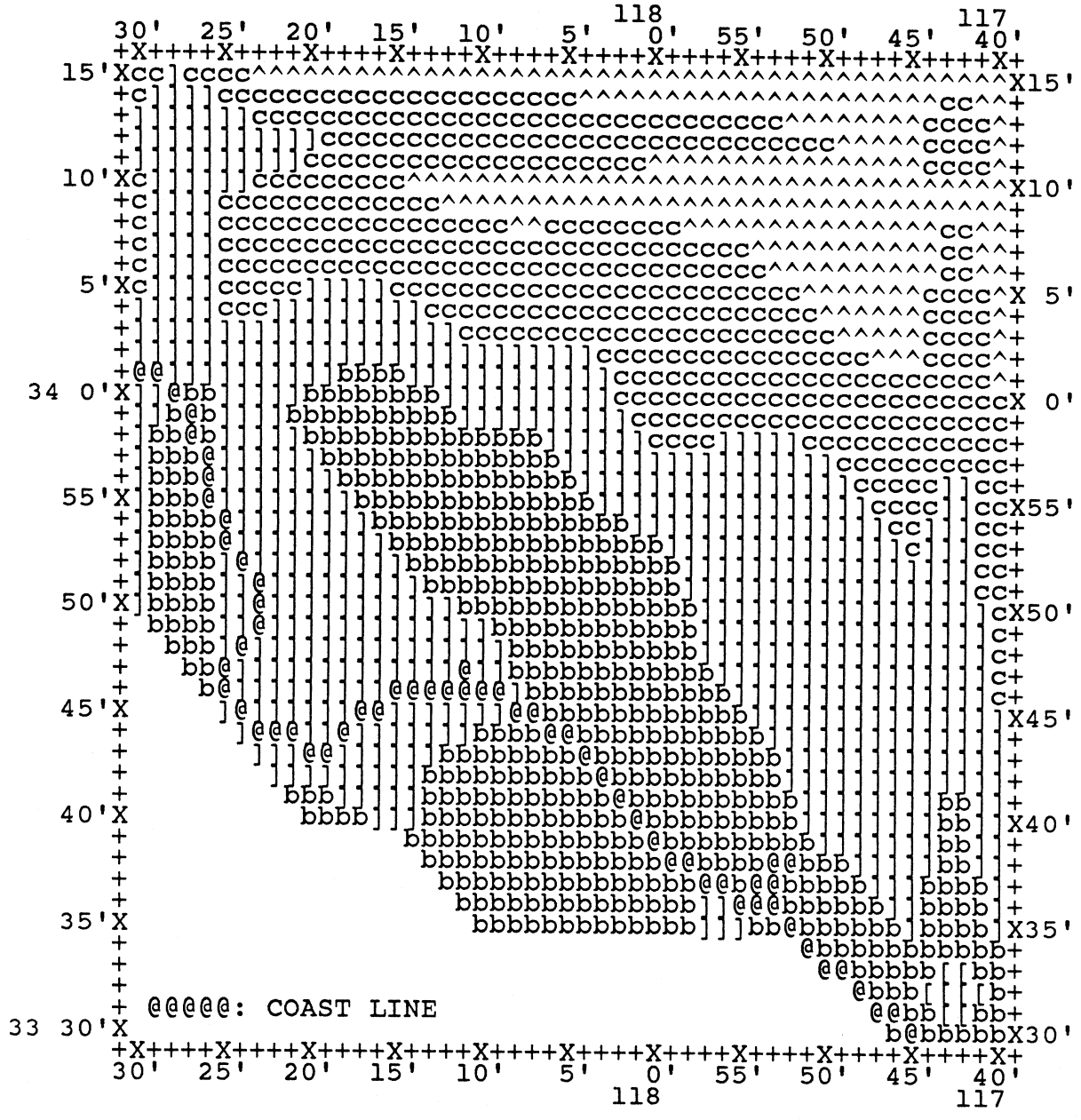

Figure B5.3

PSEUDO RELATIVE VELOCITY, PSV (IN/SEC) AT T = .190 SEC

PROBABILITY OF EXCEEDANCE = .01 FOR 50 YEARS
CALCULATED FROM ESTIMATED M.M.I. LEVELS AT SITES

CONTOUR LEVELS OF LOG(PSV):

^	d	>	e	<
1.5	1.6	1.7	1.8	1.9

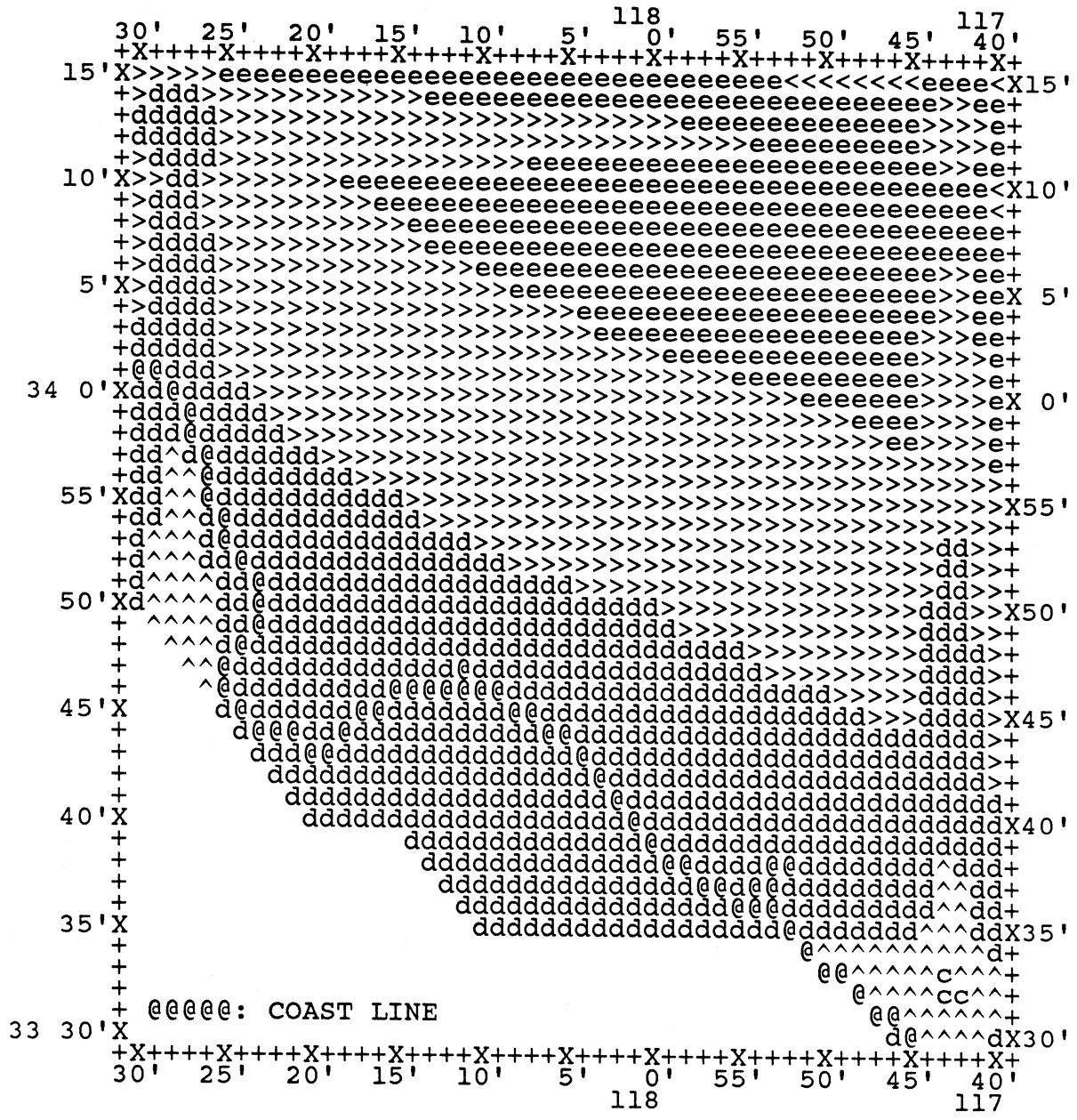

Figure B5.4

PSEUDO RELATIVE VELOCITY, PSV (IN/SEC) AT T = .340 SEC

PROBABILITY OF EXCEEDANCE = .01 FOR 50 YEARS
CALCULATED FROM ESTIMATED M.M.I. LEVELS AT SITES

CONTOUR LEVELS OF LOG(PSV):

d	>	e	<	f	\
1.6	1.7	1.8	1.9	2.0	2.1

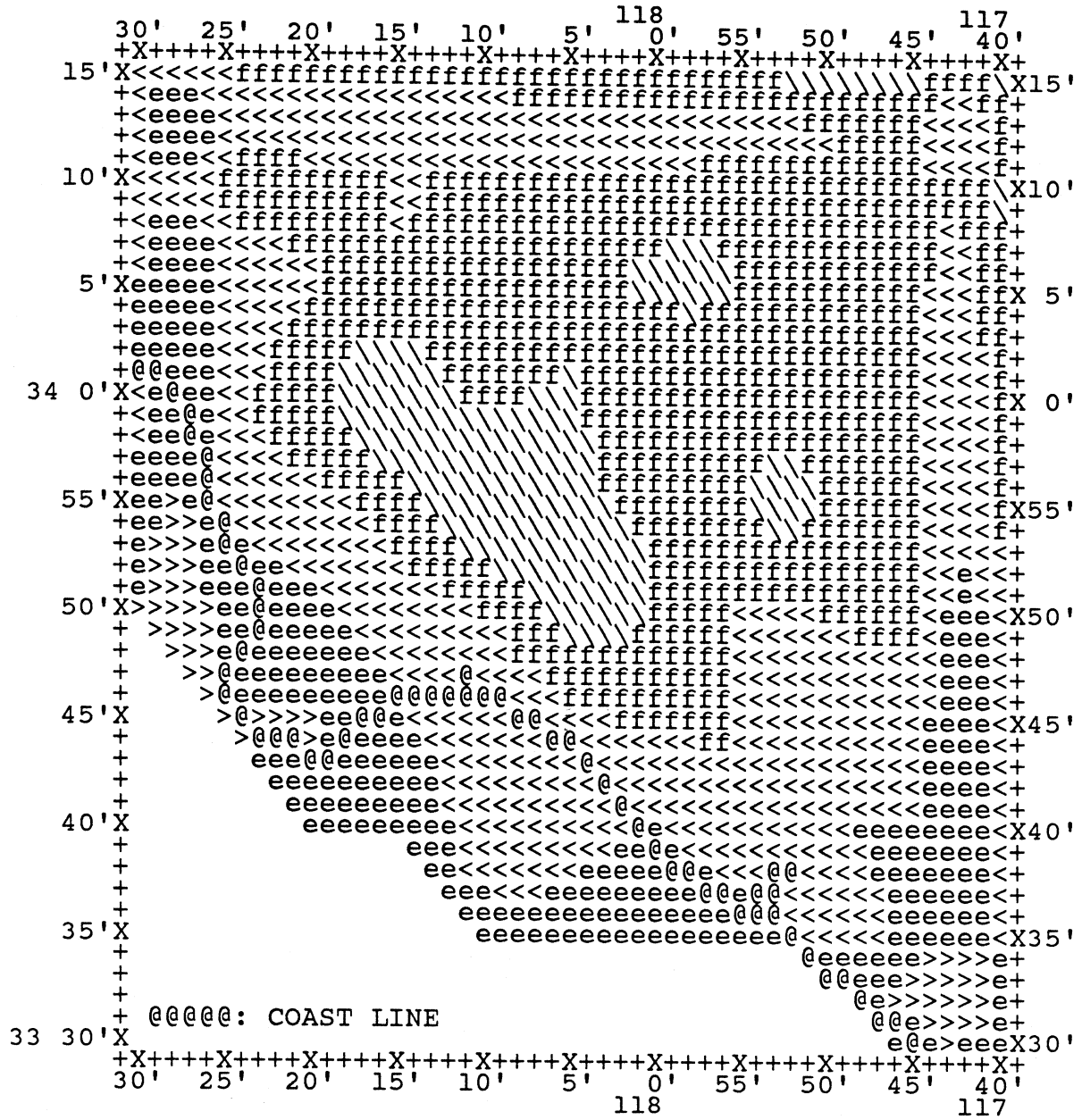

Figure B5.5

PSEUDO RELATIVE VELOCITY, PSV (IN/SEC) AT T = .500 SEC

PROBABILITY OF EXCEEDANCE = .01 FOR 50 YEARS
CALCULATED FROM ESTIMATED M.M.I. LEVELS AT SITES

CONTOUR LEVELS OF LOG(PSV):

>	e	<	f	\	g	{
1.7	1.8	1.9	2.0	2.1	2.2	2.3

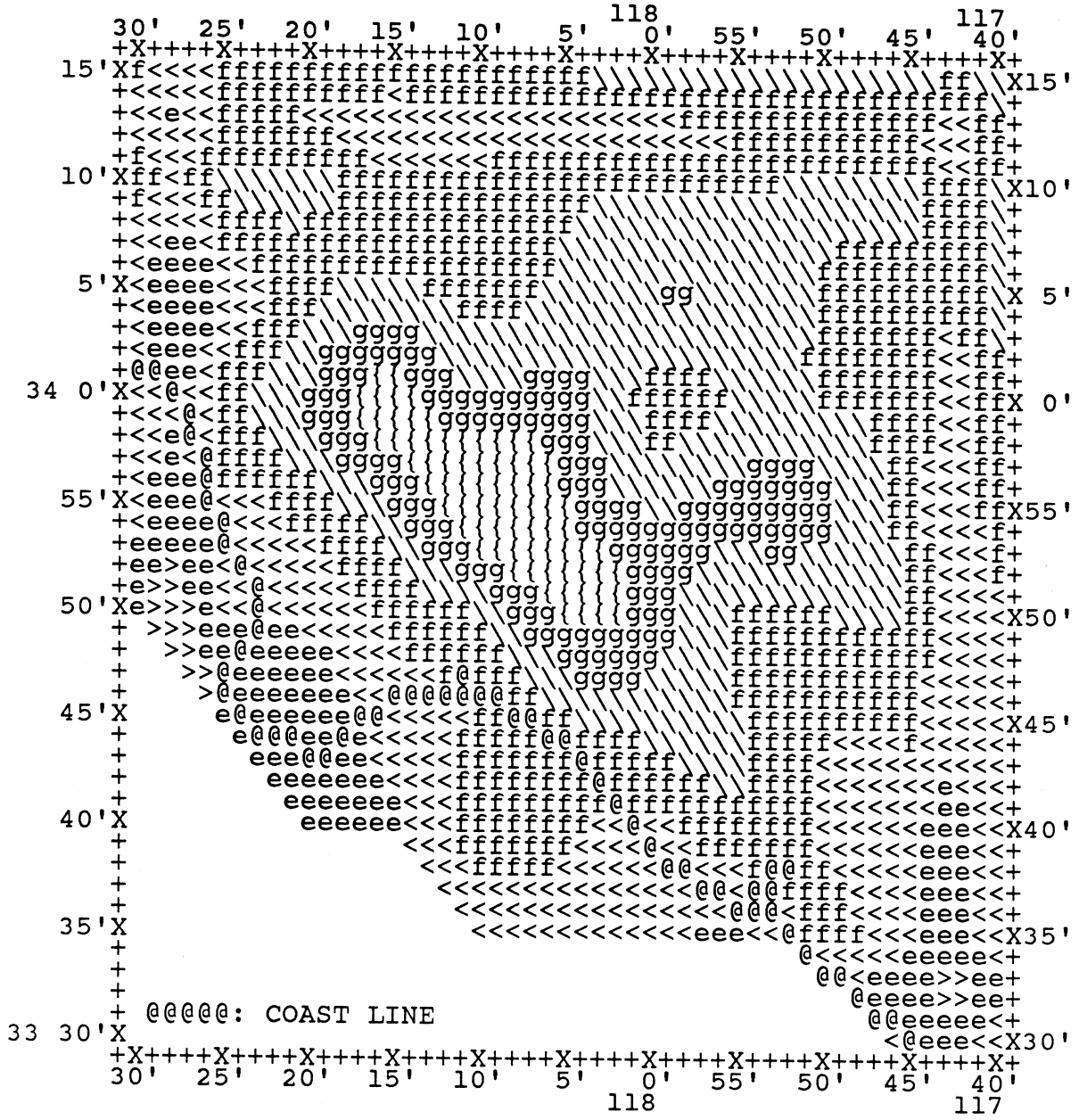

Figure B5.6

PSEUDO RELATIVE VELOCITY, PSV (IN/SEC) AT T = .900 SEC

PROBABILITY OF EXCEEDANCE = .01 FOR 50 YEARS
CALCULATED FROM ESTIMATED M.M.I. LEVELS AT SITES

CONTOUR LEVELS OF LOG(PSV):

>	e	<	f	\	g	{	h	}
1.7	1.8	1.9	2.0	2.1	2.2	2.3	2.4	2.5

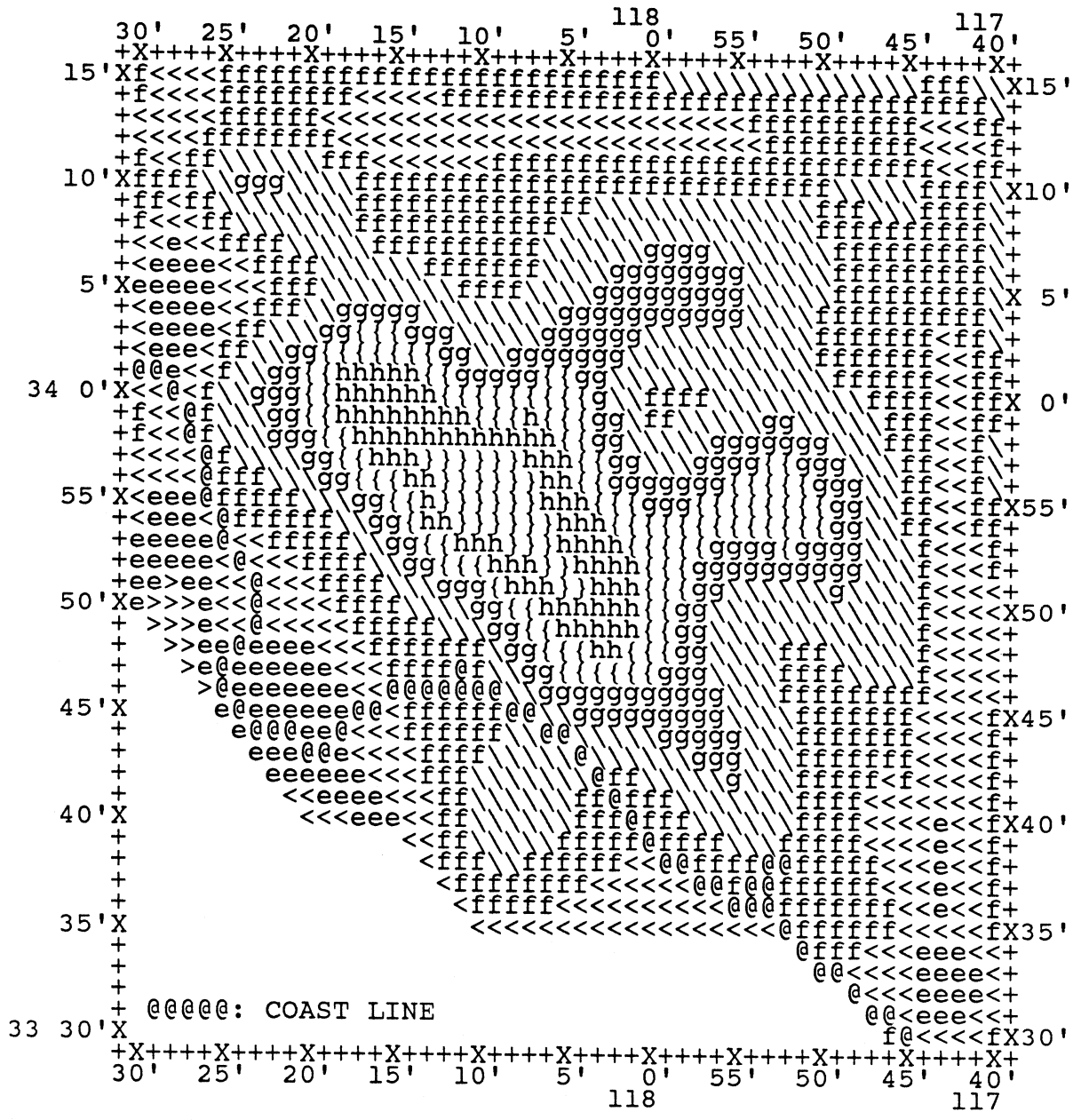

Figure B5.7

PSEUDO RELATIVE VELOCITY, PSV (IN/SEC) AT T = 1.600 SEC

PROBABILITY OF EXCEEDANCE = .01 FOR 50 YEARS
CALCULATED FROM ESTIMATED M.M.I. LEVELS AT SITES

CONTOUR LEVELS OF LOG(PSV):

>	e	<	f	\	g	{	h	}	i
1.7	1.8	1.9	2.0	2.1	2.2	2.3	2.4	2.5	2.6

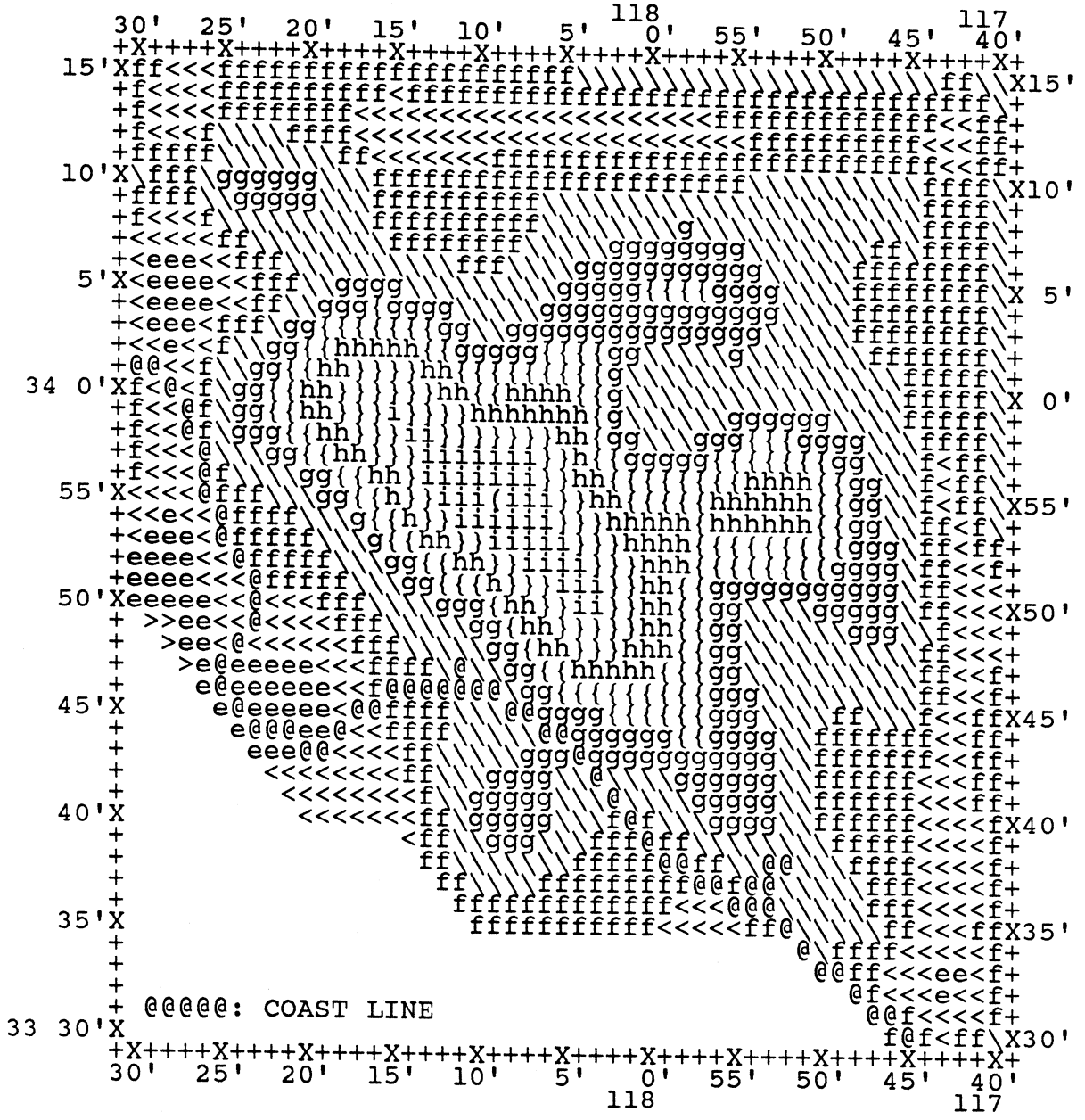

Figure B5.8

PSEUDO RELATIVE VELOCITY, PSV (IN/SEC) AT T = 2.800 SEC

PROBABILITY OF EXCEEDANCE = .01 FOR 50 YEARS
CALCULATED FROM ESTIMATED M.M.I. LEVELS AT SITES

CONTOUR LEVELS OF LOG(PSV):

d	>	e	<	f	\	g	{	h	}	i
1.6	1.7	1.8	1.9	2.0	2.1	2.2	2.3	2.4	2.5	2.6

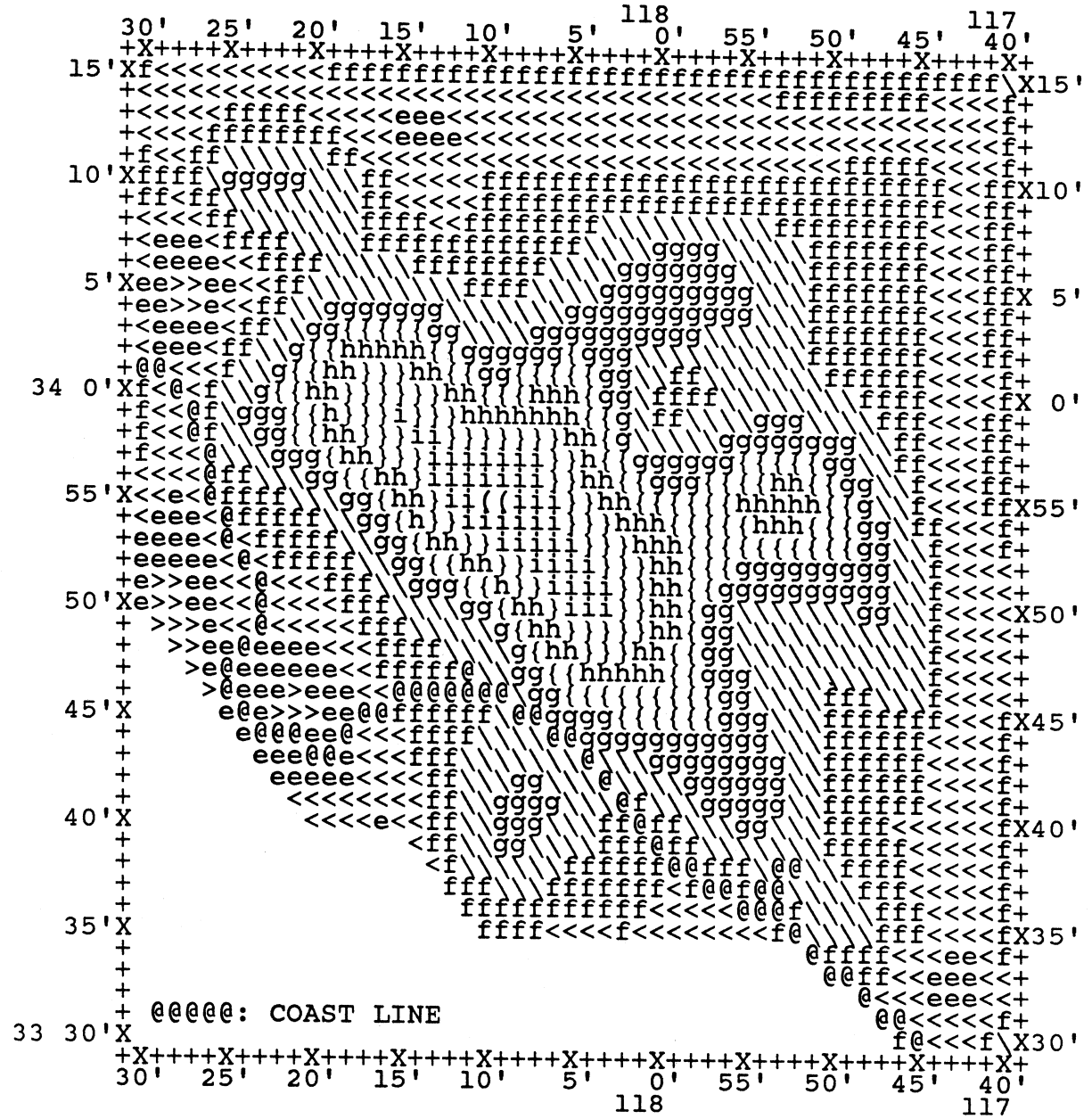

Figure B5.9

PSEUDO RELATIVE VELOCITY, PSV (IN/SEC) AT T = 4.400 SEC

PROBABILITY OF EXCEEDANCE = .01 FOR 50 YEARS
CALCULATED FROM ESTIMATED M.M.I. LEVELS AT SITES

CONTOUR LEVELS OF LOG(PSV):

^	d	>	e	<	f	\	g	{	h	}
1.5	1.6	1.7	1.8	1.9	2.0	2.1	2.2	2.3	2.4	2.5

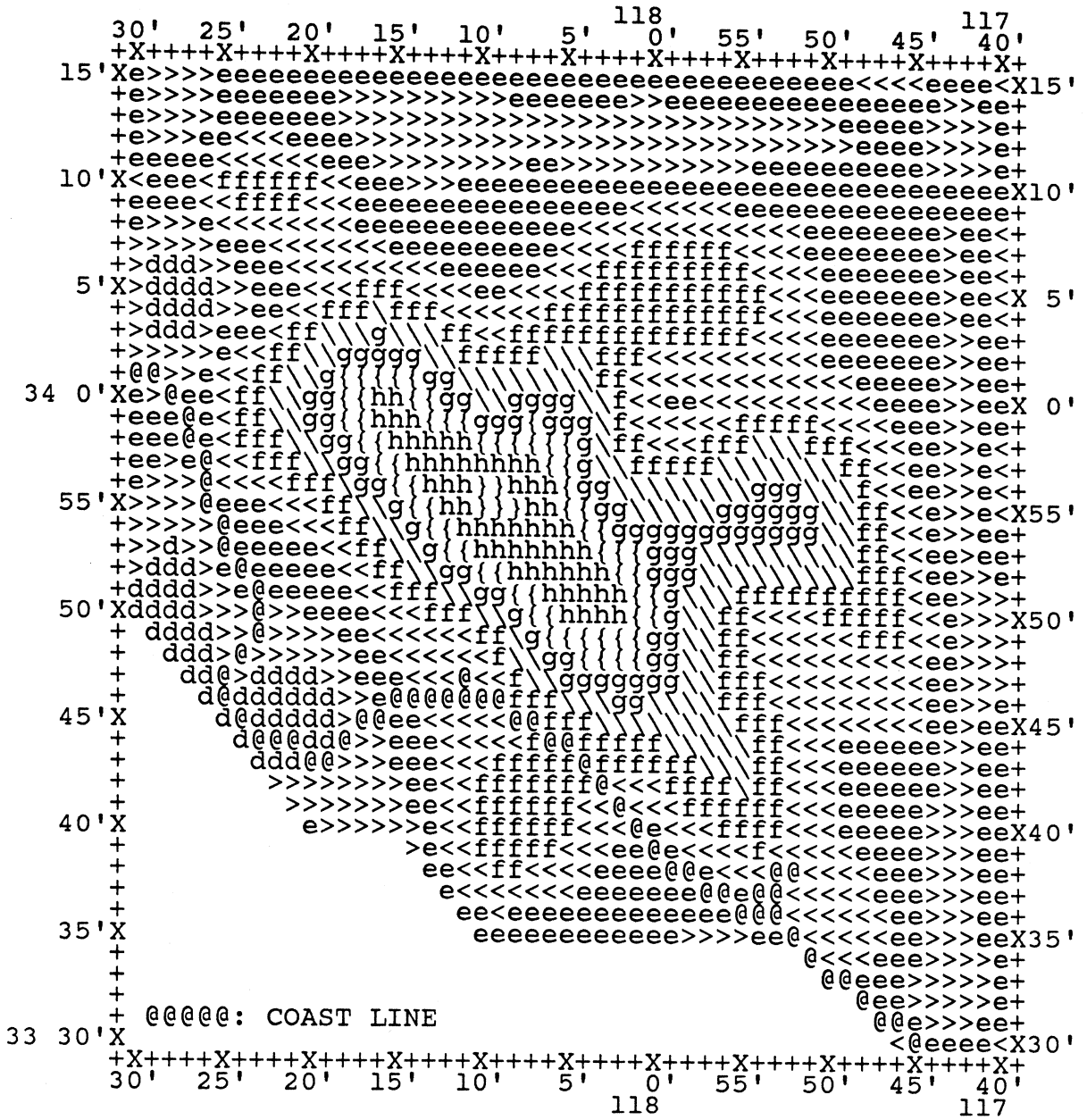

Figure B5.10

PSEUDO RELATIVE VELOCITY, PSV (IN/SEC) AT T = 7.500 SEC

PROBABILITY OF EXCEEDANCE = .01 FOR 50 YEARS
CALCULATED FROM ESTIMATED M.M.I. LEVELS AT SITES

CONTOUR LEVELS OF LOG(PSV):

b	]	c	^	d	>	e	<	f
1.2	1.3	1.4	1.5	1.6	1.7	1.8	1.9	2.0

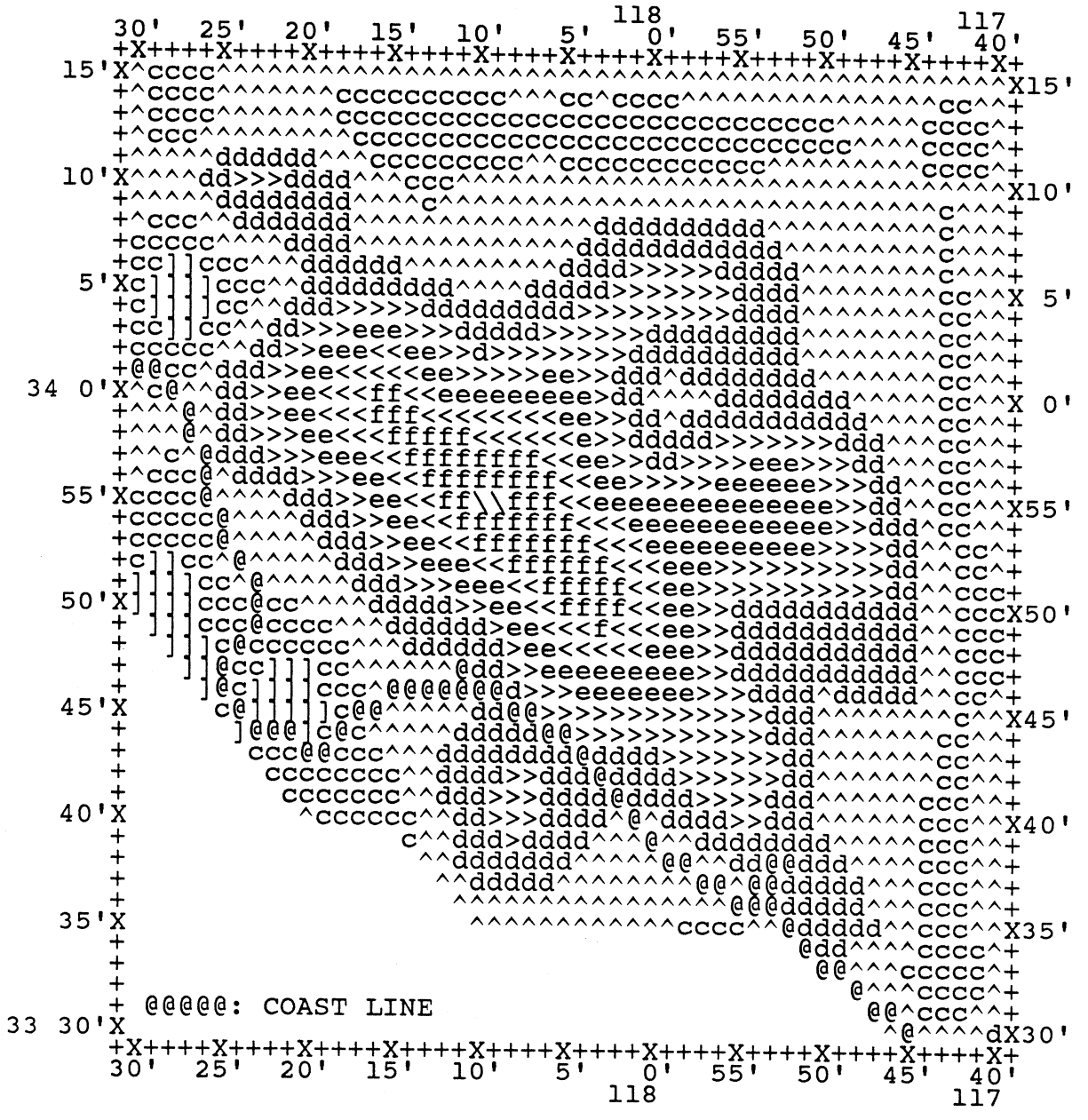

Figure B5.11